

Performance evaluation of optical communication networks

Citation for published version (APA):

Tafur Monroy, I. (1999). *Performance evaluation of optical communication networks*. [Phd Thesis 1 (Research TU/e / Graduation TU/e), Electrical Engineering]. Shaker-Verlag. <https://doi.org/10.6100/IR526283>

DOI:

[10.6100/IR526283](https://doi.org/10.6100/IR526283)

Document status and date:

Published: 01/01/1999

Document Version:

Publisher's PDF, also known as Version of Record (includes final page, issue and volume numbers)

Please check the document version of this publication:

- A submitted manuscript is the version of the article upon submission and before peer-review. There can be important differences between the submitted version and the official published version of record. People interested in the research are advised to contact the author for the final version of the publication, or visit the DOI to the publisher's website.
- The final author version and the galley proof are versions of the publication after peer review.
- The final published version features the final layout of the paper including the volume, issue and page numbers.

[Link to publication](#)

General rights

Copyright and moral rights for the publications made accessible in the public portal are retained by the authors and/or other copyright owners and it is a condition of accessing publications that users recognise and abide by the legal requirements associated with these rights.

- Users may download and print one copy of any publication from the public portal for the purpose of private study or research.
- You may not further distribute the material or use it for any profit-making activity or commercial gain
- You may freely distribute the URL identifying the publication in the public portal.

If the publication is distributed under the terms of Article 25fa of the Dutch Copyright Act, indicated by the "Taverne" license above, please follow below link for the End User Agreement:

www.tue.nl/taverne

Take down policy

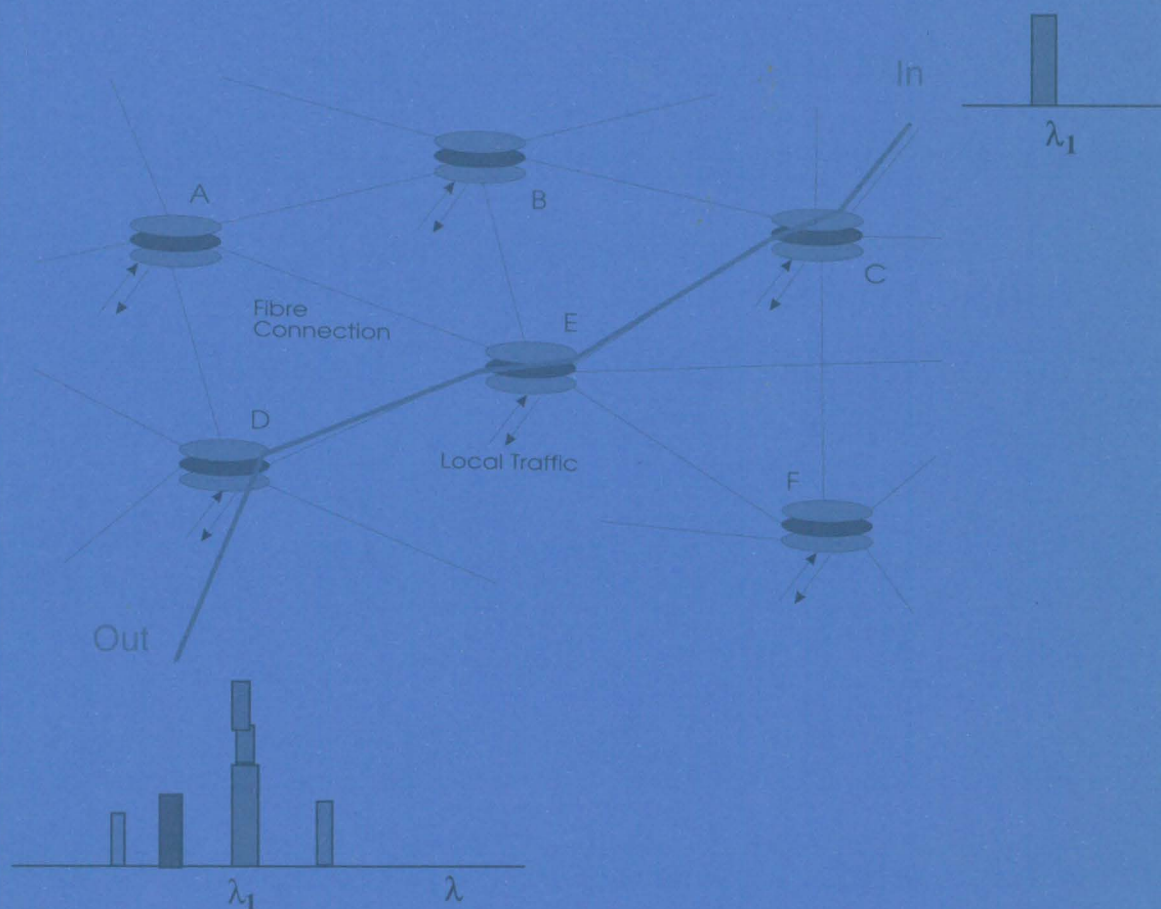
If you believe that this document breaches copyright please contact us at:

openaccess@tue.nl

providing details and we will investigate your claim.

Performance Evaluation of Optical Communication Networks

Idelfonso Tafur Monroy



Performance Evaluation of Optical Communication Networks

Performance Evaluation of Optical Communication Networks

Proefschrift

ter verkrijging van de graad van doctor aan de
Technische Universiteit Eindhoven, op gezag van de
Rector magnificus, prof.dr. M. Rem, voor een
commissie aangewezen door het College voor
Promoties in het openbaar te verdedigen op
donderdag 9 september 1999 om 16.00 uur

door

Idelfonso Tafur Monroy

geboren te El Catillo (Meta), Colombia

Copyright Shaker 1999

Alle rechten voorbehouden. Niets van deze uitgave mag worden verveelvoudigd,
opgeslagen in een geautomatiseerd gegevensbestand, of openbaar gemaakt,
in enige vorm, zonder toestemming van de uitgever.

ISBN 90-423-0087-6

Shaker Publishing B.V.
St. Maartenslaan 26
6221 AX Maastricht
tel.: 043-3500424
fax.: 043-3255090
<http://www.shaker.nl>

Dit proefschrift is goedgekeurd door de promotoren:

prof.ir. G.D. Khoe
en
prof. G. Einarsson

Copromotor:

dr.ir. H. de Waardt

Abstract

Optical communications networks are an essential part of the world wide telecommunication infrastructure. The number of users of present and future telecommunication services like Internet, web browsing and tele-education will increase dramatically. As a consequence there is an imminent demand for broadband and high capacity communication systems. A promising solution is the concept of all-optical networks. Major research efforts in areas such as photonic integration and semiconductor technology, among others, are currently directed toward the development of key components that will enable the construction of all-optical networks.

This thesis addresses the performance analysis of optical networks. Theoretical models are presented for a number of digital optical systems in the context of all-optical networking. The models account for the influence of significant noise arising from performance imperfections of optical devices that comprise an all-optical network. Modeling, apart from being applied to the performance assessment, gives insights into how to optimally operate the system so that a certain level of reliability is assured. The validity of the developed models has been confirmed by relevant experimental measurements.

The main results of this thesis are as follows. Firstly, an accurate statistical description of filtered interferometric crosstalk is presented. Secondly, phase scrambling to reduce the effect of crosstalk in wavelength division multiplexing networks is theoretically investigated and experimentally assessed. Thirdly, original research on optically preamplified receivers, phase noise analysis, and scalability of optical networks is presented. Finally, based on theoretical and experimental studies, this work gives a series of recommendations on how to select the optimal operating regime for systems employing phase scrambling to reduce interferometric crosstalk.

Samenvatting

Optische communicatie netwerken zijn een onderdeel van de wereldwijde telecommunicatie infrastructuur. Het aantal gebruikers van bestaande en toekomstige telecom diensten, zoals internet, web browsing en teleonderwijs, zal zeer sterk toenemen. Dit betekent voor de toekomst een zeer grote stijging van de vraag naar communicatie systemen met een hoge capaciteit en bandbreedte. Een veelbelovende oplossing wordt gezien in de ontwikkeling van communicatie netwerken die volledig optisch zijn. Tegenwoordig wordt veel onderzoek verricht naar nieuwe materialen en bouwstenen voor implementatie in het optische domein van deze netwerken.

Dit proefschrift behandelt de prestatie analyse van optische communicatie systemen. Binnen de context van optische netwerken zijn diverse modellen voor digitale optische systemen ontwikkeld. Ruis afkomstig van bouwstenen, een typerende voorbeeld daarvan is optische overspraak, tast de prestatie van optische communicatie systemen aan. De modellen zijn bestemd voor het analyseren van het nadelige effect van ruis. Modelering is niet alleen van belang voor de prestatie analyse, maar het geeft ook inzicht in de optimale keuze van de parameters opdat een gewenst niveau van betrouwbaarheid gegarandeerd wordt. De juistheid van deze modellen is bevestigd door experimentele resultaten.

De belangrijkste resultaten van dit proefschrift zijn: Ten eerste, een complete statistische beschrijving van optische overspraak in systemen die gebruik maken van golflengte multiplexing. Ten tweede, de scrambling van de fase, om het effect van overspraak te verminderen, theoretisch bestudeerd en experimenteel geëvalueerd. Ten derde, innovatief onderzoek naar optische ontvangers met optische voorversterking, fase ruis analyse en dimensionering van optische netwerken. Ten slotte worden een reeks van aanbevelingen gedaan betreffende het optimaal gebruik van fase scrambling om optische overspraak te verminderen.

Acknowledgments

It is a great pleasure to me to thank the many people who in different ways have supported my graduate studies and contributed to the process of writing this thesis.

First, I would like to thank my supervisors Professor G. D. Khoe and Dr. Huig de Waardt for their support during my PhD research at the Eindhoven University of Technology. I also would like to thank Professor Göran Einarsson for introducing me to the area of optical communication theory and for his support and encouragement during my time as a graduate student at the Royal Institute of Technology, Stockholm.

I would like to express my gratitude to all my colleagues, in particular to those at the Electro-optical Communication Division of the Eindhoven University of Technology for their support, cooperation and fruitful discussions on diverse research topics. Special thanks go to Dr. Gerard Hooghiemstra at the Delft University of Technology for his stimulating course on Brownian motion and his cooperation.

I want to thank my family and friends for their sincere interest in my work and their moral support. I'm very grateful to Ruud for his understanding. Finally, above all I thank the Lord for his guidance.

Contents

Abstract	i
Samenvatting	iii
Acknowledgments	v
Contents	vii
List of Abbreviations	ix
1 General Introduction	1
1.1 Brief historical review	1
1.2 All-optical networks	2
1.3 Subject of the thesis	3
1.4 Structure of the thesis	4
2 Summary of Original Work	5
2.1 List of papers	5
2.2 Description of the papers	6
2.3 Main results	11
3 All-Optical Networks	13
3.1 Building blocks	13
3.2 Evolution path towards all-optical networking	15
3.3 Enabling technologies	19
3.4 Performance limitations in optical networks	21
3.5 Further reading	23
4 Phase Noise Analysis	25
4.1 Phase noise model	25
4.2 Phase noise in optical system	26
Paper A: Error Probability Evaluation of Optical Systems Disturbed by Phase Noise and Additive Noise	29
Paper B: On a Recursive Formula for the Moments of Phase Noise	37

5	Optically Preamplified Direct Detection Receivers	43
5.1	Problem statement	43
5.2	Performance analysis	44
5.3	Communication theory	44
	Paper C: Bit Error Evaluation of Optically Preamplified Direct Detection Receiver with Fabry-Perot Optical Filters	47
	Paper D: Error Rate Analysis of Optically Preamplified Receivers with Fabry-Perot Optical Filter and Equalizing Postdetection Filtering	57
	Paper E: On Analytical Expressions for the Distribution of the Filtered Output of Square Envelope Receivers with Signal and Colored Gaussian Noise Input	65
	Paper F: An Optically Preamplified Receiver with Low Quantum Limit	73
6	Crosstalk in Optical Networks	77
6.1	Crosstalk mechanism	77
6.2	Characteristics of crosstalk	77
6.3	Reduction techniques for crosstalk	79
6.4	Phase scrambling	79
6.5	Scalability of optical networks	81
	Paper G: Performance Evaluation of Optical Cross-Connects by Saddlepoint Approximation	83
	Paper H: Statistical Analysis of Interferometric Noise in Optical ASK/Direct Detection Systems	93
	Paper I: On the Distribution and Performance Implications of Interferometric Crosstalk in WDM Networks	101
	Paper J: Performance of Optically Preamplified Receivers in WDM Systems Disturbed by Interferometric Crosstalk	113
	Paper K: Interferometric Crosstalk Reduction in Optical WDM Networks by Phase Scrambling	123
	Paper L: Scalability of All-Optical Networks: Study of Topology and Crosstalk Dependence	135
	Paper M: How Does Crosstalk Accumulate in WDM Networks?	145
	Paper N: Scalability of Optical Networks: Crosstalk Limitations	153
7	Conclusion, Recommendations, and Further Work	163
7.1	Conclusions	163
7.2	Recommendations	165
7.3	Further work	167
	Appendix A: Characteristics of Interferometric Crosstalk	169
A.1	Polarization statistics	169
A.2	Detection threshold	170
A.3	Non-perfect extinction ratio	171
	References	173
	Curriculum Vitae	179

List of Abbreviations

ASE	Amplified spontaneous emission
ASK	Amplitude shift keying
AWG	Array waveguide grating
BER	Bit-error rate
CDMA	Code division multiplexing access
DD	Direct detection
DFB	Distributed feedback
DPSK	Differential phase shift keying
EDFA	Erbium-doped fiber amplifier
FWM	Four wave mixing
ISI	Intersymbol interference
LAN	Local area network
MAN	Metropolitan area network
MGF	Moment generating function
OADM	Optical add drop multiplexing
OOK	On-off keying modulation
OTDM	Optical time division multiplexing
OXC	Optical cross-connect
PDF	Probability density function
PDG	Polarization dependent gain
PHASAR	Phased array
PIC	Photonic integrated circuit
PMD	Polarization mode dispersion
SOA	Semiconductor optical amplifier
SRS	Stimulated Raman scattering
SSMF	Standard single mode fiber
TDM	Time division multiplexing
WDM	Wavelength division multiplexing

Chapter 1

General Introduction

The growth of telecommunications is expected to continue, spurred on by several factors, including the globalization of the world economy, the strong dependence of modern industry and society on telecommunication and information systems, and the public demand for access to information. Indeed, the continuous and increasing demand for high information capacity systems assures the presence of fiber optical communication systems in the information era.

Although optical communication by use of fire, smoke, semaphore flags and optical telegraphs, has long been used for information transmission, it was not until the first half of the 19th century with the invention of the telegraph, the introduction of telephony and later of television that the infrastructure of telecommunication networks started to emerge. Soon higher and higher transmission capacities were needed from these telecommunication networks. At first, twisted pair cables were replaced by coaxial cables providing a higher transmission capacity. Other transmission media were introduced, such as microwave links and satellite communications. Later, optical fibers were proposed as an alternative for coaxial cables. These optical fibers have beneficial characteristics for information transmission, such as low attenuation and dispersion, large bandwidth, immunity to electrical noise. They also have durability, flexibility, and soon became a key part of the telecommunication network infrastructure.

The area of optical fiber communication has undergone a rapid technical development. This is mainly due to a combination of innovations in semiconductor, optical waveguide, and photonic integration technology. Today, throughout the world, telecommunications operators use optical fibers for transmission of information in long-distance systems, undersea systems, local area networks, metropolitan area networks, and in access and distribution networks.

1.1 Brief historical review

In 1966 Kao and Hockman [1] and Werts [2] suggested that if it would be possible to produce a glass fiber of sufficiently low attenuation, then optical fibers would be an alternative to coaxial cables for information transmission. The idea is based on the fact that light can propagate in an optical fiber by confining it in a guiding structure with different refractive indices n_1 and n_2 as shown in Fig. 1.1.

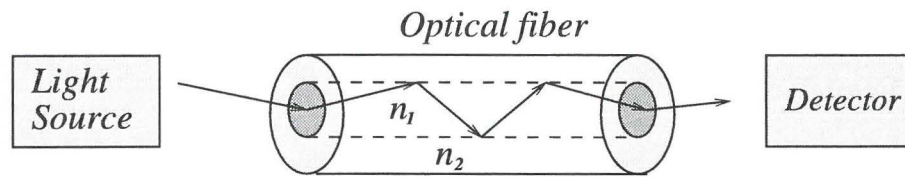


Figure 1.1: Principle of optical fiber communication. The refractive index n_1 is larger than n_2 .

Improvements in the quality of the optical fiber made possible the introduction of the first generation of optical fiber communication in the 1970's. These systems used laser sources operating at the wavelength region of 800 nm. The next development has been to operate at 1300 nm and 1550 nm wavelengths due to superior silica fiber dispersion and attenuation properties; the so-called second and third generation of optical communication systems. The development of low loss fiber of approximately 0.2dB/km and single mode laser sources has made it possible to deploy long-distance fiber optical communication systems. An event of major impact on the development of optical fiber communication was the advent of the optical fiber amplifier EDFA (erbium-doped fiber amplifier) in 1987 [3]. The introduction of the EDFA, replacing opto-electrical regeneration, revolutionized the field of fiber optical communication, mainly because of its potential to enhance the transmission length, transparency to modulation formats, polarization insensitivity, low noise and crosstalk and ease of splicing to the fiber transmission system. The fourth generation of fiber optical communication systems uses wavelength division multiplexing (WDM) to increase the information capacity and EDFAs to extend the transmission length. The principle of WDM is the simultaneous transmission of several signals at different wavelengths through a single optical fiber filament. In 1996, WDM point-to-point systems were commercially introduced and has become the preferred choice to expand and upgrade the transmission capacity of optical fiber transmission systems. The next generation of communication systems is expected to be based on advanced transmission techniques like optical soliton transmission, novel modulation schemes, and intelligent nodes. Research on the coming generation of optical systems is in progress both at industry and university research centers. A series of theoretical studies and experimental trials have been reported investigating different aspects of optical soliton communication [4]. Optical neural networks are being considered for the realization of intelligent optical nodes [5, 6]. Finally, most research efforts are focused in the areas of materials, devices and technologies, which will enable the introduction of the so-called all-optical transport networks.

1.2 All-optical networks

The transmission capacity of the current optical communications systems has been substantially enhanced in recent years. For example, by using WDM techniques systems supporting

400 Gbits/s over a single fiber are on offer. There is an increasing demand on even larger transmission capacity and flexibility in future optical networks. A promising solution to this situation is the concept of all-optical networks.

Briefly, by an all-optical network is meant the combination of transmission techniques such as WDM and optical TDM (time division multiplexing), which together with routers, optical add-drop nodes, switches, crossconnects and other photonic components that allows bit rate, flexible and reliable information transmission to be implemented entirely in the optical domain. By using this approach transparency with respect to transmission hierarchy or different code formats can be achieved while using common physical optical fibers and nodes. With all these features, transparent all-optical networks are regarded as the transport network for the growing traffic volume caused by existing and emerging communication and information services.

Let us first briefly look at the history of all-optical networking. The idea of cross-connecting WDM channels was reported in 1987 [7] and the development of optical routed networks was proposed in 1988 [8]. Soon after, a series of experimental demonstrations on optical switching and WDM networks were reported [9]. These successful demonstrations were followed by the creation of research projects on the feasibility, management, photonic integration, and related issues of optical transparent networks [10]. A WDM cross-connected layer was also proposed for LAN (local area network) applications [11]. Currently, photonic networks and their enabling technologies are a hot research topic [12–14]. One area of intensive activity is the opto-electronic integration of photonic devices like optical (de)multiplexers, optical add-drops, optical cross-connects and photoreceivers [15–17].

Within the framework of the European Commission ACTS (Advanced Communications Technologies and Services) program, the project BLISS (Broadband Light Sources and Systems) demonstrated the integration of an optical cross-connect on a single chip. Within the scope of the project the routing and switching of four WDM channels employing the new developed cross-connect chip was also demonstrated in laboratory trials. The realization of a cross-connect chip supporting a larger number of channels, the study of the scalability of cross-connected networks, and the use of techniques to reduce transmission impairments like crosstalk all fall under the heading of the recently established research project ACTS-APEX (Advance Photonic Experimental Cross-connect) [18].

1.3 Subject of the thesis

The subject of this thesis mainly stems from the performance analysis of optical cross-connected networks like those investigated in the BLISS and APEX projects. The quality of a digital communication system is usually described by how fast and reliable the information is transmitted. The speed is given in bits per second and the reliability is measured by the rate of correctly received (detected) bits; the error probability or also the so-called bit-error rate (BER). The performance analysis of a communication system is mostly based on the BER evaluation. By a proper modeling of a communication system we can effectively assess its performance. Moreover, modeling help us to identify parameters that influence the performance and to provide insights into how to operate the system so that a certain level of reliability is assured.

Firstly, this thesis covers the analysis of optical signals corrupted by phase noise. Laser phase noise, due to the spontaneous emission of photons, affects the performance of a large number of communication systems.

Secondly, performance analysis of optically preamplified receivers is the topic of the second part of this thesis. Optical amplifiers are often used to amplify signals before detection, so that a higher receiver sensitivity is achieved. Optical amplifiers introduce ASE (Amplified Spontaneous Emission) noise and are therefore often followed by an optical filter to reduce their noise contribution. Optical filtering reduces the ASE noise but it also distorts the optical signal introducing possibly intersymbol interference (ISI). This fact suggests that there is a tradeoff between ASE noise reduction and ISI and hence it is important to determine the regime of optimum operation.

Finally, the subject of the third part of this thesis concerns the modeling and reduction techniques of interferometric crosstalk in WDM networks. Interferometric crosstalk, arising from performance imperfections in optical (de)multiplexers and switching fabrics, has proved to be a serious limiting factor for the performance of optical cross-connected networks. Phase scrambling as a technique to reduce interferometric crosstalk is theoretically studied and experimentally assessed in this thesis. Additionally, performance analysis and scalability of cross-connected optical networks is presented.

1.4 Structure of the thesis

This thesis contains three key chapters that are based on publications and papers submitted for publication. Chapter 4 is devoted to the analysis of optical systems disturbed by phase noise. Chapter 5 covers the performance analysis of optically preamplified, direct detection receivers. The analysis of cross-connected optical networks is the topic of Chapter 6. The rest of this thesis is organized as follows. First, in Chapter 2, a summary is presented of each paper included in this thesis. Chapter 3 gives an introduction to all-optical networking. It therefore introduces the general context of this thesis work. A list of suggested literature is also given for the reader who may want a deeper treatment of the subject. Secondly, Chapters 4, 5 and 6 are presented. Each of these chapters starts with an introductory section to the topic of study. Subsequently, reprints of the papers are enclosed. Finally, Chapter 7 presents recommendations, suggestions for further work and conclusions.

Chapter 2

Summary of Original Work

The purpose of this chapter is to present a summary of the publications forming this thesis. The problem statement, the method and the main results are shortly described.

2.1 List of papers

The following papers are included in this thesis. In the sequel they will be referred to by their letters.

- A Göran Einarsson, Johan Strandberg, Idelfonso Tafur Monroy
Error Probability Evaluation of Optical Systems Disturbed by Phase Noise and Additive Noise
IEEE/OSA J. Lightwave Technol., September 1995, Vol. 13, No. 9, pp. 1847-1852.
- B Idelfonso Tafur Monroy and Gerard Hooghiemstra
On a Recursive Formula for the Moments of Phase Noise
IEEE Trans. Comm., Submitted for publication.
- C Idelfonso Tafur Monroy and Göran Einarsson
Bit Error Evaluation of Optically Preamplified Direct Detection Receiver with Fabry-Perot Optical Filters
IEEE/OSA J. Lightwave Technol., Vol. 15, No. 8, pp. 1546-1553, Aug. 1997.
- D Göran Einarsson and Idelfonso Tafur Monroy
Error Rate Analysis of Optically Preamplified Receivers with Fabry-Perot Optical Filter and Equalizing Postdetection Filtering
Journal of Optical Communications, Submitted for publication.
- E Idelfonso Tafur Monroy
On Analytical Expressions for the Distribution of the Filtered Output of Square Envelope Receivers with Signal and Colored Gaussian Noise Input
IEEE Trans. Comm., Submitted for publication.
- F Idelfonso Tafur Monroy
An Optically Preamplified Receiver with Low Quantum Limit

Partially presented at 1998 IEEE/LEOS Benelux Symposium, Nov. 26, 1998, Gent, Belgium, pp. 197-200.

- G Idelfonso Tafur Monroy and E. Tangdionga
Performance Evaluation of Optical Cross-Connects by Saddlepoint Approximation
IEEE/OSA J. Lightwave Technol., Vol. 16, No. 3. pp. 317-323, March 1998.
- H Idelfonso Tafur Monroy
Statistical Analysis of Interferometric Noise in Optical ASK/Direct Detection Systems
Syben'98, Zurich, Switzerland, May 18-22, 1998, pp. 178-182.
- I Idelfonso Tafur Monroy, E. Tangdionga, R. Jonker, and H. de Waardt
On the Distribution and Performance Implications of Interferometric Crosstalk in WDM Networks
IEEE/OSA J. Lightwave Technol., Vol. 17, No. 6, pp. 989-997, June, 1999.
- J Idelfonso Tafur Monroy, E. Tangdionga, and H. de Waardt
Performance of Optically Preamplified Receivers in WDM Systems Disturbed by Interferometric Crosstalk
Photonic Network Communications, Submitted for publication.
- K Idelfonso Tafur Monroy, E. Tangdionga, H. de Waardt
Interferometric Crosstalk Reduction in Optical WDM Networks by Phase Scrambling
IEEE/OSA J. Lightwave Technol., Submitted for publication.
- L Idelfonso Tafur Monroy, J. Siffels, H. de Waardt and H. J. S. Dorren
Scalability of All-Optical Networks: Study of Topology and Crosstalk Dependence
Syben'98, Zurich, Switzerland, May 18-22, 1998, pp 201-207.
- M H. J. S. Dorren, H. de Waardt, and Idelfonso Tafur Monroy
How Does Crosstalk Accumulate in WDM Networks?
IEEE/OSA J. Lightwave Technol., Submitted for publication.
- N Idelfonso Tafur Monroy
Scalability of Optical Networks: Crosstalk Limitations
Photonic Network Communications, Submitted for publication.

2.2 Description of the papers

In Chapter 4

Paper A: Error Probability Evaluation of Optical Systems Disturbed by Phase Noise and Additive Noise. This paper presents a direct and efficient method for the evaluation of the error probability of optical heterodyne receivers in the presence of phase noise. The analysis is

based on a power series expansion of the filtered phase noise. A closed form expression for the statistics of the receiver decision variable is derived, including shot noise and receiver thermal noise. Error probabilities are computed using the saddlepoint approximation. The optimal prefilter bandwidth for the phase noise rejection can easily be determined.

Contributions by the author of this thesis: 1) The theoretical part on DPSK (Differential Phase Shift Keying) system together with G. Einarsson. 2) Numerical computations for the DPSK receiver.

Paper B: On a Recursive Formula for the Moments of Phase Noise. This paper derives a simple recursive formula for the moments of phase noise, for both its real and imaginary part. In fact, the recursion is valid for any integral of a properly chosen function of Brownian motion. It also gives the moments for any arbitrary starting value. Approximate probability density functions can be found through a maximum entropy approach or an orthogonal polynomial series expansion. Moments may also be used for the calculation of error probabilities by Gaussian quadrature rules.

Contributions by the author of this thesis: 1) The applications section. 2) All numerical computations.

The mathematical derivation was done by G. Hooghiemstra.

In Chapter 5

Paper C: Bit Error Evaluation of Optically Preamplified Direct Detection Receiver with Fabry-Perot Optical Filters. This paper presents the performance analysis for an optically preamplified, direct detection receiver using a Fabry-Perot optical filter. A closed form expression is derived for the moment generating function (MGF) of the decision variable. The standard quantum limit is computed by exact analysis, using the derived MGF, and also by a Gaussian approximation. The optimum value of the optical filter bandwidth bit-time product is determined while the postdetection filter is considered to be an integrate-and-dump filter.

Contributions by the author of this thesis: 1) The theoretical part of the paper. 2) All numerical computations.

The section on the Gaussian approximation was introduced by G. Einarsson.

Paper D: Error Rate Analysis of Optically Preamplified Receivers with Fabry-Perot Optical Filter and Equalizing Postdetection Filtering. This work expands the analysis of the previous paper by considering a modified integration interval of the postdetection filter, as well as an equalizing postdetection filter. Performance enhancement can be achieved in this way. By using the simple Gaussian approximation, bounds on the error probability are proposed for a more general case of optical and electrical filtering.

Contributions by the author of this thesis: Extension of the theoretical part of the previous paper by G. Einarsson together with the author.

Numerical computations on the modified integration and equalizing receiver were done by G. Einarsson.

Paper E: *On Analytical Expressions for the Distribution of the Filtered Output of Square Envelope Receivers with Signal and Colored Gaussian Noise Input.* The analysis of optically preamplified receivers constitutes an example of the classical problem in communication theory of determining the statistics of the filtered output of square envelope receivers. In this paper we derive closed form expressions for the MGF of the filtered output of a squared envelope receiver with colored Gaussian noise input. The Gaussian processes considered are: the Wiener process, a Gaussian process with linear covariance (moving average), and the Ornstein-Uhlenbeck process. The derived MGFs are then applied to the problem of finding the quantum limit for optically preamplified, direct detection receivers.

Paper F: *An Optically Preamplified Receiver with Low Quantum Limit.* Optical amplifiers prove to efficiently enhance the receiver sensitivity of optical communication systems. In optical communications it is common practice to compare the systems ultimate sensitivity in terms of the quantum limit. The standard *quantum limit* is defined as the average number of photons per bit in the optical signal needed to achieve a bit-error probability of 10^{-9} assuming ideal detection conditions, which for a preamplified receiver means that a large amplifier gain is assumed. In this paper we first summarize the results on the quantum limit for different optically preamplified, OOK/DD receivers found in the literature. Subsequently, we present a receiver scheme that is expected to outperform previously studied configurations.

In Chapter 6

Paper G: *Performance Evaluation of Optical Cross-Connects by Saddlepoint Approximation.* An accurate and numerically simple statistical method is introduced to analyze crosstalk in cross-connected networks. It is the so-called saddlepoint approximation that makes use of the MGF for the receiver decision variable. Experimental results using a system with a directly modulated light source yielded results that are in good agreement with the theoretical predictions. The presented model accounts for crosstalk statistics (arc-sine distribution), linear random polarization, data statistics, non-perfect extinction ratio, and receiver thermal noise.

Contributions by the author of this thesis: 1) The theoretical part of the paper. 2) All simulations and numerical computations. Experiment performed by E. Tangdiongga.

Paper H: *Statistical Analysis of Interferometric Noise in Optical ASK/Direct Detection Systems.* Interferometric crosstalk affects a variety of optical communication systems. Crosstalk may arise from reflections, Rayleigh scattering, and performance imperfections of components like optical switches and (de)multiplexers both in OTDM and WDM systems. This paper presents a performance analysis of interferometric noise based on the use of the MGF for the receiver decision variable together with the saddlepoint approximation.

Paper I: *On the Distribution and Performance Implications of Interferometric Crosstalk in WDM Networks.* It has been experimentally observed that the effect of interferometric crosstalk is more severe in systems employing externally modulated light sources than in

those using directly modulated diode sources. This paper derives an accurate statistical description of filtered interferometric noise. Statistical moments are derived that account for the relationship between the source spectral bandwidth and the electrical filter bandwidth. It is this relationship that explains why systems with directly modulated sources (having a broad spectrum due to chirping) incurred smaller power penalties due to filtered interferometric crosstalk than systems employing externally modulated sources (having a spectrum mainly determined by the modulation rate). Experimental data from systems employing both types of modulation for the light source confirm the theoretical model.

Contributions by the author of this thesis: 1) The theoretical part of the paper. 2) All simulations and numerical computations. 3) Experiment performed together with E. Tangdiongga and H. de Waardt.

Paper J: *Performance of Optically Preamplified Receivers in WDM Systems Disturbed by Interferometric Crosstalk.* Optical amplifiers are commonly used as preamplifiers to enhance receiver sensitivity. This paper investigates, both theoretically and experimentally the performance of optically preamplified receivers in the presence of interferometric crosstalk. The theoretical model accurately incorporates the statistics of filtered interferometric crosstalk and the non-Gaussian statistics of detected amplified spontaneous emission (ASE). The main result is that optical preamplification does not enhance the system tolerance toward interferometric crosstalk. Moreover, it introduces additional power penalties due to crosstalk-spontaneous emission beat noise contributions. The theoretical results and experimental measurements for power penalties, for systems employing directly and externally modulated light sources, are found to be in good agreement.

Contributions by the author of this thesis: 1) The theoretical part of the paper. 2) All simulations and numerical computations. 3) Experiment performed together with E. Tangdiongga and H. de Waardt.

Paper K: *Interferometric Crosstalk Reduction in Optical WDM Networks by Phase Scrambling.* Optical networks impose strict requirements on the crosstalk level for the components involved in the optical nodes. For instance, a crosstalk level better than -35 dB has to be used to incur power penalties less than 1 dB even when a small number of crosstalk interferers are present. This still is a stringent requirement for the performance of state-of-the-art integrated optical cross-connects. In order to allow WDM networking while making use of presently available integrated optical components, phase scrambling is proposed as a technique to mitigate interferometric crosstalk. By modulating the phase of the signals with a noise source, the crosstalk noise power is redistributed to frequencies outside the electrical receiver bandwidth. In this way, a significant part of the crosstalk noise power is filtered out by the postdetection electrical filter.

This paper presents a study of interferometric crosstalk reduction by phase scrambling. A theoretical model is developed that includes the effect of phase noise to intensity noise conversion by chromatic dispersion during propagation. It is experimentally demonstrated that by using phase scrambling a network tolerance toward crosstalk is significantly enhanced. Moreover, by properly selecting the parameters for phase scrambling the effect of dispersion during transmission may be kept reasonably low. For instance, power penalties smaller than 1 dB for crosstalk values up to -18 dB are measured in a 2.5 Gbit/s link of 100 km of

standard single mode fiber (SSMF). Power penalties smaller than 2 dB for crosstalk values up to -15 dB and -16 dB are measured after transmission over 100 km and 200 km of SSMF fiber. This corresponds to an enhancement of the system tolerance to crosstalk of 7dB and 5.3 dB, respectively. This result proves the feasibility of optical networking in a LAN/MAN domain while tolerating the relatively high crosstalk levels of the present integrated optical cross-connect technology.

Contributions by the author of this thesis: 1) The theoretical part of the paper. 2) All simulations and numerical computations.

Experiment performed by E. Tangdionga, R. Jonker and H. de Waardt.

Paper L: *Scalability of All-Optical Networks: Study of Topology and Crosstalk Dependence.* In this paper, the influence of inband crosstalk on the error performance of all-optical networks with different topologies is studied. A statistical crosstalk model is used for evaluating the bit-error rate. We show that there is a delicate relationship between the network topology and crosstalk accumulation. We show also that it is possible to select the network topology with the best performance with respect to crosstalk accumulation from among several topologies. The criterion for the comparison is the bit-error rate of the largest shortest transmission path (LSTP) in the network. A LSTP criterion means that we consider the set of shortest paths between any pair of nodes in the network. We select from this set the path that traverses the greatest number of cross-connect nodes.

Contributions by the author of this thesis: 1) The theoretical system model. 2) Numerical computations for a preamplified receiver.

J. Siffels, H. de Waardt and H. J. S. Dorren initiated this work.

Paper M: *How Does Crosstalk Accumulate in WDM Networks?* The analysis of optical networks with respect to crosstalk presented in the previous paper is continued and extended. Instead of using the largest shortest optical path as a criterion, a statistical approach is applied to study the network performance. In this way, the obtained results are made more independent of the particular lay-out studied, allowing us to draw conclusions about the performance of large generic classes of optical networks. The study shows that there is a trade-off between network connectivity, number of nodes, and robustness with respect to inband crosstalk.

Contributions by the author of this thesis: The statistical model for crosstalk.

H. de Waardt and H. J. S. Dorren initiated this work.

Paper N: *Scalability of Optical Networks: Crosstalk Limitations.* This paper presents a simple model for the performance analysis of optical networks with regard to linear optical crosstalk and accumulated spontaneous emission noise. Both inband and interchannel crosstalk are considered. Based on the proposed method we evaluate the requirements imposed on the devices for scalable optical networks. Scalability with respect to the numbers of nodes, number of input fibers to a node, and number of channels per fiber is studied. We observe that in the presence of accumulated ASE noise the requirements placed on crosstalk isolation of optical switches become more stringent.

2.3 Main results

This thesis is based on a set of articles submitted for publication and articles already published in journals and conference proceedings. Naturally, some parts of the material appear in more than one article. This is due to the fact that some of the included articles treat the same subject and subsequently present progress beyond a previous paper. In this case, sections such as introduction and method may be repeated. This section outlines the main results presented in the included papers, pointing out the main contributions of this thesis.

The contributions of this thesis are as follows:

- **Paper A:** A direct and efficient method is provided for phase noise analysis in optical heterodyne systems. The method is based on the saddlepoint approximation, which makes use of the moment generating function (MGF) for the receiver decision variable.
- **Paper B:** A recursive formula is given for the moments of phase noise in communications systems.
- **Paper C:** A closed form expression is given for the MGF of the decision variable of an optically preamplified direct detection receiver. The MGF implicitly incorporates a Fabry-Perot optical filter. The MGF is used for the performance analysis.
- **Paper D:** A complete analytic solution is provided for the analysis of optical receivers with a Fabry-Perot optical filter and equalizing postdetection filtering. Based on the results of Paper C the performance analysis of optical receivers is expanded to account for arbitrary optical and postdetection filtering.
- **Paper E:** Closed form expressions are derived for the MGF of the filtered output of square envelope receivers with signal and colored Gaussian noise input. The Gaussian processes considered are the Wiener process, a process with linear covariance, and the Ornstein-Uhlenbeck process.
- **Paper F:** An optically preamplified receiver with low quantum limit is proposed. The proposed receiver scheme outperforms previously studied receiver configurations. Special comments on this paper are given in Sec. 5.3.
- **Paper G:** A simple numerical method is developed for assessing the performance of optical cross-connects that are disturbed by optical crosstalk. The method is based on a derived MGF for the decision variable which account for multiple sources of optical crosstalk.
- **Paper H:** A statistical method is given for the analysis of interferometric noise in optical ASK/direct detection systems. This method is an extension of the work presented in paper G to the case of interferometric noise in general.
- **Paper I:** A complete statistical description of filtered interferometric crosstalk is provided. The main result is the implicit incorporation in the model of the relationship

between the optical bandwidth of the signal and the bandwidth of the postdetection filter. The interferometric delay is also taken into account. Experimental results have shown good agreement with theory.

- **Paper J:** An accurate model is described for the performance of optical receivers in the presence of both amplified spontaneous emission noise and optical crosstalk. The theoretical results are confirmed by experiments.
- **Paper K:** A complete assessment is given, theoretically and experimentally, of crosstalk reduction by phase scrambling in WDM networks. There is a demonstration of the feasibility of optical networking in a LAN/MAN environment while dealing with the relatively high crosstalk values of cross-connects with the state-of-the-art technology. The theoretical framework is partially based on the results of paper I.
- **Paper L:** A study is made of the scalability of optical networks with respect to optical crosstalk and network topology. A largest shortest transmission path (LSTP) is considered for the comparison of the performance of different topologies. By a LSTP criterion is meant that we consider the set of shortest paths between any pair of nodes in the network. We select from this set the path that traverses the greatest number of cross-connect nodes.
- **Paper M:** A study is made of the accumulation of crosstalk in optical networks. This work is related to the work in paper L in the sense that instead of a LSTP criterion a statistical average over all possible paths is used for the performance analysis.
- **Paper N:** A simple model is given for the performance analysis of optical networks with regard to linear optical crosstalk (inband and interband) and accumulated spontaneous emission noise. A simple model is presented for determining the amount of interband crosstalk in WDM systems. This model incorporates results obtained in papers I and L.

Chapter 3

All-Optical Networks

All-optical networks are considered to be a promising solution for the increasing demand for bandwidth and flexibility in future communications networks. The concept of optical networks can be described as networks in which signals are transported, switched, and routed entirely in the optical domain with electro-optical conversion taking place only at the borders of the network. The use of photonic switching solves the current limitations of electronic switching to cope with higher and higher optical transmission speeds. Such optical network can be made transparent to data rate, are flexible and are particularly suitable for bulk transport of broadband signals and services [10]. At present, much research effort is focused on the development, optimization, and photonic integration of key components to enable the introduction of all-optical networks.

This chapter is intended as an introduction to optical networking. Firstly, we analyze the node functionalities in an all-optical network. The evolution path from the present WDM networks towards optical cross-connected networks is also discussed. Secondly, we describe several performance limiting factors in all-optical networks. At this point we will have introduced the general context of this thesis. The study, for instance, of limitations due to interferometric crosstalk is the subject of Chapter 6. Finally, a list of suggested literature is also given for the reader who may want a more extensive treatment of fiber optical communications and optical networking.

3.1 Building blocks

Optical transmitters and receivers

Sources of optical signals and optical detectors are key components of an optical network. Optical transmitters usually incorporate laser diodes. Transmitter modules generate optical signals at wavelengths given by the operator or at standard wavelength specifications. The main requirements for these modules are wavelength stability with time and temperature, ease of control of the laser module, low cost, manufacturability, and reliability. The data to be transmitted are conveyed in the optical signal by modulating the light source either directly or by using an external modulator. At the receiver end, optical networks employ high sensitivity photodetectors together with adequate amplification and electrical processing to

provide the best recovery of the transmitted data.

Optical multiplexing

The bandwidth of a transmission medium can be more effectively used by means of multiplexing techniques. This also applies for optical communications. One method of optical multiplexing is optical time division multiplexing (OTDM). The principle of OTDM is based on the bit interleaving of N independent RZ (return-to-zero) format channels operating at a certain bitrate. The aggregate data rate is equal to N times the data rate of each of the tributary channels. Another common multiplexing technique is wavelength division multiplexing (WDM). In WDM channels on different wavelengths are multiplexed into a single optical fiber. In this way the bandwidth of the fiber is more effectively exploited by dividing it into non-overlapping spectral bands. Both WDM and OTDM are interesting techniques for expanding the capacity of optical transmission systems. There are other multiplexing techniques like CDMA (code division multiplex access). The optical networks analyzed in this work use WDM as the optical multiplexing method. We will therefore focus on WDM systems.

Optical add-drop multiplexers

The optical add-drop multiplexer (OADM) performs the function of extracting (drop) and/or inserting (add) wavelengths (carrying an information channel) from an optical link. The schematic diagram of an OADM is presented in Fig. 3.1. The OADM in Fig. 3.1 allows extraction and insertion of different information channels using the same wavelength carrier (at wavelength λ_4) while the remaining multiplexed channels are left unaltered. OADMs enhance the flexibility of optical networks. There are other functionalities that may be performed by OADMs, e.g., signal routing, dispersion accommodation, processing of optical channel layer information, and optical signal monitoring, etc. If wavelength conversion is also used, then more advanced functionalities like cross-connecting can also be performed by an OADM [19].

Optical cross-connects

Optical cross-connects are an essential element of future optical networks, enabling high speed data switching and network flexibility. An optical cross-connect will perform functionalities like: signal demultiplexing, (non)blocking switching, signal equalization and amplification, add-drop functionalities, and wavelength conversion. Roughly speaking, optical cross-connects are intended to perform the same function as that of electronic digital switches in telephone networks. A schematic diagram of such an optical cross-connect is given in Fig. 3.2. There are other possible configurations for OXC like the one investigated in the MWTN project [10].

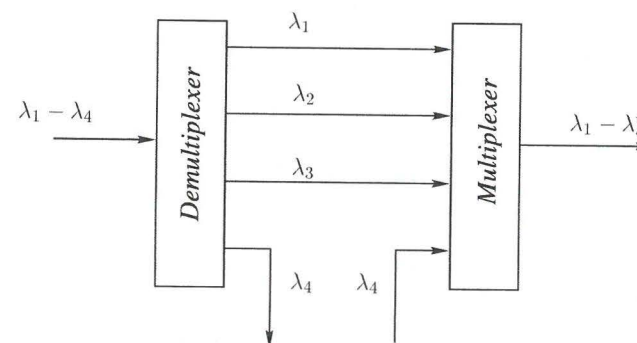


Figure 3.1: Optical add-drop multiplexer. The signals carried by λ_4^* are different from those carried by λ_4 .

Network management

Network management is an important aspect of all-optical networking. The area of management for the all-optical networks has received much attention and is full of research challenges. New techniques for effective and low cost parameter monitoring are under development [20–22]. Management strategies are also being considered and evaluated by several researchers [23]. Monitoring and management of all-optical networks is also a matter of discussion in standardization bodies [24, 25].

3.2 Evolution path towards all-optical networking

WDM point-to-point systems

Wavelength division multiplexing is already being introduced for point-to-point transmission. WDM technology is the preferred choice for upgrading fiber transmission systems to higher capacities. Figure 3.3 schematically presents a WDM point-to-point system. In a WDM point-to-point system, signals originating from different destinations (possibly, with different data formats) are fed into an optical transponder where each signal is now emitted on a different wavelength. After multiplexing, all the channels are coupled into the fiber for transmission. Erbium-doped fiber amplifiers (EDFA) are used to boost the signal (all wavelengths simultaneously). EDFAs are also used as in-line amplifiers to compensate for fiber loss and as preamplifiers for receiver sensitivity enhancement. At the receiver end, the signals are demultiplexed and subsequently converted to the electrical domain.

WDM transmission, together with the use of EDFAs (which allow for multichannel amplification) significantly increase the capacity of long-distance communication systems.

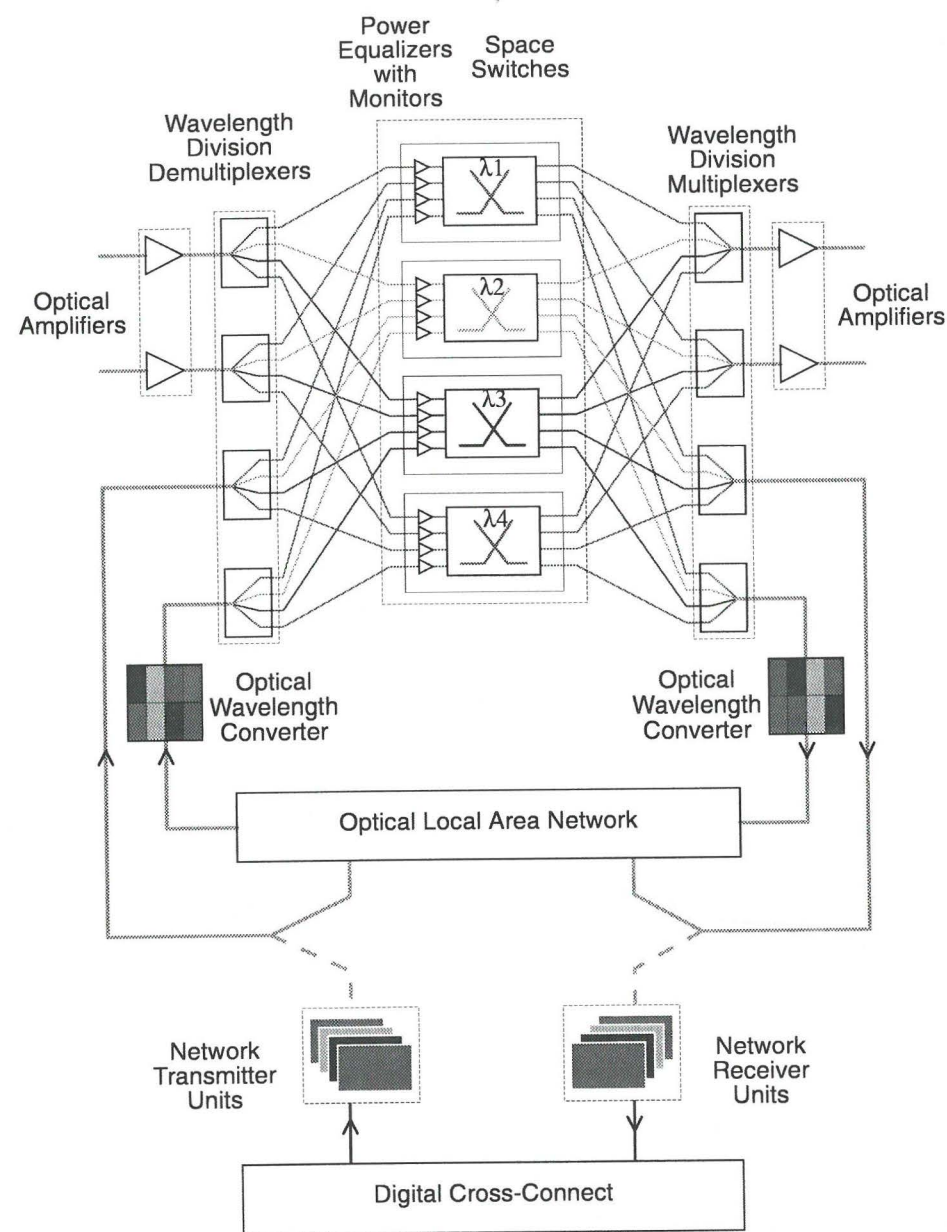


Figure 3.2: Schematic diagram of an optical cross-connect.

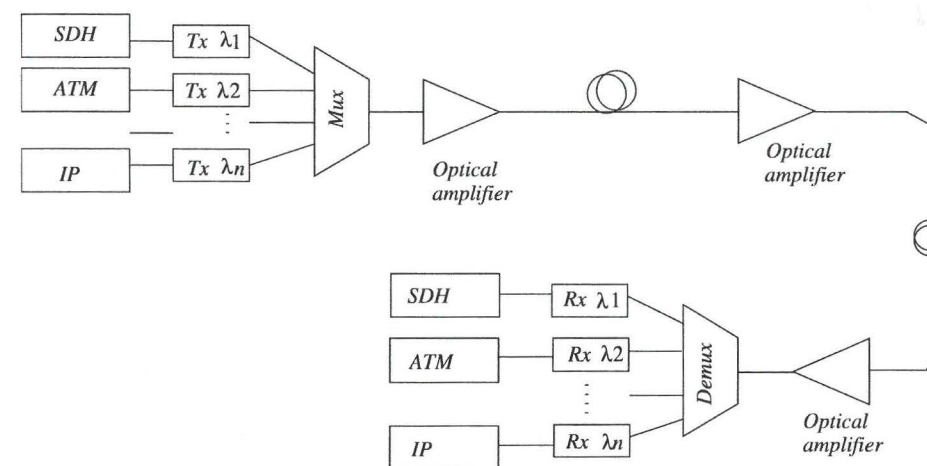


Figure 3.3: WDM point-to-point transmission system.

All-optical Networks

The structure of a telecommunication transport networks is usually divided in three levels: national, regional, and local (see Fig. 3.4). Operations like as signal routing and switching are performed in the electrical domain in each node. With the increase of transmission rates in the optical links, the nodes will be more likely to become electronic bottlenecks. In order to overcome the speed limitations of electronic switching, optical cross-connects (OXC) using fast photonic switching have been proposed. If the nodes in the present optical transport networks (see Fig. 3.4) are replaced by OXCs, and moreover with the use of transmission techniques such as WDM and optical TDM, we will then have an optical transport network supporting high bit rates, flexibility and reliable information transmission entirely in the optical domain. By using this approach transparency with respect to transmission hierarchy or different code formats can be achieved while using a common physical layer like optical fibers and nodes. This scenario is what is referred to as all-optical networking.

The evolution path from the present point-to-point WDM system to all-optical networks is a much discussed topic. There are different visions, interpretations, assumptions and opinions on the subject. However, it is expected that the introduction of all-optical networking into the telecommunication structure will take place in stages. It is expected that WDM technology will soon make an entrance in broadcast and select networks such as LANs and MANs. In wavelength routed networks the most visible first step is the implementation of optical self-healing rings. Next, cross-connected networks may follow, with all the above-mentioned properties and functionalities.

Obviously, before introduction, all-optical networking will have to offer attractive cost levels for delivering bandwidth and services. Furthermore, the all-optical networking enabling technology has to prove reliable and futureproof.

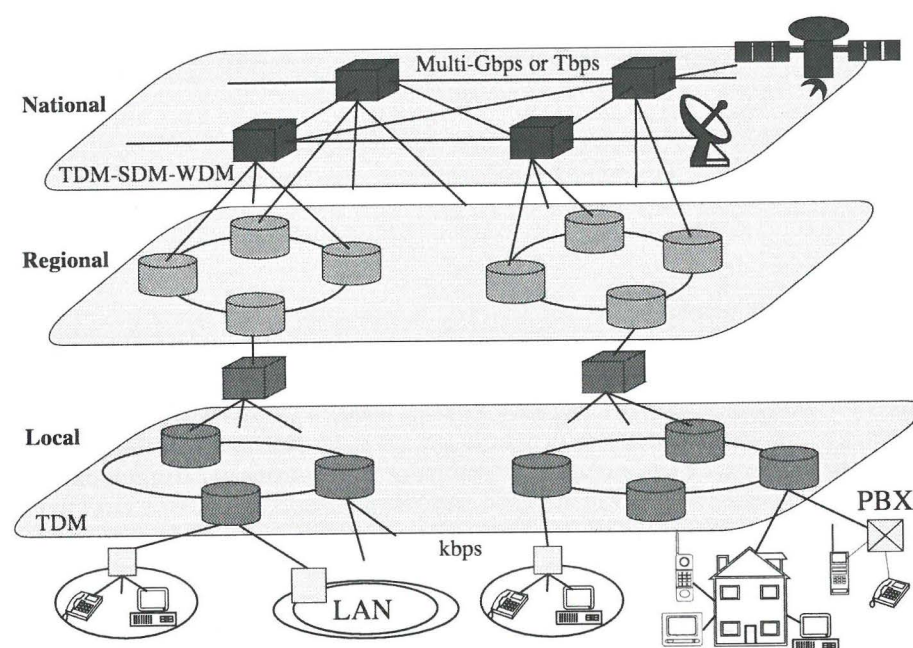


Figure 3.4: Structure of a telecommunication transport network.

3.3 Enabling technologies

The successful implementation of all-optical networks lies in the performance of critical components. The building blocks of the all-optical networks include tunable and multi-channel sources, tunable and multichannel receivers, optical amplifiers, dispersion compensation, wavelength (de)multiplexers, switches, circulators, isolators, and other devices. Researchers in the area have explored different technologies and materials for the fabrication of key optical components. Recently, important advances have been made in the development of components for routing and switching, and in photonic integration of optical cross-connects [15, 26]. An introduction to some basic components for WDM networks is presented in [27]. Below we present a short description of the main technologies that enable all-optical networking.

Light sources and receivers

Light sources for WDM systems can be divided into fixed wavelengths and tunable types. In the first class, there is a commercial available solution, namely, a set of DFB laser diodes with fixed wavelengths. Tunability is a desirable property for light sources. Tunability allows a laser to operate in different channels in a potentially very wide range of wavelengths. Intensive research is being done to develop wavelength tunable laser diodes. A review on tunable laser diodes is given in [28]. The integration of multi-wavelength transmitters is reviewed in [29]. The integration of multi-wavelength receivers has recently received much attention [17]. For example, one technical approach is based on a PHASAR (phased array) demultiplexer in InP with monolithically integrated pin photodetectors. This work is part of the ACTS research project APEX.

Optical amplifiers

Optical amplifiers allow for the direct amplification of light, without the need for optical-to-electrical conversion. Two main types of optical amplifiers are developed for used in telecommunications, namely the erbium-doped fiber amplifier (EDFA), based on silica fiber, and semiconductor optical amplifiers (SOA). The EDFA, in particular, has proved to be a key component enabling the development of optical networks. Optical amplifiers compensate for losses, allow for multichannel amplification, and they are transparent to signal format and bit-rate. Optical amplifiers provide high gain over wide bandwidth (approximately 4 THz).

EDFAs operate at the wavelength region of 1550 nm. At present, research is being done on the possibility of extending the wavelength amplification region to 1330 nm and 1600 nm. The reason is to provide amplification for a larger number of channels, thus lifting the capacity restrictions imposed by the limited amplification window. Three rare-earth materials are currently being studied as potential dopants for 1300-nm amplification: praseodymium, dysprosium, and neodymium [30]. The 1600-nm wavelength region is expected to be exploited by the use of Raman amplifiers.

Semiconductor amplifiers have demonstrated good performance in the wavelength region of 1300 nm. In WDM networking SOAs have been applied in the fabrication of devices for

	Filter shape	Temperature dependence	$d\$/d\lambda$	$ddB/d\lambda$
Fiber Bragg grating	Excellent	High ($\approx 10\text{pm}/^\circ\text{C}$) ₂	High	Medium ₄
Dielectric filter	Very good	Low ($\approx 1\text{pm}/^\circ\text{C}$)	High ₃	High
Arrayed waveguide	OK ₁	High ($\approx 10\text{pm}/^\circ\text{C}$)	Low	Low

Table 3.1: (De)multiplexing performance comparison (From [33]). (1) Can be improved. (2) Needs temperature control. (3) Allows incremental upgrade. (4) Depends on design. $d\$/d\lambda$: Dependence of cost on wavelength count.

wavelength conversion and optical switching. SOAs have proved to be a key component for the upgrade of the 1310-nm transmission systems [31].

Dense WDM (de)multiplexer

Wavelength multiplexing allows for a more efficient way of exploiting the vast bandwidth of the optical fiber. There are three main options of technology for WDM (de)multiplexing. First, we have dielectric filters, based on the interference effect created by a stack of thin film layers deposited on a glass substrate. This type of filters appears to have low temperature dependence, low loss and to be cost-efficient for a number of channels, approximately up to 16 channels.

Second, there is the arrayed waveguide grating (AWG) or PHASAR. PHASAR demultiplexers are based on the interference effect between different waveguides of progressively longer optical path lengths. Signals of different wavelengths coming into an input port will be routed to a different output port. PHASARs have proven suitable for (de)multiplexing large numbers of wavelengths. A PHASAR with $N \times N$ number of inputs-output ports can manage a maximum of N^2 connections. It is an integrated device and has the potential of being produced at low cost and with improved characteristics, like a flatter filter shape and low losses. A review of PHASAR technology for WDM applications is found in [32]. The third technology is based on fiber Bragg gratings (FBG). (De)multiplexers made from FBG exhibit excellent filter shapes. However, manufacturing complications are encountered when the number of wavelengths increases, and with temperature dependence. In Table 3.1 a comparison of the three main options is presented.

Optical switching

Optical switching has been demonstrated using different technologies. Switches can be grouped into three main types. First, we have opto-mechanical switches. These devices are characterized by low crosstalk and low insertion loss. However, they are bulky and slow compared to other alternatives. There are also micro-mechanical structures promising good performance and small dimensions [34, 35].

Second, there are thermo-optic switches. The switching operation relies on the change of refraction index with temperature. They are usually based on waveguides made in polymers or silica. They are relatively slow.

The third type of switches are electro-optics switches. Their operation is based on the change of the refractive index by an electric field. These devices are usually LiNbO_3 based, and therefore they are intrinsically suitable for high-speed operation and integration [36].

Wavelength conversion

Wavelength conversion will enhance the flexibility of optical networks. Wavelength translation is attractive for failure recovery and network reconfiguration. Wavelength conversion is also an important tool in the realization of optical packet switching [26]. In the mean time, research is underway to clarify the benefits of wavelength conversion (allocation) in all-optical networks. There are different technologies to realize wavelength conversion. These include opto-electronic conversion, laser converters, coherent converter (four-wave mixing based), and converters based on controlled optical gates. For a detailed presentation of these technologies we refer to [37].

Photonic integration

Integrated optics has been identified as key enabler for WDM all-optical networks. Photonic integration promises to provide compact devices and modules, needed to build reconfigurable all-optical networks of high-performance and reliability. Integration also has the prospect of delivering modules and devices at low cost. There are already photonic integrated circuit (PIC) implementations of add/drop (de)multiplexers, and cross-connects [15]. However, these devices still suffer from several performance limitations like inband crosstalk. Further research efforts are being directed towards improved realizations of PICs.

3.4 Performance limitations in optical networks

The building blocks for all-optical networks may suffer from performance imperfections. They may also have inherent noise sources that will limit the reach and/or performance of all-optical networks. We will briefly discuss the most common and known limitations. One of these impairments is linear optical crosstalk. The study of crosstalk and ways to mitigate its effects is the subject of Chapter 6 of this thesis.

Optical amplifiers

Optical amplifiers (EDFA and semiconductor) are used to compensate for fiber and component losses. The gain spectrum of the EDFA is not flat over the amplification bandwidth. This may cause irregular gain levels for channels at different wavelengths, which translates into unwanted power fluctuations. Different techniques to avoid this problems have been proposed. These include equalizing filters, host glasses with flatter spectra, and hybrid amplifiers [38]. The inherent amplified spontaneous emission accumulates in a cascade

of amplifiers and represents a scalability limiting factor. Therefore, special gain management techniques should be considered when designing optical systems with cascaded amplifiers [10].

Fiber Nonlinearities

When the intensity of the propagating signals in a fiber is sufficiently high, nonlinear effects may occur. Nonlinearities in a fiber may result in crosstalk, distortion, and attenuation. Nonlinearities are potential limits on the maximum power per channel, channel spacing, and maximum bit-rate.

The two principal nonlinear effects are Four-Wave Mixing (FWM), characterized by the generation of third harmonics, and Stimulated Raman Scattering (SRS), the transfer of power from shorter-wavelength channels to the higher wavelength channels. FWM can be reduced by allowing a certain amount of dispersion to destroy the phase relationship between inter-modulation products. For SRS there is no known reduction method yet. The study of nonlinearities in optical transmission systems is a complex task. We refer to a recently published book [39], where a detailed treatment of the subject is given.

Dispersion in fiber

Dispersion introduces time broadening of a pulse as it propagates along a fiber. Dispersion may lead to intersymbol interference and imposes a limit on the maximum transmission rate. Dispersion in single mode fibers is composed of chromatic and waveguide dispersion. The former is related to fact that the refractive index of a fiber is a function of the wavelength. The latter is related to the waveguide characteristics such as the indices and the particular structure of the fiber core and cladding.

There are different techniques to deal with fiber dispersion. This ranges from dispersion shifted fibers, mid-span compensation, coding, modulation schemes to electronic equalization. A review of dispersion compensating techniques is presented in [40].

Polarization effects

If the optical fiber is slightly birefringent, the two polarization states of the signal will have different propagation velocity along the fiber. This will cause pulse broadening. This effect is known as polarization mode dispersion (PMD).

PMD causes signal distortion which translates into receiver sensitivity penalties. PMD seems to be a potential limitation to multi-gigabit transmission. Different compensation schemes for PMD have been studied by workers in the field. The most promising technique appears to be adaptive compensation of first order PMD. A review on polarization mode dispersion effects on optical communication systems is given in [41].

Many components used in WDM systems exhibit varying degrees of polarization dependence. The polarization dependent loss (PDL) is defined as the difference in loss between the lowest and highest loss polarization state entering an optical element. In long systems PDL may give rise to systems power fluctuation or fading.

In an EDFA a polarization hole burning effect may take place that depends on the amplifier

saturation. The effect is called polarization dependent gain (PDG). PDG gain favors ASE noise polarized orthogonal to the signal, thus resulting in a signal-to-noise ratio degradation. There are various techniques to mitigate this problem, based on polarization scrambling of the signal and/or depolarizing of the pump source [42, 43].

Component tolerance and aging

Optical components may have a small drift in their parameter values. The parameter values may change with temperature and age. This means that the overall system performance changes in time and degrades with age. Therefore systems are designed with extra margin and tolerance towards nominal parameter deviation at the time of initial installation. There are techniques like noise loading to measure the required margins in an optical communication system [44].

Optical crosstalk

Power leakage from other channels, at the same or different nominal wavelength carrier as the signal channel, is referred to as crosstalk. This phenomenon has proved to be a serious limitation in all-optical networking. The first mechanism of crosstalk is a nonlinear effect (FWM or SRS as mentioned in a previous section) that can occur if the optical power in the fiber is sufficiently high. The second mechanism is linear power leakage due to imperfect crosstalk isolation of optical devices like switching fabrics and (de)multiplexers. Linear crosstalk can be classified as inband or interband crosstalk, depending on whether it has the same nominal wavelength as the desired signal or not. The effect of interband crosstalk can be reduced by concatenating narrow-bandwidth optical filters. Inband crosstalk, however, cannot be removed as the signal and the crosstalk operates at the same wavelength. The detrimental effect of inband crosstalk is further intensified in cascaded optical nodes due to its accumulative behavior. A further classification can be made regarding whether the interferometric delay time is shorter or longer than the light source coherence time; coherent and incoherent crosstalk, respectively. It should be noted that there are differences in terminology and denomination in the literature when referring to different types of crosstalk. Chapter 6 of this thesis studies the effect of inband crosstalk on the performance of optical systems in detail.

3.5 Further reading

An introduction is given in [45] on lightwave communication, which presents a mathematical approach to the performance analysis of optical communication systems from the signal theory point of view. Fiber communication systems and the physics of their comprising components are comprehensively explained in [46]. An introduction to optical networks is given in [47]. Systems and technologies related to high capacity transmission are excellently explained in [40]. Recent developments in optical networks and WDM technologies are presented in [12, 14, 48, 49].

Chapter 4

Phase Noise Analysis

Phase noise is known to afflict a number of communication systems. For instance, coherent and weakly optical coherent systems are sensitive to laser phase noise; see e.g., [50, 51]. Optical phase locked loops [45] and analog optical links are also reported to be influenced by laser phase noise [52]. The performance of multi-carrier orthogonal frequency division multiplexing systems is also affected by phase noise generated by oscillators [53, 54]. In general, phase noise impairs a wide range of communication systems that use oscillators as signal sources [55]. The statistical analysis of phase noise is a complex task. Different approaches have been applied. Several approximation to the statistics have been introduced [50, 51, 56]. The authors in [57, 58] use a moment characterization, numerical methods are used in [59], while in [50] simulation techniques are applied. Firstly, this chapter presents a performance analysis for optical heterodyne receivers in the presence of phase noise. Secondly, a recursive formula is derived for the statistical moments of phase noise.

4.1 Phase noise model

Light from a laser suffers from phase uncertainty or the so-called phase noise. It is caused by the intrinsic process of spontaneous emission of photons in a laser cavity. The complex baseband model for an optical field signal is

$$S(t) = Ae^{j[2\pi f + \phi(t) + \phi_0]}, \quad (4.1)$$

where f is the optical frequency, A is the amplitude, and ϕ_0 is the initial phase value. The phase noise is denoted by $\phi(t)$. Laser phase noise is modeled as a continuous Brownian motion (Wiener process) [60] defined by

$$\phi(t) = 2\pi \int_0^t n(s) ds, \quad (4.2)$$

where $n(s)$ is a zero mean white Gaussian noise process. The power spectral density of the optical laser signal turns out to be the so called Lorentzian spectrum [60]. The process $\phi(t)$ is Gaussian distributed with zero mean and with a variance

$$\sigma_\phi^2 = \text{Var}\{\phi(t)\} = 2\pi\Delta\nu t,$$

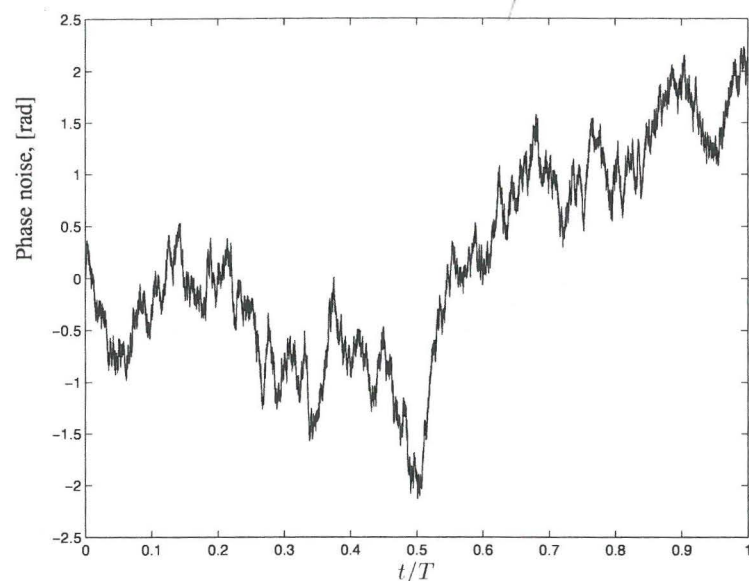


Figure 4.1: A realization of phase noise up to time T .

where $\Delta\nu$ is the 3-dB Lorentzian laser linewidth (or oscillator linewidth). Figure 4.1 presents a realization of a phase noise process, up to time T , with a given value of the parameter $\beta = 2\pi\Delta\nu$.

4.2 Phase noise in optical system

Consider the stochastic process

$$z = \int_0^t e^{j\phi(\tau)} d\tau, \quad (4.3)$$

with $\phi(\tau)$ as defined in (4.2). This process represents baseband filtering of a phase noise that may originate from a laser source. The performance evaluation of a number of optical communication systems is mainly reduced to the problem of statistically describing the complex process z in (4.3) [50].

Paper A presents a direct and efficient method for evaluating the error probability of optical heterodyne receivers in the presence of phase noise. The analysis is based on a power series expansion of the filtered phase noise. The error probabilities are computed by the saddle-point approximation which uses the moment generating function of the decision variable. The optimal pre-filter bandwidth for best phase noise rejection is easily determined.

In paper B a recursive formula for the moments of filtered phase noise is presented. In fact, the recursion is valid for any integral of a properly chosen function of Brownian motion.

It also gives the moments for any arbitrary starting value. Approximate probability density functions can be found through a maximum entropy approach or an orthogonal polynomial series expansion. Moments may also be used for the calculation of error probabilities by Gaussian quadrature rules [61].

Paper A

Error Probability Evaluation of Optical Systems Disturbed by Phase Noise and Additive Noise

Göran Einarsson, Johan Strandberg, Idelfonso Tafur Monroy

© 1995 IEEE. Reprinted, with permission, from *IEEE/OSA J. Lightwave Technol.*, Vol. 13, No. 9, pp. 1847-1852, September 1995.

Error Probability Evaluation of Optical Systems Disturbed by Phase Noise and Additive Noise

Göran Einarsson, Member, IEEE, Johan Strandberg, and Idelfonso Tafur Monroy

Abstract—A direct and efficient method for evaluation of the error probability of optical heterodyne receivers in the presence of phase noise is presented. A closed form expression for the statistics of the decision variable, including photodetector shot noise and thermal noise from electronic circuitry, is derived. The analysis assumes simple integrating filters in the receiver and is based on a power series expansion of the filtered phase noise. The error probability is calculated using a saddle point approximation which is numerically simple and gives accurate results. The optimal prefilter bandwidth for best phase noise rejection is easily determined.

I. INTRODUCTION

THE DECISION variable, in complex signal notation, of a heterodyne optical system with an envelope detector receiver has the form

$$|V|^2 = |\mathcal{Y} + X|^2 \quad (1)$$

where \mathcal{Y} represents phase noise and X additive noise. The phase noise is produced by the transmitting and local oscillator lasers. The additive noise X is photodetector shot noise and thermal noise from the electric circuitry. For large local oscillator amplitudes the shot noise can be modeled as additive white Gaussian noise.

To decide on which signal was transmitted the decision variable is compared with a threshold. If the moment generating function (mgf) of the decision variable is known the error probability can easily be determined by the saddle point method. We derive a closed form expression for the mgf of $|V|^2$ in terms of the mgf for $|\mathcal{Y}|^2$ and the result is used to calculate the error probability of different modulation schemes for heterodyne reception.

The results also apply to direct detection systems with optical preamplifier receiver.

II. AMPLITUDE-SHIFT KEYING

A block diagram of a heterodyne receiver for amplitude-shift keying (ASK) is shown in Fig. 1. It contains an envelope detector together with a bandpass prefilter and a lowpass postfilter. We consider binary on-off intensity modulation with rectangular pulses of amplitude A and duration T . When the local oscillator amplitude C is much greater than A the output current from the photodetector can with proper scaling, be

modeled as

$$i(t)/C \approx C/2 + A \cos(\omega_h t + \theta(t)) + n_1(t) \quad (2)$$

where $\theta(t) = \theta_2(t) - \theta_0(t)$ is the difference between the phase noise of the local oscillator and of the transmitting laser and $n_1(t)$ is white Gaussian noise with intensity $N_1 = 1/2$.

To simplify the analysis let the prefilter H_1 be a bandpass integrator operating at the heterodyne frequency. During the data symbol interval the prefilter output is sampled L times at $t = kT'$, $k = 1, 2, \dots, L$, generating a sequence of complex valued stochastic variables

$$V_k = A\mathcal{Y}_k + X_k \quad (3)$$

where

$$\mathcal{Y}_k = \frac{1}{T'} \int_{(k-1)T'}^{kT'} e^{j\theta(t)} dt \quad (4)$$

is filtered phase noise and X_k , filtered white noise, is a complex valued, zero mean Gaussian variable. The quadrature components of X_k have equal variance, in the absence of thermal noise, equal to

$$\sigma^2 = 1/T'. \quad (5)$$

The envelope detector forms the square of the magnitude (absolute value) of V_k . The lowpass postfilter H_2 is assumed to be a discrete time integrator producing the decision variable

$$U = \frac{T'}{2} \sum_{k=1}^L |V_k|^2. \quad (6)$$

The fact that the additive noise is white and Gaussian and that the phase noise $\theta(t)$ is a random walk process with independent increments makes $|V_k|^2$ a sequence of independent and equally distributed random variables.

The probability distribution of U is related in a simple way to the mgf of

$$|V|^2 = |\mathcal{Y} + X|^2 \quad (7)$$

where the factor A and the index k are temporarily omitted.

It is shown in Appendix A that the mgf of $|V|^2$ is

$$\Psi_V(s) = \frac{1}{1 - 2\sigma^2 s} \Psi_{\mathcal{Y}}\left(\frac{s}{1 - 2\sigma^2 s}\right) \quad (8)$$

where

$$\Psi_{\mathcal{Y}}(s) = E\{\exp(|\mathcal{Y}|^2 s)\} \quad (9)$$

is the mgf of the squared envelope $|\mathcal{Y}|^2$.

Manuscript received November 16, 1994; revised May 29, 1995. This work was supported by the Swedish Research Council for Engineering Sciences.

The authors are with the Department of Signals, Sensors and Systems, Royal Institute of Technology, S-100 44 Stockholm, Sweden.

IEEE Log Number 9413654.

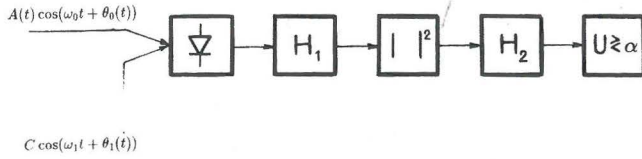


Fig. 1. Heterodyne ASK receiver with envelope detector. The predetector filter H_1 is a bandpass filter at the heterodyne frequency and the postdetector filter H_2 is a lowpass filter.

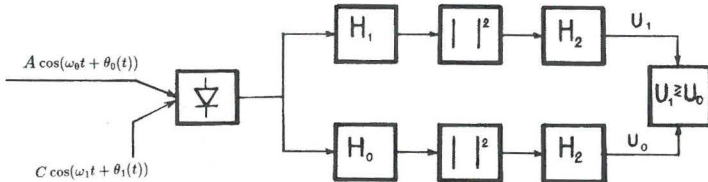


Fig. 2. Heterodyne FSK receiver with envelope detectors. The predetector filters H_1 and H_0 are bandpass filters at the heterodyne frequencies representing data symbols "one" and "zero," respectively. The postdetector filters H_2 are lowpass filters.

The phase noise is a continuous Brownian motion (Wiener-Lévy) process with Gaussian statistics. The primary statistical properties of $\theta(t)$ are easily specified but the probability distribution of $|\mathcal{Y}|^2$ is difficult to determine. A closed form approximate result is obtained by expanding the integrand $e^{j\theta(t)}$ in (4) in a Taylor series and keeping the first terms, [1]

$$\mathcal{Y} \approx \hat{\mathcal{Y}} = 1 - \frac{1}{2T'} \int_0^{T'} \theta^2(t) dt + \frac{j}{T'} \int_0^{T'} \theta(t) dt \quad (10)$$

where the index k is dropped since all \mathcal{Y}_k have the same statistics.

The statistical distribution of the approximate variable $\hat{\mathcal{Y}}$ has been determined by Foschini and Vannucci [1]. The mgf of $|\hat{\mathcal{Y}}|^2$ is

$$\Psi_{\hat{\mathcal{Y}}}(s) = \exp(s) [\sinh \sqrt{2\beta's}]^{-1/2} \quad (11)$$

where "sinh" denotes the hyperbolic sinc-function

$$\sinh x = \frac{\sinh x}{x} = \frac{e^x - e^{-x}}{2x} \quad (12)$$

The parameter $\beta' = 2\pi B_L T'$ is equal to 2π times the product of B_L and the integration interval T' with B_L the sum of the 3-dB linewidths of the lasers at the transmitter and the local oscillator.

Substitution of (11) into (8) gives a useful approximate expression for the mgf of $|V_k|^2$. Including the factor A the result is

$$\Psi_V(s) = \frac{1}{1-2\sigma^2 s} \exp\left(\frac{A^2 s}{1-2\sigma^2 s}\right) \times \left[\sinh \sqrt{\frac{2\beta' A^2 s}{1-2\sigma^2 s}} \right]^{-1/2} \quad (13)$$

The decision variable (6) is the sum of L equally distributed independent variables $|V_k|^2$ and the mgf of U is (14) with s

replaced by $sT'/2$ and raised to the power L . From (5) follows that $\sigma^2 T' = 1$ and

$$\begin{aligned} \Psi_U(s) &= [\Psi_V(sT'/2)]^L \\ &= \frac{1}{(1-s)^L} \exp\left(\frac{m_1 s}{1-s}\right) \left[\sinh \sqrt{\frac{2\beta m_1 s}{(1-s)L^2}} \right]^{-L/2} \end{aligned} \quad (14)$$

where

$$\beta = 2\pi B_L T \quad (15)$$

and the parameter $m_1 = A^2 T'/2 = A^2 L T'/2$ is the expected number of photoelectrons in the received optical pulse.

The error probability is easy to calculate from $\Psi_U(s)$ using the saddle point approximation as outlined in Appendix B. The procedure includes determination of the optimal receiver threshold minimizing P_e .

The result is shown in Fig. 4 for various values of the phase noise parameter $B_L T$. The values of L indicated in the diagram are those resulting in the lowest P_e .

The prefilter bandwidth is proportional to $B' = 1/T'$ and $L = T/T' = B'/B$ is a measure of the magnitude of B' relative to the rate or bandwidth B of the data signal.

A. Frequency-Shift Keying

Frequency-Shift Keying (FSK) is readily analyzed utilizing the results from ASK since each branch of the FSK receiver in Fig. 2 is equal to an ASK receiver of Fig. 1.

Assume that the signal corresponding to the upper branch is transmitted. The stochastic variable obtained by sampling the postfilter in the upper branch of Fig. 2 is then equal to (6)

$$U_1 = T' \sum_{k=1}^L |A\mathcal{Y}_k + X_{1k}|^2 \quad (16)$$

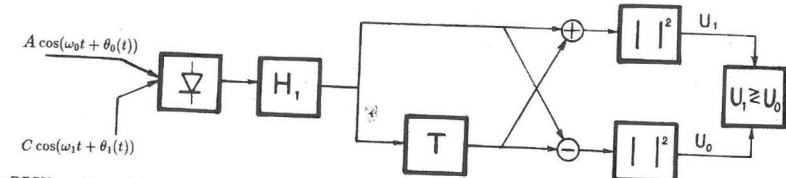


Fig. 3. Heterodyne DPSK receiver with envelope detector. The predetector filter H_1 is a bandpass filter at the heterodyne frequency.

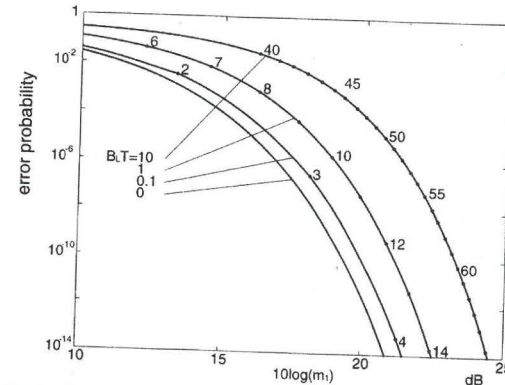


Fig. 4. Bit error probability for heterodyne ASK (on-off modulation) with envelope detector receiver calculated from the Taylor expansion of the filtered phase noise for various values of $B_L T$. The optimal prefilter bandwidth parameter L is indicated along the curves. The parameter m_1 is the expected number of photoelectrons in the received "on" pulse.

The output of the lower branch is noise only

$$U_0 = T' \sum_{k=1}^L |X_{0k}|^2 \quad (17)$$

It has a (central) chi-square distribution with $2L$ degrees of freedom and its mgf is equal to (15) with $m = 0$.

The receiver makes its decisions by comparing U_1 with U_0 or equivalently

$$U = U_1 - U_0 \quad (18)$$

with a zero threshold. The stochastic variable U is the difference between two independent variables and its mgf is the product

$$\Psi_U(s) = \Psi_{U_1}(s) \cdot \Psi_{U_0}(-s). \quad (19)$$

The approximate mgf function of U_1 is equal to (15).

Fig. 5 shows the calculated error probability, using the saddlepoint approximation with the optimal values of L indicated in the diagram. The calculations are simpler than for ASK since the threshold for FSK is fixed.

B. Differential Phase-Shift Keying

In Differential Phase-Shift Keying (DPSK) the phase of the transmitted optical field is modulated and the phase of the previous signal is used as a phase reference in the receiver.

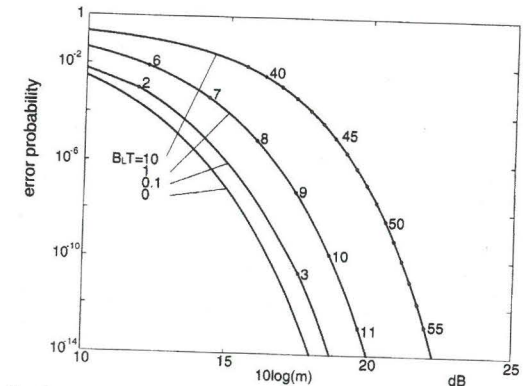


Fig. 5. Bit error probability for heterodyne FSK with envelope detector receiver, calculated from the Taylor expansion of the filtered phase noise for various values of $B_L T$. The optimal prefilter bandwidth parameter L is indicated along the curves. The parameter m is the average number of received photoelectrons per bit.

We consider the case without predetector filtering where $T' = T$ and one sample per signal interval is generated.

The receiver, Fig. 3 has two branches obtained by adding or subtracting the signal and a delayed copy from the previous time interval. The resulting signals V_+ and V_- are analogous to (3)

$$V_{\pm} = b_0 A \mathcal{Y}_1 + X_1 \pm [A \mathcal{Y}_0 + X_0] \quad (20)$$

with

$$\begin{aligned} \mathcal{Y}_1 &= \frac{1}{T} \int_0^T e^{j\theta(t)} dt \\ \mathcal{Y}_0 &= \frac{1}{T} \int_{-T}^0 e^{j\theta(t)} dt \end{aligned} \quad (21)$$

and where $b_0 = e^{j(\phi_1 - \phi_0)} = \pm 1$ represents the transmitted data symbol.

The performance of DPSK does not depend on the start up value of the signal phase and it is convenient to let the phase noise $\theta(t)$ be equal to zero at $t = 0$. The phase noise integrals (21) are then independent and equally distributed stochastic variables. The quantities X_1 and X_0 are filtered shot noise from the photodetector. They are independent, complex valued, zero mean, Gaussian variables with quadrature components of equal variance $\sigma^2 = 2 N_1/T = 1/T$.

DPSK is sensitive to phase noise and we use a first order approximation obtained by keeping the linear term only in a

A saddlepoint approximation for the lower tail is obtained in the same way

$$q_-(\alpha) = \int_{-\infty}^{\alpha} p(x)dx \approx [2\pi\psi''(s_1)]^{-1/2} \exp[\psi(s_1)] \quad (B7)$$

with s_1 equal to the negative root of (B6). The error probability for a specific threshold α is

$$P_e \approx \frac{1}{2}[q_+(\alpha, s_0) + q_-(\alpha, s_1)] \quad (B8)$$

The threshold minimizing (B8) can be obtained by setting the derivative with respect to α equal to zero

$$\frac{dP_e}{d\alpha} = -\frac{1}{2}[s_0q_+(\alpha, s_0) + s_1q_-(\alpha, s_1)] = 0 \quad (B9)$$

The saddlepoint approximation requires the numerical solution of three nonlinear equations, two times (B6) and (B9).

Two terms in the Taylor expansion (B4) are used in the derivation above. The approximation can be improved by including higher-order terms [7] but this is not necessary for ordinary system evaluation at error probability values normally encountered in practice.

ACKNOWLEDGMENT

The authors thank P. J. Smith and G. Jacobsen for helpful discussions on DPSK.

REFERENCES

- [1] G. J. Foschini and G. Vannucci, "Characterizing filtered light waves corrupted by phase noise," *IEEE Trans. Info. Theory*, vol. 34, pp. 1437-1448, Nov. 1988.
- [2] O. K. Tonguz and R. E. Wagner, "Equivalence between preamplified direct detection and heterodyne receivers," *IEEE Photon. Technol. Lett.*, vol. 3, pp. 835-837, Sept. 1991.
- [3] G. Einarsson, *Principles of Lightwave Communications*. Chichester, UK: Wiley, 1995.
- [4] G. J. Foschini, L. J. Greenstein, and G. Vannucci, "Noncoherent detection of coherent lightwave signals corrupted by phase noise," *IEEE Trans. Commun.*, vol. 6, pp. 306-314, Mar. 1988.
- [5] G. Jacobsen and I. Garrett, "The effect of crosstalk and phase noise in multichannel coherent optical DPSK systems with tight IF filtering," *J. Lightwave Tech.*, vol. 9, pp. 1609-1617, Nov. 1991.
- [6] C. P. Kaiser, M. Shafi, and P. J. Smith, "Analysis methods for optical heterodyne DPSK receivers corrupted by laser phase noise," *J. Lightwave Technol.*, vol. 11, pp. 1820-1830, Nov. 1993.

- [7] C. W. Helstrom, "Approximate evaluation of detection probabilities in radar and optical communications," *IEEE Trans. Aerospace Electron. Syst.*, vol. AES-14, pp. 630-640, July 1978.
- [8] C. W. Helstrom, "Performance analysis of optical receivers by the saddlepoint approximation," *IEEE Trans. Commun.*, vol. COM-27, pp. 186-191, Jan. 1979.



Göran Einarsson (S'61-M'64) received the M.S. degree in electrical engineering from the Massachusetts Institute of Technology in 1962, and the Doctorate from the Royal Institute of Technology, Stockholm, Sweden, in 1968. He was with the Long Distance Division of the L. M. Ericsson Corporation, Sweden, from 1953 to 1960 and from 1962 to 1968, working on carrier and PCM systems. From 1960 to 1962 he was with the Research Laboratory of Electronics at M.I.T., engaged in research on multipath communication. During part of 1979 he served as a consultant at Bell Laboratories, Crawford Hill, NJ, USA. From 1969 to 1990 he has been Professor of Communication Theory at the University of Lund, and he now holds the same position at the Royal Institute of Technology, Stockholm, Sweden.



Johan Strandberg was born on July 14, 1963. He graduated from the Royal Institute of Technology, Sweden, in 1991 and has since been engaged in a Ph.D. program at the Division of Telecommunication Theory. His main interests are optical communication theory and the statistical properties of phase noise.



Idelfonso Tafur Monroy was born in El Castillo (Meta), Colombia, in 1968 and graduated from the Bonch-Bruевич Institute of Communications, St. Petersburg, Russia, in 1992, where he received the M.Sc. degree in Multichannel Telecommunications. Since then he has been a graduate student at the Division of Telecommunication Theory of the Royal Institute of Technology, Stockholm, Sweden. His current research interests are in the area of optical communication theory.

Paper B

On a Recursive Formula for the Moments of Phase Noise

Idelfonso Tafur Monroy and Gerard Hooghiemstra

© 1998 IEEE. Reprinted, with permission, from *IEEE Trans. Comm.*, Submitted for publication.

On a recursive formula for the moments of phase noise

Idelfonso Tafur Monroy and Gerard Hooghiemstra

Abstract— In this paper we present a recursive formula for the moments of phase noise in communication systems. The phase noise is modeled using continuous Brownian motion. The recursion is simple and valid for an arbitrary initial phase value. The moments obtained by the recursion are used to calculate approximations to the probability density function of the phase noise, using orthogonal polynomial series expansions and a maximum entropy criterion.

Keywords— Brownian motion, phase noise, optical communication, error analysis, derivation of moments, maximum entropy.

I. INTRODUCTION

Phase noise has proven to be a major performance-limiting factor in a number of communication systems. For example, in optical coherent or weakly coherent systems e.g. [1, 2]. Multicarrier transmission, using orthogonal frequency division multiplexing (OFDM), for instance in wireless indoor systems, is very sensitive to phase noise [3, 4]. Phase noise is also reported to degrade the performance of coherent analog amplitude-modulated wide-band rectifier narrowband (AM-WIRNA) optical links [5], among others. The statistical properties of phase noise (in the context of optical communication systems) have been studied by several authors e.g. [1, 2] and by those authors they are referring to. It is a complex problem for which different types of approximative solutions have been presented (cf. [2]). The authors in [1] use simulation techniques; a characterization through moments has been given by [6] and [7], whereas a numerical approach is given in [8]. The list of references on phase noise analysis cited here is by no means complete but demonstrates the range of different approaches.

From a mathematical point of view, characterizing phase noise is equivalent to the study of the complex-

valued stochastic process (cf. [1]),

$$Z(t) = \int_0^t e^{jB(s)} ds, \quad t \geq 0, \quad (1)$$

where $\{B(s), s \geq 0\}$ is Brownian motion with zero mean and variance

$$\sigma_s^2 = \text{var}(B(s)) = \beta s.$$

The parameter $\beta = 2\pi\Delta\nu$, where $\Delta\nu$ is the Lorentz linewidth of the oscillator (laser linewidth in the case of optical systems).

The process $\{Z(t), t \geq 0\}$ can be decomposed in its real and imaginary part:

$$Z(t) = \int_0^t \cos B(s) ds + j \int_0^t \sin B(s) ds = X(t) + jY(t). \quad (2)$$

We present a recursive formula, expression (8), for the moments of $X(t)$ and $Y(t)$, for fixed $t \geq 0$. The recursion has two advantages over the one given in [6]. It is simpler in form and it is valid for arbitrary initial value $x \in \mathbb{R}$ of Brownian motion $\{B(s), s \geq 0\}$, whereas the recursion of [6] is restricted to the initial value $x = 0$.

We close the section with a definition and some notation. We denote by P_x the probability measure of the Brownian motion starting from $x \in \mathbb{R}$. More specifically for each Borel set A , consisting of continuous functions on $[0, \infty)$,

$$P_x((B(s))_{s \geq 0} \in A) = P((x + B(s))_{s \geq 0} \in A),$$

where $P = P_0$ is the probability measure of Brownian motion $\{B(s), s \geq 0\}$, starting from 0. The symbol E_x is used for the mathematical expectation with respect to the probability measure P_x . Finally, we often write B_s instead of $B(s)$.

II. RECURSIVE FORMULA

We consider the following functional of the Brownian motion:

$$A_t = A_t((B_s)_{s \geq 0}) = \int_0^t f(B_s) ds, \quad t \geq 0, \quad (3)$$

I. Tafur Monroy works at the Eindhoven University of Technology, Telecommunications Technology and Electromagnetics, P. O. Box 513, 5600 MB Eindhoven, The Netherlands

G. Hooghiemstra works at the Delft University of Technology, Faculty of Technical Mathematics and Informatics, Department of Statistics, Probability and Operations Research, P. O. Box 5031, NL- 2600 GA Delft, The Netherlands

where f is a measurable, non-negative function. Moreover for some $\lambda > 0$ the function f should satisfy

$$\int_{-\infty}^{\infty} f(y) e^{-|y|\sqrt{\lambda}} dy < \infty. \quad (4)$$

Denote for fixed t , by $E_x e^{-bA_t}$, $b > 0$, the Laplace-Stieltjes transform of the random variable A_t . We first derive from a simplified form of the Feynman-Kac formula (cf. [9], p. 272) a functional equation for the double Laplace transform:

$$\int_0^{\infty} e^{-\lambda t} E_x e^{-bA_t} dt, \quad \lambda, b > 0,$$

of the random variable A_t . From this functional equation the moment recursion (8), which is surprisingly simple, follows.

Observe that

$$A_t = \int_0^t f(B_s) ds$$

is a so-called additive functional:

$$A_{s+u} - A_s = A_u \circ \theta_s,$$

where θ_s is the shift operator (θ_s maps the set of continuous functions on $[0, \infty)$ on the set of the continuous functions on $[0, \infty)$ and is defined by: $\theta_s(g)(u) = g(s+u)$, where g is a continuous function on $[0, \infty)$). The proof that $\{A_t, t \geq 0\}$ is additive is straightforward:

$$\begin{aligned} A_{s+u} - A_s &= \int_0^{s+u} f(B_v) dv - \int_0^s f(B_v) dv \\ &= \int_s^{s+u} f(B_v) dv = \int_0^u f(B_{s+v}) dv \\ &= \int_0^u f(\theta_s(B_v)) dv = A_u \circ \theta_s, \end{aligned}$$

where it is implicitly assumed that both sides $A_{s+u} - A_s$ and $A_u \circ \theta_s$ are applied to the random continuous function $\{B(v), v \geq 0\}$.

Following ([9], p. 272), we obtain for $\lambda, b > 0$,

$$\begin{aligned} E_x \int_0^{\infty} e^{-\lambda t - bA_t} (e^{bA_t} - 1) dt \\ &= E_x \int_0^{\infty} e^{-\lambda t - bA_t} \left\{ \int_0^t b f(B_s) e^{bA_s} ds \right\} dt \\ &= E_x \int_0^{\infty} e^{-\lambda s} b f(B_s) \left\{ \int_s^{\infty} e^{-\lambda(t-s) - b(A_t - A_s)} dt \right\} ds \\ &= E_x \int_0^{\infty} e^{-\lambda s} b f(B_s) \left\{ \int_0^{\infty} e^{-\lambda u - bA_u \circ \theta_s} du \right\} ds \\ &= E_x \int_0^{\infty} e^{-\lambda s} b f(B_s) E_{B_s} \left\{ \int_0^{\infty} e^{-\lambda u - bA_u} du \right\} ds. \end{aligned} \quad (5)$$

Here the first equality sign follows from:

$$\frac{d}{ds} e^{bA_s} = b f(B_s) e^{bA_s},$$

which implies:

$$\int_0^t b f(B_s) e^{bA_s} ds = e^{bA_t} - 1.$$

Changing the order of integration (this is permitted by Fubini's theorem since the integrand is non-negative) yields the third line. The third equality is justified by a change of variables: $u = t - s$, and by:

$$A_t - A_s = A_{s+u} - A_s = A_u \circ \theta_s,$$

where we use the additivity of the functional $\{A_t, t \geq 0\}$. Finally, the last equality is the (weak) Markov property (see [9] or Freedman [10]): the Brownian motion starts afresh from position B_s .

Define

$$\phi_b(x, \lambda) = \int_0^{\infty} e^{-\lambda t} E_x e^{-bA_t} dt.$$

The left-hand side of (5) can be written as:

$$\begin{aligned} E_x \int_0^{\infty} e^{-\lambda t - bA_t} (e^{bA_t} - 1) dt &= \int_0^{\infty} e^{-\lambda t} dt - \int_0^{\infty} e^{-\lambda t} E_x e^{-bA_t} dt = \\ &= \frac{1}{\lambda} - \phi_b(x, \lambda); \end{aligned}$$

the right-hand side as:

$$\begin{aligned} E_x \int_0^{\infty} e^{-\lambda s} b f(B_s) E_{B_s} \left\{ \int_0^{\infty} e^{-\lambda u - bA_u} du \right\} ds \\ &= \int_0^{\infty} e^{-\lambda s} \int_{-\infty}^{\infty} b f(y) \phi_b(y, \lambda) \frac{e^{-(y-x)^2/2\sigma_s^2}}{\sigma_s \sqrt{2\pi}} ds dy \\ &= b \int_{-\infty}^{\infty} f(y) \phi_b(y, \lambda) \int_0^{\infty} e^{-\lambda s} \frac{e^{-(y-x)^2/2\sigma_s^2}}{\sigma_s \sqrt{2\pi}} dy ds \\ &= b \int_{-\infty}^{\infty} \phi_b(y, \lambda) f(y) \frac{e^{-|y-x|\sqrt{2\lambda/\beta}}}{\sqrt{2\lambda\beta}} dy. \end{aligned}$$

Hence we get the functional equation:

$$\frac{1}{\lambda} - \phi_b(x, \lambda) = b \int_{-\infty}^{\infty} \phi_b(y, \lambda) f(y) \frac{e^{-|y-x|\sqrt{2\lambda/\beta}}}{\sqrt{2\lambda\beta}} dy. \quad (6)$$

By expanding on both sides of (6) the expression e^{-bA_t} in a power series in $b \in (0, 1)$ and comparing the co-

efficients of b^n we obtain:

$$\begin{aligned} \int_0^{\infty} e^{-\lambda t} E_x A_t^n dt \\ &= n \int_{-\infty}^{\infty} f(y) \int_0^{\infty} \frac{e^{-\lambda s - |y-x|\sqrt{2\lambda/\beta}}}{\sqrt{2\lambda\beta}} E_y A_s^{n-1} ds dy. \end{aligned}$$

A recursive formula for $E_x A_t^n$ can be obtained by taking on both sides of the above equation the inverse Laplace transform. Note that the inverse Laplace transform of

$$\frac{e^{-\lambda s - |y-x|\sqrt{2\lambda/\beta}}}{\sqrt{2\lambda\beta}},$$

is equal to:

$$g_{y-x}(t-s) 1(t > s), \quad t \in (0, \infty), \quad (7)$$

where

$$g_a(t) = \frac{1}{\sqrt{2\pi\beta t}} e^{-\frac{a^2}{2\beta t}}.$$

So,

$$\begin{aligned} E_x A_t^n &= n \int_{-\infty}^{\infty} f(y) \int_0^{\infty} g_{y-x}(t-s) 1(t > s) E_y A_s^{n-1} ds dy \\ &= n \int_{-\infty}^{\infty} f(y) \int_0^t \frac{e^{-(y-x)^2/2\beta(t-s)}}{\sqrt{2\pi\beta(t-s)}} E_y A_s^{n-1} ds dy. \end{aligned}$$

This proves the following recursion:

$$E_x A_t^n = n \int_{-\infty}^{\infty} f(y) \int_0^t E_y A_s^{n-1} p(t-s; x, y) ds dy, \quad (8)$$

where

$$\begin{aligned} p(s; x, y) &= P_x(B_s \in dy) / dy \\ &= (2\pi\beta s)^{-1/2} \exp\{-(y-x)^2/2\beta s\}. \end{aligned}$$

The above recursion has two advantages over the recursion given in [6]. It is simpler in form and it gives the moments starting from arbitrary $x \in \mathbb{R}$.

III. APPLICATIONS

We apply (8) to find the moments of

$$X(t) = \int_0^t \cos B_s ds.$$

Note that the cosine can be negative; however, it is not difficult to show that both the functional equation (6) and the recursion (8) also hold for functions that are

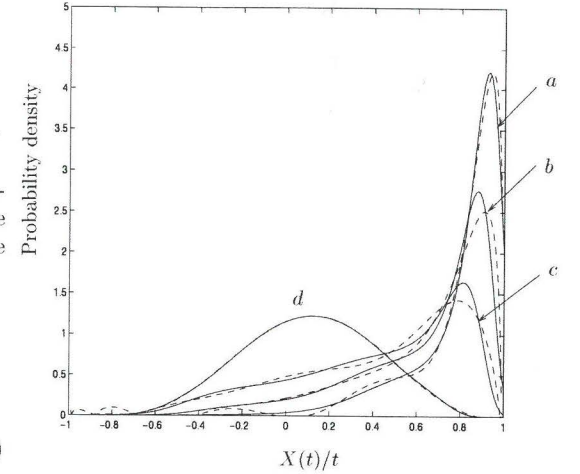


Fig. 1. Probability density of $X(t)/t$. Zero initial value: $x = 0$. Solid lines represent the results by a maximum entropy approach while dashed lines is the Chebyshev polynomial series expansion. a) $\beta t = 1$, b) $\beta t = 2$, c) $\beta t = 4$, d) $\beta t = 18$.

bounded from below and satisfy (4). From $E_y X(t)^0 = 1$, and

$$\operatorname{Re}\left\{ \int_{-\infty}^{\infty} e^{iy} p(t-s; x, y) dy \right\} = \cos x \exp\left\{-\frac{1}{2}\beta(t-s)\right\},$$

we obtain

$$\begin{aligned} E_x X(t) &= \cos x \int_0^t \exp\left\{-\frac{1}{2}\beta(t-s)\right\} ds \\ &= \frac{2 \cos x (1 - e^{-\beta t/2})}{\beta}. \end{aligned} \quad (9)$$

For the second moment we obtain

$$\begin{aligned} E_x X(t)^2 &= \frac{4}{\beta} \int_{-\infty}^{\infty} \cos^2 y \left\{ \int_0^t (1 - e^{-\beta s/2}) p(t-s; x, y) ds \right\} dy \\ &= \frac{2}{\beta} \int_0^t (1 - e^{-\beta s/2}) (1 + e^{-2\beta(t-s)} \cos 2x) ds \\ &= \frac{1}{\beta^2} \{2\beta t - 4 + 4e^{-\beta t/2}\} + \\ &\quad + \frac{\cos 2x}{3\beta^2} \{3 + e^{-2\beta t} - 4e^{-\beta t/2}\}. \end{aligned} \quad (10)$$

The third moment can be expressed in terms involving $\cos x$ and $\cos 3x$:

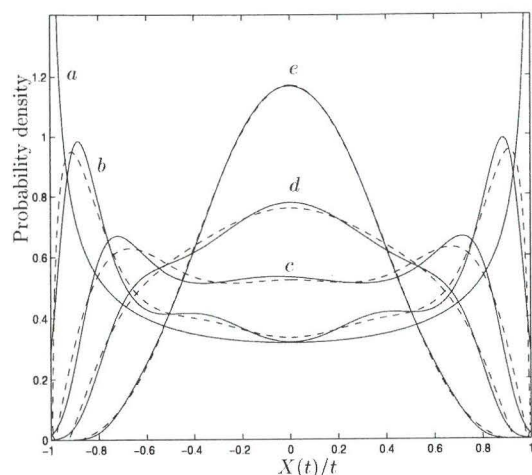


Fig. 2. Probability density of $X(t)/t$. Steady-state regime. Solid lines represent the results by a maximum entropy approach while dashed lines is the Chebyshev polynomial series expansion. a) $\beta t = 0$, b) $\beta t = 1$, c) $\beta t = 4$, d) $\beta t = 8$, e) $\beta t = 18$.

$$E_x X(t)^3 = \frac{\cos x}{3\beta^3} \{136e^{-\beta t/2} - e^{-2\beta t} + 6\beta t(6 + 5e^{-\beta t/2}) - 135\} + \frac{\cos 3x}{30\beta^3} \{6e^{-2\beta t} - 15e^{-\beta t/2} - e^{-9\beta t/2} + 10\}.$$

As the order increases the expressions become more complex. We used a computer program supporting symbolic integration to find the moments up to the fifteenth order.

Based on the moments we used a maximum entropy criterion (cf. [11]) to obtain an approximation for the probability density function (pdf) of $X(t)/t$. We also used a series expansion involving Chebyshev polynomials for comparison. Two cases were treated: (i) zero starting value $x = 0$, and (ii) a random, uniformly distributed on $(-\pi, \pi)$, initial value x (steady-state regime [7]). In Fig. 1 we present the results of the case of zero initial value for different values of βt . The results of the steady-state regime are displayed in Fig. 2. In both figures the solid lines represent calculations with the maximum entropy approach, while the dashed lines represent the Chebyshev polynomial series expansion. Both approaches yield a similar shape of the pdf of $X(t)/t$. However, the maximum entropy approach seems to converge faster than the orthogonal polynomial

representation.

The results for the steady-state regime are found to be in good agreement with previously published results [7]. As one can observe in Fig. 1 and Fig. 2, for large values of βt (what can be considered as strong filtering) the pdf of $X(t)/t$ tends to acquire a Gaussian shape.

IV. CONCLUSIONS

A simple recursive formula for the moments of phase noise, its real and imaginary part is presented. In fact, the recursion is valid for any integral of a function of the Brownian motion provided that the function is measurable, bounded from below, and satisfies (4). The recursion also gives the moments for an arbitrary starting value. Approximative pdf's can be found through a maximum entropy approach or a orthogonal polynomial series expansion. Moments may also be used for the calculation of error probabilities by Gaussian quadrature rules; see [12].

REFERENCES

- [1] G. Foschini and G. Vannucci, "Characterizing filtered light waves corrupted by phase noise," *IEEE Trans. Inform. Theory*, vol. 34, pp. 1437-1448, Nov. 1988.
- [2] I. Garret and G. Jacobsen, "Phase noise in weakly coherent systems," *IEE Proceedings*, vol. 136, pp. 159-165, June 1989.
- [3] T. Pollet, M. van Bladel, and M. Moeneclaey, "BER sensitivity of OFDM systems to carrier frequency offset and Wiener phase noise," *IEEE Trans. Commun.*, vol. 43, pp. 191-193, Feb./March/April 1995.
- [4] L. Tomba, "On the effect of wiener phase noise in OFDM systems," *IEEE Trans. Commun.*, vol. 46, no. 5, pp. 580-583, 1998.
- [5] R. Taylor, V. Poor, and S. Forrest, "Phase noise in coherent analog AM-WIRNA optical links," *J. Lightwave Technol.*, vol. 15, no. 4, pp. 565-575, 1997.
- [6] D. J. Bond, "The statistical properties of phase noise," *Br. Telecom Technol. J.*, vol. 7, pp. 12-17, Oct. 1989.
- [7] G. L. Pierobon and L. Tomba, "Moment characterization of phase noise in coherent optical systems," *J. Lightwave Technol.*, vol. 9, pp. 996-1005, Aug. 1991.
- [8] J. B. Waite and D. S. L. Lettis, "Calculation of the properties of phase noise in coherent optical receivers," *Br. Telecom Technol. J.*, pp. 18-26, Oct. 1989.
- [9] L. C. G. Rogers and D. Williams, *Diffusions, Markov Processes and Martingales*. Wiley, second ed., 1997.
- [10] D. Freedman, *Brownian Motion and Diffusion*. Amsterdam: Holden-Day, 1971. ISBN: 0-8162-3024-2.
- [11] M. Kavehrad and M. Joseph, "Maximum entropy and the method of moments in performance evaluation of digital communications systems," *IEEE Trans. Commun.*, vol. COM-34, pp. 1183-1189, Dec. 1986.
- [12] G. H. Golub and J. H. Welsh, "Calculation of Gaussian quadrature rules," *Math. Comput.*, vol. 23, April 1969.

Chapter 5

Optically Preamplified Direct Detection Receivers

The first results published on light amplification in a glass fiber date back to 1961 [62] and 1964 [63] in papers by Snitzer and Koester, respectively. Early work on fiber amplifiers was also conducted by Letokhov and Pavlik [64]. It is interesting to note that a significant amount of work on fiber amplifiers was already done long before the idea of using optical fibers in telecommunications was discussed by Kao and Hockman in 1966 [1]. In the subsequent years considerable improvements in fiber fabrication, and in semiconductor pump laser technology were of great importance for the development of fiber lasers and amplifiers. In 1985 lasing in a doped fiber was demonstrated [65] and soon after, in 1987, the first erbium-doped fiber amplifier (EDFA) was constructed [3]. Today, the EDFA is a key component in optical fiber links or optical networks. Optical amplifiers are used as boosters, in-line amplifiers (compensating for fiber loss), and preamplifiers. The subject of this chapter originates from the application of EDFAs as preamplifiers in optical communication systems.

5.1 Problem statement

The fundamental components of a preamplified, direct detection receiver are an optical amplifier, an optical filter, a photodetector, an electrical postdetection filter, and a decision circuit. The block diagram of such a receiver is depicted in Fig. 5.1.

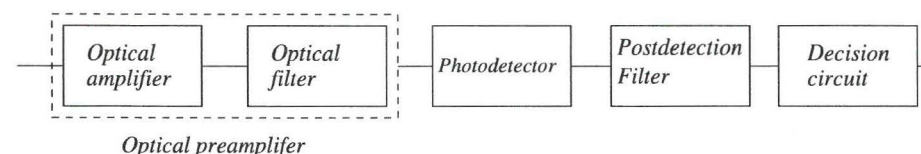


Figure 5.1: Block diagram of an optically preamplified direct detection receiver.

In the receiver under discussion the optical amplifier increases the power level. At the same time, the EDFA generates spontaneous emission noise which is added to the photodetector input signal. Amplified spontaneous emission (ASE) noise is an inherent noise source of the fiber optical amplifier which impairs the receiver performance. At the output of the optical amplifier, the average noise power measured in a bandwidth B is [66]

$$P_0 = n_{sp} h f_0 (G - 1) B \quad \text{Watts} \quad (5.1)$$

where G is the amplifier power gain, f_0 denotes the optical frequency, h is the Planck's constant and n_{sp} is the *spontaneous emission factor*. For available EDFAs the value of G is in the range 20-30 dB. For an ideal amplifier $n_{sp} = 1$ whereas for a practical EDFA $n_{sp} > 1$. The effect of ASE noise can be limited by an optical filter after amplification, but at the same time filtering distorts the optical pulse and introduces intersymbol interference (ISI). In WDM systems optical filters may also be used for the selection of channels. ASE noise and ISI impair the signal detectability, but it is not directly clear how the overall receiver performance is influenced. This fact suggests that there is a tradeoff between ASE noise reduction and ISI and hence it is important to determine the regime of optimum operation.

5.2 Performance analysis

This chapter addresses the performance analysis of optically preamplified, direct detection receivers impaired both by ASE noise and ISI. The question is to determine the statistics of the receiver decision variable, taking into consideration ISI, and to further evaluate the bit-error probability. The statistics are described by the moment generating function (MGF). In this part, closed form expressions for the MGF of the decision variable are derived. This MGF is believed to be new.

Exact expressions for the MGF, including ISI, facilitate the calculation of error probabilities and yield a more complete performance analysis of optically preamplified receivers.

In paper C the case for a receiver with a Fabry-Perot optical filter is studied. A closed form expression for the MGF of the decision variable is presented. Moreover, it is found that there is an optimum relation between the optical filter (Fabry-Perot) bandwidth, bit-rate, and postdetection filtering that results in the lowest error probability for a given received power level. In paper D, an extended study is conducted to show that postdetection electrical equalization results in a better performance. It also shows how the better performance can be achieved, based on a Gaussian approximation for the error rate analysis, for a wide class of optical and postdetection filters.

5.3 Communication theory

Determining the distribution of the output of square envelope receivers with colored Gaussian noise input constitutes a classic problem in communication theory e.g. [67-71]. Although the mathematical formalism for determining the statistics of the output of such receivers is well known, e.g. [67, 69, 71, 72], deriving closed form expressions for the distribution is a complex task. Moreover, if at the input both signal and noise are present, this task becomes even more formidable. For the case of noise only input, expressions for the MGF

and analytical approximations to the probability density function have been reported for several covariance kernels, e.g. [69, 71, 73]. For both signal and noise being present at the input, closed form expressions for the distribution are scarcely documented in the literature. In paper E, closed form expressions for the MGF are derived for the case of an input signal composed of a binary sequence of rectangular pulses. The considered Gaussian processes are: the Wiener process, a Gaussian process with linear covariance (moving average), and the Ornstein-Uhlenbeck process.

The analysis of optically preamplified, OOK direct detection receivers is an example of square envelope detection followed by filtering. This means that the derived MGFs are applicable to the problem of finding the quantum limit for optically preamplified OOK receivers (see paper E).

Comments on paper F

The question of what is the ultimate quantum limit for optically preamplified OOK receivers is the topic of paper F. To find the answer, first, the results presented in the literature for different optically preamplified, OOK/DD receivers are summarized. Subsequently, a receiver scheme is presented that is expected to outperform previously studied configurations.

The quantum limit for an optically preamplified receiver with an ideal bandpass optical filter is 38.4 photons/bit [45]. The result of the analysis in paper F suggests that an optically preamplified receiver can operate with a quantum limit smaller than 38.4 photons/bit. This is an intriguing result as one would expect that any other receiver will have a larger quantum limit than in the case of an ideal optical bandpass filter. The analysis in paper F should be considered as an intermediate presentation rather than a complete and final result. This paper is therefore particularly open for discussion. The validity of the mathematical derivations and the accuracy of the numerical computations still have to be rigorously proved. Work to clarify these issues is in progress.

Paper C

Bit Error Evaluation of Optically Preamplified Direct Detection Receiver with Fabry-Perot Optical Filters

Idelfonso Tafur Monroy and Göran Einarsson

© 1997 IEEE. Reprinted, with permission, from *IEEE/OSA J. Lightwave Technol.*, Vol. 15, No. 8, pp. 1546-1553, Aug. 1997.

Bit Error Evaluation of Optically Preamplified Direct Detection Receivers with Fabry-Perot Optical Filters

Idelfonso Tafur Monroy and Göran Einarsson

Abstract—The error performance of a preamplified, direct detection receiver with an optical filter of the Lorentzian type is studied. The analysis takes into account the influence of the optical intersymbol interference (ISI). A closed-form expression of the moment generating function (MGF) of the decision variable is derived. Error probabilities are evaluated from the MGF using a saddlepoint approximation. The Gaussian approximation is also examined. The detection sensitivity in terms of a quantum limit is calculated. The results show that there exists an optimum optical bandwidth, the reason being a tradeoff between the effect of ISI and the spontaneous emission noise. It is also shown that the Gaussian approximation gives a good estimate of the error probability, allowing to find in a simple manner the optimum parameters of optically preamplified, direct detection receiver.

Index Terms—Error analysis, intersymbol interference, optical amplifiers, optical communication, optical filters, optical receivers.

I. INTRODUCTION

IN optically preamplified direct detection receiver the optical amplifier increases the power levels, but at the same time, the erbium-doped fiber amplifier (EDFA) generates spontaneous emission noise which is added to the photodetector input signal. Amplified spontaneous emission (ASE) noise is an inherent noise source of the fiber optical amplifier which impairs the receiver performance. To limit the effect of ASE, which is a wide band noise source, an optical filter is needed. Filtering, however, can distort the optical pulse and introduces intersymbol interference (ISI). Fabry-Perot filters are widely used in experimental optical transmission systems, e.g., [14]. They are well described by a Lorentzian impulse response [28].

The main question of the performance analysis is to determine the statistics of the receiver decision variable, taking into consideration ISI, and to further evaluate the bit-error probability. Most of the previous analysis of optically preamplified receivers were made under the assumption that the signal passes the optical filter unaltered, which means that the ISI is neglected or the optical filter bandwidth is assumed to be large [1]–[5]. The performance analysis for a receiver with a perfect rectangular bandpass optical filter is documented in [6], [7], and in [8] for a receiver with a traveling-wave semiconductor

optical preamplifier. Ben-Ali *et al.* [25] derived upper bounds on the bit error probability. Chernoff and modified Chernoff bounds together with an improved bound on the bit error probability are presented in [26]. Chinn [27] considered a probability density function (pdf) of the decision variable obtained by convolving individual pdf for a finite number of modes of a Karhunen-Loève expansion of the signal and noise. A Karhunen-Loève expansion approach is also used in [13] for deriving a moment generating function (MGF), but the use of the MGF is limited to finding the first and second moment of the decision variable. These works take into consideration the significance of the ISI, but a closed-form expression of the MGF, (statistics), of the decision variable that explicitly incorporate a Fabry-Perot optical filter is not given.

In this paper, a closed-form expression of the MGF of the decision variable, explicitly incorporating a Fabry-Perot optical filter, is derived. The MGF is then used to calculate bit-error probabilities by the so called saddlepoint approximation (spa). Some previous works have considered the decision variable to be Gaussian distributed [9]–[13]. In this paper the Gaussian approximation, including ISI, is also examined. The results shows that the Gaussian approximation gives a fairly accurate estimate of the error probability of optically preamplified receivers.

This paper is organized as follow: In Section II the reference scheme and the model of the receiver under analysis is presented. The general form of the MGF for the decision variable is derived with the help of a Karhunen-Loève expansion of the signal and noise. The method of deriving the MGF for the decision variable is also presented. In Section III, the expression for the error probability is presented and the saddlepoint approximation is introduced. A closed-form expression of the MGF for the decision variable is given. The performance of the Gaussian approximation is also studied. Numerical results, and comparison with previous work are presented in Section IV. Finally, in Section V, summarizing conclusions are drawn.

II. SYSTEM MODEL

The system under analysis is depicted schematically in Fig. 1. The optical preamplifier (EDFA) is characterized by an optical field amplifier with power gain G , an additive noise source $N(t)$, representing the spontaneous emission and an optical filter with complex equivalent baseband impulse

Manuscript received September 10, 1996; revised April 24, 1997.

I. T. Monroy is with the Electrical Engineering Department, Eindhoven University of Technology, 5600 MB Eindhoven, The Netherlands.

G. Einarsson is with the Department of Signals, Sensors, and Systems, Royal Institute of Technology, Stockholm S-100 44 Sweden.

Publisher Item Identifier S 0733-8724(97)05914-8.

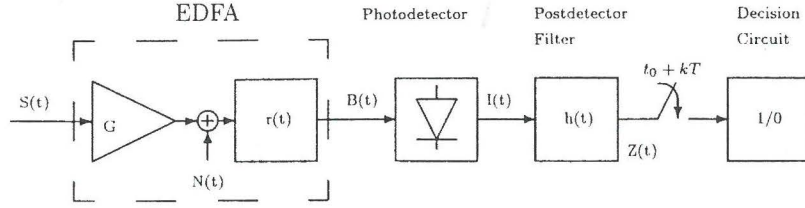


Fig. 1. Complex baseband model of preamplified direct detection receiver.

response $r(t)$. The equivalent baseband form of the optical field at the output of the EDFA is

$$B(t) = [\sqrt{G}S(t) + N(t)] * r(t) \quad (1)$$

where $*$ stands for a convolution operation and $S(t)$ is the envelope (modulation) of the input optical signal $s(t)$, expressed as the real part of a complex field function

$$s(t) = \text{Re} \{ S(t) \exp j\omega t \} \quad (2)$$

where $\omega = 2\pi f$, f being the optical frequency.

The optical field $B(t)$ illuminating the photodetector produces an output shot noise current $I(t)$. The signal at the output of the postdetector filter, with impulse response $h(t)$, is

$$Z(t) = I(t) * h(t).$$

This signal is sampled at $t = t_0 + kT$ time instants to form the decision variable. The decision device derives the estimate of a transmitted bit in a particular bit interval by comparing the decision variable with an optimal, preselected, detection threshold α . By an optimal threshold α is meant the detection threshold that yields the lowest error probability.

To continue further, we introduce some definitions and normalizations. The input signal $S(t)$ is assumed to be a rectangular pulse of duration T . The amplitude of $S(t)$ is chosen (normalized) such as m is the average number of photons contained in $S(t)$. In the sequel, it is assumed that for a transmitted "zero" bit "zero" photons are received. For equally likely symbols "one" and "zero," m is the average number of received photons per bit at the input to the EDFA.

For a given bit pattern $B = (\dots, b_{-1}, b_0, b_1, \dots)$ the normalized information signal at the output of the optical filter is denoted by $Y(t)$

$$Y(t) = \sqrt{G}S(t) * r(t) = \sqrt{\frac{G2m}{T}} \sum_{k=-\infty}^{\infty} b_k g(t - kT) * r(t) \quad (3)$$

$$Y(t) = \sqrt{\frac{G2m}{T}} \left[b_0 l(t) + \sum_{k \neq 0} b_k l(t - kT) \right] \quad (4)$$

where

- $l(t)$ $g(t) * r(t)$;
- b_k statistically independent binary symbols representing a data "zero" and a "one," respectively. $b_k \in \{0, 1\}$;
- m average number of received photons per bit;
- $g(t)$ input unit rectangular pulse of duration T ;

The first term in (4) represents the desired information signal while the last term is the ISI. At the output of the optical amplifier, the average noise power measured in a bandwidth B is [1]

$$P_0 = n_{sp} h f (G - 1) B \quad W$$

where h is the Planck's constant and n_{sp} is the spontaneous emission factor of the amplifier. For reason of compatibility with the normalization of $S(t)$ the density of $N(t)$ should be expressed in photons per second. The photon intensity corresponding to the stochastic optical field $N(t)$ is [35]

$$N_0 = n_{sp}(G - 1) \text{ photons/s.}$$

At the output of the optical filter the real and imaginary parts of the Gaussian noise $X(t) = N(t) * r(t)$ are independent, with mean zero and autocorrelation

$$K(\tau) = \frac{n_{sp}}{2} (G - 1) R(\tau) \quad (5)$$

where [15]

$$R(\tau) = \int_{-\infty}^{\infty} r(t) r^*(t + \tau) dt \quad (6)$$

with $*$ denoting complex conjugate.

With the above notations the optical field at the output of the EDFA becomes

$$B(t) = Y(t) + X(t).$$

The photo-electron intensity is proportional to the square of the optical field (optical power) falling upon the photodetector [28]. It is assumed that the photodetector quantum efficiency η is equal to one, and the optical field is normalized so that the photo-electron intensity is

$$\lambda(t) = |Y(t) + X(t)|^2. \quad (7)$$

The signal $Z(t)$, the postdetection filter $h(t)$ output signal, is a doubly stochastic process: it depends on the information bit pattern and on the stochastic mechanism of photodetection. The mathematical model for $Z(t)$ is the filtered compound Poisson stochastic process [16], [17] whose stochastic intensity is $\lambda(t)$. With no loss of generality we consider a time interval of duration T and denote the decision variable by $Z = Z(t = T)$. Conditioned on the value of $\lambda(t)$ the MGF for Z is [16]

$$M_Z(s) | \lambda = \exp \left(\int_0^T \lambda(\tau) [\exp \{sh(t - \tau)\} - 1] d\tau \right). \quad (8)$$

In this work, we restrict ourselves to a specific type of postdetector filter: the integrate-and-dump filter. The impulse response of the integrate-and-dump filter is given by

$$h(t) = \begin{cases} 1, & 0 \leq t \leq T \\ 0, & \text{otherwise.} \end{cases} \quad (9)$$

Thus, the unconditional MGF of Z is given by

$$M_Z(s) = \int_0^\infty \exp \left\{ \int_0^T \lambda(t) [\exp(s) - 1] dt \right\} p(\lambda) d\lambda \quad (10)$$

$p(\lambda)$ being the probability density function of $\lambda(t)$. In terms of the MGF for Λ

$$M_Z(s) = M_\Lambda(e^s - 1) \quad (11)$$

where

$$\begin{aligned} \Lambda &= \int_0^T \lambda(t) dt \\ &= \int_0^T |Y(t) + X(t)|^2 dt. \end{aligned} \quad (12)$$

Λ is also called the *Poisson parameter function* [16]. The expression (11) appears in an early paper by Personick [19]. The MGF $M_\Lambda(s)$ is given by

$$M_\Lambda(s) = E \{ e^{s\Lambda} \}. \quad (13)$$

We expand $V(t) = Y(t) + X(t)$ in a Karhunen-Loève expansion, in the time interval $[0, T]$, choosing the set of orthonormal functions $\{f_n\}$ such that

$$V(t) = \sum_{n=1}^{\infty} v_n f_n(t) \quad \text{with } v_n = x_n + y_n$$

and

$$\begin{aligned} y_n &= \int_0^T Y(t) f_n^*(t) dt \\ x_n &= \int_0^T X(t) f_n^*(t) dt \end{aligned}$$

with f_n and λ_n being the eigenfunctions and eigenvalues, respectively, related to the following equation [20]:

$$\int_0^T K(t, u) f_n(u) du = \lambda_n f_n(t) \quad 0 \leq t \leq T \quad (14)$$

where $K(t, u) = \frac{1}{2} E \{ X(t) X^*(u) \}$. By Parseval's theorem, the integral (12) becomes

$$\begin{aligned} \Lambda &= \sum_{n=1}^{\infty} |y_n + x_n|^2 \\ &= \sum_{n=1}^{\infty} |v_n|^2. \end{aligned} \quad (15)$$

The coefficients x_n are zero mean Gaussian independent variables whose real and imaginary part (x_{nc} and x_{ns} , respectively) have a variance $\text{Var} \{x_{nc}\} = \text{Var} \{x_{ns}\} = \lambda_n/2$ [20]. We observe that v_n are independent variables with mean

y_n ; hence, the MGF of a particular $|v_n|^2$ is that of a stochastic variable with a noncentral chi-square distribution [15]

$$M_{|v_n|^2}(s) = \frac{1}{1 - \lambda_n s} \exp \left\{ \frac{|y_n|^2 s}{1 - \lambda_n s} \right\}.$$

From (13) and (15), we have that

$$M_\Lambda(s) = \prod_{n=1}^{\infty} E \left\{ e^{s|v_n|^2} \right\}.$$

Thus, the general mathematical form for the MGF of Λ is [18], [19]

$$\begin{aligned} M_\Lambda(s) &= \prod_{n=1}^{\infty} \frac{1}{(1 - \lambda_n s)} \exp \left(\sum_{n=1}^{\infty} \frac{|y_n|^2 s}{1 - \lambda_n s} \right) \\ \text{Re } s &< \frac{1}{\max_n \lambda_n}. \end{aligned} \quad (16)$$

The choice of the integrate-and-dump filter simplifies the analysis, but it yields a suboptimum receiver. An MGF in the form of (16) can also be obtained for a general postdetector filter [25], [36].

The MGF (16) can be represented in terms of the resolvent kernel $h(t, u; s; \tau)$ [21], [24], [30] related to the integral equation

$$\begin{aligned} h(t, u; s; T) - s \int_0^T h(t, v; s; \tau) K(v, u) dv &= K(t, u) \\ 0 \leq (t, u) \leq T \end{aligned} \quad (17)$$

as

$$M_\Lambda(s) = [D(s)]^{-1} \exp [F(s)] \quad (18)$$

where

$$\begin{aligned} F(s) &= m_h s + s^2 \int_0^T \int_0^T Y^*(t) h(t, u; s; T) Y(u) dt du \\ m_h &= \int_0^T |Y(t)|^2 dt \end{aligned} \quad (19)$$

and $D(s)$, also called the Fredholm determinant, is given by [22]

$$D(s) = \exp \left\{ - \int_0^T \int_0^T h(t, t; v; T) dt dv \right\}. \quad (20)$$

The MGF given in the form of (18) is more convenient for numerical computations than the MGF expressed in terms of an infinite product [cf. (16)].

III. ANALYSIS

A. The Error Probability

The error performance analysis is conducted by conditioning on the sent symbol b_0 and considering the finite sequence $\tilde{B} = (b_{-L}, \dots, b_{-1}, b_1, \dots, b_L)$ of symbols surrounding b_0 . Assuming that the symbols $b_0 = 1$ and $b_0 = 0$ are *a priori*

equally probably, the conditional error probability given a sequence \tilde{B} is

$$P_e|\tilde{B} = \frac{1}{2} P_r(Z < \alpha | \tilde{B}|_{b_0=1}) + \frac{1}{2} P_r(Z > \alpha | \tilde{B}|_{b_0=0}) \quad (21)$$

$$P_e|\tilde{B} = \frac{1}{2} \{q_+(\alpha) + q_-(\alpha)\}$$

As it is shown in [31], the tail probability $q_+(\alpha)$ is approximately equal to

$$q_+(\alpha) \approx \frac{\exp[\phi(s_0)]}{\sqrt{2\pi\phi''(s_0)}} \quad (22)$$

the so-called *saddlepoint approximation*. The function $\phi(s)$ is related to the MGF for Z , $M_Z(s)$ by

$$\phi(s) = \ln[M_Z(s)] - s\alpha - \ln|s|. \quad (23)$$

The parameter s_0 is the positive root of the equation

$$\phi'(s) = 0 \quad (24)$$

and $\phi''(s_0)$ stands for the second derivative of (23) at $s = s_0$. The lower probability tail is approximated by

$$q_-(\alpha) \approx \frac{\exp[\phi(s_1)]}{\sqrt{2\pi\phi''(s_1)}} \quad (25)$$

with s_1 equal to the negative root of (24). See [31] or [35] for further details. The error probability is minimized by adjusting the detection threshold α . The optimum value of α and the parameters s_0 and s_1 may be found numerically by solving an appropriate set of equations [35]. The saddlepoint approximation has been proposed by Helstrom [31], as an efficient and numerically simple tool for analyzing communication systems. The saddlepoint approximation has shown a reasonably high degree of accuracy in the analysis of optical communication systems [32]–[34].

The average error probability, for a fixed threshold α , is obtained by averaging the conditional error probability with respect to \tilde{B} with a b_0 given

$$P_e = \frac{1}{2} E_{\tilde{B}}\{P_r(Z < \alpha | \tilde{B}|_{b_0=1})\} + \frac{1}{2} E_{\tilde{B}}\{P_r(Z > \alpha | \tilde{B}|_{b_0=0})\}. \quad (26)$$

The expression (26) is general with respect to the statistics of the transmitted binary message. In this paper, we consider the case in which the message consists of mutually independent binary symbols.

In optical communications, the (standard) *Quantum limit* is defined as the average number of photons per bit in the optical signal $S(t)$ needed to achieve a bit error probability of 10^{-9} assuming ideal detection conditions, which means that $G \gg 1$ and $n_{sp} = 1$.

B. Lorentzian Optical Filter

The normalized Lorentzian filter impulse response is specified by

$$r(t) = \sqrt{2}\mu e^{-\mu|t|} \quad t \geq 0 \quad (27)$$

and consequently the covariance kernel is

$$R(\tau) = \mu e^{-\mu|\tau|} \quad \tau \in \mathbf{R} \quad (28)$$

where $B = \mu/\pi$ is the 3-dB optical filter bandwidth.

The output signal of the EDFA (after the optical filter) is given by

$$Y(t) = \sqrt{\frac{4Gm}{T}} \left[\int_0^t b_0 \mu e^{-\mu\nu} d\nu + \sum_{k=1}^{\infty} b_{-k} \int_{(k-1)T+t}^{kT+t} \mu e^{-\mu\nu} d\nu \right]$$

$$= \sqrt{\frac{4Gm}{T}} \left[b_0(1 - e^{-\mu t}) + \sum_{k=1}^{\infty} b_{-k}(e^{\mu T} - 1)e^{-\mu t} \right].$$

A more concise expression for $Y(t)$ is presented in [25]

$$Y(t) = \sqrt{\frac{4Gm}{T}} [b_0 + \rho e^{-\mu t}] \quad t \in [0, T] \quad (29)$$

in which

$$\rho = (e^{\mu T} - 1) \sum_{k=-\infty}^{-1} b_k e^{\mu k T} - b_0. \quad (30)$$

In order to obtain an expression for the MGF of the type in (18) the resolvent kernel $h(t, u, s; T)$ should be known. For the case of the Lorentzian filter the resolvent kernel is given in the literature, e.g., [20], [30]

$$h(t, u, s; T) = \frac{[h_1 e^{\beta t} + h_2 e^{-\beta t}][h_1 e^{\beta(T-u)} + h_2 e^{-\beta(T-u)}]}{v[h_1^2 e^{\beta T} - h_2^2 e^{-\beta T}]} \quad (31)$$

for $0 \leq t \leq u \leq T$. For $u < t$ the roles of u and t just interchange in (31), in which

$$h_1 = v + 1$$

$$h_2 = v - 1$$

with

$$v = \sqrt{1 - 2\sigma^2 s}$$

$$\beta = v\mu$$

and

$$\sigma^2 = n_{sp}(G - 1).$$

The Fredholm determinant is given by (see the Appendix)

$$D(s) = \frac{(v+1)^2 e^{\beta T} - (v-1)^2 e^{-\beta T}}{4v e^{\mu T}}. \quad (32)$$

The expression for

$$F(s) = m_h s + s^2 F(s)$$

in which

$$F(s) = \int_0^T \int_0^T Y^*(t) h(t, u; s; T) Y(u) dt du$$

turns out to be

$$F(s) = \frac{4mG}{\mu T} [b_0^2 F_1(s) + b_0 \rho F_2(s) + \rho^2 F_3(s)]. \quad (33)$$

The expressions for $F_1(s)$, $F_2(s)$, and $F_3(s)$ are shown in (33a), (33b), and (33c) at the bottom of the next page. The derivation of the above expressions is straightforward but

tedious. In the Appendix a more detailed presentation is given. According to (11) the MGF for the decision variable, Z , is

$$M_Z(s) = M_\Lambda(e^s - 1). \quad (34)$$

The validity of the derived MGF can be tested by considering the following cases: 1) Only noise being present. The MGF for the decision variable is then given only in terms of the Fredholm determinant $D(s)$. We obtain the same result as for the well studied case of detecting purely incoherent light with a Lorentz spectral density, e.g., [21]. 2) If both signal and noise are present, then the mean and variance of the decision variable derived from (36) and those obtained from (37) and (38) are identical, as expected from the properties of the MGF.

C. The Gaussian Approximation

The Gaussian approximation to the error probability $P_e|\tilde{B}$ [cf. (21)] is given by

$$P_e|\tilde{B} = \frac{1}{2} Q\left(\frac{E_1 - \alpha}{\sigma_1}\right) + \frac{1}{2} Q\left(\frac{\alpha - E_0}{\sigma_0}\right) \quad (35)$$

with $E_{0,1}$ and $\sigma_{0,1}^2$ being the mean and the variance of the decision variable for a transmitted binary symbol "zero" and "one," respectively. The function $Q(x)$ is the normalized Gaussian tail probability

$$Q(x) = \frac{1}{\sqrt{2\pi}} \int_x^\infty e^{-s^2/2} ds.$$

If the MGF for Λ is known, the mean E_Λ and variance σ_Λ^2 are given by [15]

$$E_\Lambda = \frac{d[\ln M_\Lambda(s)]}{ds} \Big|_{s=0}$$

$$\sigma_\Lambda^2 = \frac{d^2[\ln M_\Lambda(s)]}{ds^2} \Big|_{s=0} \quad (36)$$

respectively. Alternatively, E_Λ and σ_Λ^2 are also given by the following relations:

$$E_\Lambda = \int_0^T |Y(t)|^2 dt + \int_0^T K(t, t) dt \quad (37)$$

and

$$\sigma_\Lambda^2 = 2 \int_0^T \int_0^T Y(t) Y(u) K(t, u) dt du$$

$$+ \int_0^T \int_0^T K^2(t, u) dt du \quad (38)$$

respectively. The mean and the variance of the decision variable Z are given in term of the mean and the variance

of Λ according to the *Poisson transform* by [29]

$$E_Z = E_\Lambda$$

$$\sigma_Z^2 = E_\Lambda + \sigma_\Lambda^2. \quad (39)$$

For the case of the Lorentzian optical filter the covariance of the noise $X(t)$ is from (28)

$$K(\tau) = K(t - u)$$

$$= \sigma^2 \mu e^{-\mu|\tau|}. \quad (39)$$

The mean of Λ results to be

$$E_\Lambda = 4mG b_0^2 + \frac{8mG}{\mu T} b_0 \rho (1 - e^{-\mu T})$$

$$+ \frac{2mG}{\mu T} \rho^2 (1 - e^{-2\mu T}) + \sigma^2 \mu T \quad (40)$$

and the variance

$$\sigma_\Lambda^2 = \frac{\sigma^4}{2} (2\mu T + e^{-2\mu T} - 1)$$

$$+ \frac{16mG\sigma^2}{\mu T} b_0^2 (e^{-\mu T} + \mu T - 1)$$

$$+ \frac{8mG\sigma^2}{\mu T} \rho b_0 (e^{-2\mu T} - 4e^{-\mu T} - 2\mu T e^{-\mu T} - 3)$$

$$+ \frac{4mG\sigma^2}{\mu T} \rho^2 (1 - 2\mu T e^{-2\mu T} - e^{-2\mu T}). \quad (41)$$

IV. RESULTS

The Lorentzian filter is a causal filter [see (27)] and the ISI is caused by the bits preceding the information bit. We are going to examine the situation for two past information bits. Averaging over a larger sequence of past bits does not substantially changes the result for the average error probability [25], [36]. The computations are performed for the On-Off keying (OOK) modulation format with a value $G = 100$ and $n_{sp} = 1$. The observation time is the interval $[0, T]$. The value of ρ was calculated for all possible sequences $\mathcal{B} = \{b_{-2}, b_{-1}, b_0\}$ and the average error probability was evaluated by (26) using a saddlepoint approximation for each term. The receiver optimum threshold α , yielding the lowest error probability, is determined numerically.

The quantum limit for different values of the bandwidth bit-time product BT, yielded both by the saddlepoint and the Gaussian approximation, is displayed in Fig. 2. The quantum limit, with optimized BT = 7 and optimum decision threshold, is 49.9 [photons/bit] compared to the 38 [photons/bit] for a receiver with a matched optical filter [1]. The bounds on the error probability derived in [25] yielded a quantum limit of

$$F_1(s) = \mu T s + \frac{2\mu T s^2 \sigma^2}{v^2} + \frac{4s^2 \sigma^2 \{2 - [(v+1)e^{\beta T} - (v-1)e^{-\beta T}]\}}{v^3 [(v+1)^2 e^{\beta T} - (v-1)^2 e^{-\beta T}]} \quad (33a)$$

$$F_2(s) = 2s \left\{ 1 - \frac{4 - 2s\sigma^2 [(v+2)e^{\beta T} - (v-2)e^{-\beta T}]}{v[(v+1)^2 e^{\beta T} - (v-1)^2 e^{-\beta T}]} \right\} \quad (33b)$$

$$F_3(s) = s \left\{ \frac{1}{2} + \frac{\sigma^2 s (e^{\beta T} - e^{-\beta T}) - [(v-1)e^{\beta T} + (v+1)e^{-\beta T}]}{[(v+1)^2 e^{\beta T} - (v-1)^2 e^{-\beta T}]} \right\}. \quad (33c)$$

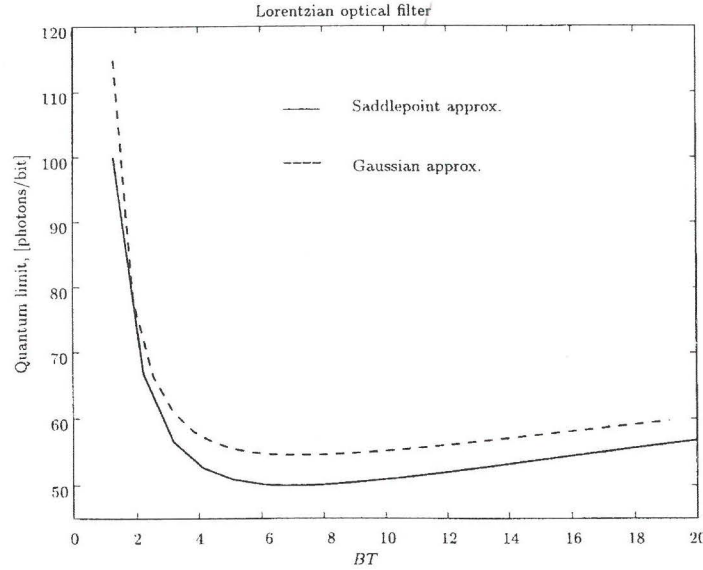


Fig. 2. The Quantum limit as a function of the bandwidth bit-time product BT . The solid line shows the results of the exact analysis (spa). The dotted line illustrates the results by the Gaussian approximation. $G = 100$, $n_{sp} = 1$.

56.5 [photons/bit] for an optimum $BT = 8$. The quantum limit derived in [27] is 44.5 [photons/bit] for an optimum $BT = 3.7$ and optimized observation time. Experimental results for a receiver with a value $BT = 7$ reported a quantum limit of 76 [photons/bit] [14]. The present work predicts for this case a quantum limit of 49.9 [photons/bit], which is in good agreement with the experimental result, considering that penalties may be incurred in the postdetection signal treatment.

The Gaussian approximation, the dotted line in Fig. 2, gives a good estimate of the error probability. The resultant quantum limit is 54.5 compared to 49.9 [photons/bit] yielded by the exact analysis (spa). The Gaussian approximation also predicts the optimum bandwidth bit-time product with high degree of accuracy.

V. CONCLUSIONS

In this paper, the impact of ISI on the performance of optically preamplified, direct detection OOK receivers with a Lorentzian optical filter has been studied. A closed-form expression for the MGF of the decision variable has been derived. Bit-error probabilities have been calculated by the spa (exact analysis) and the Gaussian approximation. The optimum filter bandwidth, minimizing the bit-error probability, and the penalty incurred by using a nonmatched filter, Lorentzian, is found.

The Gaussian approximation predicts the performance of the optically preamplified receiver with good accuracy; see Fig. 2. The parameters required by the Gaussian approximation, the variance and the mean of the decision variable, may be found without the knowledge of the MGF. Different type of optical filters [covariance kernels $K(t, u)$] may be considered with no

need of solving integral equations of the Fredholm type. Thus, optimum parameters of optically preamplified, OOK direct detection receiver may be determined by the simple method of the Gaussian approximation.

Although this paper deals only with OOK modulation format, the technique employed here can be used for receivers with other types of modulation. Independent additive noise contributions at the receiver can be incorporated in the exact analysis by just multiplying their MGF. The Gaussian approximation is expected to work well for modulation schemes with nonzero decision threshold [37].

APPENDIX

In this Appendix is presented the derivation of the MGF for the direct detection, optically preamplified receiver with an optical filter of the Lorentzian type.

Introducing the following auxiliary functions:

$$\begin{aligned} f_1(t; s) &= (\beta + \mu)e^{\beta t} + (\beta - \mu)e^{-\beta t} \\ f_1(u; s; T) &= (\beta + \mu)e^{\beta(T-u)} + (\beta - \mu)e^{-\beta(T-u)} \\ f_2(t; s; T) &= (\beta + \mu)e^{\beta(T-t)} + (\beta - \mu)e^{-\beta(T-t)} \\ f_2(u; s) &= (\beta + \mu)e^{\beta u} + (\beta - \mu)e^{-\beta u} \end{aligned}$$

and

$$C(s; T) = \frac{\mu^2}{\beta[(\beta + \mu)^2 e^{\beta T} - (\beta - \mu)^2 e^{-\beta T}]}$$

$h(t, u; s; T)$ in (31) can be expressed as

$$h(t, u; s; T) = C(s; T) \{f_1(u; s; T)f_1(t; s)\theta(u - t) + [1 - \theta(u - t)]f_2(u; s)f_2(t; s; T)\}$$

with

$$\theta(t - u) = \begin{cases} 0 & t < u \\ 1 & t > u. \end{cases} \quad (42)$$

The moment generating function is expressed as [see (18)]

$$M_A(s) = [D(s)]^{-1} \exp[F(s)]$$

where

$$F(s) = m_h s + s^2 \int_0^T \int_0^T Y^*(t)h(t, u; s; T)Y(u) du dt \quad (43)$$

$$m_h = \int_0^T |Y(t)|^2 dt$$

and $D(s)$, the Fredholm determinant, is given by [22]

$$D(s) = \exp \left\{ - \int_0^T \int_0^T h(t, u; s; T) dt du \right\}. \quad (44)$$

We start by integrating with respect to u in (19)

$$\mathcal{I}_1 = \int_0^T h(t, u; s; T)Y(u) du. \quad (45)$$

After substitution of (29) \mathcal{I}_1 can be expressed as

$$\begin{aligned} \mathcal{I}_1 &= \sqrt{\frac{4mG}{T}} C(s; T) \{f_1(t; s) \underbrace{\int_0^T f_1(u; s; T)(b_o + \rho e^{-\mu u})}_{g_1(u)} \\ &\quad \times \theta(u - t) du + f_2(t; s; T) \underbrace{\int_0^T [1 - \theta(u - t)]}_{g_2(u)} \\ &\quad \times \underbrace{f_2(u; s)(b_o + \rho e^{-\mu u})}_{g_2(u)} du. \end{aligned} \quad (46)$$

We recall that

$$\begin{aligned} \int_0^T g(u)\theta(u - t) du &= [G(u) - G(t)]\theta(u - t)|_0^T \\ &\quad \text{in our case } 0 \leq t \leq T \\ &= G(T) - G(t) \end{aligned} \quad (47)$$

where $G(t)$ is the primitive function of $g(t)$. Then

$$\begin{aligned} \mathcal{I}_1 &= \sqrt{\frac{4mG}{T}} C(s; T) [f_1(t; s)G_1(T) - f_1(t; s)G_1(t) \\ &\quad - f_2(t; s; T)G_2(0) + f_2(t; s; T)G_2(u)] \\ &\equiv \sqrt{\frac{4mG}{T}} C(s; T) [I_1^1 - I_2^1 - I_3^1 + I_4^1]. \end{aligned} \quad (48)$$

The integration operation leading to I_n^1 , $n = 1 \dots 4$, is straightforward but tedious. The resulting expressions contain

many terms. In the derivation that follows we do not reproduce the long intermediate expressions, but focus on the main steps toward the final result for the desired MGF.

Continuing with the derivation, we now perform integration with respect to t

$$\begin{aligned} &\int_0^T \int_0^T Y^*(t)h(t, u; s; T)Y(u) dt du \\ &= \int_0^T \mathcal{I}_1 Y^*(t) dt \\ &= \frac{4mG}{T} C(s; T) \int_0^T \mathcal{I}_1 (b_o + \rho e^{-\mu t}) dt. \end{aligned}$$

The expression for the variable m_h turns out to be

$$\begin{aligned} m_h &= \int_0^T |Y(t)|^2 dt \\ &= \frac{4mG}{T} \int_0^T (b_o + \rho e^{-\mu t})^2 dt \\ &= \frac{4mG}{\mu T} \left[b_o^2 \mu T + 2b_o \rho (1 - e^{-\mu T}) + \frac{\rho^2}{2} (1 - e^{-2\mu T}) \right]. \end{aligned} \quad (49)$$

Finally, rearranging common terms in b_o^2 , $b_o \rho$, and ρ^2 we get

$$F(s) = \frac{4mG}{\mu T} [b_o^2 F_1(s) + b_o \rho F_2(s) + \rho^2 F_3(s)]$$

where $F_1(s)$, $F_2(s)$, and $F_3(s)$ are shown at the bottom of the page and the Fredholm determinant takes the form

$$D(s) = \frac{(v + 1)^2 e^{\beta T} - (v - 1)^2 e^{-\beta T}}{4v e^{\mu T}}$$

with

$$v = \sqrt{1 - 2\sigma^2 s}$$

and

$$\beta = v\mu$$

The same result for $D(s)$ (considering the difference in notation) is given in an early paper by Helstrom [21].

ACKNOWLEDGMENT

The authors would like to thank one of the reviewers for constructive comments that helped to improve this presentation.

$$\begin{aligned} F_1(s) &= \mu T s + \frac{2\mu T s^2 \sigma^2}{v^2} + \frac{4s^2 \sigma^2 \{2 - [(v + 1)e^{\beta T} - (v - 1)e^{-\beta T}]\}}{v^3 [(v + 1)^2 e^{\beta T} - (v - 1)^2 e^{-\beta T}]} \\ F_2(s) &= 2s \left[1 - \frac{4 - 2s\sigma^2 [(v + 2)e^{\beta T} - (v - 2)e^{-\beta T}]}{v [(v + 1)^2 e^{\beta T} - (v - 1)^2 e^{-\beta T}]} \right] \\ F_3(s) &= s \left\{ \frac{1}{2} + \frac{\sigma^2 s (e^{\beta T} - e^{-\beta T}) - [(v - 1)e^{\beta T} + (v + 1)e^{-\beta T}]}{[(v + 1)^2 e^{\beta T} - (v - 1)^2 e^{-\beta T}]} \right\} \end{aligned}$$

REFERENCES

- [1] P. S. Henry, "Error-rate performance of optical amplifiers," in *Proc. OFC 1989*, paper THK3.
- [2] D. Marcuse, "Derivation of analytical expressions for the bit-error probability in lightwave systems with optical amplifiers," *J. Lightwave Technol.*, vol. 8, pp. 1816-1823, Dec. 1990.
- [3] L. G. Carliolaro, R. Corvaja, and G. L. Pierobon, "Exact performance evaluation of lightwave systems with optical preamplifier," *Optic. Commun.*, vol. 5, no. 6, pp. 757-766, Nov./Dec. 1994.
- [4] D. Marcuse, "Calculation of bit-error probability for a lightwave system with optical amplifiers and post-detection Gaussian noise," *J. Lightwave Technol.*, vol. 9, pp. 505-513, Apr. 1991.
- [5] P. A. Humblet and M. Azizoglu, "On the bit error rate of lightwave systems with optical amplifiers," *J. Lightwave Technol.*, vol. 9, pp. 1576-1582, Nov. 1991.
- [6] L. F. B. Ribeiro, J. R. F. Da Rocha, and J. L. Pinto, "Performance evaluation of EDFA preamplified receivers taking into account intersymbol interference," *J. Lightwave Technol.*, vol. 13, pp. 225-232, Feb. 1995.
- [7] S. L. Danielsen et al., "Detailed noise statistics for an optically preamplified direct detection receiver," *J. Lightwave Technol.*, vol. 13, pp. 977-981, May 1995.
- [8] J. C. Cartledge and A. F. Elrefaie, "Effect of chirping-induced waveform distortion on the performance of direct detection receivers using traveling-wave semiconductor optical preamplifiers," *J. Lightwave Technol.*, vol. 9, pp. 209-219, Feb. 1991.
- [9] R. C. Steele, G. R. Walker, and N. G. Walker, "Sensitivity of optically preamplified receivers with optical filtering," *IEEE Photon. Technol. Lett.*, vol. 3, pp. 545-547, June 1991.
- [10] O. K. Tonguz and L. G. Kazovsky, "Theory of direct-detection lightwave receivers using optical amplifiers," *J. Lightwave Technol.*, vol. 9, pp. 174-181, Feb. 1991.
- [11] N. A. Olsson, "Lightwave systems with optical amplifiers," *J. Lightwave Technol.*, vol. 7, pp. 1071-1082, July 1989.
- [12] I. Jacobs, "Effect of optical amplifier bandwidth on receiver sensitivity," *IEEE Trans. Commun.*, vol. 38, pp. 1863-1864, Oct. 1990.
- [13] C. Lawetz and C. J. Cartledge, "Performance of optically preamplified receivers with Fabry-Perot optical filters," *J. Lightwave Technol.*, vol. 14, pp. 2467-2474, Nov. 1996.
- [14] J. C. Livas, "High sensitivity optically preamplified 10 Gb/s receiver," in *Proc. OFC 96*, paper PD4.
- [15] A. Papoulis, *Probability, Random Variables, and Stochastic Processes*, 3rd ed. Singapore: McGraw-Hill International Edition, 1991.
- [16] L. Snyder, *Random Point Processes*. New York: Wiley-Interscience, 1975.
- [17] K. W. Cattermole and J. J. O'Reilly, *Mathematical Topics in Telecommunications*. London, England: Pentech, 1984, vol. 2.
- [18] M. Kac and A. J. F. Siegert, "On the theory of noise in radio receivers with square law detectors," *J. Appl. Phys.*, vol. 18, pp. 383-397, Apr. 1947.
- [19] S. D. Personick, "Applications for quantum amplifiers in simple digital optical communication systems," *Bell Syst. Tech. J.*, pp. 117-133, Jan. 1973.
- [20] H. L. Van Trees, *Detection, Estimation, and Modulation Theory, Part I*. New York: Wiley, 1968.
- [21] C. W. Helstrom, "Computation of photoelectron counting distributions by numerical contour integration," *J. Opt. Soc. Amer. A*, vol. 2, no. 5, pp. 674-682, May 1985.
- [22] A. J. F. Siegert, "A systematic approach to a class of problems in the theory of noise and other random phenomena—Part II, examples," *IRE Trans. Inform. Theory*, pp. 38-43, Mar. 1957.
- [23] I. M. Schwartz, "Distribution of the time-average power of a Gaussian process," *IEEE Trans. Inform. Theory*, vol. IT-16, pp. 17-26, Jan. 1970.
- [24] A. J. F. Siegert, "Passage of stationary process through linear and nonlinear devices," *Trans. IRE, Inform. Theory*, vol. PGIT-3, pp. 4-25, Mar. 1954.
- [25] D. Ben-Eli, E. D. Yeheskel, and S. Shamai, "Performance bounds and cutoff rates of quantum limited OOK with optical amplification," *IEEE J. Select. Areas Commun.*, vol. 13, pp. 510-530, Apr. 1995.
- [26] Y. R. Zhou and L. R. Watkins, "Rigorous approach to performance modeling of nonlinear, optically amplified IM/DD systems," *IEEE Proc.-Optoelectron.*, vol. 142, no. 6, pp. 271-278, Dec. 1995.
- [27] S. R. E. Chinn, "Error-rate performance of optically amplifiers with Fabry-Perot filters," *Electron. Lett.*, vol. 31, no. 9, pp. 756-757, Apr. 1995.
- [28] B. E. A. Saleh and M. C. Teich, *Fundamentals of Photonics*. New York: Wiley, 1991.
- [29] B. Saleh, *Photoelectron Statistics*. Berlin, Germany: Springer-Verlag, 1978.
- [30] C. W. Helstrom, "Distribution of the filtered output of a quadratic rectifier computed by numerical contour integration," *IEEE Trans. Inform. Theory*, vol. 32, pp. 450-463, July 1986.
- [31] ———, "Approximate evaluation of detection probabilities in radar and optical communications," *IEEE Trans. Aerospace Electron. Syst.*, vol. AES-14, pp. 630-640, July 1978.
- [32] ———, "Performance analysis of optical receivers by the saddlepoint approximation," *IEEE Trans. Commun.*, vol. 27, pp. 186-190, Jan. 1979.
- [33] ———, "Computing the performance of optical receivers with avalanche diode detectors," *IEEE Trans. Commun.*, vol. 36, pp. 61-66, Jan. 1988.
- [34] ———, "Analysis of avalanche diode receivers by saddlepoint integration," *IEEE Trans. Commun.*, vol. 40, pp. 1327-1338, Aug. 1992.
- [35] G. Einarsson, *Principles of Lightwave Communications*. New York: Wiley, 1996.
- [36] I. Tafur Monroy, "Performance analysis of optically preamplified direct detection receivers," Royal Inst. Technol., Stockholm, Rep. TRITA-TTT-9603, 1996.
- [37] G. Einarsson and M. Sundelin, "Performance analysis of optical receivers by Gaussian approximation," *J. Opt. Commun.*, vol. 16, pp. 227-232, 1995.



Idelfonso Tafur Monroy was born in El Castillo (Meta), Colombia, in 1968, and received the M.Sc. degree in multichannel telecommunications from the Bonch-Bruевич Institute of Communications, St. Petersburg, Russia, in 1992. In 1993, he enrolled as a graduate student in the Department of Signals, Sensors, and Systems at the Royal Institute of Technology, Stockholm, Sweden, and received the Technology Licentiate degree in telecommunication theory in 1996. He is currently pursuing the Ph.D. degree in the Department of Electrical Engineering at the Eindhoven University of Technology, The Netherlands.



Göran Einarsson received the M.S. degree in electrical engineering from the Massachusetts Institute of Technology (M.I.T.), Cambridge, MA, in 1962, and the Doctorate from the Royal Institute of Technology, Stockholm, Sweden, in 1968.

From 1953 to 1960, he was with the Long Distance Division of the L. M. Ericsson Corporation and from 1962 to 1968, he was working on carrier and PCM systems. From 1960 to 1962, he was with the Research Laboratory of Electronics at M.I.T., engaged in research on multipath communication.

During part of 1979, he served as a Consultant at Bell Laboratories, Crawford Hill, NJ, working on CDMA systems. From 1969 to 1990, he was Professor of Communication Theory at the University of Lund, Sweden, and he now holds the same position at the Royal Institute of Technology, Stockholm, Sweden. His current activities are in the field of optical communication theory.

Paper D

Error Rate Analysis of Optically Preamplified Receivers with Fabry-Perot Optical Filter and Equalizing Postdetection Filtering

Göran Einarsson and Idelfonso Tafur Monroy

Journal of Optical Communications, Submitted for publication.

Error Rate Analysis of Optical Receivers with Fabry-Perot Optical Filter and Equalizing Postdetection Filtering

Göran Einarsson and Idelfonso Tafur Monroy

Abstract— A complete analytic solution in form of the moment-generating function is presented for the statistical distribution of the decision variable of an on-off system with a Fabry-Perot optical filter. The results include ASE noise, photodetector shot noise and dark current together with thermal noise in the decision circuit. The influence of intersymbol interference is incorporated into the analysis and the optimal bandwidth of the optical filter is determined. It is shown that an equalizing electrical postdetection filter may make a significant improvement in performance. The analysis is extended to cover receivers with an arbitrary optical filter and arbitrary postdetection filtering by making use of a Gaussian approximation.

I. INTRODUCTION

Optical amplifiers, used as preamplifiers, have proven to efficiently enhance the receiver detection sensitivity. An optical amplifier must be followed by an optical filter to reduce the amplified spontaneous emission (ASE) noise which is of wide bandwidth character. The analysis of an optical preamplifier receiver is complicated. The photodetector is a quadratic device and linear signal analysis does not apply. Hence, an optical filter with narrow bandwidth reduces the ASE noise but will cause intersymbol interference (ISI) which deteriorates performance. An important design parameter is the optimal filter bandwidth accomplishing the best balance between filtered ASE noise and ISI.

The repertoire for optical processing design is limited. In this paper we present a simple analytical approach to the performance analysis of optically preamplified receivers. Firstly, we consider an optical preamplifier receiver with a Fabry-Perot optical filter. A Fabry-Perot etalon is a widely used device for optical filtering in optical fiber communication systems. The analysis is based on an exact analytic expression for the bit error probability. Secondly, a Gaussian approximation is introduced which allows an accurate, and simple analysis for arbitrary optical filter shapes in combination with a wider class of electrical postdetection filters. It is shown that an equalizing electrical postdetection filter may make a significant improvement in performance. Moreover, a proper combination of optical filter 3-dB bandwidth and electrical equalizing postdetection allows the use of narrower optical filtering. This may be of relevance in dense wavelength division multiplexing (DWDM) systems with closely spaced channels.

Göran Einarsson is with the Royal Institute of Technology, Telecommunication Theory, Dept. of Signals, Sensors and Systems, Stockholm, Sweden.

Idelfonso Tafur Monroy is with the Eindhoven University of Technology, Telecommunications Technology and Electromagnetics, Eindhoven, The Netherlands.

The rest of the paper is organized as follows. Section II introduces the receiver model under investigation. The performance analysis and the strategies for equalizing postdetection are explained in Sec. III. A Gaussian approximation to the performance analysis, and how it can be used for the analysis of receivers incorporating an arbitrary optical and electrical postdetection filter is introduced in Sec. IV. Finally, summarizing conclusions are drawn in Sec. V.

II. SYSTEM MODEL

A block diagram of an optically preamplified receiver is shown in Figure 1. The optical and postdetection filter are denoted by H_1 and H_2 , respectively. Their impulse responses are, accordingly, denoted by $h_1(t)$ and $h_2(t)$. The optical field signal, in equivalent lowpass representation, at the output of the optical filter H_1 is

$$Z(t) = [S(t) + X(t)] * h_1(t) = S_1(t) + X_1(t), \quad (1)$$

where $*$ denotes convolution, the envelope (modulation) of the optical signal is $S(t)$, and $X(t)$ represents the spontaneous emission noise from the optical amplifier.

The response of the photodetector depends on the random optical intensity $\Gamma(t) = |Z(t)|^2/2$. The decision is based on the output $V(t)$ from the postdetection filter H_2 , sampled at time T , the end of the symbol interval. If the photon intensity $\Gamma(t)$ is a deterministic function, then the moment-generating function (MGF) for $V(T)$ is, [1]: eqn (5.111),

$$\Psi_V(s) = \exp\left[\int_{-\infty}^{\infty} \Gamma(\tau)(\exp[sh_2(t-\tau)] - 1) d\tau\right] \quad (2)$$

However, $\Gamma(t)$ is random and $V(t)$ is a doubly stochastic process whose MGF is obtained by forming a statistical average with respect to $\Gamma(t)$. For the important special case when $h_2(t)$ is an integrate-and-dump filter

$$h_2(t) = \begin{cases} 1 & ; \quad 0 < t < T \\ 0 & ; \quad \text{otherwise,} \end{cases} \quad (3)$$

acting as a photoelectron counter, $V(T)$ is equal to the number N of photoelectrons observed in the bit time interval $[0, T]$. The expression for the MGF then simplifies to

$$\begin{aligned} \Psi_V(s) &= E \left\{ \exp \left[\int_0^T \Gamma(t)(e^s - 1) dt \right] \right\} \\ &= E \{ \exp[\mathcal{M}(e^s - 1)] \}, \end{aligned} \quad (4)$$

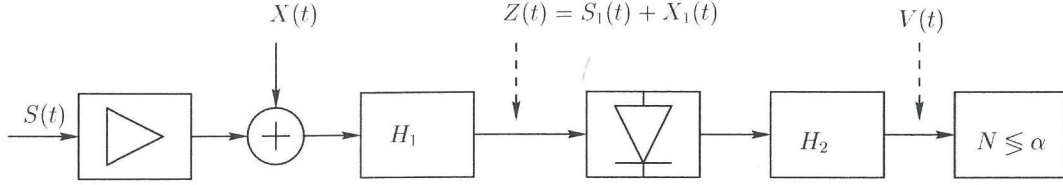


Fig. 1. A preamplified receiver with optical bandpass filter H_1 and postdetection filter H_2 .

where \mathcal{M} is the average optical intensity

$$\mathcal{M} = \int_0^T \Gamma(t) dt = \frac{1}{2} \int_0^T |Z(t)|^2 dt. \quad (5)$$

For a photodetector (PIN diode) with quantum efficiency η the output photoelectron intensity is equal to $\Gamma(t)$ multiplied by η and (4) is equal to

$$\Psi_V(s) = \Psi_{\mathcal{M}}(\eta[c^s - 1]), \quad (6)$$

with $\Psi_{\mathcal{M}}(s)$ the MGF of \mathcal{M} .

A photodetector dark current of intensity γ_d adds an independent Poisson process to $V(t)$. Thermal noise in the decision circuit is an independent Gaussian process and the complete MGF has the form

$$\Psi_V(s) = \Psi_{\mathcal{M}}(\eta[c^s - 1]) \exp[\gamma_d T (c^s - 1)] \exp(s^2 \sigma^2 / 2), \quad (7)$$

with σ^2 the variance of the thermal noise.

For an integrating postdetection filter the statistics of the decision variable is determined by the integral (5) of a non-stationary and non-Gaussian random process $\Gamma(t)$. A standard procedure for the analysis is to expand the stochastic process $Z(t)$ into a series with orthogonal coefficients, a Karhunen-Loeve expansion. This approach has been used by [2, 3] and [4], among others. It requires the solution of an integral equation and the results are expressed in terms of infinite series.

III. PERFORMANCE ANALYSIS

A. Fabry-Perot Filter

A Fabry-Perot (F-P) or Lorentzian filter has the impulse response

$$h_1(t) = \begin{cases} \sqrt{2}\mu e^{-\mu t} & ; t > 0 \\ 0 & ; t < 0 \end{cases} \quad (8)$$

The 3-dB filter bandwidth $B_L = \mu/\pi$.

The filter output $A_1(t)$ for a rectangular (non-return-to-zero) input signal of amplitude A is

$$A_1(t) = \begin{cases} A(1 - e^{-\mu t}) & ; 0 \leq t \leq T \\ A(e^{\mu T} - 1)e^{-\mu t} & ; t \geq T \end{cases} \quad (9)$$

It is shown in Figure 2.

An explicit expression for the MGF of the decision variable for an optical system with a Fabry-Perot optical

filter and an integrating postdetection filter has been presented by Tafur and Einarsson [5]. The MGF for the optical intensity variable (5) has the form

$$\Psi_{\mathcal{M}}(s) = [D(s)]^{-1} \exp[F(s)], \quad (10)$$

where $D(s)$ is the Fredholm determinant representing the system noise.

$$D(s) = \frac{(v+1)^2 e^{vu} - (v-1)^2 e^{-vu}}{4ve^u}, \quad (11)$$

where $v = \sqrt{1 - 2\mathcal{N}_0 s}$ and $u = \mu T$.

It is convenient in the further analysis to consider the MGF for a signal of the form

$$S_1(t) = A(c_0 + \rho e^{-\mu t}). \quad (12)$$

The function $F(s)$ is then

$$F(s) = \frac{4mG}{u} [c_0^2 F_1(s) + c_0 \rho F_2(s) + \rho^2 F_3(s)] \quad (13)$$

with $F_1(s)$, $F_2(s)$, and $F_3(s)$ given at the top of next page. In (13) the number of received photons is denoted by m . It is assumed that a linear polarizer is used to reduce the ASE noise. The analysis applies to a receiver without polarizer after a slight generalization, cf. [4].

B. Intersymbol Interference

Let $c_k = \{0, 1\}$ be a transmitted sequence of binary symbols where $k = 0$ denotes the symbol under detection located in the time interval $[0, T]$ and $k \geq 1$ are symbols of previous intervals $[-kT, (-k+1)T]$. For a F-P filter ISI is caused by previous data symbols only and the optical field signal at the output of the optical filter is

$$\begin{aligned} S_1(t) &= c_0 A_1(t) + \sum_{k=1}^{\infty} c_k A_1(t + kT) \\ &= c_0 A(1 - e^{-\mu t}) + \sum_{k=1}^{\infty} c_k A(e^{\mu kT} - 1)e^{-\mu(t+kT)} \end{aligned} \quad (14)$$

This can be expressed as $S_1(t) = A(c_0 + \rho e^{-\mu t})$ with

$$\rho = (e^{\mu T} - 1) \sum_{k=1}^{\infty} c_k e^{-\mu kT} - c_0 \quad (15)$$

The relation (15) shows that, for a F-P filter, the effect of ISI is controlled by the real valued parameter $-1 \leq \rho \leq 1$.

$$\begin{aligned} F_1(s) &= us + \frac{2us^2 \mathcal{N}_0}{v^2} + \frac{4s^2 \mathcal{N}_0 \{2 - [(v+1)e^{vu} - (v-1)e^{-vu}]\}}{v^3[(v+1)^2 e^{vu} - (v-1)^2 e^{-vu}]} \\ F_2(s) &= 2s \left\{ 1 - \frac{4 - 2s \mathcal{N}_0 [(v+2)e^{vu} - (v-2)e^{-vu}]}{v[(v+1)^2 e^{vu} - (v-1)^2 e^{-vu}]} \right\} \\ F_3(s) &= s \left\{ \frac{1}{2} + \frac{s \mathcal{N}_0 (e^{vu} - e^{-vu}) - [(v-1)e^{vu} + (v+1)e^{-vu}]}{(v+1)^2 e^{vu} - (v-1)^2 e^{-vu}} \right\} \end{aligned}$$

The MGF of the exact and complete distribution for the decision variable, including ISI, is obtained by forming the average of $\Psi_V(s)$ or $\Psi_{\mathcal{M}}(s)$ with respect to ρ

$$\Psi(s) = \sum_{\rho} P(\rho) \Psi(s, \rho). \quad (16)$$

The probability distribution for ρ is readily determined assuming that the data symbols c_k are independent and taking values $\{0, 1\}$ with equal probability. For a F-P filter the ISI is dominated by a few preceding symbols and a very limited number of terms need to be included in (16).

C. Quantum Limit

The sensitivity of an optical receiver under ideal conditions is often expressed as a quantum limit, defined as the minimal number of received photons per transmitted bit, needed to achieve a bit error probability not greater than 10^{-9} . Figure 3 shows the quantum limit for a fixed threshold receiver as a function of the F-P filter 3-dB bandwidth. The curve is calculated by a saddlepoint approximation based on (16). The average number of received photons for a transmitted "one" is denoted by m_1 . The optimal filter bandwidth is $B_L T = 7.5$ yielding a quantum limit of 49.8 photons per bit.

The quantum limit for single symbol transmission is shown as the dashed curve in Figure 3. It constitutes a lower bound on the quantum limit for an optical preamplifier receiver with a Fabry-Perot optical filter.

D. Modified postdetection filter

A well known method for reduction of the effect of ISI is to design the detector filter as an equalizer. Such a filter modifies the received signal in such a way that the influence between signals is reduced.

The ISI generated by a F-P filter is present in the beginning of the signal interval, as illustrated in Figure 2. A simple modification of the postdetection filter for improved performance is to let the integrating filter disregard a small time interval $[0, \varepsilon T]$ at the beginning of the signal interval, where the ISI is most severe.

The decision variable is now; cf. (5)

$$\mathcal{M}_{\varepsilon} = \int_{\varepsilon T}^T \Gamma(t) dt = \frac{1}{2} \int_{\varepsilon T}^T |Z(t)|^2 dt. \quad (17)$$

The performance of an optical receiver with an optical F-P filter and a restricted integrating postdetection filter is

easy to analyze. A change in the integration variable gives the relation

$$\int_{\varepsilon}^1 (c_0 + \rho e^{-us})^2 ds = \int_0^1 (c_0 + \tilde{\rho} e^{-\tilde{u}s})^2 ds, \quad (18)$$

where $\tilde{\rho} = \rho e^{-\varepsilon u}$ and $\tilde{u} = u(1 - \varepsilon)$, which means that the analysis derived for the standard filter can be used for the modified filter also. The number of received photons is reduced from m to $m(1 - \varepsilon)$ which combined with simple transformations of the parameters ρ and u produces the results for the modified filter.

The quantum limit for a receiver with a modified postdetection filter is shown in Figure 3. A suitable relation for the parameter ε turned out to be $\varepsilon = 0.4/B_L T$. The modified filter should be used in combination with an optical filter of bandwidth $B_L T = 3.7$ resulting in a quantum limit of 44.9 photons per bit. This agrees with the results by S. R. Chinn [6]. The improvement is mainly due to the lower filter bandwidth which reduces the amount of ASE at the filter output. The possibility of using narrower optical filters is of interest in dense wavelength division multiplexing (DWDM) systems with closely spaced channels. A postdetection filter with restricted integration is not an optimal equalizer but comparison with the lower bound in Figure 3 indicates that it works well.

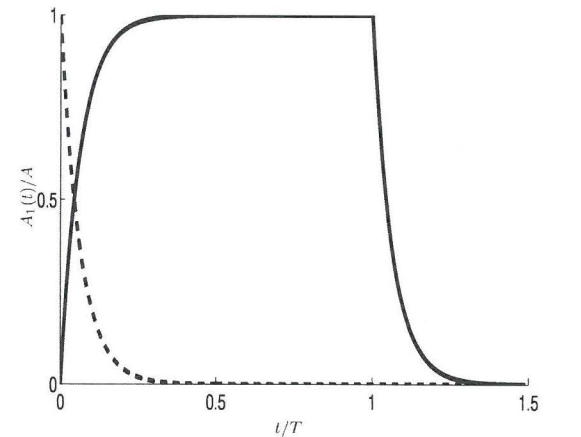


Fig. 2. The output signal from a Fabry-Perot filter with bandwidth $B_L = 5/T$ for a rectangular input signal. Intersymbol interference is indicated by the dotted curve.

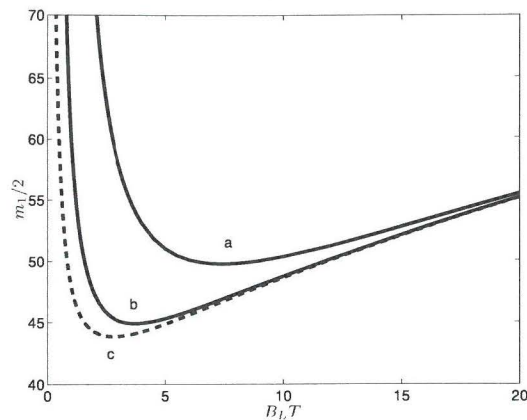


Fig. 3. Quantum limit for a receiver with Fabry-Perot optical filter as a function of $B_L T$. (a) Ordinary integrating postdetection filter. (b) Modified filter (equalizer). (c) A lower bound, neglecting intersymbol interference.

IV. GAUSSIAN APPROXIMATION

The Gaussian approximation is simpler than an exact evaluation based on the true statistics of the decision variable. It can be applied to an arbitrary optical filter and the effect of an arbitrary postdetection filter can easily be included in the analysis.

The decision is based on the output $V(t)$ from the post detector filter H_2 , sampled at time T , the end of the symbol interval. The Gaussian approximation requires the mean and variance of $V(T)$ for the "one" and "zero" signal conditions. Expressions for these quantities are presented in [5]. For a real valued received signal $S_1(t)$ and an optical filter with a real valued impulse response

$$E\{V\} = \frac{\eta}{2} \int_{-\infty}^{\infty} [S_1^2(t) + 2r(0)]v(t)dt \quad (19)$$

and

$$\text{Var}\{V\} = \eta^2 \int_{-\infty}^{\infty} \int_{-\infty}^{\infty} [S_1(s)S_1(t)r(s,t) + r^2(s,t)]v(s)v(t)dsdt + \frac{\eta}{2} \int_{-\infty}^{\infty} [S_1^2(t) + 2r(0)]v^2(t)dt, \quad (20)$$

where $v(t) = h_2(T-t)$ is the weight function of the post-detection filter.

The function $r(s,t)$ is the autocorrelation function of the noise at the optical filter output and the parameter η is the quantum efficiency of the photodetector.

A. Fabry-Perot Optical Filter

For a Gaussian approximation analysis of an optical system with F-P filter the integrals in (19) and (20) is evaluated for the signal $S_1(t) = A(c_0 + \rho e^{-\mu t})$ introduced in

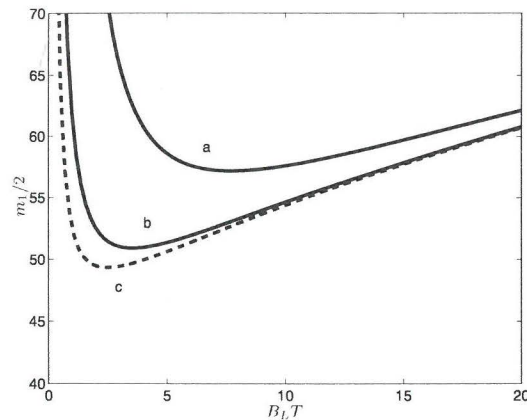


Fig. 4. Quantum limit for a receiver with Fabry-Perot optical filter calculated by the Gaussian approximation. (a) Upper bound based on a worst case ISI analysis. Ordinary integrating postdetection filter. (b) Upper bound for receiver with modified filter (equalizer). (c) A lower bound, neglecting intersymbol interference.

(12). For the special case when the postdetection filter function $v(t) = 1$ for $0 < t < T$ and zero elsewhere, after substitution of $N_0 = n_{sp}(G-1)$, see [5],

$$E\{V\} = m\eta G[2uc_0^2 + 4c_0\rho(1-e^{-u}) + \rho^2(1-e^{-2u})]/2u + \eta n_{sp}(G-1)u/2 \quad (21)$$

and

$$\text{Var}\{V\} = m\eta^2 n_{sp} G(G-1) [2c_0\rho(e^{-2u} + 3 - (2u+4)e^{-u}) + 4c_0^2(e^{-u} + u - 1) + \rho^2(1 - (2u+1)e^{-2u})]/2u + [\eta n_{sp}(G-1)]^2 [e^{-2u} + 2u - 1]/8 + E\{V\}, \quad (22)$$

where m is the (average) number of received photons.

The Gaussian approximation estimate of the transmission error probability is obtained from the standard relation, see i.e. [1],

$$P_e = \frac{1}{\rho\sqrt{2\pi}} \exp(-r^2/2) \quad (23)$$

with r equal to the signal-to-noise ratio

$$r = \frac{E_1 - E_0}{\sigma_1 - \sigma_0}, \quad (24)$$

in which $E_{1,0}$ is the mean value of the receiver decision variable for a received symbol "one", and "zero", respectively. The standard deviation is denoted, accordingly, as $\sigma_{1,0}$. A comparison with the error probability calculated by the saddlepoint approximation shows that the Gaussian

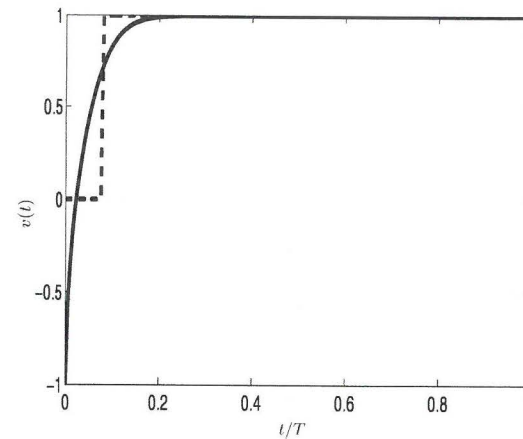


Fig. 5. Weight function for an equalizing postdetection filter derived from an optimal filter for the Poisson channel. The dashed curve indicates the weight function of a restricted integration equalizer with $\varepsilon = 0.4/B_L T$.

approximation gives a reliable estimate of the error probability. As an example, for a receiver with a F-P filter having a 3-dB bandwidth bit-time product $B_L T = 5$, gain $G = 100$ and spontaneous emission factor $n_{sp} = 1.5$. The bit error probability calculated by the Gaussian approximation is $P_e = 1.33 \times 10^{-6}$ to be compared with $P_e = 7.95 \times 10^{-7}$ from the true distribution using a saddlepoint approximation. A discussion of the properties of the Gaussian approximation can be found in [7].

B. Intersymbol Interference

The Gaussian approximation can be used to estimate upper and lower bounds on the degradation of error probability caused by ISI. A lower bound is obtained by considering single symbol transmission and an upper bound by a worst case analysis.

In (14) the signals are added coherently. A more realistic assumption is that signals from different data symbols adds non-coherently which means power addition. Assume that the phases of the signals received in different time-slots take random and independent values in relation to the received signal $S_1(t)$ in the bit interval under detection ($k=0$). The signal at the output of the optical filter is

$$S_1(t) = c_0 A_1(t) + \sum_{k=1}^{\infty} c_k e^{j\phi_k} A_1(t+kT) \quad (25)$$

The parameters ϕ_k are independent random variables, uniformly distributed in $[0, 2\pi]$.

Substitution of (9) into (25) and taking the average with

respect to ϕ_k gives

$$E\{S_1(s)S_1(t)\} = A^2 c_0 (1 - e^{-\mu s})(1 - e^{-\mu t}) + A^2 (e^{\mu T} - 1)^2 \sum_{k=1}^{\infty} c_k e^{-\mu(s+kT)} e^{-\mu(t+kT)}. \quad (26)$$

In a worst case ISI analysis the interfering symbols c_k are zero for all $k \geq 1$ making $S_1(t) = A_1(t)$, for a binary "one" transmitted ($c_0 = 1$). For a transmitted "zero" ($c_0 = 0$) the parameters c_k are set equal to one for all $k \geq 1$ corresponding to maximal ISI. The summation in (26) can then be evaluated and for $c_0 = 0$

$$E\{S_1(s)S_1(t)\} = \frac{A^2 (e^{\mu T} - 1)^2 e^{-\mu(s+t)}}{e^{2\mu T} - 1} \quad (27)$$

From (27) follows that for non-coherent ISI, a worst case analysis corresponds to a parameter

$$\rho = \frac{e^u - 1}{\sqrt{e^{2u} - 1}}. \quad (28)$$

Upper and lower bounds on the quantum limit calculated by the Gaussian approximation as a function of the F-P filter bandwidth are shown in Figure 4. The lower bound is single signal transmission and the upper bound is from a worst case analysis as described above. Also shown is the reduced upper bound produced by a modified postdetection filter.

C. Modified postdetection filter

The effect of an arbitrary postdetection filter can be estimated by the Gaussian approximation. As an example consider a filter function of the form $v(t) = \ln[\Gamma_1(t)/\Gamma_0(t)]$ inspired by the optimum filter for direct detection, cf. [1]: eqn (5.149),

$$v(t) = C \ln \left[\frac{(1 - e^{-\mu t})^2 + g_0}{e^{-2\mu t} + g_0} \right], \quad (29)$$

where g_0 represents the background (ASE) noise and C is a normalizing constant. The appearance of $v(t)$ for $g_0 = 0.1$, which turns out to be a suitable value at $B_L = 5/T$, is shown in Figure 5. Substitution of (29) into (19) and (20) using numerical integration results in $P_e = 1.09 \times 10^{-6}$ for a system with $m_1 = 100$, $G = 100$, and $n_{sp} = 1.5$ which is better than obtained by a restricted integration filter yielding $P_e = 1.42 \times 10^{-6}$.

V. CONCLUSIONS

This paper presents a simple analytical approach to the analysis of optically preamplified receivers. A receiver using a Fabry-Perot optical filter is implicitly incorporated in the analysis. It is shown that by using electrical equalizing postdetection a significant improvement in performance can be achieved. Moreover, it is also shown that a proper combination of the optical filter 3-dB bandwidth together

with equalizing postdetection allows the use of narrower optical filters; which is of relevance in DWDM systems with closely spaced channels. Finally, a Gaussian approximation to the performance analysis is introduced. This approximation, which is numerically simple and gives accurate results, makes easy the finding of the optimum 3-dB bandwidth of the optical filter for receivers with an arbitrary optical filter shape and with arbitrary electrical postdetection filtering.

REFERENCES

- [1] G. Einarsson, *Principles of Lightwave Communications*. Chichester: John & Wiley, 1996.
- [2] S. R. Chinn, D. M. Boroson, and J. C. Livas, "Sensitivity of optically preamplified dsk receivers with fabry-perot filters," *J. Lightwave Technol.*, vol. 14, pp. 370-375, 1996.
- [3] C. Lawetz and J. C. Cartledge, "Performance of optically preamplified receivers with fabry-perot optical filters," *J. Lightwave Technol.*, vol. 14, pp. 2467-2474, November 1996.
- [4] S. Herbst, P. Meissner, M. Baussmann, and M. Erbach, "Sensitivity of a direct wdm-system with a frequency selective optical receiver and optical preamplifier," *J. Lightwave Technol.*, vol. 16, pp. 32-36, January 1998.
- [5] I. Tafur Monroy and G. Einarsson, "Bit error evaluation of optically preamplified direct detection receivers with fabry-perot optical filters," *J. Lightwave Technol.*, vol. 15, pp. 1546-1553, August 1997.
- [6] S. R. Chinn, "Error-rate performance of optical amplifiers with fabry-perot filters," *Elec. Lett.*, vol. 31, pp. 756-757, April 1995.
- [7] G. Einarsson and M. Sundelin, "Performance analysis of optical receivers by gaussian approximation," *J. Opt. Commun.*, vol. 16, pp. 272-232, 1995.

BIOGRAPHY



Göran Einarsson received the M.S. degree in electrical engineering from the Massachusetts Institute of Technology in 1962, and the Doctorate from the Royal Institute of Technology, Stockholm, Sweden, in 1968. He was with the Long Distance Division of the L. M. Ericsson Corporation from 1953 to 1960 and from 1962 to 1968 working on carrier and PCM systems. From 1960 to 1962 he was with the Research Laboratory of Electronics at M.I.T., engaged in research on multipath communication. During

part of 1979 he served as a consultant at Bell Laboratories, Crawford Hill, NJ, USA, working on CDMA systems. From 1969 to 1990 he has been Professor of Communication Theory at the University of Lund, Sweden, and he now holds the same position at the Royal Institute of Technology, Stockholm, Sweden. His current activities are in the field of optical communication theory.



Idelfonso Tafur Monroy was born in El Castillo (Meta), Colombia, in 1968 and graduated from the Bonch-Bruévich Institute of Communications, St. Petersburg, Russia, in 1992, where he received the M.Sc. degree in Multichannel Telecommunications. In 1993 he enrolled as a graduate student in the Department of Signals, Sensors and Systems at the Royal Institute of Technology, Stockholm, Sweden, where he received in 1996 the Technology Licentiate degree in Telecommunication Theory. He is currently pursuing the PhD degree in the Department of Electrical Engineering at the Eindhoven University of Technology, The Netherlands. His research interests are in the area of optical communication theory.

Paper E

On Analytical Expressions for the Distribution of the Filtered Output of Square Envelope Receivers with Signal and Colored Gaussian Noise Input

Idelfonso Tafur Monroy

© 1999 IEEE. Reprinted, with permission, from *IEEE Trans. Comm.*,
Submitted for publication.

On Analytical Expressions for the Distribution of the Filtered Output of Square Envelope Receivers

Idelfonso Tafur Monroy, *Student Member, IEEE*

Abstract—Closed form expressions for the moment generating function (MGF) of the filtered output of square envelope receivers with signal and colored Gaussian noise input are derived. The informative signal is a binary sequence of rectangular pulses. The considered Gaussian processes are: the Wiener process, a Gaussian process with linear covariance (moving average), and the Ornstein-Uhlenbeck process. The derived MGFs are then applied to the problem of finding the quantum limit for optically preamplified, direct detection receivers.

Keywords—Communication theory, envelope receivers, error analysis, optical communication, preamplified receivers.

I. INTRODUCTION

Determining the distribution of the output of square envelope receivers with colored Gaussian noise input constitutes a classic problem in communication theory; see e.g. [1–5]. Although the mathematical formalism for determining the statistics of the output of such receivers is well known, e.g. [1,3,5,6], deriving closed form expressions for the distribution is a complex task. Moreover, if both signal and noise are present at the input, this task becomes even more formidable. For the case of noise only input expressions for the moment generating function (MGF) and analytical approximations to the probability density function have been reported for several covariance kernels, e.g. [3,5,7]. For both signal and noise being present at the input closed form expressions for the distribution are scarcely documented in the literature. In this letter, closed form expression for the MGF are derived for the case of an input informative signal composed of a binary sequence of rectangular pulses. The considered Gaussian processes are: the Wiener process, a Gaussian process with linear covariance (moving average), and the Ornstein-Uhlenbeck process.

The remain of this letter is structured as follow: in Sec. II the system model to be discussed is presented. The mathematical formalism to obtain closed form expressions for the MGF of the receiver's output is also described. Closed form expressions for the MGF for the the considered Gaussian processes are derived in Sec. III. Section IV is devoted to the application of the derived MGFs to find the quantum limit for optically preamplified, direct detection receivers. Finally, summarizing conclusions are presented in Sec. V.

II. SYSTEM MODEL

In this section we present the reference model for the system under investigation. The receiver schematic diagram is presented in Fig. 1. This receiver has the classic configuration of pre-detection filter $r(t)$, square envelope detector and post-detection filter. The input is an informative signal corrupted by an additive white Gaussian noise (AWGN) $n(t)$ with spectral density parameter N_0 . In the sequel, equivalent bandpass representation of signal and noise is assumed. The incoming signal is a binary sequence of rectangular pulses $S(t)$. For a given bit pattern, $\mathcal{B} = (\dots, b_{-1}, b_0, b_1, \dots)$, at the output of the filter $r(t)$ the signal is given by

$$Y(t) = S(t) \star r(t) = \sqrt{\frac{m}{T}} \left[b_0 l(t) + \sum_{k \neq 0} b_k l(t - kT) \right] \quad (1)$$

where:

$r(t)$ is the pre-detection filter impulse response,
 $l(t) = g(t) \star r(t)$, in which \star denotes convolution.
 $g(t)$ is unit rectangular pulse of duration T ,
 $b_k \in \{0, 1\}$ are statistically binary symbols representing a data "zero" and a "one", respectively.
 m is the energy content of the signal $S(t)$ in a bit-duration time interval: $m = \frac{1}{2} \int_0^T |S(t)|^2 dt$.

At the pre-detection filter output the resultant colored Gaussian noise is denoted by $X(t)$, whose in-phase and quadrature components have zero mean and autocovariance

$$K(\tau) = \frac{N_0}{2} R(\tau), \quad R(\tau) = \int_{-\infty}^{\infty} r(t) r^*(t + \tau) dt, \quad (2)$$

where \star means complex conjugate.

With the above notations the input of the square envelope detector becomes: $B(t) = Y(t) + X(t)$. If we consider and integrate-and-dump post-detection filter, then the receiver's output is given by

$$\Lambda = \int_0^T |Y(t) + X(t)|^2 dt. \quad (3)$$

The general mathematical form for the MGF of Λ , $M_\Lambda(s) = E\{e^{s\Lambda}\}$, is well known, e.g. [1,7]

$$M_\Lambda(s) = \prod_{n=1}^{\infty} \frac{1}{(1 - \lambda_n s)} \exp \left(\sum_{n=1}^{\infty} \frac{|y_n|^2 s}{1 - \lambda_n s} \right), \quad (4)$$

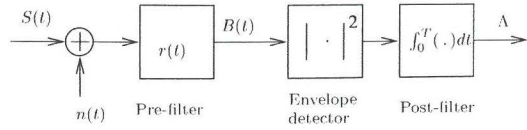


Fig. 1. Square envelope receiver

where $y_n = \int_0^T Y(t) f_n^*(t) dt$. The set of orthonormal functions $\{f_n\}$ are the eigenfunctions and λ_n are the eigenvalues of the integral equation

$$\int_0^T K(t, u) f_n(u) du = \lambda_n f_n(t), \quad 0 \leq t \leq T, \quad (5)$$

in which $K(t, u)$ is the covariance kernel of the process $X(t)$. Let $h(t, u; s; \tau)$ stand for the resolvent kernel associated with the integral equation (5). The MGF in (4) can be represented in terms of the resolvent kernel as [7]

$$M_\Lambda(s) = [D(s)]^{-1} \exp[F(s)], \quad (6)$$

where

$$F(s) = s \int_0^T |Y(t)|^2 dt + s^2 \int_0^T \int_0^T Y^*(t) h(t, u; s; T) Y(u) dt du, \quad (7)$$

and $D(s)$, also called the Fredholm determinant, is given by

$$D(s) = \exp \left[\int_0^s \int_0^T h(t, t; v; T) dt dv \right]. \quad (8)$$

III. MOMENT GENERATING FUNCTION

In this section, closed form expressions for $M_\Lambda(s)$ are presented for three different Gaussian processes.

Case 1 The Wiener process

Suppose that $r(t)$ is the (normalized) impulse response of an integrate-and-dump filter, then

$$X(t) = \int_0^\infty r(t-s) n(s) ds, \quad (9)$$

$$r(t-s) = \begin{cases} \frac{1}{T} & s < t \\ 0 & s > t \end{cases}$$

The process $X(t)$ is the Wiener process which has covariance given by

$$K(t, u) = \frac{N_0}{T^2} \int_0^t \int_0^u \delta(t-u) dt du = \frac{N_0}{T^2} \min(t, u). \quad (10)$$

As one can observe from the character of $r(t)$, the integrate-and-dump filter does not introduce intersymbol interference (ISI). The resulting expression for the MGF is (see

Appendix A for a derivation)

$$M_Z(s) = \cos(\sqrt{N_0 s})^{-1} \exp \left[-\frac{m}{N_0} + \frac{m \tan(\sqrt{N_0 s})}{\sqrt{N_0 s}} \right] \quad (11)$$

Case 2 Gaussian process with linear covariance

Let $r(t)$ be a finite-time bandpass integrator (moving average) whose impulse response is given by

$$r(t) = \begin{cases} \frac{1}{T} & 0 \leq t \leq T \\ 0 & \text{otherwise.} \end{cases} \quad (12)$$

The covariance kernel of $X(t)$ is the triangular function (linear covariance [5])

$$K(\tau) = \begin{cases} \frac{N_0}{T} \left(1 - \frac{|\tau|}{T}\right) & 0 \leq \tau \leq T \\ 0 & \text{otherwise.} \end{cases} \quad (13)$$

The analysis for the observation time $[0, T]$ shows that the MGF for Λ is of the same character as (11). As already reported in [5], it can be derived from Eq. 11 by substitution of \sqrt{s} by $\sqrt{2s}$. The result is

$$M_Z(s) = \cos(\sqrt{2N_0 s})^{-1} \exp \left[-\frac{m}{N_0} + \frac{m \tan(\sqrt{2N_0 s})}{\sqrt{2N_0 s}} \right].$$

In contradistinction to the integrate-and-dump filter the finite-duration integrator introduces ISI. Communication is only possible if the observation time is shifted from $[0, T]$ to $[\frac{T}{2}, \frac{3T}{2}]$. For this type of filter only a single past and one succeeding bit produce ISI on the present transmitted bit. Hence the bit sequence of interest is: $B = (b_{-1}, b_0, b_1)$. The expression for $F(s)$ is given by

$$F(s) = \frac{m[b_0^2 H_1(s) + (b_{-1} b_0 + b_0 b_1) H_2(s) + (b_{-1}^2 + b_1^2) H_3(s)]}{4N_0 \cos(\beta)}, \quad (14)$$

with

$$H_1(s) = \text{sinc}(\beta)(5N_0 s + 4) - 2 \text{sinc}(\beta/2)(N_0 s + 1) - 2 \cos(\beta/2)$$

$$H_2(s) = \text{sinc}(\beta)(N_0 s - 4) - \text{sinc}(\beta/2)(N_0 s - 2) + 2 \cos(\beta/2)$$

$$H_3(s) = \text{sinc}(\beta)(N_0 s/2 + 2) - \text{sinc}(\beta/2) - \cos(\beta/2),$$

where $\beta = \sqrt{2N_0 s}$, and $\text{sinc}(x) = \sin(x)/x$. The Fredholm determinant is given by $D(s) = \cos(\sqrt{2N_0 s})$. Appendix B explains the derivation of (15).

Case 3 The Ornstein-Uhlenbeck process

If $r(t)$ is the impulse response of the Lorentzian filter:

$$r(t) = \sqrt{2} \mu e^{-\mu t}, \quad t \geq 0, \quad (15)$$

then the process $X(t)$ is the so called Ornstein-Uhlenbeck process with covariance given by

$$K(\tau) = \mu e^{-\mu|\tau|}, \quad \tau \geq 0. \quad (16)$$

The information signal for $t \in [0, T]$ is given by

$$Y(t) = \sqrt{\frac{2m}{T}} [b_0 + \rho e^{-\mu t}], \quad \rho = (e^{\mu T} - 1) \sum_{k=-\infty}^{-1} b_k e^{\mu k T} - b_0.$$

The Lorentzian filter is a causal filter; hence when studying the effect of ISI only a sequence of previous bits with respect to the present transmitted bit b_0 is treated: $B = (\dots b_{-2}, b_{-1}, b_0)$. In practice only a small number of previous bit is considered [8]. For this case the resolvent kernel is well known e.g. [5, 7]. The closed form expression for $M_\Lambda(s)$ and its detailed derivation has been reported in an earlier paper by the (co)author [8]. The resulting expressions for $D(s)$ and $F(s)$ are presented here:

$$F(s) = \frac{2mG}{\mu T} [b_0^2 F_1(s) + b_0 \rho F_2(s) + \rho^2 F_3(s)], \quad (17)$$

where

$$F_1(s) = \mu T s + \frac{2\mu T s^2 \sigma^2}{v^2} + \frac{4s^2 \sigma^2 (2 - [(v+1)e^{\beta T} - (v-1)e^{-\beta T}])}{v^3 [(v+1)^2 e^{\beta T} - (v-1)^2 e^{-\beta T}]},$$

$$F_2(s) = 2s \left[1 - \frac{4 - 2s\sigma^2 [(v+2)e^{\beta T} - (v-2)e^{-\beta T}]}{v [(v+1)^2 e^{\beta T} - (v-1)^2 e^{-\beta T}]} \right],$$

$$F_3(s) = s \left[\frac{1}{2} + \frac{\sigma^2 s (e^{\beta T} - e^{-\beta T}) - [(v-1)e^{\beta T} + (v+1)e^{-\beta T}]}{[(v+1)^2 e^{\beta T} - (v-1)^2 e^{-\beta T}]} \right]$$

in which $v = \sqrt{1 - 2\sigma^2}$, $\beta = v\mu$.

$$D(s) = \frac{(v+1)^2 e^{\beta T} - (v-1)^2 e^{-\beta T}}{4v e^{\mu T}}. \quad (18)$$

The mean and the variance of Z can be found from the properties of the MGF. Namely, from the first and second derivative of the MGF evaluated at $s = 0$ [9]. The mean and the variance of Z can also be expressed in terms of the covariance kernel without the knowledge of the MGF [8]. The validity of the previous derived MGFs has been tested by confirming that the mean and the variance obtained by both methods are identical. Moreover, if only noise is present, then the MGF is given only in terms of the Fredholm determinant $D(s)$ and their expressions are in agreement with those already known in the literature e.g., [5, 7].

IV. APPLICATIONS

In this section we applied the derived MGFs to determine the quantum limit for optically preamplified, On-Off keying (OOK) direct detection receivers. The schematic diagram of such a receiver is illustrated in Fig. 2. The preamplifier is an EDFA (erbium-doped fiber amplifier) which is

modeled as linear optical field amplifier with gain G and AWGN noise $n(t)$ representing the ASE (amplified spontaneous emission) noise. The spectral parameter of $n(t)$ is given by $N_0 = n_{sp}(G-1)h\nu$, where n_{sp} is the amplifier spontaneous emission factor, h is the Planck's constant, and ν optical frequency. An optical filter $r(t)$ is used to limit the effect of ASE on the system performance, and in the case of WDM (wavelength division multiplexing) systems to select the desired channel.

By introducing a proper normalization (see [8]) m represents the average number of photons contained in an optical signal $S(t)$ for a transmitted binary "one". The spectral parameter of $n(t)$ is then given by $N_0 = n_{sp}(G-1)$. At the output of the photodetector the photocurrent is directly proportional to the square magnitude of the received optical field. Further, the photocurrent is filtered and sampled to form the decision variable Z . Thus, the analysis of optically preamplified, OOK direct detection receivers (Fig. 2), is an example of the classic communication situation of square envelope detectors followed by filtering with colored Gaussian input. Assume that the postdetection filter is an integrate-and-dump filter. The MGF for the receiver decision variable Z is then given by $M_Z(s) = M_\Lambda(e^s - 1)$, where Λ is the so-called Poisson parameter (c.f (3)) e.g., [8, 10]. Assuming independent, equally likely binary symbols the average error probability is given by

$$P_e = \frac{1}{2} [\text{E}_B \{P_r(Z < \alpha | B|_{b_0=1}) + P_r(Z > \alpha | B|_{b_0=0})\}] \quad (19)$$

Based on the MGF for the decision variable Z , error probabilities are expeditiously computed by the so-called saddlepoint approximation. For further details on the saddlepoint approximation see [7, 11], and [8] for an application to performance analysis of optically preamplified receivers.

In optical communications, the (standard), quantum limit is defined as the average number of photons per bit in the optical signal $S(t)$ needed to achieve a bit-error probability of 10^{-9} assuming ideal detection conditions, which for a preamplified receiver means that a large G is assumed. Suppose we have optical filters described by the impulse responses (equivalent baseband representation) of cases 1-3 (Eqs. 9, 12, 15). The above derived MGFs for these cases can then be used (substituting $m \mapsto mG$ to account for amplification, and with $N_0 = n_{sp}(G-1)$) to find the corresponding quantum limits. In Table I are presented the obtained results. For comparison, the quantum limit for the situation when the optical signal is assumed to pass the optical filter undistorted and that $X(t)$ is Gaussian bandlimited (ideal bandpass filter) is also included. When the effect of optical filtering is taken into account penalties are observed compared to the case assuming ideal bandpass filtering. For the analyzed optical filters this penalty in the quantum limit is at least of eight photons per bit. It should be noted that of the considered optical filters only the Lorentzian filter (case 3) represents practical interest. Widely used in optical transmission systems Fabry-

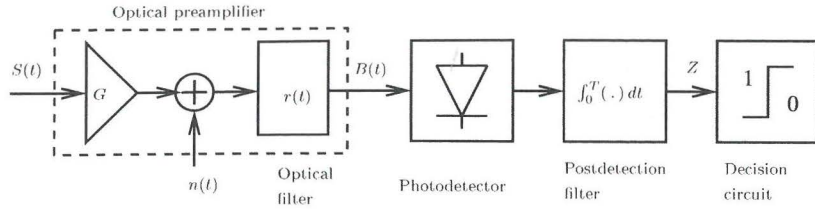


Fig. 2. Optically preamplified OOK receiver

Optical filter type	Quantum limit
Ideal situation	38.4 [11]
Integrate-and-dump	46.3
Finite-time Bandpass Integrator	59.6
Lorentzian, Optimal $\mu T = 7$	49.9

TABLE I

QUANTUM LIMIT FOR OPTICALLY PREAMPLIFIED OOK DIRECT DETECTION. $G = 100$ AND $n_{sp} = 1$.

Perot filters are well described by the Lorentzian impulse response of Eq. 15. We observe also that there exists an optimum bandwidth bit-time product $BT = \mu T/\pi$, the reason being a trade off between ISI and ASE noise (see Table I).

V. CONCLUSIONS

Closed form expressions, believed to be new, for the MGF of the filtered output of square envelope receivers with signal and colored Gaussian noise have been derived. The Wiener process, a Gaussian process with linear covariance and the Ornstein-Uhlenbeck process are considered. The informative signal is a binary sequence of rectangular pulses. We present an application of the derived MGFs in the performance analysis of optically preamplified, direct detection receivers.

APPENDICES

A. Derivation of the MGF: case 1

For the covariance function given by Eq. 10 the resolvent kernel is given by [5]

$$h(t, u; s; \tau) = \underbrace{\frac{\sigma^2}{\beta} [\sin(\beta t) \cos(\beta u) - \theta(t-u) \sin(\beta t) \cos(\beta u)]}_{h_1} + \underbrace{q \frac{\sigma^2}{\beta} \sin(\beta t) \sin(\beta u)}_{h_2} + \underbrace{\theta(t-u) \frac{\sigma^2}{\beta} \cos(\beta t) \sin(\beta u)}_{h_3}, \quad (20)$$

where $\sigma^2 = N_0/T^2$, $\beta = \sqrt{\sigma^2 s}$,

$$q = \tan(\beta T), \quad \text{and} \quad \theta(t-u) = \begin{cases} 0 & t < u \\ 1 & t > u. \end{cases}$$

We perform integration in Eq. 7 first with respect to t and with respect to u .

$$I_1 = \int_0^T Y^*(u) \underbrace{\int_0^T h(t, u; s; T) Y(t) dt}_{I_2} du,$$

$$I_2 = \int_0^T \underbrace{Y(t) h_1}_{a} + \underbrace{Y'(t) h_2}_{b} + \underbrace{Y(t) h_3}_{c} dt$$

in which $Y(t) = \sqrt{\frac{2m}{T}} t \equiv At$. Solving the integrals a, b, c we get:

$$I_2 = -A \frac{\sigma^2 u}{\beta^2} + A \frac{\sigma^2 \sin(\beta u)}{\beta^3 \cos(\beta T)}$$

Subsequently,

$$I_1 = \int_0^T A u I_2 du = -A^2 T^3 \frac{\sigma^2}{3\beta^2} + \frac{A^2 \sigma^2}{\beta^5} (\tan(\beta T) - \beta T).$$

$$F(s) = s \int_0^T |Y(t)|^2 dt + s^2 I_1, \quad \text{resulting in}$$

$$F(s) = -\frac{m}{N_0} + \frac{m \tan(\sqrt{N_0 s})}{N_0 \sqrt{N_0 s}}. \quad (21)$$

The Fredholm determinant is given by (see Eq. 8)

$$D(s) = \exp \left\{ \int_0^s \frac{\sigma T}{\sqrt{v}} \tan(\sigma T \sqrt{v}) dv \right\} = \cos(\sqrt{N_0 s}). \quad (22)$$

A result already obtained in [5] and references therein.

B. Derivation of the MGF: case 2

For the covariance kernel given in (13) and an observation interval $[-T/2, T/2]$, the resolvent kernel is presented in [5]. If the observation time is extended to $[0, 2T]$, then the resultant resolvent kernels is given by

$$h(t, u; s; T) = \frac{N_0}{\beta T} \left[\tan \beta \cos \left[\frac{\beta(t-u)}{T} \right] - \sin \left[\frac{\beta|t-u|}{T} \right] \right], \quad (23)$$

with $\beta = \sqrt{2N_0 s}$. The MGF is found by performing integration in (7) and (8) with the proper integration limits and the corresponding expression for $Y(t)$. The algebraic procedure is similar to that presented in Appendix A.

REFERENCES

- [1] M. Kac and A. J. F. Siegert, "On the theory of noise in radio receivers with square law detectors," *J. of Applied Physics*, vol. 18, pp. 383-397, April 1947.
- [2] S. O. Rice, "Mathematical analysis of random noise," *Bell Sys. Tech. J.*, vol. 23 and 24, pp. 282-332 and 46-156, 1954.
- [3] A. J. F. Siegert, "A systematic approach to a class of problems in the theory of noise and others random phenomena -part ii, examples," *IRE Trans. Information Theory*, pp. 38-43, March 1957.
- [4] D. Slepian, "Fluctuations of random noise power," *Bell Sys. Tech. J.*, pp. 163-184, Jan. 1958.
- [5] M. I. Schwartz, "Distribution of the time-average power of a gaussian process," *IEEE Trans. Inform. Theory*, vol. 16, pp. 17-26, Jan. 1970.
- [6] C. W. Helstrom, "Distribution of the filtered output of a quadratic rectifier computed by numerical contour integration," *IEEE Trans. Inform. Theory*, vol. 32, pp. 450-463, July 1986.
- [7] C. W. Helstrom, *Elements of Signal Detection and Estimation*. ISBN 0-13-808940-x, Englewood Cliffs, NJ.: Prentice Hall, 1995.
- [8] I. T. Monroy and G. Einarsson, "Bit error evaluation of optically preamplified direct detection receivers with fabry-perot optical filters," *J. Lightwave Technol.*, vol. 15, pp. 1546-1553, August 1997.
- [9] A. Papoulis, *Probability, Random Variables, and Stochastic Processes*. McGraw-Hill Int. Editions, second ed., 1991.
- [10] S. D. Personick, "Applications for quantum amplifiers in simple digital optical communication systems," *Bell Systems Tech. Journal*, vol. 52, pp. 117-133, Jan. 1973.
- [11] G. Einarsson, *Principles of Lightwave Communications*. John & Wiley, 1996.

Paper F

An Optically Preamplified Receiver with Low Quantum Limit

Idelfonso Tafur Monroy

Partially presented at *1998 IEEE/LEOS Benelux Symposium*, Nov. 26, 1998, Gent, Belgium., pp. 197-200.

An Optically Preamplified Receiver with Low Quantum Limit

Idelfonso Tafur Monroy

Abstract—An optically preamplified receiver configuration resulting in a very low quantum limit is presented.

Indexing terms: Optical communications, quantum limit, noise analysis, preamplified receiver, optical amplifier.

Introduction: Optical amplifiers are proven to efficiently enhance the receiver sensitivity of optical communication systems. In optical communications it is of common practice to compare the systems ultimate sensitivity in terms of the quantum limit. The (standard) *quantum limit* is defined as the average number of photons per bit in the optical signal needed to achieve a bit-error probability of 10^{-9} assuming ideal detection conditions, which for a preamplified receiver means that a large amplifier gain is assumed. In this paper we firstly summarize the results on the quantum limit for different optically preamplified, OOK/DD receivers presented in the literature. Subsequently, we present a receiver scheme foreseen to outperform previously studied configurations.

System model: The schematic diagram of the studied receiver is illustrated in Fig. 1. The preamplifier is an EDFA (erbium-doped fiber amplifier) which is modeled as linear optical field amplifier with gain G and AWG (additive white Gaussian) noise $n(t)$ representing the ASE (amplified spontaneous emission) noise. The spectral parameter of $n(t)$ is given by $N_0 = n_{sp}(G - 1)h\nu$, where n_{sp} is the amplifier spontaneous emission factor, h is the Planck's constant, and ν optical frequency. An optical filter $r(t)$ is used to limit the effect of ASE on the system performance, and in the case of WDM (wavelength division multiplexing) systems, to select the desired channel. The incoming signal is a binary sequence of rectangular pulses $S(t)$. At the output of the filter $r(t)$ and the signal is denoted by $Y(t)$ the resultant colored Gaussian noise by $X(t)$. With the above notations the incident optical field on the photodetector becomes: $B(t) = Y(t) + X(t)$. The optical filter is a finite-time integrator over the bit duration time $[0, T]$ whose impulse response $r(t)$ is given by

$$r(t) = \begin{cases} \frac{1}{T}, & 0 \leq t \leq T \\ 0, & \text{otherwise.} \end{cases} \quad (1)$$

The postdetection filter is assumed to be an integrate-and-dump filter. The integration interval I is chosen to be $[T - dT/2, T + dT/2]$. The parameter d is going to be selected so that it yields the lowest bit-error probability.

Performance Analysis: For the performance analysis we need a complete statistical description of the receiver decision variable. The moment generating function (MGF)

Eindhoven University of Technology, Telecommunications Technology and Electromagnetics, P. O. Box 513, 5600 MB Eindhoven The Netherlands, E-mail: i.tafur@ele.tue.nl

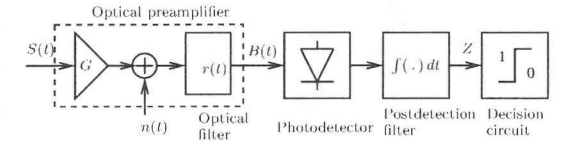


Fig. 1. Optically preamplified OOK receiver

provides us with such statistical information. The MGF for the receiver decision variable Z is given by $M_Z(s) = M_\Lambda(e^s - 1)$, where Λ is the so-called Poisson parameter [1]. For an integrate-and-dump post-detection filter $\Lambda = \frac{1}{2} \int_I |Y(t) + X(t)|^2 dt$. Based on the MGF for the decision variable Z , error probabilities are expeditiously computed by the so-called saddlepoint approximation [2, 3].

The general mathematical form for the MGF of Λ , $M_\Lambda(s) = E\{e^{s\Lambda}\}$, is well known, e.g. [2] and can be represented as

$$M_\Lambda(s) = [D(s)]^{-1} \exp[F(s)], \quad (2)$$

where $F(s)$ and $D(s)$ are found by solving the so-called Fredholm integral equations, e.g., [2, 4]. For the present case we have that

$$F(s) = mG[b_0^2 H_1(s) + (b_{-1}b_0 + b_0b_1)H_2(s) + (b_{-1}^2 + b_1^2)H_3(s)], \quad (3)$$

with

$$\begin{aligned} H_1(s) &= \frac{s}{\beta \cos \beta} [\sin x(2d - 4) + \sin \beta(4 - d^2/2 - 2d)] \\ &\quad + \frac{2}{\sigma^2 \beta \cos \beta} [\sin \beta - \sin(x)] - d \frac{\cos x}{\sigma^2 \cos \beta} \\ H_2(s) &= \frac{s}{\beta \cos \beta} [d \sin \beta - d \sin x - d^2 \sin \beta/2] \\ &\quad + d \frac{\cos x}{\sigma^2 \cos \beta} + \frac{2}{\sigma^2 \beta \cos \beta} [\sin x - \sin \beta] \\ H_3(s) &= \frac{1}{\beta \cos \beta} [sd^2 \sin \beta/4 \\ &\quad - \frac{1}{\sigma^2} (d\beta \cos x/2 + \sin \beta - \sin x)] \end{aligned}$$

where m is the number of received photons in an optical pulse for a transmitted symbol "one". The parameter $\sigma^2 = n_{sp}(G - 1)$, $\beta = \sqrt{2\sigma^2}s$, and $x = \beta(1 - d/2)$. The Fredholm determinant is given by $D(s) = \cos(\sqrt{2\sigma^2}s)^d$. We observe that for this receiver configuration only a single past and one succeeding bit (with respect to the present observed bit b_0) produce intersymbol interference on the present transmitted bit. Hence the bit sequence of interest is (b_{-1}, b_0, b_1) .

Optical filter type	Quantum limit
Match filter	38.4 [3, 5] ^a
Integrate-and-dump	46.3 [6] ^a
Lorentzian, Optimal $B_{3dB}T = 7$	49.9 [4] ^a
Lorentzian, Optimal $B_{3dB}T = 3.7$	44.5 [5] ^b
Finite-time integrator	59.6 (Fig. 2) ^a
Finite-time integrator	16.2 (Fig. 2) ^b

TABLE I

Quantum limit for optically preamplified OOK/DD receivers. Postdetection integration interval a) : regular $[0, T]$, b) : optimized.

A plot of the quantum limit as a function of the integration interval dT is presented in Fig. 2. We observe that the lowest quantum limit is 16.2 photons/bit for a factor $d = 0.12$ and a value of $G = 20$ dB. If the value of G is large and the integration interval dT is made small and optimized (yielding the lowest error probability) the proposed receiver scheme has a lower quantum limit compare to the previously studied configurations; see Table I. In Table I is presented the reported quantum limit for preamplified receivers with different optical filters. The match filter situation is the case when the optical signal is assumed to pass the optical filter undistorted and that $X(t)$ is Gaussian band-limited (ideal bandpass filter assumed).

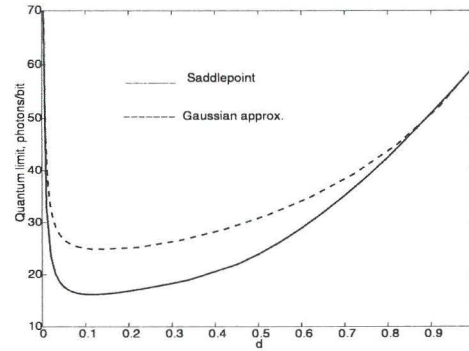
Gaussian approximation: The error probabilities may also be computed by using the common Gaussian approximation for the statistics for the receiver decision variable. This approximation requires the mean E_A and variance Var_A to be known. The mean and variance of A can be found either by using the properties of the MGF or by solving a set of integrals involving $Y(t)$ and the autocorrelation function of $X(t)$ [4]. The resultant expressions are:

$$E_A = mG[b_0^2(2d - d^2 + d^3/6) + (b_{-1} + b_1)d^3/12 + (b_{-1}b_0 + b_1b_0)(d^2/2 - d^3/6)] + \sigma^2 d \quad (4)$$

$$\text{Var}_A = mG\sigma^2\left[\frac{b_0^2}{120}(240d^2 - 160d^3 - 2d^5 + 35d^4) + \frac{(b_{-1}b_0 + b_1b_0)}{120}(60d^3 + 2d^5 - 25d^4) + \frac{(b_{-1}^2 + b_1^2)}{240}(15d^4 - 2d^5)\right] + \frac{2}{3}\sigma^4 d \quad (5)$$

In Fig. 2 is displayed the result of the Gaussian approximation for the quantum limit (dotted line). The minimum value is 24.8 photons/bit for an integration interval $d = 0.12$.

Summary: We have shown that if the optical filter is a finite-time integrator and the postdetection filter an integrator over a small interval centered around the end of each bit interval a quantum limit of 16.2 photons/bit can be achieved. Although a finite-time integrator optical filter (corresponding to a filter with a sinc shaped transfer function) is probably difficult to realize, the presented receiver configuration outperforms previously studied schemes (Table I). An interesting question, open for study, is which

Fig. 2. Quantum limit as a function of the integration interval d

value constitutes the ultimate theoretical lowest quantum limit for optically preamplified OOK/DD receivers.

References

- [1] S. D. Personick, "Applications for quantum amplifiers in simple digital optical communication systems," *Bell Systems Tech. Journal*, vol. 52, pp. 117-133, Jan. 1973.
- [2] C. W. Helstrom, *Elements of Signal Detection and Estimation*. ISBN 0-13-808940-x, Englewood Cliffs, NJ.: Prentice Hall, 1995.
- [3] G. Einarsson, *Principles of Lightwave Communications*. Chichester: John & Wiley, 1996.
- [4] I. Tafur Monroy and G. Einarsson, "Bit error evaluation of optically preamplified direct detection receivers with fabry-perot optical filters," *J. Lightwave Technol.*, vol. 15, pp. 1546-1553, August 1997.
- [5] S. R. Chinn, "Error-rate performance of optical amplifiers with fabry-perot filters," *Elec. Lett.*, vol. 31, pp. 756-757, April 1995.
- [6] I. Tafur Monroy, "On analytical expressions for the distribution of the filtered output of square envelope receivers with signal and colored gaussian noise input," *IEEE Trans. Commun.*, 1998, submitted for publication.

Chapter 6

Crosstalk in Optical Networks

This part of the thesis presents an extensive study of interferometric crosstalk in WDM optical networks. A statistical description is given, and ways to reduce its effects on the performance of WDM systems are outlined. This chapter is intended as an introduction to the general context of the papers included. Firstly, we describe the crosstalk mechanism, the characteristics of crosstalk, and the influence on the system performance. Secondly, methods to reduce interferometric crosstalk are discussed. Special emphasis is placed on phase scrambling; this reduction technique is investigated in detail in paper K.

6.1 Crosstalk mechanism

Let us consider a channel at a particular wavelength λ_1 at one extreme of an optical transparent network: mark "in" in Fig. 6.1. Due to performance imperfections of components in the optical nodes at the other extreme ("out" in Fig. 6.1), the channels will experience crosstalk interference from other channels operating at the same wavelength (inband crosstalk). Channels operating at different wavelengths may also fall within the receiver bandwidth giving rise to interband crosstalk. The effect of interband crosstalk can be reduced by concatenating narrow-bandwidth optical filters. Inband crosstalk, however, cannot be removed as the signal and the crosstalk operate at the same wavelength. The detrimental effect of inband crosstalk is further intensified in cascaded optical nodes due to its accumulative behavior.

6.2 Characteristics of crosstalk

If an optical signal $E_s(t)$ and a crosstalk interferer $E_x(t)$ are present at the input of a photodetector, the total optical field is given by their superposition. The output of a photodetector is a photocurrent proportional to the intensity of the detected optical field. This nonlinear operation on the detected field results in a photocurrent composed of three terms. The two first terms are the contribution of the average optical power in the signal and in the crosstalk, respectively. The third term is a fluctuating term due to the randomly changing phase difference between the signal and crosstalk. This is the interferometric crosstalk noise term. Postdetection filtering is used in optical receivers. The interferometric crosstalk

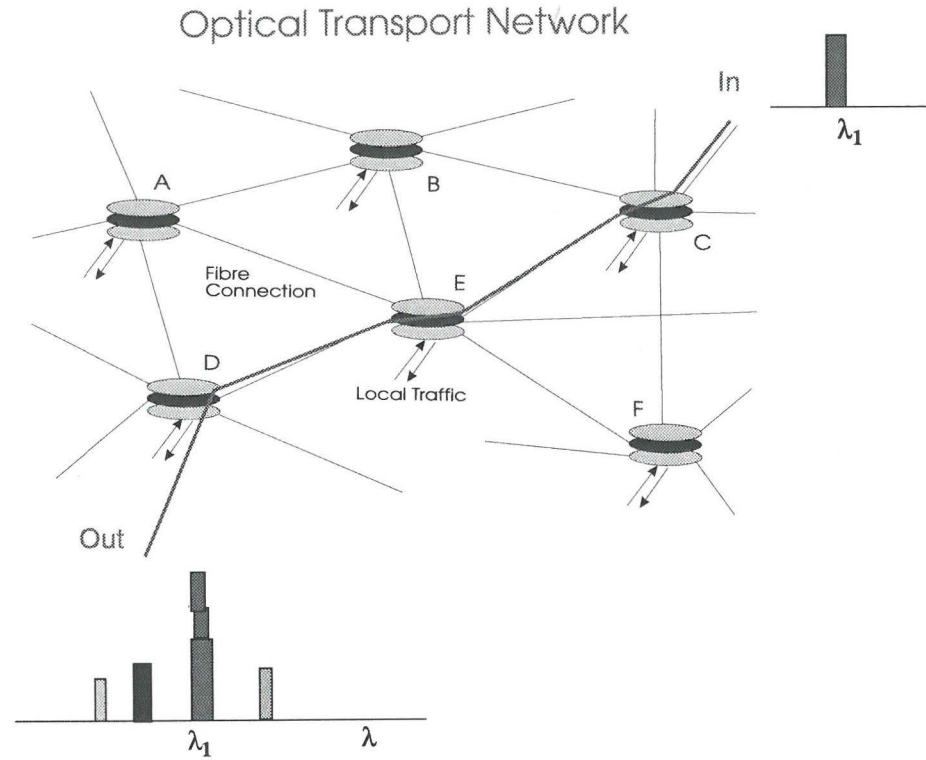


Figure 6.1: Crosstalk in optical cross-connected networks

contribution to the filtered photocurrent can be mathematically described as (see paper I):

$$\xi_{s,x} = \vec{r}_s \vec{r}_x \int_0^T \sqrt{g_s(t)g_x(t-\tau_d)} \cos[\phi_s(t) - \phi_x(t-\tau_d)] dt \quad (6.1)$$

if we consider an integrate-and-dump postdetection filter. The bit duration time is denoted by T . $\phi(t)$ is the phase, and $g(t) > 0$ is the optical pulse shape. The interferometric delay time is denoted by τ_d . \vec{r}_s and \vec{r}_x are unit vectors representing the signal and interferer polarization state, respectively. Expression (6.1) is difficult to describe statistically. It is composed of the $\cos(\cdot)$ operation on the phase difference between the signal and crosstalk. The laser phase is modeled as a Wiener process (variables $\phi_s(t)$, $\phi_x(t)$). Based on this assumption a statistical description is derived in paper I. It was found that if the bandwidth of the laser is of a larger magnitude than the receiver bandwidth, crosstalk can be substantially reduced by low-pass filtering. This is the idea behind crosstalk reduction by phase scrambling. We also observe that crosstalk depends on the interferometric delay time. It is found that the most detrimental effect takes place for τ_d in the order of the coherence time of the light source [74]. In several applications of interest the delay time is of a larger magnitude

than the coherence time ($B_L \tau_d \gg 1$). This situation is called the incoherent interferometric noise regime. We can also observe that if the delay time is such that the signal and crosstalk are in total bit misalignment, the signal-crosstalk beating term will disappear. This fact has been employed to demonstrate crosstalk reduction by bit misalignment [75].

Another variable present is the polarization state. The study of the effect of polarization statistics on the system performance has shown that polarization has a tendency toward its worst case alignment. No substantial performance difference was found between a worst case polarization matching and a linear polarization state of signal and crosstalk [76] (see also paper G). Other characteristics of crosstalk are related to non-perfect extinction ratio and optimized detection threshold. It is found that the crosstalk is more detrimental in systems with non-perfect extinction ratio. It also found that a proper optimization of the detection threshold yields more tolerance toward crosstalk compared to the commonly used midway (between digital zero and one) threshold setting [77, 78]. Appendix A gives some examples on how the performance of a system is related to the abovementioned characteristics of interferometric crosstalk.

6.3 Reduction techniques for crosstalk

As mentioned in the previous section there are some characteristics of crosstalk that can be used to reduce its detrimental effect on the systems performance. These techniques include phase scrambling, bit misalignment, and polarization scrambling. Crosstalk reduction by other techniques like coding [79] and intra-bit modulation [77] have also been proposed. Crosstalk reduction by coding will be at the cost of information redundancy and transmitter/receiver complexity. Reduction by bit-pattern misalignment is based on the assumption that we can manipulate the interferometric delay before crosstalk signals are switched, thus before crosstalk is added to the signal. This situation can be a difficult one to implement in complex cross-connect nodes. Another assumption of this technique is bit synchronization at the entrance of optical switching elements. Synchronization imposes a series of technical challenges. Another way to reduce crosstalk is to manipulate the phase of the optical signals. Based on this observation intra-bit modulation of DFB (distributed feedback) lasers has been proposed for crosstalk reduction purposes [77]. Alternatively, phase modulation may be performed by external modulation of the light source with a noise signal, i.e. phase scrambling [80–82]. This technique is explained in the following section. Crosstalk has also been considered as a traffic conflict. In this context, different approaches have been proposed based on the concept of dilation, both in space and time [83]. Although these techniques have not been fully explored yet, their hardware implementation and the finding of effective algorithms appear to be challenging.

6.4 Phase scrambling

The mechanism behind crosstalk reduction by phase scrambling is the redistribution of noise energy into higher frequencies permitting an improved noise rejection by the receiver filter. This idea is illustrated in Fig. 6.2. The schematic diagram of phase scrambling implementation in a transmitter is presented in Fig. 6.3.

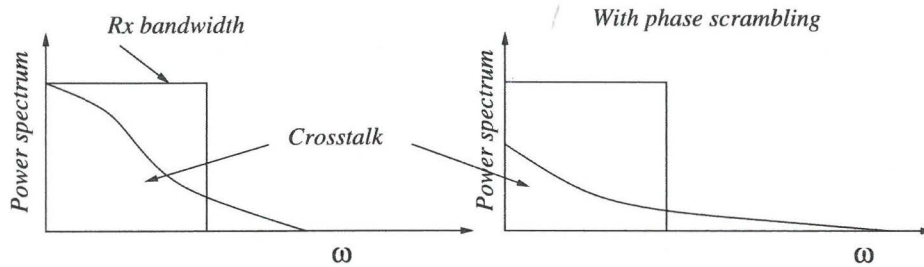


Figure 6.2: Redistribution of noise energy by phase scrambling.

The phase modulation is induced via a noise signal. This is done to assure that crosstalk reduction takes place for all possible interferometric delay times and simultaneously for the several crosstalk sources present. This is the main reason why phase modulation with a deterministic signal is not preferred.

Benefits of phase scrambling

WDM systems impose severe requirement on the optical crosstalk isolation of the constituent elements. For instance, crosstalk isolation levels better than 35 dB should be used to have power penalties smaller than 1 dB when even a moderate number of crosstalk interferers are present [84]. This still is a strict requirement for the performance of integrated optical switches and cross-connects at the current state-of-the-art [85]. Although improvements in device performance is foreseen, a substantial relaxation of the crosstalk requirements from individual components in an optical network can be achieved by using phase scrambling. Phase scrambling has been shown to significantly reduce crosstalk (see paper K). It is efficient in the presence of multiple crosstalk sources as well as for any interferometric time delay. It is possible to share the external phase modulator between several channels. This is an advantage of phase scrambling over coding techniques where dedicated equipment is required for each channel and receiver. Moreover, phase scrambling may be beneficial in preventing nonlinear effects during transmission. Namely, it can assure the required phase un-correlation (walk-off) needed to avoid the four-wave mixing effect discussed earlier in Sec. 3.4.

Limitations

Phase scrambling results in broadening of the signal spectrum. This implies that penalties as a result of phase noise to intensity noise conversion due to chromatic dispersion may be incurred. In fact, the spectrum can not be made arbitrarily broad as large power penalties due to dispersion will then take place. In conclusion, phase scrambling reduces crosstalk but introduces limitations with respect to the transmission distance due to dispersion penalties. This aspect is investigated in paper K. The main result is that by properly choosing the parameters for phase scrambling, crosstalk can be reduced and transmission is possible up

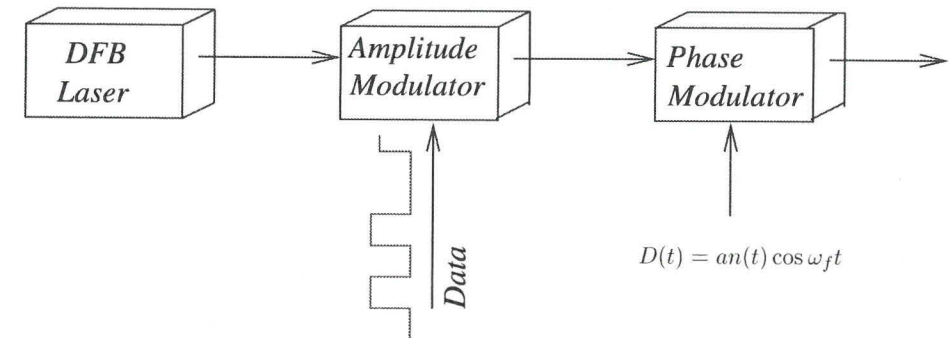


Figure 6.3: The signal is phase modulated with noise $D(t)$, centered at an arbitrary frequency ω_f and modulation index a .

to 100 - 200 km SSMF (standard single mode fiber) with acceptable power penalties. This result shows that phase scrambling can be used to reduce crosstalk (allowing for the use of today optical integrated technology) in networks covering LAN and MAN distances.

6.5 Scalability of optical networks

Consider a network of interconnected cross-connects. Scalability addresses the issues of how many cross-connects can be traversed before falling below a certain measure of quality service (QoS), for example, a level of bit-error rate (BER). We can distinguish scalability with respect to the following:

- Number of input fibers to a cross-connect node
- Number of channels per fiber
- Channel spacing
- Accumulated ASE and power budgets
- Optical crosstalk
- Network topology

Scalability in WDM networks is strongly limited by interferometric crosstalk. Other limiting aspects include accumulated ASE, deterioration of the extinction ratio (contrast between power level for a binary "one" and a "zero"), dispersion, and the aspects already mentioned in section 3.4 such as the effects of nonlinearities.

Paper L studies scalability of optical networks with respect to crosstalk and topology. A largest shortest transmission path (LSTP) in the network is considered. A LSTP criterion means that we consider the set of shortest paths between any pair of nodes in the network.

We select from this set the path that traverses the greatest number of cross-connect nodes.

The study is generalized to a wider class of network topologies in paper **M** by including statistics over all possible connections in a given network. The main conclusion is that the performance of networks with respect to crosstalk is closely related to the network topology. Hence, for a given number of nodes there are ways of connecting them that make them less vulnerable to crosstalk.

The use of optical amplifiers also imposes scalability limitations due to the increase of the signal power needed to maintain a satisfactory signal-to-noise ratio against accumulated ASE. This aspect of scalability of networks is presented in paper **N**. Scalability of networks employing phase scrambling is reduced to the study of limitations imposed by fiber dispersion. Paper **K** presents more details and experimental results on this topic.

Paper G

Performance Evaluation of Optical Cross-Connects by Saddlepoint Approximation

Idelfonso Tafur Monroy and E. Tangdiongga

© 1998 IEEE. Reprinted, with permission, from *IEEE/OSA J. Lightwave Technol.*, Vol. 16, No. 3, pp. 317-323, March 1998.

Performance Evaluation of Optical Cross-Connects by Saddlepoint Approximation

Idelfonso Tafur Monroy and Eduward Tangdionga

Abstract—The impact of in-band crosstalk on the transmission performance of optical cross-connects, incorporating (de)multiplexers and space switches, is studied. A statistical description of the receiver decision variable that yields a performance analysis in good agreement with experiment is given. Bit error rate and power penalties are calculated using the so-called saddlepoint approximation which is numerically simple and gives accurate results.

Index Terms—Error analysis, optical communication, optical cross-connects, optical crosstalk.

I. INTRODUCTION

OPTICAL cross-connects are regarded as a promising solution to the increasing demand of routing flexibility and transport capacity of broadband communication systems. An example of the structure of an optical multiwavelength cross-connect is presented in Fig. 1.

Linear crosstalk in cross-connects can be classified as in-band or interband crosstalk, according to whether it has the same nominal wavelength as the desired signal or not. The effect of interband crosstalk can be reduced by concatenating narrow-bandwidth optical filters. In-band crosstalk, however, cannot be removed as the signal and the crosstalk operates at the same wavelength. The deteriorating effect of in-band crosstalk is further intensified in cascaded optical nodes due to its accumulative behavior. This paper studies the effect of in-band crosstalk on the error performance of optical cross-connects. It has been observed that the crosstalk induced noise shows a highly non-Gaussian (bounded) statistics [1]. The use of an approximate Gaussian (nonbounded) distribution results in performance analyzes predicting greater penalties than those using a bounded distribution [2]; see Fig. 6.

In this paper, a statistical description of the receiver decision variable is given through the moment generating function (mgf). The performance evaluation is carried out with the help of the so-called saddlepoint approximation, using the mgf for the decision variable, that is numerically simple and gives accurate results. The analysis takes into consideration the effects of linear random polarization, nonideal extinction ratio, and receiver thermal noise together with transmitted data statistics. Power penalties due to inband crosstalk have

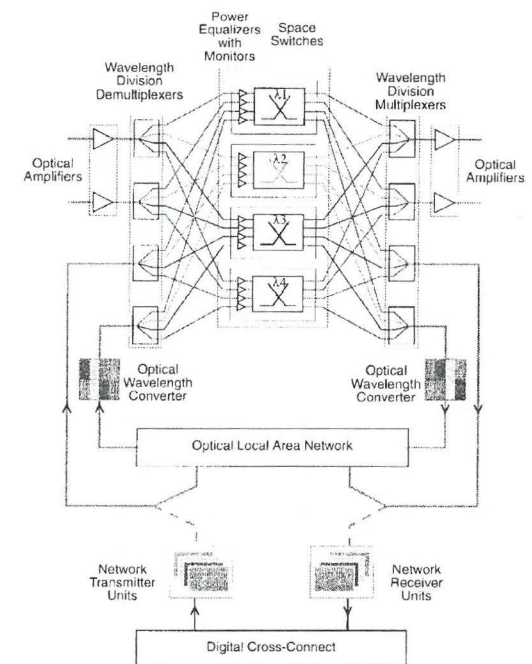


Fig. 1. An optical multiwavelength cross-connect.

been measured in an experimental setup that uses a directly modulated light source. Experimental results are in good agreement with the theory.

The paper is structured as follows: In Section II, the model of the system under analysis is presented. Section III presents the derivation of the mgf of the decision variable while Section IV introduces the saddlepoint approximation for calculating error probabilities. Section V describes the experiments. Comparison of experimental results and theory is also presented. Finally, in Section VI, summarizing conclusions are drawn.

II. SYSTEM MODEL

We consider an optical signal which has traversed an optical cross-connect consisting of (de)multiplexers and space switches (Fig. 1). The equivalent baseband form of the total

Manuscript received March 5, 1997; revised November 12, 1997. This work was supported in part by the European Community ACTS-BLISS project and IOP Electro-Optics phase 3 program.

The authors are with the Eindhoven University of Technology, Telecommunication Technology and Electromagnetics, 5600 MB Eindhoven, The Netherlands.

Publisher Item Identifier S 0733-8724(98)01905-7.

optical field is given by

$$\vec{S}_{\text{tot}}(t) = \vec{S}_s(t) + \vec{S}_x(t) \quad (1)$$

where, in general, $\vec{S}(t)$ is the envelope (modulation) of the input optical signal $\vec{s}(t)$, expressed as the real part of a complex field function

$$\vec{s}(t) = \text{Re}\{\vec{S}(t)\exp(j\omega_0 t)\} \quad (2)$$

$$\vec{S}(t) = A(t)\vec{r}\exp(j\phi(t)) \quad (3)$$

where $\omega_0 = 2\pi f$, f is the optical frequency, $\phi(t)$ is the phase, and $A(t) > 0$ is the optical pulse shape. The vector \vec{r} indicates the state of linear polarization. $\vec{S}_s(t)$ and $\vec{S}_x(t)$ represent the optical field, equivalent baseband form, of the desired signal and crosstalk interferer, respectively.

The output of the photodetector $I_{\text{sh}}(t)$ is a shot noise process characterized by a photoelectron intensity $\lambda(t)$. The time varying intensity of the photoelectron process is proportional to the instantaneous optical signal power. The instantaneous optical power is proportional to the squared magnitude of the electromagnetic field quantity. Hence, the photoelectron intensity can be written as

$$\lambda(t) = \frac{1}{2} \frac{\eta}{h f} |\vec{S}_{\text{tot}}(t)|^2 \quad \text{photoelectrons/s} \quad (4)$$

where η is the photodetector quantum efficiency and h is Planck's constant. This relation provides a connection between the electro-magnetic field model and the photon model of light, constituting the so called semiclassical approach of optical detection [3].

To continue the analysis, we return to the description of the optical field of the desired signal and the crosstalk, $\vec{S}_s(t)$ and $\vec{S}_x(t)$, respectively

$$\vec{S}_s(t) = \sqrt{b_k^s} A_s(t) \vec{r}_s e^{j(\phi_s(t))} \quad (5)$$

$$\vec{S}_x(t) = \sqrt{cb_k^x} A_x(t) \vec{r}_x e^{j(\phi_x(t))} \quad (6)$$

where ϵ is the component power crosstalk parameter: the ratio of leakage crosstalk to signal power. The quantity b_k ($k = 0, \pm 1, \pm 2, \dots$) is introduced to represent the binary symbols: $b_k \in \{\rho, 1\}$ ($0 \leq \rho < 1$). For the case of perfect extinction ratio we have $\rho = 0$. $\phi_{s,x}$ is the phase of the signal and crosstalk, respectively. \vec{r}_s and \vec{r}_x are real (we consider only linear polarization states) unit vectors representing the signal and crosstalk polarization state, respectively.

It is convenient to normalize the optical field (to avoid carrying the factor $\frac{\eta}{hf}$ along in further calculations) so that the photoelectron intensity can be written as

$$\lambda(t) = \frac{1}{2} |\vec{S}_{\text{tot}}(t)|^2 = \frac{1}{2} |\vec{S}_s(t) + \vec{S}_x(t)|^2. \quad (7)$$

It is assumed that the optical pulses are of identical shape, $A_s(t) = A_x(t) = A(t)$, and confined in the time interval $[0, T]$, implying absence of intersymbol interference (ISI). For a transmitted binary "one" m photons are contained in an optical pulse of duration T and for a binary "zero" ρm photons

are in the optical pulse. The amplitude of $A(t)$, following the normalization, is chosen such that

$$m = \frac{1}{2} \int_0^T |A(t)|^2 dt \quad (8)$$

where the factor $1/2$ comes from the complex notation.

The receiver thermal noise, denoted by $I_{\text{th}}(t)$, is modeled as an additive, zero mean, white Gaussian stochastic process. The shot noise and thermal noise current pass the electrical postdetector filter. Note that the shot and thermal noise are independent stochastic processes. The filtered signal $Z(t)$ is further sampled at $t = t_0 + kT$ time instants to form the decision variable. By comparing the sample value with a preselected threshold, the decision circuit provides an estimate of a transmitted bit in a particular bit interval.

III. THE MOMENT GENERATING FUNCTION

The postdetector filter is assumed to be an integrator over the time interval $[0, T]$. With no loss of generality we consider the time interval $[0, T]$ ($k = 0$) and denote the decision variable by $Z = Z(t=T)$

$$Z = \int_0^T [I_{\text{sh}}(t) + I_{\text{th}}(t)] dt \\ = X_{\text{sh}} + X_{\text{th}} \quad (9)$$

X_{th} is a zero mean, Gaussian distributed random variable (r.v.) with variance σ_{th}^2 given by

$$\sigma_{\text{th}}^2 = \frac{2K_B T_k T}{q_e^2 R_L} \quad (10)$$

K_B being the Boltzmann's constant, T_k the temperature in Kelvin, q_e the electron charge, and R_L the receiver resistance load. The mgf of the decision variable is

$$M_Z(s) = E\{e^{sZ}\} = M_{\text{sh}}(s)M_{\text{th}}(s) \quad (11)$$

where M_{th} is the mgf for a zero-mean Gaussian variable with variance σ_{th}^2

$$M_{\text{th}}(s) = e^{s^2 \sigma_{\text{th}}^2 / 2} \quad (12)$$

$M_{\text{sh}}(s)$ is the mgf of X_{sh} : the filtered shot noise contribution to the decision variable Z . The product of mgf in (11) is a consequence of the stochastic independence of the shot and thermal noise.

The filtered shot noise is well modeled by a doubly stochastic Poisson process with intensity $\lambda(t)$. Hence, for the case of an integrator postdetection filter, M_{sh} is given by [7]

$$M_{\text{sh}}(s) = M_{\Lambda}(e^s - 1) \quad (13)$$

where $M_{\Lambda}(s) = E\{e^{s\Lambda}\}$ and $\Lambda = \int_0^T \lambda(t) dt$ is the Poisson parameter.

A. Single Crosstalk Source

For the case of a single crosstalk source the parameter Λ has the form

$$\Lambda = \frac{1}{2} \int_0^T |\vec{S}_{\text{tot}}(t)|^2 dt \\ = m(b_0^s + cb_0^x) + 2m\sqrt{b_0^s b_0^x} \vec{r}_s \cdot \vec{r}_x \cos(\phi_s - \phi_x). \quad (14)$$

The bit alignment between the signal and crosstalk interferer is assumed to be perfect. Expression (14) is derived under the assumption that the relative phase difference is constant at least within one bit duration. The phase difference $\phi_s - \phi_x$ is assumed to be a uniformly distributed random variable in the interval $[0, 2\pi]$. The probability distribution function (pdf) of the variable $\xi = \cos(\phi_s - \phi_x)$ is the so called arcsine distribution. The pdf of ξ is given by [8]

$$f(\xi) = \begin{cases} \frac{1}{\pi\sqrt{1-\xi^2}}, & -1 < \xi < 1 \\ 0, & \text{elsewhere.} \end{cases} \quad (15)$$

Experimental measurements have shown that the statistics of in-band crosstalk induced noise approaches the form described by (15) [1].

The signal and crosstalk are assumed to exhibit linear polarizations with random, independent orientation angles θ_s and θ_x , respectively. The parameter Λ takes the form

$$\Lambda = m(b_0^s + cb_0^x) + 2m\sqrt{b_0^s b_0^x} \zeta(\theta_s, \theta_x) \xi \quad (16)$$

where the function $\zeta(\theta_s, \theta_x)$ is given by [4]

$$\zeta(\theta_s, \theta_x) = |\cos(\theta_s - \theta_x)| \quad (17)$$

$\theta_s - \theta_x$ is taken to be uniformly distributed in $[0, 2\pi]$. The pdf of ζ is given by the doubled, nonnegative part of an arcsine distribution [8]

$$f(\zeta) = \begin{cases} \frac{2}{\pi\sqrt{1-\zeta^2}}, & 0 < \zeta < 1 \\ 0, & \text{elsewhere.} \end{cases} \quad (18)$$

The mgf for Λ is derived from the pdf of the random variables involved in it. The result is (see Appendix for a derivation)

$$M_{\Lambda}(s) = \exp[sm(b_0^s + cb_0^x)] I_0^2(sm\sqrt{b_0^s b_0^x} \epsilon) \quad (19)$$

where $I_0(x)$ is the modified Bessel's function of zero order. The final expression of the mgf for Z is then

$$M_Z(s) = M_{\Lambda}(e^s - 1)M_{\text{th}}(s). \quad (20)$$

B. Multiple Crosstalk Sources

This section treats the case of in-band crosstalk when N interfering fields are present. We assume that each interferer has relative crosstalk power ϵ . The expression for the decision variable takes then the following form:

$$Z = mb_0^s + 2\sqrt{cm} \sum_{n=1}^N \sqrt{b_0^s b_0^{x,n}} \vec{r}_s \cdot \vec{r}_{x,n} \times \cos(\phi_s - \phi_{x,n}) \\ + 2cm \sum_{j=n+1}^N \sum_{n=1}^{N-1} \sqrt{b_0^{x,n} b_0^{x,j}} \cos(\phi_{x,n} - \phi_{x,j}) \\ + cm \sum_{n=1}^N b_0^{x,n} + X_{\text{th}}. \quad (21)$$

The decision variable (21) consists of the signal term, the signal-crosstalk beat terms, the crosstalk-crosstalk beat terms, self crosstalk beat term, and the receiver thermal noise. The third terms (crosstalk-crosstalk beat terms) have a variance smaller by $O(\sqrt{\epsilon})$ than the signal-crosstalk beating terms. However, in this paper the crosstalk-crosstalk beat terms are not neglected, but considered statistically independent and will be included in the performance analysis.

The error probability analysis is conducted by a weighted statistically average of the error probability for each value μ of the N crosstalk term being simultaneously "one." This probability is given by the binomial distribution

$$p(\mu) = \frac{N!}{(N-\mu)! \mu! 2^N}. \quad (22)$$

Hence, the average error probability P_e , for a given threshold α , is given by

$$P_e = \sum_{\mu=0}^N P_e(\alpha, \mu) p(\mu). \quad (23)$$

The N crosstalk sources are considered statistically independent. Hence, the mgf for Z is easily derived using (19) due to the fact that the mgf of a sum of independent r.v. is the product of the mgf for each r.v. in the sum. Note that the effect of nonperfect extinction ratio is also easily incorporated in the analysis by considering the total crosstalk field as the sum of μ field terms of amplitude $A(t)$ and $\nu = N - \mu$ field terms with amplitude $\sqrt{\rho}A(t)$. The bit-error rate for a given μ is calculated by the saddlepoint approximation; see Section IV-A.

IV. PERFORMANCE ANALYSIS

The question is to evaluate the average error rate P_e of the system under discussion. We are going to treat the case of amplitude shift keying (ASK) modulation format. The error probability, given that a binary "one" is transmitted is

$$q_-(\alpha) = P_{r1}(Z < \alpha) \quad (24)$$

where α denotes the decision threshold. Similarly, the error probability, given a binary "zero" is transmitted is

$$q_+(\alpha) = P_{r0}(Z > \alpha). \quad (25)$$

Assuming that the symbols are *a priori* equally probable, the average error probability is

$$P_e = \frac{1}{2} [q_-(\alpha) + q_+(\alpha)]. \quad (26)$$

A. Analysis by Saddlepoint Approximation

The saddlepoint approximation (spa) has been proposed by Helstrom [9], as an efficient and numerically simple tool for analyzing communication systems. The spa has shown a reasonably high degree of accuracy in the analysis of optical communication systems, e.g., [10].

As shown in [9], the tail probability $q_+(\alpha)$ is approximately equal to

$$q_+(\alpha) \approx \frac{\exp[\Phi(s_0)]}{\sqrt{2\pi}\Phi''(s_0)} \quad (27)$$

the so-called *saddlepoint approximation*. The function $\Phi(s)$ is related to the mgf for Z , $M_Z(s)$ by

$$\Phi(s) = \ln[M_Z(s)] - s\alpha - \ln|s|. \quad (28)$$

The parameter s_0 is the positive root of the equation

$$\Phi'(s) = 0 \quad (29)$$

and $\Phi''(s_0)$ stands for the second derivative of (28) at $s = s_0$. The lower probability tail

$$q_-(\alpha) = \int_{-\infty}^{\alpha} p(z) dz \quad (30)$$

is approximated by

$$q_-(\alpha) \approx \frac{\exp[\Phi(s_1)]}{\sqrt{2\pi}\Phi''(s_1)} \quad (31)$$

with s_1 equal to the negative root of (29). See [9] or [3] for further details. The error probability is minimized by adjusting the detection threshold α . The optimum value of α and the parameters s_0 , s_1 may be found numerically by solving an appropriate set of equations [3].

V. EXPERIMENTAL RESULTS AND DISCUSSION

The experimental arrangement depicted in Fig. 2 has been used to model the crosstalk interference in a cross-connect system. As transmitter, a DFB laser which has an unmodulated linewidth of 50 MHz at center wavelength of 1550 nm is directly driven by a pulse pattern generator. The generator produces repetitive $2^7 - 1$ PRBS of 2.5 Gb/s electrical signals. The extinction ratio is measured to be 8 dB. The laser light is divided into two paths. One path is regarded as the desired signal and the other the crosstalk. The crosstalk path is further divided into N channels by an $1 \times N$ photonic splitter. An optical attenuator, and polarization controller are located and adjusted to give each crosstalk channel an equal interference to the desired signal and obtain matched polarizations at the receiver. Fiber delays with different lengths are used to decorrelate all crosstalk channels.

In the experiment only three fiber delays are used with a different length of 500 m which far exceeds the laser coherence length. At the end the crosstalk channels are combined by an $N \times 1$ photonic coupler, and the desired signal after being interfered by the crosstalk is detected and examined using the bit error rate tester. As receiver, an InGaAs PIN photodetector with a responsivity of 0.9 A/W followed by a transimpedance amplifier has been used. The detector's sensitivity is about -26 dBm for a bit error rate of 10^{-9} . The electrical amplifier (EA) can give a maximum gain of 32 dB and has a noise figure of 5 dB. The electrical filter for suppressing the receiver thermal noise has a bandwidth of 1.75 GHz. The performance is

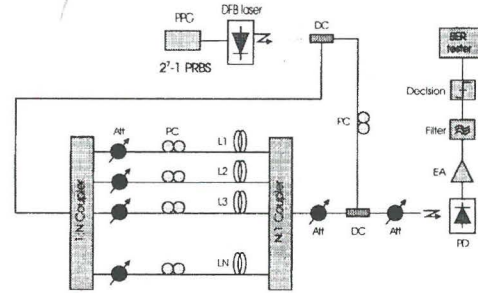


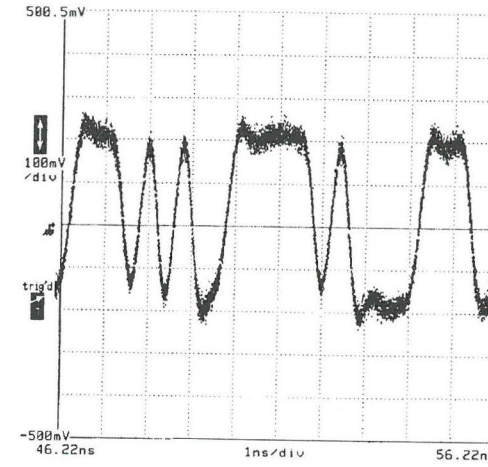
Fig. 2. Experimental setup used to model the crosstalk interference in a cross-connect system. PPG: Pulse pattern generator. DC: Directional coupler. Att: Attenuator. PC: Polarization control. PD: Photodetector. EA: Electrical amplifier.

measured using a fixed decision-threshold at midway between "one" and "zero."

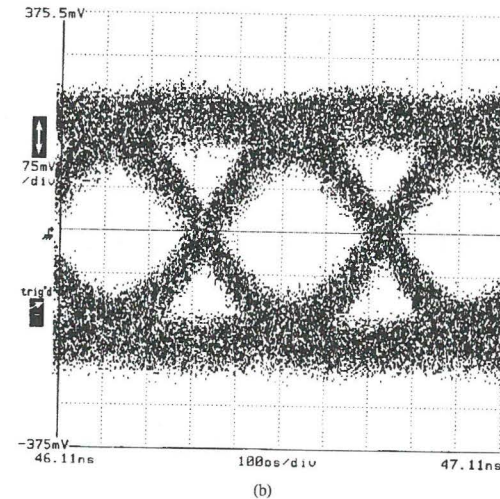
Fig. 3 shows the output of the receiver when there is no crosstalk source added in the system. We can see the presence of receiver thermal noise in bit "one" and "zero" as well. Next, the crosstalk channels are added to the signal channel. As an example, Fig. 4 gives a plot of the signal channel contaminated by three crosstalk channels of -20 dB each, relative to the signal channel power. The envelope of the interference is not constant. At the edges of the pulses where the frequency variation due to chirp are maximum, small distortion can be observed. The shapes of the envelopes are further varied by bit delays as the results of different fiber delay used in the experiment setup.

Measured and theoretical bit-error rate curves for a single crosstalk source and different values of ϵ are presented in Fig. 5. In Fig. 6 measured results are presented for power penalties together with the theoretical curves, calculated by the spa using the derived statistics for the receiver decision variable (solid lines). The result are in good agreement with the theory considering that discrepancies may arise due to additional penalties introduced by the signal processing and measurement errors. Analysis with linear randomly polarized signals resulted in power penalties non substantially different from those obtained for the worst case: precisely matched signal and crosstalk polarizations. This observation is in good agreement with an earlier published result stating that systems with randomly polarized fields show a statistical preference for near-worst-case operation [4]. In the experiment the polarization of signal and crosstalk are matched to simulate the worst case situation.

Measurements of crosstalk-induced power penalties in an optical cross-connect switch have been reported in [5] and [6]. The experimental setup reported in [5] and [6] uses an external modulated light source in contrast to a directly modulated source used in our experiment making a direct comparison of results difficult. Power penalties measured using a directly modulated source are reported in [2] for a single crosstalk source and at lower bit rate than that employed in the present work. Our result (see Fig. 6) shows the same general

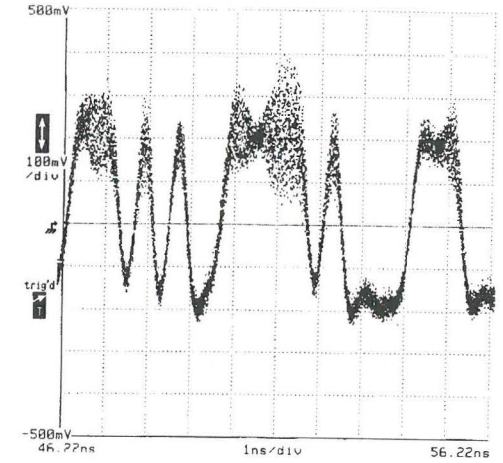


(a)

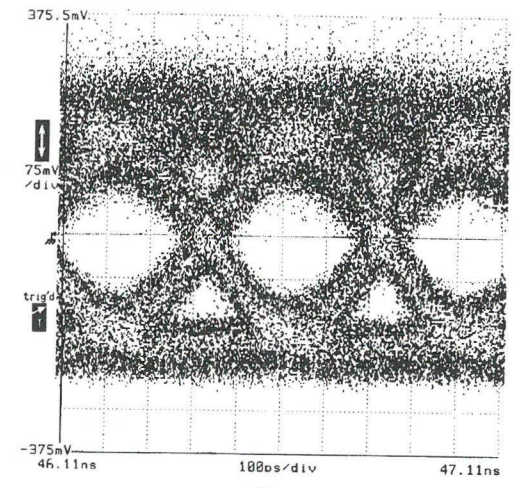


(b)

Fig. 3. The detected laser pulse pattern (a) and eye diagram (b) used in the crosstalk measurement. The laser is directly modulated with 2.5 Gb/s $2^7 - 1$ pseudo-random binary sequences.



(a)



(b)

Fig. 4. Optical pulses after interference by three crosstalk channels. The power of each crosstalk interferer is 20 dB under the signal power.

appearance as that in [2]: good agreement with experiment, assuming a bounded statistics for crosstalk.

The results for power penalties yielded by the Gaussian approximation are also shown in Fig. 6 (dash-dot lines). It can be observed that the analysis using a Gaussian distribution yields considerably greater power penalties than the bounded statistics approach, and than the measurement results.

VI. CONCLUSION

Performance analysis of in-band crosstalk in an optical cross-connect has been studied using a comprehensive statistical approach. Supporting measurements, using a directly

APPENDIX

This appendix gives a short derivation of the mgf for the signal-crosstalk term of the receiver decision variable in (16).

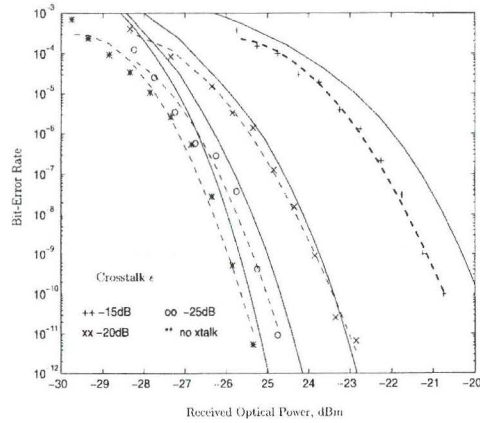


Fig. 5. Bit error rate for a single crosstalk source and different values of the parameter ϵ . The dotted lines are obtained by interpolation of the experimental data. The solid lines are the theoretical curves calculated by the spa.

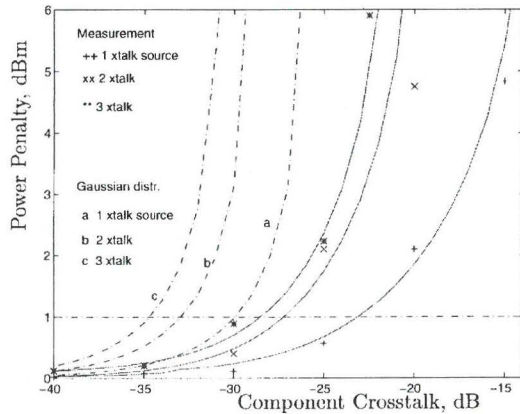


Fig. 6. Power penalties for a single, two, and three crosstalk sources. Signal and crosstalk polarizations are aligned to simulate a worst-case operation. The solid lines are the theoretical curves calculated by the spasing the bounded statistics approach. The dash-dot lines are the results when the crosstalk induced noise is assumed to be Gaussian distributed.

The r.v in consideration, simplified in notation, is of the type $y = \zeta\xi$. Conditioning on the value of ζ the mgf for y is

$$M_{y|\zeta}(s) = E_{\xi|\zeta}\{e^{s\zeta\xi}\} \quad (32)$$

or in terms of the pdf of ξ , expression (15),

$$M_{y|\zeta}(s) = \int_{-1}^1 \frac{e^{s\zeta\xi}}{\pi\sqrt{1-\xi^2}} d\xi. \quad (33)$$

An analytical solution to the integral (33) is given by (9.6.18) in [11]

$$M_{y|\zeta}(s) = I_0(s\zeta) \quad (34)$$

where $I_0(x)$ is the modified Bessel's function of zero order.

As we know the pdf of ζ , cf. (18), the unconditioned mgf $M_y(s)$ can be written as

$$M_y(s) = \int_0^1 \frac{2I_0(s\zeta)}{\pi\sqrt{1-\zeta^2}} d\zeta. \quad (35)$$

An analytical expression for (35) can be found by using [12, eq. (6.567)]. Finally, the result, which is used in the derivation of (19), is

$$M_y(s) = I_0^2(s/2). \quad (36)$$

ACKNOWLEDGMENT

The authors would like to thank Dr. M. O. van Deventer, KPN Research, Leidschendam, The Netherlands, for the support in carrying out the measurements. Prof. G. Einarsson, Prof. H. J. Butterweck, Dr. H. de Waardt, and Dr. H. Dörren are acknowledged for valuable discussions. The authors thank the anonymous reviewers for comments improving the presentation.

REFERENCES

- [1] M. Tur and E. L. Goldstein, "Probability distribution of phase-induced intensity noise generated by distributed feed-back lasers," *Opt. Lett.*, vol. 15, no. 1, pp. 1-3, Jan. 1990.
- [2] P. T. Legg, M. Tur, and I. Andonovic, "Solution paths to limit interferometric noise induced performance degradation in ask/direct detection lightwave networks," *J. Lightwave Technol.*, vol. 14, pp. 1943-1953, Sept. 1996.
- [3] G. Einarsson, *Principles of Lightwave Communications*. New York: Wiley, 1996.
- [4] E. L. Goldstein, L. Eskildsen, Y. Silberberg, and C. Lin, "Polarization statistics of crosstalk-induced interferometric noise in transparent lightwave networks," in *Proc. ECOC'95-Brussels*, Brussels, Belgium, pp. 689-692.
- [5] E. L. Goldstein and L. Eskildsen, "Scaling limitations in transparent optical networks due to low-level crosstalk," *IEEE Photon. Technol. Lett.*, vol. 1, pp. 93-95, Jan. 1995.
- [6] E. L. Goldstein, L. Eskildsen, and A. F. Elrefaie, "Performance implications of component crosstalk in transparent lightwave networks," *IEEE Photon. Technol. Lett.*, vol. 6, pp. 657-660, May 1994.
- [7] L. Snyder, *Random Point Processes*. New York: Wiley-Interscience, 1975.
- [8] A. Papoulis, *Probability, Random Variables, and Stochastic Processes*, 2nd ed. New York: McGraw-Hill, 1991.
- [9] C. W. Helstrom, "Approximate evaluation of detection probabilities in radar and optical communications," *IEEE Trans. Aerosp. Electron. Syst.*, vol. 14, pp. 630-640, July 1978.
- [10] C. W. Helstrom, "Performance analysis of optical receivers by saddle-point approximation," *IEEE Trans. Commun.*, pp. 186-190, Jan. 1979.
- [11] M. Abramowitz and I. A. Stegun, *Handbook of Mathematical Functions with Formulas, Graphs, and Mathematical Tables*, vol. XIV of *Dover Books on Advanced Mathematics*. New York: Dover, 1965.
- [12] I. S. Gradshteyn and I. M. Ryzhik, *Table of Integrals, Series, and Products*, 4th ed. New York: Academic, 1965.

Idelfonso Tafur Monroy was born in El Castillo (Meta), Colombia, in 1968 and graduated from the Bonch-Bruевич Institute of Communications, St. Petersburg, Russia, in 1992, where he received the M.Sc. degree in multichannel telecommunications. In 1993 he enrolled as a graduate student in the Department of Signals, Sensors and Systems at the Royal Institute of Technology, Stockholm, Sweden, where he received the Technology Licentiate degree in telecommunication theory in 1996. He is currently pursuing the Ph.D. degree in the Department of Electrical Engineering at the Eindhoven University of Technology, The Netherlands.

His research interests are in the area of optical cross-connect systems and optical communication theory.



Eduward Tangdionga was born in Makassar, Indonesia, in November 1968. He received the Diploma degree in electrical engineering (elektroniek ingenieur) from Eindhoven University of Technology (EUT), The Netherlands, in August 1994.

In December 1994, he joined the EUT Stan Ackermans Institute working on crosstalk in optical cross-connect networks. Currently, he is a Research Assistant at the Electro-Optical Communication Systems Group at EUT, where he is taking part in the ACTS project BLISS (Broadband Lightwave Sources and Systems).

Paper H

Statistical Analysis of Interferometric Noise in Optical ASK/Direct Detection Systems

Idelfonso Tafur Monroy

Syben'98, Zurich, Switzerland, May 18-22, 1998, pp 178-182.

Statistical analysis of interferometric noise in optical ASK/direct detection systems

Idelfonso Tafur Monroy

Eindhoven University of Technology, Telecommunication Technology and Electromagnetics.

P.O. Box 513, 5600 MB Eindhoven, The Netherlands.

ABSTRACT

An efficient method for evaluating the error probability of optical ASK/DD systems subject to interferometric noise is presented. The receiver decision variable is statistically described by its moment generating function (mgf). The theoretical results, obtained with the aid of the new derived mgf, are in good agreement with experiment, employing directly modulated light sources, while the common used Gaussian statistics for the photocurrent yields larger power penalties. The analysis takes into consideration polarization statistics, photodetector shot noise, non-ideal extinction ratio, and receiver thermal noise. Error probabilities are calculated using the saddlepoint approximation which is numerically simple and gives accurate results.

Keywords: Optical noise, interferometric noise, optical communication, error analysis, bit-error rate.

1. INTRODUCTION

Interferometric noise has been reported to degrade the performance, introducing large power penalties and bit-error rate floors, of a variety of optical networks, e.g., all-optical trunk networks; see ¹ and references therein. Although for a proper performance analysis the statistical modeling of the noise is important, in the literature it has been of common practice to consider the interferometric noise to be Gaussian distributed, e.g., ^{2,1} in the analysis of ASK/DD optical system corrupted by a multiple number of interferers. For a very large number of interferers, according to the Central Limit Theorem, the Gaussian approximation may be invoked, but for a small and medium number of interferers the Gaussian approximation yields larger power penalties than those obtained by the exact analysis. A recursive convolution method for the analysis of interferometric noise is presented in ³ but convolving a large number of probability density functions is numerically complex. In this paper, an effective and numerical simple method for the performance analysis of optical systems disturbed by interferometric noise is presented. The decision variable is statistically described by its moment generating function (mgf). The mgf is then used to calculate bit-error probabilities by the so called saddlepoint approximation. The analysis takes into consideration polarization statistics, photodetector shot noise, non-ideal extinction ratio, and receiver thermal noise together with transmitted data statistics. Experimental results of power penalties due to interferometric induced noise, measured in an experimental setup that uses a directly modulated light source, are in good agreement with the theory.

2. SYSTEM MODEL

We consider the case of an optical informative signal disturbed by a number N of interferers operating at the same nominal wavelength. The optical field of the information signal $\vec{S}_s(t)$ and the interferers $\vec{S}_x(t)$ is given by their complex amplitude vectors

$$\vec{S}_s(t) = \sqrt{b_k} A_s(t) \vec{r}_s e^{j\phi_s(t)}, \quad (1)$$

$$\vec{S}_x(t) = \sum_{n=1}^N \sqrt{\epsilon_n b_k^{x,n}} A_{x,n}(t) \vec{r}_{x,n} e^{j\phi_{x,n}(t)}, \quad (2)$$

where ϵ is the crosstalk parameter: the ratio of leakage crosstalk to signal power. The indicator b_k is introduced to represent the binary symbols: $b_k \in \{\rho, 1\}$ ($0 \leq \rho < 1$). For the case of perfect extinction the ratio $\rho = 0$. $\phi_{s,x}$ is the

phase of the signal and interferer, respectively. \vec{r}_s and \vec{r}_x are real unit vectors representing the signal and interferer linear polarization state, respectively.

The output of the photodetector, $I_{sh}(t)$, is a shot noise process characterized by a photoelectron intensity $\lambda(t)$, which normalized can be written as

$$\lambda(t) = \frac{1}{2} |\vec{S}_s(t) + \vec{S}_x(t)|^2, \quad (3)$$

where the factor 1/2 comes from the complex notation.

The receiver thermal noise, denoted by $I_{th}(t)$, is modeled as an additive, zero mean, white Gaussian stochastic process. It is assumed that the optical pulses are of identical shape and confined in the time interval $[0, T]$, i.e. no intersymbol interference (ISI) is assumed. For a transmitted binary "one"

$$m = \frac{1}{2} \int_0^T |A(t)|^2 dt$$

photons are contained in an optical pulse of duration T and for a binary "zero" ρm photons are in the optical pulse.

3. PERFORMANCE ANALYSIS

The postdetector filter is assumed to be an integrator over the time interval $[0, T]$. With no loss of generality we consider the time interval $[0, T]$ ($k = 0$) and denote the decision variable by $Z = Z_{(t=T)}$.

$$Z = \int_0^T [I_{sh}(t) + I_{th}(t)] dt = X_{sh} + X_{th}. \quad (4)$$

X_{th} is a zero mean, Gaussian distributed random variable (r.v) with variance σ_{th}^2 given by

$$\sigma_{th}^2 = \frac{2K_B T_k T}{q_e^2 R_L}, \quad (5)$$

K_B being the Boltzmann's constant, T_k the temperature in Kelvin, q_e the electron charge, and R_L We are going to treat the case of amplitude shift keying (ASK) modulation format. The error probability, assuming that the binary symbols are *a priori* equiprobable, is

$$P_e = \frac{1}{2} [P_{r1}(Z < \alpha) + P_{r0}(Z > \alpha)] = \frac{1}{2} [q_-(\alpha) + q_+(\alpha)], \quad (6)$$

where α denotes the decision threshold. $q_-(\alpha), q_+(\alpha)$ is the error probability, given a binary "one" and a "zero" is transmitted, respectively.

3.1. Analysis by saddlepoint approximation

As it is shown in⁴ the tail probabilities $q_+(\alpha)$ and $q_-(\alpha)$ are approximately equal to

$$q_+(\alpha) \approx \frac{\exp[\Phi(s_0)]}{\sqrt{2\pi\Phi''(s_0)}} \quad \text{and} \quad q_-(\alpha) \approx \frac{\exp[\Phi(s_1)]}{\sqrt{2\pi\Phi''(s_1)}}, \quad (7)$$

the so called *saddlepoint approximation*. The function $\Phi(s)$ is related to the mgf for Z , $M_Z(s) = E\{e^{sZ}\}$, by

$$\Phi(s) = \ln[M_Z(s)] - s\alpha - \ln|s|. \quad (8)$$

The parameter $s_{0,1}$ is the positive and negative root of the equation $\Phi'(s) = 0$, respectively. $\Phi''(s_{0,1})$ stands for the second derivative of (8) at $s = s_{0,1}$. See⁴ or⁵ for further details. The error probability is minimized by adjusting the detection threshold α . The optimum value of α and the parameters s_0, s_1 may be found numerically by solving an appropriate set of equations.⁵

4. THE MOMENT GENERATING FUNCTION

The mgf of the decision variable is given by

$$M_Z(s) = M_{sh}(s)M_{th}(s), \quad (9)$$

where M_{th} is the mgf for a zero mean Gaussian variable with variance σ_{th}^2 : $M_{th}(s) = \exp(s\sigma_{th}^2/2)$. $M_{sh}(s)$ is the mgf of the filtered shot noise contribution to the decision variable Z . The shot noise is well modeled as a doubly stochastic Poisson process with intensity $\lambda(t)$. Hence, for the case of an integrator postdetection filter, M_{sh} is given by⁶

$$M_{sh}(s) = M_\Lambda(e^s - 1), \quad (10)$$

where $\Lambda = \int_0^T \lambda(t) dt$ is the *Poisson parameter*.

4.1. Single interferer source

The bit alignment between the information signal and the interferer is assumed to be perfect. The relative phase difference $\Delta\phi = \phi_s - \phi_x$ is assumed to be constant at least within one bit duration, and uniformly distributed in the interval $[0, 2\pi]$. The signal and the interferer are assumed to exhibit linear polarizations with random, independent orientation angles θ_s and θ_x , respectively. With the above mentioned assumptions the parameter Λ takes the form

$$\Lambda = m(b_0^s + \epsilon b_0^x) + 2m \sqrt{b_0^s b_0^x} \underbrace{\epsilon \zeta(\theta_s, \theta_x) \times \xi(\phi_s, \phi_x)}_{\text{Interferometric noise}}, \quad (11)$$

where the function $\zeta(\theta_s, \theta_x)$ and $\xi(\phi_s, \phi_x)$ are given by

$$\zeta(\theta_s, \theta_x) = |\cos(\theta_s - \theta_x)|, \quad \xi(\phi_s, \phi_x) = \cos(\phi_s - \phi_x), \quad (12)$$

with $\Delta\theta = \theta_s - \theta_x$ being uniformly distributed in $[0, 2\pi]$. The mgf for Λ is derived from the probability density function (pdf) of the random variables involved in it. The result is (see Appendix A for a derivation)

$$M_\Lambda(s) = \exp[sm(b_0^s + \epsilon b_0^x)] I_0^2\left(sm \sqrt{b_0^s b_0^x} \epsilon\right), \quad (13)$$

where $I_0(x)$ is the modified Bessel's function of zero order. The final expression for the mgf of Z is then

$$M_Z(s) = M_\Lambda(e^s - 1)M_{th}(s). \quad (14)$$

4.2. Multiple interfering sources

We assume that each interferer has relative interfering power ϵ . The expression for the decision variable takes then the following form

$$\begin{aligned} Z = & m b_0^s + 2m \sqrt{\epsilon} \sum_{n=1}^N \sqrt{b_0^s b_0^{x,n}} \zeta(\theta_s, \theta_{x,n}) \times \xi(\phi_s, \phi_{x,n}) + \\ & 2\epsilon m \sum_{j=n+1}^N \sum_{n=1}^{N-1} \sqrt{b_0^{x,n} b_0^{x,j}} \zeta(\theta_{x,n}, \theta_{x,j}) \times \xi(\phi_{x,n}, \phi_{x,j}) + \\ & \epsilon m \sum_{n=1}^N b_0^{x,n} + X_{th}. \end{aligned} \quad (15)$$

The error probability analysis is conducted by a weighted statistically average of the error probability for each value μ of the N interfering terms being simultaneously "one". This probability is given by the binomial distribution

$$p(\mu) = \frac{N!}{(N - \mu)! \mu! 2^N}. \quad (16)$$

Hence, the average error probability, for a given threshold α , is given by

$$P_e = \sum_{\mu=0}^N P_e(\alpha, \mu) p(\mu). \quad (17)$$

The N interfering sources are considered statistical independent. Hence, mgf for Z is easily derived using (13) due to the fact that the mgf of a sum of independent r.v is the product of the mgf for each r.v in the sum. Note that the effect of non-perfect extinction ratio is also easily incorporated in the analysis by considering the total interfering field as the sum of μ field terms of amplitude $A(t)$ and $\nu = N - \mu$ field terms with amplitude $\sqrt{\rho}A(t)$. The bit-error rate for a given μ is calculated by the saddlepoint approximation; see Sect. 3.1.

5. NUMERICAL RESULTS

In Fig. 1 are presented the results for power penalties, calculated by the spa using the derived mgf for the receiver decision variable (solid lines). The system parameters are those of the system presented in⁷ employing a directly modulated light source with $2.5 \text{ Gb/s } 2^7 - 1$ PRBS. The system operates at a central wavelength of 1550 nm. The extinction ratio is measured to be 8 dB, and the receiver resistance load is equal to 250Ω . The power penalties are related to a bit-error rate of 10^{-9} . The results yielded by the Gaussian approximation are also shown (dashed lines). As it can be observed in Fig. 1 good agreement between theory and experimental results exists. It is also observed that the analysis using a Gaussian distribution results in considerable greater power penalties for small number of interferers. However, as the number of interferers increases the Gaussian approximation performs better.

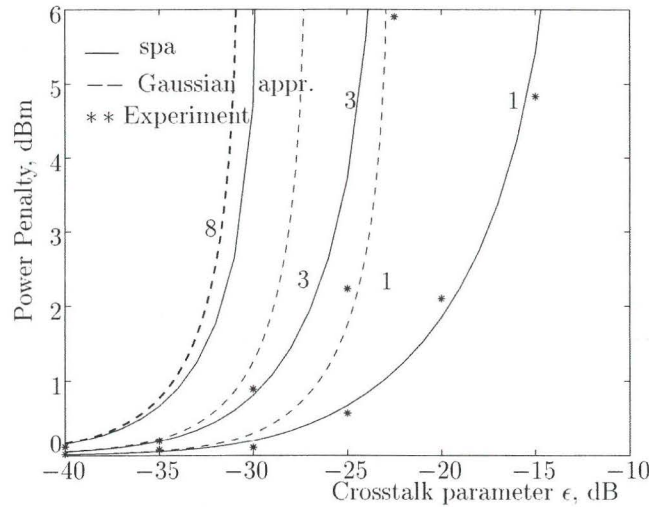


Figure 1. Power penalties for a single, three, and eight interfering sources. The solid lines are the power penalties, calculated by the spa using the exact statistics approach. The dashed lines are the results when the interferometric noise is assumed to be Gaussian distributed. The ** points are the experimental data for a single, and three interferers (data from Ref. 7. A directly modulated light source is used).

6. CONCLUSIONS

An analytical expression for the mgf of the decision variable of an optical ASK/DD system disturbed by interferometric noise is presented. The mgf is then used to calculate bit-error probabilities by the saddlepoint approximation,

which is numerically simple. The analysis accounts for the Poisson nature of the problem (shot noise) as well as for the case of linear polarization statistics of the interferometric noise, non-ideal extinction ratio and the thermal noise from the receiver electronic circuitry. The theory is in good agreement with experiment, considering differences due to experimental error. It is also shown that for a small and medium number of interferers the Gaussian approximation predicts more severe restrictions on the system crosstalk parameter than those yielded by the exact analysis.

APPENDIX A

This appendix gives a short derivation of the mgf for the signal-interferer term of the receiver decision variable in (11). The r.v in consideration, simplified in notation, is of the type $y = \zeta\xi$. In terms of the pdf of $\Delta\theta$, and $\Delta\phi$, the mgf of y is

$$M_y(s) = \frac{1}{(2\pi)^2} \int_0^{2\pi} \int_0^{2\pi} \exp[s|\cos \Delta\theta| \cos \Delta\phi] d\theta d\phi. \quad (18)$$

Integration over $\Delta\phi$, using the standard definition of the modified Bessel function $I_0(x)$, gives

$$M_y(s) = \frac{1}{2\pi} \int_0^{2\pi} I_0(s|\cos \Delta\theta|) d\theta = I_0^2(s/2), \quad (19)$$

with the aid of (6.6.681.3) in.⁸ The result in (19) is used for the derivation of (13).

ACKNOWLEDGEMENT

The author would like to thank Prof. G. Einarsson, Dr. J. Boersma and E. Tangdionga for their valuable comments and discussions. This work was performed in part within the framework of the European Community ACTS-BLISS project.

REFERENCES

1. P. T. Legg, M. Tur, and I. Andonovic, "Solution paths to limit interferometric noise induced performance degradation in ASK/direct detection lightwave networks," *J. Lightwave Technol.* **14**, pp. 1943-1953, Sept. 1996.
2. J. L. Gimlet and N. K. Cheung, "Effects of phase-to-intensity noise conversion by multiple reflections on gigabits-per-second DFB laser transmission systems," *J. Lightwave Technol.* **7**, pp. 888-895, June 1989.
3. W. D. Cornwell and I. Andonovic, "Interferometric noise for a single interferer: comparison between theory and experiment," *Elec. Letters* **32**, pp. 15001-15002, August 1996.
4. C. Helstrom, "Approximate evaluation of detection probabilities in radar and optical communications," *IEEE Trans. Aerosp. Electron. Syst.* **14**, pp. 630-640, July 1978.
5. G. Einarsson, *Principles of Lightwave Communications*, John & Wiley, 1996.
6. L. Snyder, *Random Point Processes*, Wiley-Interscience Publ., 1975.
7. E. Tangdionga and *et al.*, "Crosstalk penalties in cross-connected networks using externally and directly modulated lightwaves," *IEEE J. Sel. Areas Commun.*, 1998. Submitted for publication.
8. I. S. Gradshteyn and I. M. Ryzhik, *Table of Integrals, Series, and Products*, Academic press, fourth ed., 1965.

Paper I

On the Distribution and Performance Implications of Interferometric Crosstalk in WDM Networks

Idelfonso Tafur Monroy, E. Tangdionga, R. Jonker, and H. de Waardt
© 1999 IEEE. Reprinted, with permission, from *IEEE/OSA J. Lightwave Technol.*, Vol. 16, No. 6, pp 989-997, June 1999.

On the Distribution and Performance Implications of Filtered Interferometric Crosstalk in Optical WDM Networks

Idelfonso Tafur Monroy, Eduward Tangdiongga, and Huig de Waardt

Abstract—The distribution and performance implications of filtered interferometric crosstalk in optical networks is theoretically and experimentally studied. The probability density function is estimated by using a maximum entropy approach based on analytically derived statistical moments. The theoretical results are confirmed by relevant experimental data obtained from an amplitude shift keying direct detection (ASK/DD) system using directly, and externally modulated light sources. Power penalties are measured for both types of source modulation. The experimental results are in good agreement with theory.

Index Terms—Error analysis, optical crosstalk, optical communication, wavelength division multiplexing (WDM) networks.

I. INTRODUCTION

INTERFEROMETRIC crosstalk has been reported to degrade the performance, introducing large power penalties and bit error rate floors, of a variety of optical networks, e.g., all-optical trunk networks and wavelength division multiplexing (WDM) systems; see, e.g., [1]–[5]. For a reliable performance analysis of a communication system an accurate statistical description of the noise is required. Although the impact of interferometric noise on the performance of optical networks has been widely studied, the performance evaluation is commonly based on weakly crosstalk statistical assumptions. For instance, crosstalk has been assumed to be either arc-sine or Gaussian distributed, e.g., [2]–[7]. Performance analyzes assuming a two pronged arc-sine distribution for interferometric crosstalk have shown good agreement with experiment when the system uses a directly modulated light source, e.g., [4]–[7], while the Gaussian approximation gives pessimistic results. For systems employing externally modulated sources analyzes using the arc-sine distribution assumption appear to be too optimistic, while analyzes assuming Gaussian statistics have shown good agreement with experiment, e.g., [2]–[4], [8]. Furthermore, it has been observed that systems employing a directly modulated light source incurred smaller power penalties due to interferometric crosstalk than systems using external light source modulation [4], [8].

It is of relevant interest to accurately describe the statistics of filtered interferometric crosstalk for both types of source modulation in order to efficiently predict its impact on the performance of optical networks. In this paper, we present a statistical analysis of filtered interferometric crosstalk which is valid for arbitrary values of the laser 3-dB linewidth, interferometric delay, and electrical filter bandwidth. Of special interest is the dependence of the filtered interferometric crosstalk statistics on the value of the 3-dB laser bandwidth due to the fact that its value can differ significantly depending on the light source modulation type.

A maximum entropy approach is used to estimate the probability density function (pdf) of interferometric noise based on derived moments. The study shows that the statistics of filtered interferometric crosstalk (and the system performance) is strongly dependent on the product of the laser 3-dB linewidth and the electrical filter bandwidth. Namely, for filters with a large bandwidth the statistics of crosstalk shows a two pronged character, while for a narrower filter bandwidth the statistics reverts to a Gaussian-like type. Measured probability density functions and computer simulations confirm the theoretical pdf's. It is also observed that the interferometric crosstalk is substantially reduced (filtered out), resulting in a better system performance, when the 3-dB laser linewidth exceeds the filter bandwidth. This fact indicates that one can reduce interferometric crosstalk in optical networks by broadening (phase dithering) the laser spectrum as already pointed out in [9]–[11].

Power penalties due to interferometric crosstalk are measured for an amplitude shift keying direct detection (ASK/DD) system using directly, and externally modulated light sources. The experimental results are in good agreement with theoretical predictions. Based on the knowledge of the variance of filtered crosstalk a simple Gaussian approximation is proposed for computing power penalties.

The rest of the paper is structured as follows. Section II presents the system model under investigation. In Section III the derivation of moments of filtered crosstalk is given. In Section IV, based on the derived moments pdf's are estimated using a maximum entropy approach. A comparison of theoretical pdf's with simulated and measured pdf's is also presented. Section V is devoted to the performance analysis of optical systems disturbed by interferometric crosstalk. Power penalties are computed using the estimated pdf for filtered interferometric crosstalk. Experimental details are presented in Section VI.

Manuscript received July 23, 1998; revised February 23, 1999. This work was supported in part by the European Commission ACTS project AC332 APEX.

The authors are with the COBRA Institute, Telecommunications Technology and Electromagnetics, Eindhoven University of Technology, Eindhoven 5600 MB The Netherlands.

Publisher Item Identifier S 0733-8724(99)04511-9.

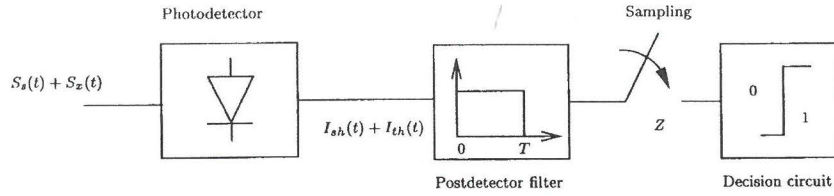


Fig. 1. Schematic diagram of an ASK/DD receiver. At the receiver input $S_s(t)$ represents the optical signal while interferometric crosstalk is denoted by $S_x(t)$.

Experimental results, their discussion and comparison with theory are the topics of Section VII. Finally, in Section VIII summarizing conclusions are presented.

II. SYSTEM MODEL

We consider the case of an optical signal disturbed by a crosstalk interfering source operating at the same nominal wavelength. The optical field of the signal $\vec{S}_s(t)$ and the crosstalk $\vec{S}_x(t)$ is given by their complex amplitude vectors

$$\vec{S}_s(t) = \sqrt{b_k} A_s(t) \vec{r}_s e^{j\phi_s(t)} \quad (1)$$

$$\vec{S}_x(t) = \sqrt{c b_k} A_x(t) \vec{r}_x e^{j\phi_x(t)} \quad (2)$$

where c is the crosstalk parameter: the ratio of leakage crosstalk to signal power. The indicator b_k is introduced to represent the binary symbols: $b_k \in \{0, 1\}$ ($0 \leq \rho < 1$). For the case of perfect extinction the ratio $\rho = 0$. The variable $\phi_{s,x}$ is the phase of the signal and interferer, respectively. The vectors \vec{r}_s and \vec{r}_x are unit vectors representing the signal and interferer polarization state, respectively.

We consider an ASK/DD receiver whose schematic diagram is depicted in Fig. 1. The output of the photodetector $I_{sh}(t)$ is a shot noise process characterized by a photoelectron intensity $\lambda(t)$, which normalized can be written as [5]

$$\lambda(t) = \frac{1}{2} |\vec{S}_s(t) + \vec{S}_x(t)|^2 \quad (3)$$

where the factor "1/2" comes from the complex notation.

The receiver thermal noise, denoted by $I_{th}(t)$, is modeled as an additive, zero mean, white Gaussian stochastic process. It is assumed that the optical pulses are of identical shape and confined in the time interval $[0, T]$, i.e., no intersymbol interference (ISI) is assumed. For a transmitted binary "one"

$$m = \frac{1}{2} \int_0^T |\Lambda(t)|^2 dt$$

photons are contained in an optical pulse of duration T and for a binary "zero" $0m$ photons are in the optical pulse.

The postdetection filter is assumed to be a finite time integrator over the interval $[0, T]$. With no loss of generality we consider the time interval $[0, T]$ ($k = 0$) and denote the decision variable by $Z = Z_{(t=T)}$

$$Z = \int_0^T [I_{sh}(t) + I_{th}(t)] dt = X_{sh} + X_{th} \quad (4)$$

X_{th} is a zero mean, Gaussian distributed random variable (RV) with variance σ_{th}^2 given by [15]

$$\sigma_{th}^2 = \frac{2K_B T_k T}{q^2 R_L} \quad (5)$$

K_B being the Boltzmann's constant, T_k denotes absolute temperature, q_e the electron charge, and R_L the receiver resistance load.

The moment generating function (MGF) of the decision variable is given by

$$M_Z(s) = E\{e^{sZ}\} = M_{sh}(s) M_{th}(s) \quad (6)$$

where M_{th} is the MGF for a zero-mean Gaussian variable with variance σ_{th}^2

$$M_{th}(s) = e^{s^2 \sigma_{th}^2 / 2} \quad (7)$$

$M_{sh}(s)$ is the MGF of X_{sh} : the filtered shot noise contribution to the decision variable Z . The product of MGF in (6) is a consequence of the stochastic independence of the shot and thermal noise.

The filtered shot noise is well modeled by a doubly stochastic Poisson process with intensity $\lambda(t)$. Hence, for the case of an integrator postdetection filter, M_{sh} is given by

$$M_{sh}(s) = M_\Lambda(e^s - 1) \quad (8)$$

where $M_\Lambda(s) = E\{e^{s\Lambda}\}$ and $\Lambda = \int_0^T \lambda(t) dt$ is the Poisson parameter [12].

The signal and the interferer are assumed to exhibit aligned state of polarization (worst case) and perfect bit alignment. With the above mentioned assumptions the parameter Λ takes the form

$$\Lambda = m(b_0^s + \epsilon b_0^x) + 2m\sqrt{b_0^s b_0^x} \epsilon \times \underbrace{\frac{1}{T} \int_0^T \xi(t) dt}_\gamma \quad (9)$$

where the function $\xi(t)$ is given by

$$\xi(t) = \cos[\phi_s(t) - \phi_x(t - \tau_d)] \quad (10)$$

in which τ_d is the interferometric delay time.

Conditioning on the value of γ the MGF for Λ is given by

$$M_{\Lambda|\gamma}(s, \gamma) = \exp[sm(b_0^s + \epsilon b_0^x)] \exp[2sm\sqrt{b_0^s b_0^x} \epsilon \gamma]. \quad (11)$$

The variable γ takes values in the interval $[-1, 1]$. Denoting the pdf of γ by $f_\gamma(\cdot)$ the unconditioned MGF for Λ can be written as

$$M_\Lambda(s) = \int_{-1}^1 M_{\Lambda|\gamma}(s, \gamma) f_\gamma(\gamma) d\gamma. \quad (12)$$

The pdf function $f_\gamma(\cdot)$ can be estimated from the moments of γ by using a maximum entropy approach [13]. Based on the knowledge of the MGF we can compute error probabilities by the so-called saddlepoint approximation as outlined in Section V.

III. MOMENT CHARACTERIZATION OF FILTERED INTERFEROMETRIC CROSSTALK

The laser phase [function $\phi_{s,x}(t)$ in (1) and (2)] is modeled as Wiener (Brownian motion) process whose autocorrelation is given by

$$R(t_1, t_2) = 2\pi\Delta\nu \min(t_1, t_2) = \beta \min(t_1, t_2) \quad (13)$$

where $\Delta\nu$ equals the 3-dB bandwidth of the Lorentzian shaped laser power spectrum [14].

The phase difference $\Delta\phi(t) = \phi_s(t) - \phi_x(t - \tau_d)$ is also a Wiener process, Gaussian distributed with zero mean and autocorrelation function given by

$$R_{\Delta\phi}(\tau) = \begin{cases} \beta(\tau_d - |\tau|), & |\tau| \leq \tau_d \\ 0, & |\tau| > \tau_d \end{cases} \quad (14)$$

The autocorrelation function of the process $\xi(t)$ is related to the autocorrelation of the process $\Delta\phi(t)$ in the following way ([15], Section VIII-C2)

$$R_\xi(\tau) = \frac{1}{2} e^{(-[R_{\Delta\phi}(0) + R_{\Delta\phi}(\tau)])} + \frac{1}{2} e^{(-[R_{\Delta\phi}(0) - R_{\Delta\phi}(\tau)])} \quad (15)$$

Substitution of (14) in (15) yields

$$R_\xi(\tau) = \begin{cases} \frac{1}{2} e^{-\beta|\tau|} [1 + e^{-2\beta(\tau_d - |\tau|)}], & |\tau| \leq \tau_d \\ e^{-\beta|\tau|}, & |\tau| > \tau_d \end{cases} \quad (16)$$

The autocorrelation functions (14) and (16) are used to derive the moments of filtered interferometric crosstalk.

A. The Moments

The filtered crosstalk [cf., (9)] is denoted by

$$\gamma = \frac{1}{T} \int_0^T \xi(t) dt = \frac{1}{T} \int_{t-T}^t \xi(t_1) dt_1. \quad (17)$$

The mean, first moment, of the variable γ is easily derived

$$\mu_1 = E\{\gamma\} = \frac{1}{T} \int_0^T E\{\cos[\Delta\phi(t)]\} dt = \exp\left(-\frac{\sigma_{\Delta\phi}^2}{2}\right). \quad (18)$$

By observing (18) and (16) we find that the process $\xi(t)$ is a wide-sense stationary stochastic (WSS) process. Thus, the second moment for γ can be found by [16]

$$\mu_2 = E\{\gamma^2\} = \frac{2}{T^2} \int_0^T (T - \tau) R_\xi(\tau) d\tau. \quad (19)$$

Inserting (16) in (19) it turns out that

$$E\{\gamma^2\} = \frac{1}{(\beta T)^2} [e^{-2\beta\tau_d} (e^{\beta T} - 1 - \beta T) + \beta T - 1 + e^{-\beta T}]. \quad \text{in which}$$

A plot of the variance of γ , $\text{Var}\{\gamma\} = E\{\gamma^2\} - (E\{\gamma\})^2$, for different values of β and τ_d is presented in Fig. 2, keeping a fixed value for T . For comparison reasons we use as reference an integrator filter with equivalent bandwidth defined as $B_e = (1/T)$. In the sequel, all considered filters are assumed to have the same noise equivalent bandwidth. As we can observe from Fig. 2 the variance of filtered interferometric crosstalk is

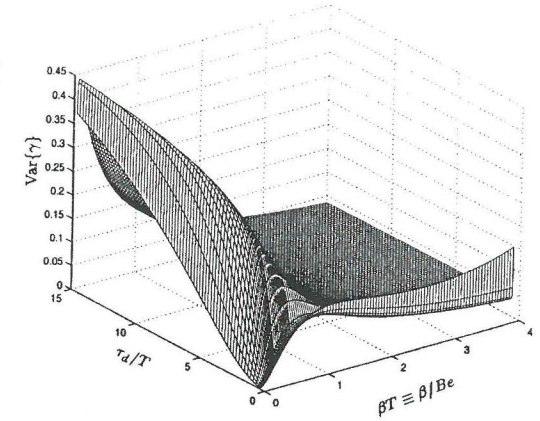


Fig. 2. Variance of filtered interferometric crosstalk.

strongly dependent on the relation between the values of β , τ_d , and T . For instance, if we consider the situation for $\beta T \rightarrow 0$ (negligible filtering), we have that the variance of γ increases with $\beta\tau_d$ from its minimum value zero to its maximum value of one-half for $\beta\tau_d \gg 1$. For the case of $\tau_d = 0$ the process $\Delta\phi(t)$ is a standard Brownian motion in contradistinction to a stationary Gaussian process when $\tau_d > 0$. For this particular case the variance of γ is an increasing function of βT .

We are interested in the regime when the interferometric noise is less damaging, i.e., when it has a small variance. It can be seen from Fig. 2 that this occurs when the values of τ_d/T and βT are large. It corresponds to the case of incoherent interferometric noise (interferometric delay time much larger than the light source coherence time) and a laser linewidth larger than the filter bandwidth. The fact that the variance decreases for large values of βT is an important characteristic of filtered interferometric crosstalk. It indicates that one can reduce interferometric crosstalk in optical networks by assuring a high value of $\beta T \equiv \beta/B_e$. As the value of the postdetection filter bandwidth is governed by the system bit rate, a high value β/B_e can be achieved, for instance, by broadening (phase dithering) the laser spectrum.

The higher moments of γ can be found by the following relation [17]:

$$\mu_k = \frac{k!}{2^{k-1} T^k} \sum_{\mathbf{a}} I_{\mathbf{a}}^{(k)}|_{t=T} \quad (20)$$

$$I_{\mathbf{a}}^{(n)} = \int_0^t e^{\beta b_n t_n} I_{\mathbf{a}}^{(n-1)} dt_n \quad (21)$$

with the initial condition $I_{\mathbf{a}}^{(0)} = e^{c\beta\tau_d}$. The parameters b_n , and c are given by (33) and (34), respectively. See Appendix A for a derivation.

The third moment is found to be equal to

$$\mu_3 = \frac{3}{8(\beta T)^3} \left[(1 + \beta T) e^{-(9/2)\beta T_d} + \left(1 + \frac{2}{3}(\beta T)^3 - 2\beta T + 2(\beta T)^2 \right) \cdot e^{-(1/2)\beta T_d} + (\beta T - 1) e^{2\beta T - (9/2)\beta T_d} - e^{-(1/2)\beta T_d - 2\beta T} \right].$$

The analytical expressions for higher moments become complex as the order increases. However, the recursion (21) is expeditiously solved by computer programs supporting symbolic integration. We have computed moments up to the twelve order.

In several applications of interest, for instance in WDM networks, the interferometric delay is of a larger magnitude than the laser coherence time ($\beta T_d \gg 1$). This situation is called the incoherent interferometric noise regime. For this case we notice that the terms containing exponentials of $-\beta T_d$ may be neglected and consequently the odd moments of the filtered interferometric crosstalk vanish and the even moments are function of the parameter βT alone. The resulting expression for even moments up to order four are given below

$$\mu_2 = \text{Var} \{ \gamma \} = \frac{1}{(\beta T)^2} [e^{-\beta T} + \beta T - 1] \quad (22)$$

$$\mu_4 = \frac{1}{48(\beta T)^4} [e^{-4\beta T} + 783 + 144(\beta T)^2 - 540\beta T - (240\beta T + 784)e^{-\beta T}]. \quad (23)$$

IV. PROBABILITY DENSITY FUNCTION OF FILTERED INTERFEROMETRIC CROSSTALK

A. Maximum Entropy Approach

The probability density of a random variable can be estimated by a maximum entropy approach based on its known moments [13]. Using this approach we have estimated the pdf of filtered interferometric crosstalk considering a laser source with a 3-dB linewidth of 45 MHz. If we use a filter with an equivalent bandwidth of 34, 141.3, 565.2 MHz, then the corresponding parameter βT is equal to 8.3, 2.0, and 0.5, respectively. In Fig. 3 is presented a plot of the estimated pdf for the three different values of βT . We observe that as the product βT increases the shape of the pdf changes from a two pronged one to a Gaussian like function shape for large values of βT .

The maximum entropy approach can be arbitrarily used for estimating an unknown pdf based on a finite number of moments. We performed computer simulations and experimental measurements to justify the use of the maximum entropy criterion in the performance evaluation of optical systems disturbed by filtered interferometric crosstalk.

B. Computer Simulation

The statistics of filtered crosstalk γ has also been studied with the aid of computer simulations. The simulations are

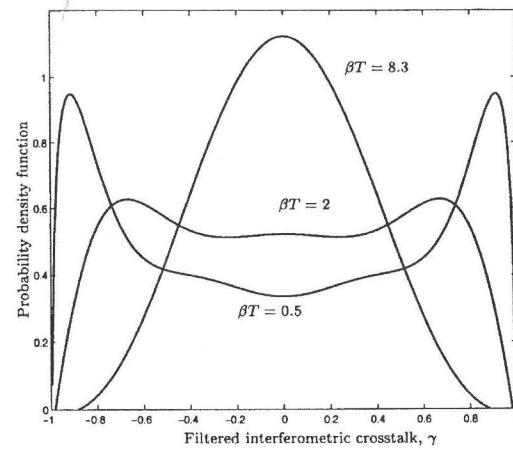


Fig. 3. Probability density function of filtered crosstalk as a function of βT . The pdf is estimated using a maximum entropy approach.

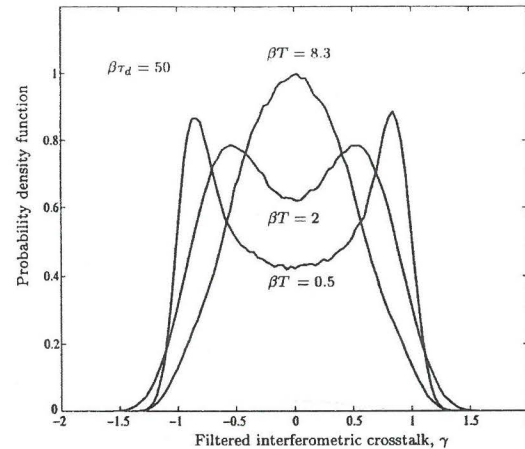


Fig. 4. Statistics of filtered interferometric crosstalk as a function of βT . Simulations results for a seventh-order Butterworth digital filter, using 10^6 samples.

performed in the following way. A process $\Delta\phi(t)$ is generated with a corresponding variance βT_d . Then the functional $\xi(t)$ is formed. Further, the process ξ is passed through a filter. The filter used is a seventh-order Butterworth digital filter. The filtered samples are then analyzed in a frequency histogram yielding an estimate of the probability density function of the filtered crosstalk. The simulated pdf of filtered crosstalk for the values of $\beta T = 0.5, 2.0$, and 8.3 with a fixed value $\beta T_d = 50.0$ is displayed in Fig. 4. It is observed again that the statistics changes from a two-pronged shape for small values of βT (wide bandwidth filter) to a Gaussian-like shape for larger values of βT (narrower bandwidth filter). This agrees well with the simulation results in [18].

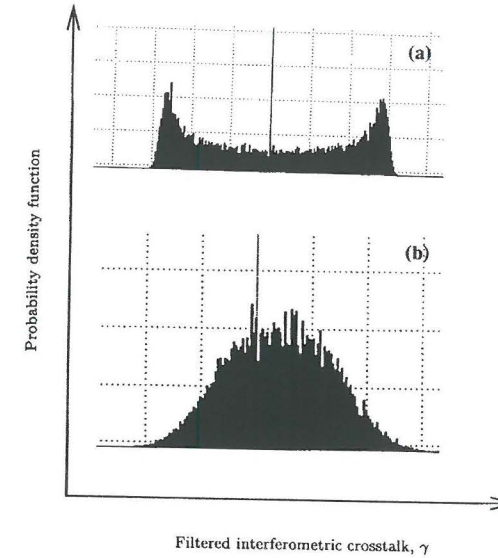


Fig. 5. Statistics of filtered interferometric crosstalk. Measured results for the incoherent regime. The 3-dB laser linewidth is 45 MHz. The filter bandwidth is (a) 2500 MHz ($\beta T = 0.11$) and (b) 34 MHz ($\beta T = 8.3$).

C. Measured pdf

Measured probability density functions of filtered interferometric crosstalk are shown in Fig. 5. Details of the experimental setup are presented in Section VI. The incoherent regime ($\beta T_d \gg 1$) is assured in the experiment. The laser 3-dB linewidth, continuous-wave (CW) operation, is measured to be 45 MHz. Two filters are used: 1) a filter with a 3-dB bandwidth of 2500 MHz. This case correspond, approximately, to having a value $\beta T = 0.11$ and 2) a filter with 34 MHz 3-dB bandwidth ($\beta T = 8.3$). The measured pdf's confirm the theoretical results (incoherent regime) on the reshaping of the statistics from a two pronged function to a Gaussian like shape as the filter bandwidth becomes smaller than the light source 3-dB linewidth; as βT increases. This result is in agreement with measurements reported by others workers in the field [1], [18], [19].

V. PERFORMANCE ANALYSIS

The question is to evaluate the average error probability for an ASK/DD system. The error probability, given that a binary "one" is transmitted is

$$q_-(\alpha) = P_{r1}(Z < \alpha)$$

where α denotes the decision threshold. Similarly, the error probability, given a binary "zero" is transmitted is

$$q_+(\alpha) = P_{r0}(Z > \alpha).$$

Assuming that the symbols are *a priori* equally probable, the average error probability is

$$P_e = \frac{1}{2} [q_-(\alpha) + q_+(\alpha)]. \quad (24)$$

A. Analysis by Saddlepoint Approximation

The saddlepoint approximation (SPA) has been proposed by Helstrom [20], as an efficient and numerically simple tool for analyzing communication systems. The SPA has shown a reasonably high degree of accuracy in the analysis of optical communication systems, e.g., [21].

As shown in [20] the tail probability $q_+(\alpha)$, and $q_-(\alpha)$, are approximately equal to

$$q_+(\alpha) \approx \frac{\exp[\Phi(s_0)]}{\sqrt{2\pi\Phi''(s_0)}} \quad \text{and} \quad q_-(\alpha) \approx \frac{\exp[\Phi(s_1)]}{\sqrt{2\pi\Phi''(s_1)}} \quad (25)$$

respectively, the so-called *saddlepoint approximation*. The function $\Phi(s)$ is related to the MGF for Z , $M_Z(s)$ by

$$\Phi(s) = \ln[M_Z(s)] - s\alpha - \ln|s|. \quad (26)$$

The parameters s_0 , and s_1 are the positive and negative root, respectively, of the equation

$$\Phi'(s) = 0 \quad (27)$$

and $\Phi''(s_{0,1})$ stands for the second derivative of (26) at $s = s_{0,1}$. (See [20] or [15] for further details.) The error probability is minimized by adjusting the detection threshold α . The optimum value of α and the parameters s_0, s_1 may be found numerically by solving an appropriate set of equations [15].

B. Gaussian Approximation

For simplicity reasons, in the performance analysis of a variety of communications systems, it is often assumed that the interfering noises are Gaussian distributed. We proposed to consider the filtered interferometric noise to be Gaussian distributed with mean zero and variance given by (22) instead of having a variance equal to one-half as assumed in previous analyzes, e.g., [2], [3]. This assumption simplifies the performance evaluation. It is found that the proposed Gaussian approximation yields reasonable good results for (small) crosstalk values ϵ that does not result in large power penalties (less than 2 dBm); see Figs. 7 and 8.

Until now we have considered the case of interferometric noise arising from a single interferer. In many applications, as in multichannel WDM networks, there will be a multiple number of interferers. Although in this work we do not present experimental results for the case of multiple interferers, in Appendix B we show how to include N sources of interferometric noise in the performance analysis.

VI. EXPERIMENT

The measurement setup to verify the theory is schematically given in Fig. 6. At the transmitter side, two light sources modulation schemes are used, namely, direct modulation in Fig. 6(a) and external modulation in Fig. 6(b). In Fig. 6(a) a distributed feedback (DFB) laser which has a CW-linewidth of 45 MHz is modulated directly by an electrical pulse pattern

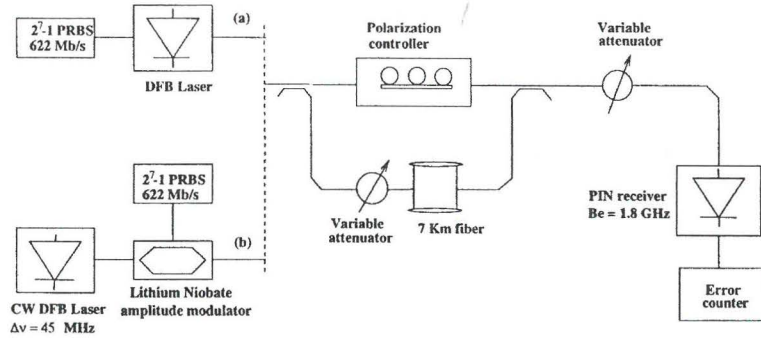


Fig. 6. Experimental setup used to measure power penalties due to filtered interferometric crosstalk. Two light source modulation schemes are used: (a) direct modulation and (b) external modulation.

generator with nonreturn-to-zero (NRZ) signals. The generated pseudorandom binary signals have a bit-rate of 622 Mb/s and their pattern is repeated after $2^7 - 1$ bits. By this direct modulation scheme we have obtained optical signals of an average extinction ratio of 15 dB.

In the external modulation scheme, Fig. 6(b), lightwaves coming from the DFB laser are coupled into a lithium niobate (LiNbO_3) modulator. The modulator is driven by the 622 Mb/s $2^7 - 1$ pseudorandom electrical signals. The resulting optical signals have an improved extinction ratio of 20 dB. Besides that, the spectral broadening or chirp which is very common in directly modulated laser is reduced. We have observed that the spectral width of external modulation is determined mainly by the modulation speed, i.e., 622 MHz whereas in direct modulation the combined effect of adiabatic and transient chirp makes the spectrum wider than that of external modulation. Measurements of the spectrum for the direct modulated light source case yielded values in the range from 1.9 to 2.4 GHz.

After the transmitter, the lightwaves are split to form a signal and a crosstalk path by a Mach-Zehnder structure with one of its arm 7 km longer than the other. The difference in the arm-length is intended to decorrelate information signals from crosstalk. The state of polarization of the information signal with respect to the crosstalk is matched to produce a worst case condition at the detection. In the crosstalk path a variable optical attenuator is located for crosstalk power adjustment relative to the signal power. Another attenuator is placed after the Mach-Zehnder structure to vary optical signal powers coupled to an optical detector for bit error rate (BER) evaluation.

As detector, a broad-band optical-to-electrical (O/E) converter followed by electrical filtering is used for studying the statistics of filtered signal-to-crosstalk beating noise. But for BER-evaluation and power penalty analysis a receiver module with a more sensitive InGaAs p-i-n photodetector incorporating also a high-gain electrical transimpedance amplifier is employed. The detector's sensitivity is around -30 dBm for a BER of 10^{-9} . The BER and power penalties measurements are performed using an optimized decision-threshold. The resulting BER values are lower than those obtained with a fixed threshold.

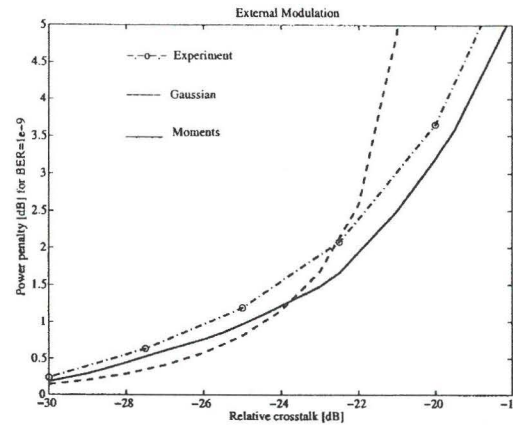


Fig. 7. Measured power penalties for the external light source modulation case (marks). The solid line represents the theoretical result (moment based) while the dotted line is the Gaussian approximation result.

VII. RESULTS AND DISCUSSION

A. External Modulation

Measured power penalties for an externally modulated light source, at a BER of 10^{-9} , as a function of the crosstalk power ϵ is presented in Fig. 7 (marks). The 3-dB laser linewidth is found to be mainly determined by the modulation rate. In Fig. 7 the solid line represents the theoretical result while the dotted line is the result by the Gaussian approximation. We can observe in Fig. 7 good agreement between theory and experiment. The Gaussian approximation gives reasonable good result for small values of ϵ that result in small power penalties while for large values of ϵ this approximation yields too pessimistic results.

B. Direct Modulation

The spectral line of light sources like a DFB laser is considerably broadened under direct modulation, e.g., [22] and [23]. This is due to the laser dynamics during the transitions from

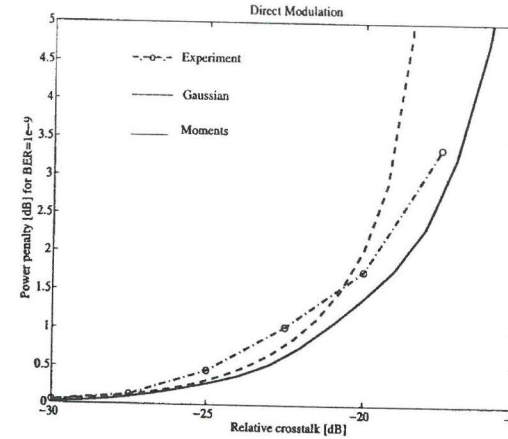


Fig. 8. Measured power penalties for a directly modulated light source (marks). The solid line represents the theoretical result (moment based) while the dotted line is the Gaussian approximation result.

one power level to another. This spectral broadening, "chirp," is a key differentiating property of directly modulated lasers from externally modulated lasers that experience negligible or smaller spectral broadening.

Interferometric noise arising from directly modulated DFB light sources has been shown to be bit-sequence dependent [24]. This fact together with the (dynamics) transient and adiabatic chirp properties of directly modulated sources make the analysis of interferometric noise a more complex task than in the case of externally modulated light sources. In the performance analysis, we proceed by assigning to the 3-dB laser linewidth the average measured value $\Delta\nu = 2.2$ GHz.

The spectral broadening by the direct modulation results in a larger value βT than in the case of an externally modulated source. Hence the resultant reduction in variance of the filtered interferometric crosstalk [cf., (22)] suggest that lower power penalties will be incurred. This is actually confirmed by the experiment. In Fig. 8 is displayed the measured power penalties for a directly modulated source (marks). Comparing with the results for the external modulated source (Fig. 7) the system with a directly modulated source experiences less power penalties due to filtered interferometric crosstalk. These results are in good agreement with previous observations by other authors [4], [8]. Interferometric noise reduction by broadening the spectrum (by, e.g., phase dithering or phase noise modulation) has already being proposed and exploited [9]–[11].

In Fig. 8 are also displayed the theoretical, moments based, results (solid line) and the results by the Gaussian approximation (dotted line). Good agreement between theory and experiment is also observed. As in the previous case (Fig. 7), the Gaussian approximation gives a reasonable good result for small values of ϵ . The experimental results show that power penalties are kept less than 1 dBm if the crosstalk parameter ϵ is better than -23 dB for a directly modulated source, and better than -26 dB for an externally modulated

source. The theoretical, simulations and experimental results clearly indicate that significant interferometric noise reduction is possible if the laser 3-dB bandwidth is larger than the postdetection filter bandwidth.

VIII. CONCLUSIONS

This paper presents a statistical analysis for filtered interferometric noise which takes into account the relation between the laser (signal and crosstalk) 3-dB bandwidth and the postdetection filter bandwidth. The impact of interferometric crosstalk on the performance of optical networks turns out to be strongly dependent on this relation, for instance, significant interferometric noise reduction is possible if the laser 3-dB bandwidth is larger than the postdetection filter bandwidth. This operating situation can be achieved by broadening (phase dithering) the laser spectrum. Research on the topic is in progress.

This paper also gives insights, both by an accurate statistical analysis and experiment, on why ASK/DD systems with directly modulated light sources incurred less power penalties due to interferometric noise than systems using externally modulated sources. The reason being the different resulting relation between the laser 3-dB bandwidth and the postdetection filter bandwidth.

The presented theoretical analysis has shown good consistency with experimental results from an ASK/DD system using externally, and directly modulated light sources.

APPENDIX A DERIVATION OF MOMENTS

In this Appendix a derivation for the moments of the variable γ is given. We follow closely the presentation by Roudas [17]. The moment of order k , $E\{\gamma^k\}$, is given by

$$\mu_k = \frac{1}{T^k} \int_{-T}^T \int_{-T}^T \cdots \int_{-T}^T E\{\cos \Delta\phi(t_1) \times \cos \Delta\phi(t_2) \times \cdots \times \cos \Delta\phi(t_k)\} dt_1 dt_2 \cdots dt_k. \quad (28)$$

Using trigonometric identities and the representation for $\cos(\cdot)$ as the real part of an exponential function we have

$$\mu_k = \frac{1}{2^{k-1} T^k} \left[\text{Re} \left\{ \int_{-T}^T \int_{-T}^T \cdots \int_{-T}^T E\{\exp(j[\Delta\phi(t_1) + \cdots + \Delta\phi(t_2) + \Delta\phi(t_k)])\} dt_1 dt_2 \cdots dt_k \right\} + \text{Re} \left\{ \int_{-T}^T \int_{-T}^T \cdots \int_{-T}^T E\{\exp(j[\Delta\phi(t_1) + \Delta\phi(t_2) - \cdots + \Delta\phi(t_k)])\} dt_1 dt_2 \cdots dt_k \right\} + \cdots + \text{Re} \left\{ \int_{-T}^T \int_{-T}^T \cdots \int_{-T}^T E\{\exp(j[\Delta\phi(t_1) - \Delta\phi(t_2) - \cdots + \Delta\phi(t_k)])\} dt_1 dt_2 \cdots dt_k \right\} \right]. \quad (29)$$

We observe that the integrands are the characteristic function of a sum of zero mean Gaussian variables $\Delta\phi(t_1)$, $\Delta\phi(t_2)$, ..., $\Delta\phi(t_k)$ which is given by [25]

$$\begin{aligned} & \mathbb{E} \left\{ \exp \left(j \sum_{k=1}^N u_k \Delta\phi(t_k) \right) \right\} \\ &= \exp \left[-\frac{1}{2} \sum_{k,l=1}^N u_k u_l R_{\Delta\phi}(t_k, t_l) \right]. \end{aligned} \quad (30)$$

Arranging the integration variables in increasing order, i.e., $t_1 < t_2 < \dots < t_k$ it can be shown that

$$\begin{aligned} \mu_k &= \frac{k!}{2^{k-1} T^k} \\ & \cdot \left[\text{Re} \left\{ \int_{t-T}^t \int_{t-T}^{t_1} \dots \int_{t-T}^{t_{k-1}} \mathbb{E} \{ \exp(j[\Delta\phi(t_1) \right. \right. \\ & \quad \left. \left. + \dots + \Delta\phi(t_2) + \Delta\phi(t_k)]) \} dt_1 dt_2 \dots dt_k \right\} \right. \\ & \quad \left. + \text{Re} \left\{ \int_{t-T}^t \int_{t-T}^{t_1} \dots \int_{t-T}^{t_{k-1}} \mathbb{E} \{ \exp(j[\Delta\phi(t_1) \right. \right. \\ & \quad \left. \left. + \Delta\phi(t_2) - \dots + \Delta\phi(t_k)]) \} dt_1 dt_2 \dots dt_k \right\} \right. \\ & \quad \left. + \dots + \text{Re} \left\{ \int_{t-T}^t \int_{t-T}^{t_1} \dots \int_{t-T}^{t_{k-1}} \mathbb{E} \{ \exp(j[\Delta\phi(t_1) \right. \right. \\ & \quad \left. \left. - \Delta\phi(t_2) - \dots - \Delta\phi(t_k)]) \} dt_1 dt_2 \dots dt_k \right\} \right]. \end{aligned} \quad (31)$$

Let denote by $\alpha = (\alpha_1, \alpha_2, \dots, \alpha_k)$ the set of signs $+1$ or -1 in front of the variables $\Delta\phi(t_1), \Delta\phi(t_2), \dots, \Delta\phi(t_k)$. We consider the general case, $t_1 < t_2 < \dots < t_k$, for which we get

$$\begin{aligned} & \mathbb{E} \{ \exp(j[\alpha_1 \Delta\phi(t_1) + \alpha_2 \Delta\phi(t_2) + \dots + \alpha_k \Delta\phi(t_k)]) \} \\ &= e^{(\beta \sum_{n=1}^k b_n u_n + c \beta \tau_d)} \end{aligned} \quad (32)$$

in which

$$b_n = \begin{cases} -1 + \sum_{l=1}^n a_l - \sum_{l=n+1}^k a_l & 1 < n < k-1 \\ -1 + a_k \sum_{l=1}^k a_l & n = k \end{cases} \quad (33)$$

and the term c is given by

$$c = \frac{k}{2} - \sum_{n=1}^k a_n \sum_{l=1}^n a_l. \quad (34)$$

Considering a particular set α and substituting (32) in (31), we have that

$$\begin{aligned} I_a &= \int_{t-T}^t \int_{t-T}^{t_1} \dots \int_{t-T}^{t_{k-1}} \mathbb{E} \{ \exp(j[\alpha_1 \Delta\phi(t_1) \\ & \quad + \dots + \alpha_2 \Delta\phi(t_2) + \alpha_k \Delta\phi(t_k)]) \} dt_1 dt_2 \dots dt_k \\ &= e^{c \beta \tau_d} \int_{t-T}^t e^{\beta b_k t_k} \int_{t-T}^{t_k} e^{\beta b_{k-1} t_{k-1}} \dots \int_{t-T}^{t_2} e^{\beta b_1 t_1} dt_1 \\ & \quad \cdot dt_2 \dots dt_k. \end{aligned}$$

The integrals in (35) obey the following recursive relation:

$$I_a^{(n)} = \int_0^t e^{\beta b_n t_n} I_a^{(n-1)} dt_n \quad (35)$$

with the initial condition $I_a^{(0)} = e^{c \beta \tau_d}$.

Finally, the μ_k moment can be expressed as

$$\mu_k = \frac{k!}{2^{k-1} T^k} \sum_{\alpha} I_a^{(k)}|_{t=T}. \quad (36)$$

APPENDIX B

PERFORMANCE ANALYSIS FOR MULTIPLE CROSSTALK INTERFERERS

This Appendix shows how to extend the performance analysis in order to include N sources of interferometric crosstalk. We proceed by following [5] in which we have that the average error probability, P_e , given a detection threshold α , is given by a weighted statistical average of the error probability $P_e(\alpha, \mu)$ for each value μ , binomially distributed, of interferers being simultaneously a digital "one" (see [5, eq. (22)]). Given a value μ , the MGF for Λ , $M_\Lambda(s)$, consists of the product of the MGF for all the resultant signal and crosstalk beat terms; see (21) in [5]. The MGF $M_\Lambda(s)$ is evaluated in a similar way as in (12) observing that we need now to determine the pdf for a sum of independent identically distributed (i.i.d) random variables (RV) of the type in (17). The performance analysis comprises the following steps.

- 1) Given a value μ determine the number of terms signal-to-crosstalk, crosstalk-to-crosstalk, beating terms in Λ ; taking into account the extinction ratio ρ .
- 2) For each resulting sum of RV of type (17) compute its pdf. This is done in the following way: compute the moments for each RV in the sum as shown in Section III-A (eventually for different values of βT). Compute the cumulants by the standard relations between moments and cumulants [26]. The cumulants for a sum of i.i.d random variables is given by the sum of the cumulants of each RV in the sum. Compute the moments of the sum from the cumulants [26]. Based on the moments estimate the pdf by the maximum entropy approach.
- 3) Evaluate the error probability by the SPA (see Section V-A) based on the MGF $M_\Lambda(s)$ (using the estimated pdf computed in step 2).
- 4) Finally, the average error probability, P_e , is evaluated.

Using the above procedure the performance analysis accounts for data statistics, interferometric crosstalk statistics, extinction ratio, shot noise and thermal noise. The Gaussian approximation, proposed in Section V-B, will simplify the analysis, requiring less computing time. It is expected that for a large number of interferers the Gaussian approximation, via the Central Limit Theorem, will yield results closed to those obtained by the accurate statistical approach.

ACKNOWLEDGMENT

The authors would like to thank I. Roudas, Corning, Inc., Photonic Research and Test Center, Somerset, NJ, for providing an English version of the original text in French of [17,

ch. 5], including a subroutine to compute the relation (20). The authors would also like to acknowledge the anonymous reviewers for comments improving the presentation.

REFERENCES

- [1] M. Tur and E. L. Goldstein, "Dependence of error rate on signal-to-noise ratio in fiber-optic communication systems with phase-induced intensity noise," *J. Lightwave Technol.*, vol. 7, pp. 2055-2057, Dec. 1989.
- [2] E. L. Goldstein, L. Eskildsen, and A. F. Elrefaie, "Performance implications of component crosstalk in transparent lightwave networks," *IEEE Photon. Technol. Lett.*, vol. 6, pp. 657-700, May 1994.
- [3] E. L. Goldstein and L. Eskildsen, "Scaling limitations in transparent optical networks due to low-level crosstalk," *IEEE Photon. Technol. Lett.*, vol. 7, pp. 93-94, Jan. 1995.
- [4] P. T. Legg, M. Tur, and I. Andonovic, "Solution paths to limit interferometric noise induced performance degradation in ASK/direct detection lightwave networks," *J. Lightwave Technol.*, vol. 14, pp. 1943-1953, Sept. 1996.
- [5] I. T. Monroy and E. Tangdiongga, "Performance evaluation of optical cross-connects by saddlepoint approximation," *J. Lightwave Technol.*, vol. 16, pp. 317-323, Mar. 1998.
- [6] W. D. Cornwell and I. Andonovic, "Interferometric noise for a single interferer: comparison between theory and experiment," *Electron. Lett.*, vol. 32, pp. 15001-15002, Aug. 1996.
- [7] K. Ho *et al.*, "Exact analysis of homodyne crosstalk penalty in WDM networks," *IEEE Photon. Technol. Lett.*, vol. 10, pp. 457-458, Mar. 1998.
- [8] L. Eskildsen *et al.*, "Interferometric noise limitations in fiber-amplifier cascade," *Electron. Lett.*, vol. 29, pp. 2040-2041, Nov. 1993.
- [9] P. K. Pepeljugoski and K. Y. Lau, "Interferometric noise reduction in fiber-optic links by superposition of high frequency modulation," *J. Lightwave Technol.*, vol. 10, pp. 957-963, July 1992.
- [10] A. Yariv, H. Blauvelt, and S. Wu, "A reduction of interferometric phase-to-intensity conversion noise in fiber links by large index phase modulation of the optical beam," *J. Lightwave Technol.*, vol. 10, pp. 978-981, July 1992.
- [11] F. W. Willems and W. Muys, "Suppression of interferometric noise in externally modulated lightwave AM-CATV systems by phase modulation," *Electron. Lett.*, vol. 29, pp. 2062-2063, Nov. 1993.
- [12] S. D. Personick, "Applications for quantum amplifiers in simple digital optical communication systems," *Bell Systems Tech. J.*, vol. 52, pp. 117-133, Jan. 1973.
- [13] M. Kavehrad and M. Joseph, "Maximum entropy and the method of moments in performance evaluation of digital communications systems," *IEEE Trans. Commun.*, vol. COM-34, pp. 1183-1189, Dec. 1986.
- [14] A. Mooradian, "Laser linewidth," *Phys. Today*, vol. 38, pp. 48-48, May 1985.
- [15] G. Einarsson, *Principles of Lightwave Communications*. New York: Wiley, 1996.
- [16] A. Papoulis, *Probability, Random Variables, and Stochastic Processes*, 2nd ed. New York: McGraw-Hill, 1991.
- [17] I. Roudas, "Conception optimale d'un système optique cohérent CPFSK avec récepteur différentiel," Ph.D. dissertation, Ecole Nationale Supérieure des Télécommunications, Paris, France, Jan. 1995.
- [18] A. Aric, M. Tur, and E. L. Goldstein, "Probability-density function of noise at the output of a two-beam interferometer," *J. Opt. Soc. Amer. A*, vol. 8, pp. 1936-1942, Dec. 1991.
- [19] M. Tur and E. L. Goldstein, "Probability distribution of phase-induced intensity noise generated by distributed feed-back lasers," *Opt. Lett.*, vol. 15, pp. 1-3, Jan. 1990.
- [20] C. Helstrom, "Approximate evaluation of detection probabilities in radar and optical communications," *IEEE Trans. Aerosp. Electron. Syst.*, vol. 14, pp. 630-640, July 1978.
- [21] —, "Performance analysis of optical receivers by saddlepoint approximation," *IEEE Trans. Commun.*, Jan. 1979, pp. 186-190.
- [22] R. A. Linke, "Modulation induced transient chirping in single frequency lasers," *IEEE J. Quantum Electron.*, vol. QE-21, pp. 593-597, June 1985.

- [23] K. Petermann, "Laser diode modulation and noise," in *Advances in Optoelectronics*. New York: Kluwer Academic, 1988.
- [24] M. Tur *et al.*, "Sequence dependence of phase-induced intensity noise in optical networks that employ direct modulation," *Opt. Lett.*, vol. 20, pp. 359-361, Feb. 1995.
- [25] E. Wong and B. Hajek, *Stochastic Processes in Engineering Systems*. Berlin, Germany: Springer, 1985.
- [26] E. Biglieri, "A recursive method for computing the coefficients of the Gram-Charlier series," *Proc. IEEE*, pp. 251-252, Feb. 1972.

Idelfonso Tafur Monroy was born in El Castillo (Meta), Colombia, in 1968 and graduated from the Bonch-Bruевич Institute of Communications, St. Petersburg, Russia, in 1992, where he received the M.Sc. degree in multichannel telecommunications. In 1993, he enrolled as a graduate student in the Department of Signals, Sensors and Systems at the Royal Institute of Technology, Stockholm, Sweden, where he received the Technology Licentiate degree in Telecommunication Theory in 1996. He is currently pursuing the Ph.D. degree at the Department of Electrical Engineering at the Eindhoven University of Technology (EUT), The Netherlands.

His research interests are in the area of optical communication networks, communication theory, stochastic processes, and applied probability theory.

Eduward Tangdiongga was born in Makassar (Ujung Pandang), Indonesia, in November 1968. He received the degree of elektrotechniek ingenieur in 1994 from Eindhoven University of Technology (EUT), Eindhoven, The Netherlands, for working on planar arrayed microstrip antennas. Then, he joined the EUT Stan Ackermans Institute, where he received in 1996 the Technology Designer degree (MTD) for a work on designing of a WDM cross-connect with good crosstalk performance.

Presently, he is a Research Assistant at the Electro-Optical Communication Division of the Department of Electrical Engineering-EUT, where he is actively involved in the European ACTS project BLISS (Broadband Lightwave Sources and Systems) and APEX (Advanced Photonics Experiment X-connect).

Huig de Waardt was born in Voorburg, The Netherlands on December 1, 1953. After finishing Gymnasium at the Christelijk Lyceum Voorburg, he studied electrical engineering and received the degree in material sciences from the Delft University of Technology, Delft, The Netherlands, in 1980. His work was in photovoltaic energy conversion in amorphous hydrogenated silicon. In 1995, he received the Ph.D. degree from the University of Delft with his dissertation "High Capacity 1300 nm Optical Transmission."

In 1981, he joined the Department of Physics, KPN Research, Leidschendam, where he was engaged into research on the performance aspects of long-wavelength semiconductor laser diodes, LED's and photodiodes. In 1989, he moved to the Department of Transmission where he has been working in the fields of high bit rate direct-detection systems, optical preamplification, wavelength division multiplexing, dispersion-related system limitations, and the system application of resonant optical amplifiers. He contributed to (inter)national standardization bodies and to the EURO-COST activities 215 and 239. In October 1995, he was appointed as an Associate Professor at the Faculty of Electrical Engineering, University of Eindhoven, The Netherlands, in the area of high-speed trunk transmission. His current research interests are in applications of semiconductor optical amplifiers, high-speed OTDM transmission, integrated optical cross-connects, and WDM optical networking. He was active in European research programs as ACTS BLISS and ACTS Upgrade. At present, he is responsible for the WDM system demonstrator within the ACTS APEX project.

Paper J

Performance of Optically Preamplified Receivers in WDM Systems Disturbed by Interferometric Crosstalk

Idelfonso Tafur Monroy, E. Tangdionga, and H. de Waardt
Photonic Network Communications, Submitted for publication.

Performance of Optically Preamplified Receivers in WDM Systems Disturbed by Interferometric Crosstalk

IDELFONSO TAFUR MONROY, EDUWARD TANGDIONGGA AND HUIG DE WAARDT *

i.tafur@ele.tue.nl

Eindhoven University of Technology

Telecommunication Technology and Electromagnetics

P. O. Box 513, 5600 MB Eindhoven, The Netherlands

Abstract. Interferometric crosstalk is a performance limiting factor of major concern in all-optical WDM transmission networks. Interferometric crosstalk arising from performance imperfections in optical components may introduce large power penalties and bit-error rate floors. Optical amplifiers are often used to increase the signal level incident on a detector so that high receiver sensitivity can be obtained. We investigate theoretically and experimentally the performance of optically preamplified, direct detection receivers in the presence of interferometric crosstalk. The model includes an accurate description of filtered interferometric crosstalk by using a maximum entropy approach. Experimental results, using both directly and externally modulated light sources, are found to be in good agreement with theory.

Keywords: Optical crosstalk, wavelength division multiplexing networks, error analysis, optical communication, optical amplifiers.

1. Introduction

All-optical WDM networks, comprising optical add/drop modules and/or optical crossconnects will employ optical components that may introduce crosstalk. Interferometric crosstalk arising from performance imperfections in (de)multiplexer and optical switches may result in large power penalties and bit-error rate floors, e.g., [1–4]. In Figure 1a is shown an example of a crossconnected optical network. Let us consider a channel at a certain wavelength λ_1 at one extreme of the network (mark “in” in Fig. 1a). Due to performance imperfections of components in the optical nodes at the other extreme (“out” in Fig. 1a) the channel will experience crosstalk interference from

other channels operating at the same wavelength; in-band crosstalk. Channels operating at different wavelengths may also fall within the receiver bandwidth producing interband crosstalk. State-of-the-art integrated optical crossconnects show a typical value of -20 dB of inband crosstalk and a value of interband crosstalk less than -40 dB [5]. Power loss of integrated crossconnects is still high due to the high refractive index of InP-based material. A loss of 13 dB was reported in [5]. When dilated optical switches are used to improve further the crosstalk performance, the loss will be even higher. All-optical networks employing the advanced integrated crossconnects are likely to incorporate optical amplifiers to compensate for power losses, and also for sensitivity enhancement resulting in a larger power budget.

Hence, it is of importance to study the performance of optically preamplified receivers in the presence of in-

*This work was supported in part by the European Commission ACTS project AC332 APEX.

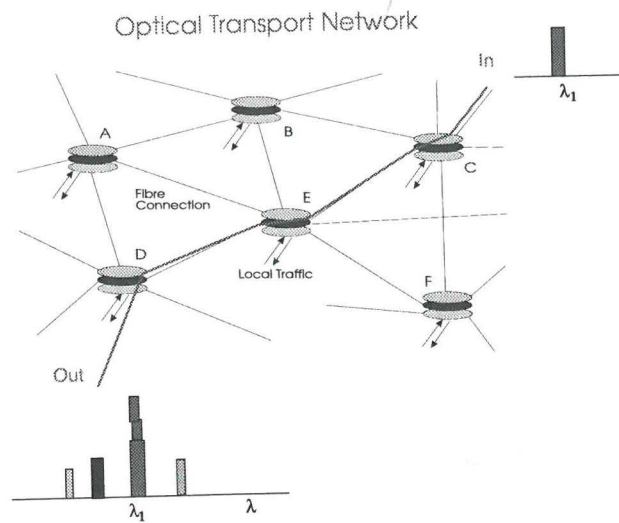


Fig. 1a. Optical crossconnected transport network.

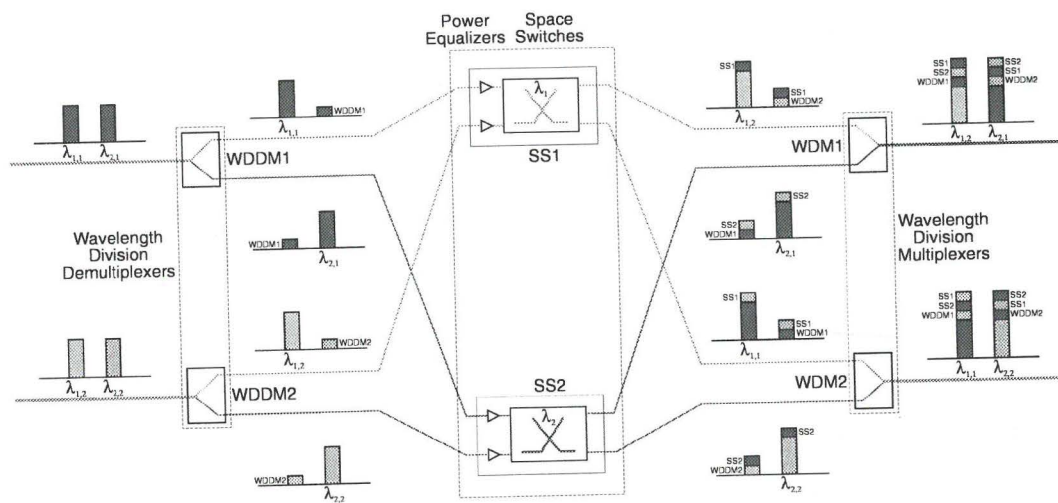


Fig. 1b. Crosstalk due to non-perfect wavelength (de)multiplexers and optical space switches. WDDM: wavelength division demultiplexer, SS: space switch, WDM: wavelength division multiplexer.

interferometric crosstalk. The main contribution of this paper is the accurate theoretical model for the receiver performance and the validation of its results by relevant experiments. The receiver model includes an accurate statistical description of noise. The statistics of filtered

interferometric noise is determined by using a maximum entropy approach. The non-Gaussian statistics of detected amplified spontaneous emission (ASE) noise is also included. We present experimental results for power penalties, due to interferometric crosstalk, for

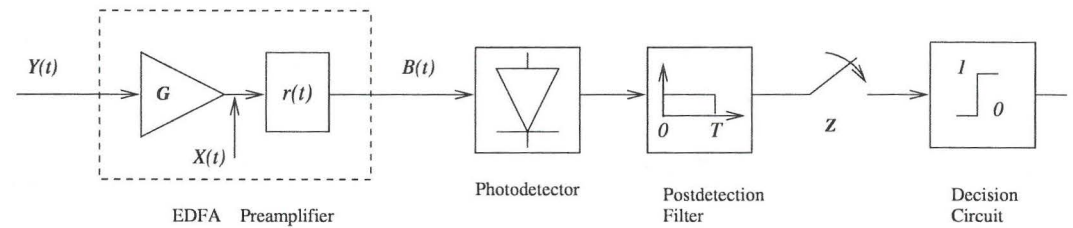


Fig. 2. Optical preamplified ASK/DD receiver

a system using directly and externally modulated light sources. We found that, regardless of the light source modulation type, optical preamplification does not improve the receiver's tolerance toward crosstalk. Additional power penalties with respect to the case of no-preamplification are observed. This is attributed to ASE-crosstalk beat noise contributions. The experimental results are found to be in good agreement with theory. The rest of the paper is structured as follows. The system model under investigation is presented in Sect. 2. The experimental setup is described in Sect. 3. Experimental results, their discussion and comparison with theory are the topic of Sect. 4. Finally, in Sect. 5 summarizing conclusions are presented.

2. System Model

A signal traversing an optical crossconnected network will accumulate crosstalk due to performance imperfections of the wavelength selective (de)multiplexers and space switches. Fig. 1b shows as an example the crosstalk mechanism in an integrated crossconnect that can switch signals at two wavelength channels, independently, from two inputs to two outputs. The crossconnect is based on an arrayed-waveguide grating (AWG) multiplexer, and implemented by connecting the demultiplexer outputs to multiplexer inputs through the space switches. A certain wavelength channel can be passed to an desired output by activating the switch either in cross or in bar state. Both inband and interband crosstalk will take place in the crossconnect due to power leakage in the optical devices. Interband crosstalk arises from inadequately suppressed wavelengths in the demultiplexers (mark "WDDM1" and "WDDM2" in Fig. 1b). In the inband crosstalk case, the desired signal and the leakage signal have the same nominal wavelength.

For example, the signal at wavelength λ_1 from input 1 ($\lambda_{1,1}$) of the first space switch suffers inband crosstalk (mark "SS1") from $\lambda_{1,2}$. At the end of the crossconnect, the multiplexers collect all wavelength channels together and the resulting output channels suffer from accumulated crosstalk (mark "WDDM, SS1, SS2"). The detrimental effects of WDDM, SS1, and SS2 on a desired channel is enhanced by the fact that they have the same nominal wavelength and the resulting beating terms fall within the receiver bandwidth. This kind of crosstalk (inband crosstalk) once being added to a desired signal cannot be removed by signal processing (optical filtering), and therefore it will accumulate as signals traverse several nodes in a crossconnected network.

Optical amplifiers are commonly used as preamplifiers (before detection) to enhance the system sensitivity. Hence it of importance to assess the performance of optically preamplified receiver in the presence of crosstalk. We will consider an ASK/DD (amplitude shift keying/direct detection), optically preamplified receiver whose schematic diagram is depicted in Fig. 2. The incoming optical signal $Y(t)$ (informative signal and crosstalk), after traversing one or several optical crossconnects, is amplified and subsequently filtered in order to reduce the effect of the ASE noise. The photodetector output is passed through an integrate-and-dump filter and sampled to form the decision variable Z . The decision device derives an estimate of a transmitted binary symbol by comparing the value of the decision variable with a preselected detection threshold.

We are interested in assessing the error performance of the system. To accomplish this goal we use an statistical method for evaluating the error probabilities: the so called saddlepoint approximation which makes use of the moment generating function (MGF) for the

receiver decision variable [6]. So, for the performance analysis we need to determine the MGF (which provides a complete statistical description) of the receiver decision variable. We proceed by following [7] where a detailed presentation of the performance analysis for ASK/DD systems subject to interferometric crosstalk is given. We have that the decision variable is composed of the contribution of the shot noise (including crosstalk and ASE) and the receiver thermal noise. The MGF of the decision variable Z is then given by [7]

$$M_Z(s) = M_{sh}(s)M_{th}(s), \quad (1)$$

where M_{th} is the MGF for a zero mean Gaussian variable with variance σ_{th}^2 : $M_{th}(s) = \exp(s\sigma_{th}^2/2)$. $M_{sh}(s)$ is the MGF of the filtered shot noise (photocurrent) contribution to the decision variable Z . The shot noise is well modeled as a doubly stochastic Poisson process with intensity $\lambda(t)$. Hence, for the case of and integrate-and-dump postdetection filter, M_{sh} is given by [11]

$$M_{sh}(s) = M_\Lambda(e^s - 1), \quad (2)$$

where $\Lambda = \int_0^T \lambda(t)dt$ is the *Poisson parameter*. The photoelectron intensity $\lambda(t)$, in a normalized way can be written as:

$$\lambda(t) = \frac{1}{2}|B(t)|^2, \quad (3)$$

in which $B(t)$ represents the optical field, equivalent baseband form, falling upon the photodetector.

2.1. Optical preamplification

Consider an optical signal $Y(t)$ at the input of the EDFA preamplifier which is modeled as an optical field amplifier with power gain G , an additive noise source $X(t)$, representing the ASE noise and an optical filter with complex equivalent baseband impulse response $r(t)$; see Fig. 2. The optical field at the output of the amplifier is

$$B(t) = \sqrt{G}Y(t) + X(t). \quad (4)$$

The density of $X(t)$ expressed in photons per second is given by [9]:

$$N_0 = n_{sp}(G - 1),$$

in which n_{sp} represents the spontaneous emission parameter. For the further analysis, we assume that $Y(t)$ is confined in the bit interval and that the impulse response $r(t)$ is limited to the same time interval. We

can therefore expand $B(t)$ in a Fourier series. Subsequently, the optical field $B(t)$ can be written as:

$$B(t) = \sum_{k=-L}^{k=L} (Y_k + X_k)e^{j\pi kt/T}, \quad (5)$$

where $\beta = 2L + 1$ (the number of temporal modes) equals the ratio of the bandwidth B_0 of the optical filter and the data rate $B = 1/T$:

$$\beta = B_0/B.$$

The ASE noise is considered to be a white Gaussian noise, hence the real and imaginary part of $X_k = X_{ck} + jX_{sk}$ are Gaussian independent variables with equal variances for all $-L \leq k \leq L$: $\text{Var}\{X_{ck}\} = \text{Var}\{X_{sk}\} = N_0B$.

We can now express Λ as:

$$\Lambda = \frac{T}{2} \left(\sum_{k=-L}^{k=L} [Y_k \sqrt{G} + X_{ck}]^2 + X_{sk}^2 \right). \quad (6)$$

We focus now on the derivation of the MGF for Z , accounting for crosstalk and optical preamplification. Our first step towards the derivation of this MGF is to condition on the value of Y_k and observe that Λ is the sum of 2β independent Gaussian variables with variance equal to $N_0/2$ of which β have mean $Y_k \sqrt{G}$. From the orthogonality of the base functions $e^{j\pi kt/T}$ we have that

$$\int_0^T |Y(t)|^2 dt = T \sum_{k=-L}^{k=L} |Y_k|^2. \quad (7)$$

The conditional (on Y_k) MGF for Z is given by a noncentral chi square distribution function [8]:

$$M_{\Lambda|Y}(s) = \frac{1}{(1 - N_0s)^\beta} \exp\left(\frac{\frac{1}{2}sT \sum_{k=-L}^{k=L} |\sqrt{G}Y_k|^2}{1 - N_0s}\right). \quad (8)$$

The second step is to average over all possible values of Y_k from which we obtain:

$$M_\Lambda(s) = \frac{1}{(1 - N_0s)^\beta} M_{\Lambda_0}\left(\frac{s}{1 - N_0s}\right), \quad (9)$$

where Λ_0 is given by

$$\Lambda_0 = \frac{1}{2} \int_0^T |\sqrt{G}Y(t)|^2. \quad (10)$$

Expression (10) is (except for the amplification factor G) the *Poisson parameter* for a receiver without optical amplification [7]. The MGF (9) agrees well with the derived results in [9–11].

The MGF for the decision variable for a receiver subject to interferometric crosstalk arising from a single interferer source (operating at the same nominal wavelength as the informative signal), without any preamplification is given by [7]

$$M_{\Lambda_0}(s) = \int_{-1}^1 M_{\Lambda_0|\gamma}(s, \tilde{\gamma}) f_\gamma(\tilde{\gamma}) d\tilde{\gamma}, \quad (11)$$

in which

$$M_{\Lambda_0|\gamma}(s, \gamma) = \exp[sm(b_0^s + \epsilon b_0^x)] \exp[2m\sqrt{b_0^s b_0^x} \epsilon \gamma]. \quad (12)$$

and $f_\gamma(\cdot)$ is the probability density function (PDF) for the filtered interferometric crosstalk γ which is given by

$$\gamma = \frac{1}{T} \int_0^T \cos[\phi_s(t) - \phi_x(t - \tau_d)] dt,$$

where τ_d is interferometric delay, and $\phi_{s,x}(t)$ is the phase of the signal and crosstalk, respectively.

Some explanation on the symbols used in (12). The number of photons contained in an optical pulse for a transmitted binary “one” is denoted by m while gm photons are contained in an optical pulse for a transmitted binary “zero”. The variable $b_k^{s,x}$ represents the binary symbols for signal and crosstalk, respectively, in a certain bit interval k . The ratio of leakage crosstalk to signal power is denoted by ϵ .

The PDF of γ is evaluated using a maximum entropy approach based on a finite number of computed statistical moments. In Appendix A is presented a short derivation for the moments of γ . In [7] a more detailed derivation is given.

Substituting (11) into (8) we obtain an expression for the MGF of the decision variable Z for a receiver subject to interferometric crosstalk and using optical preamplification.

2.2. Performance analysis

Based on the knowledge of the MGF, $M_Z(s)$, the performance analysis is carried out with the help of the

so-called saddlepoint approximation [6]. We follow closely the performance analysis approach of [7]. See also Appendix B for a presentation of the procedure for the computation of error probabilities. The derived MGF in (11) accounts for the statistics of filtered interferometric crosstalk, and noncentral chi squared statistics due to preamplification [10]. The analysis also accounts for the data statistics, all possible combinations of the interfering bit and the signal bit, and non-perfect extinction ratio. In many practical applications the delay time τ_d is much larger than the laser coherence time; the so-called incoherence interferometric noise. This type of (incoherent) interferometric crosstalk will be generated in the experimental setup.

3. Experimental setup

The measurement setup to verify the theory is schematically given in Fig. 3. At the transmitter side, two light sources modulation schemes are used, namely direct modulation (a) and external modulation (b). In Fig. 3(a) a distributed feedback (DFB) laser which has a CW-linewidth of 45 MHz is modulated directly by an electrical generator of non-return-to-zero (NRZ) signals. The generated pseudo-random binary signals have a bit-rate of 622 Mbit/s and their pattern is repeated after $2^7 - 1$ bits. Using this direct modulation scheme we have obtained optical signals of an average extinction ratio of 15 dB.

In the external modulation scheme, Fig. 3(b), lightwaves coming from the DFB laser are coupled into a lithium niobate (LiNbO₃) modulator. The modulator is driven by the 622 Mbit/s $2^7 - 1$ pseudo-random electrical signals. The resulting optical signals have an improved extinction ratio of 20 dB. It should be noticed that due to practical limitations a short binary sequence is used. This is to avoid the possible baseline wandering effect at the receiver circuit in case of a long sequence of binary “ones” and “zeros”. We have observed that the spectral width of external modulation is determined mainly by the modulation speed, i.e. 622 MHz whereas in direct modulation the combined effect of adiabatic and transient chirp makes the spectrum wider than that of external modulation. Measurements of the spectrum for the direct modulated light source case yielded values in the range of 1.9–2.4 GHz.

After the transmitter, the lightwaves are split to form a signal and a crosstalk path by a Mach-Zehnder struc-

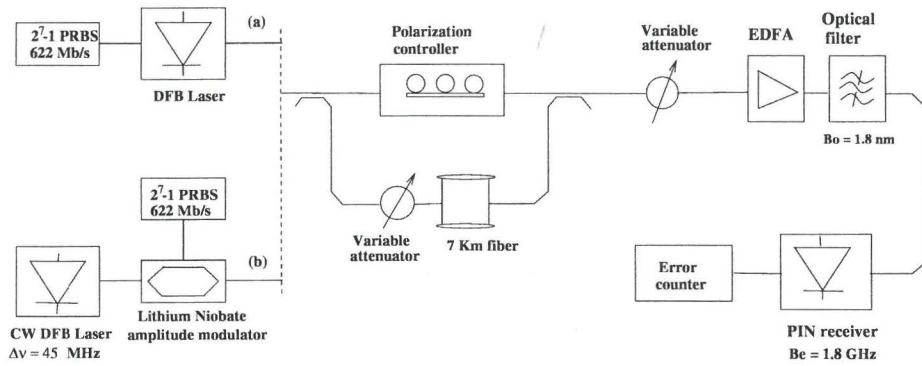


Fig. 3. Experimental setup used to measure power penalties due to filtered interferometric crosstalk. Two light source modulation schemes are used: (a) direct modulation, and (b) external modulation.

ture with one of its arm 7 km longer than the other. The difference in the arm-length is intended to decorrelate information signals from crosstalk. The state of polarization of the information signal with respect to the crosstalk is matched to produce a worst case condition at the detection. In the crosstalk path a variable optical attenuator is located for crosstalk power adjustment relative to the signal power. Another attenuator is placed after the Mach-Zehnder structure to vary optical signal powers coupled to an optical detector for bit error rate (BER) evaluation.

An erbium-doped fiber amplifier (EDFA) followed by a 1.8 nm bandwidth optical filter is used to preamplify the signal before detection. The receiver has an electrical bandwidth of 1.8 GHz with is sufficient to ensure that the signal, crosstalk and ASE noise beating at 622 Mbit/s are detected. The power penalties measurements at a BER of 10^{-9} are performed using an optimized decision threshold.

4. Results and discussion

The experimental and theoretical results for power penalties as a function of the crosstalk parameter ϵ : the ratio of leakage crosstalk to signal power, are presented in Fig. 4. As we can see from Fig. 4 the system employing an externally modulated laser source incurred larger power penalties than the system using a directly modulated laser. This difference is attributed to the fact that the spectrum of the directly modulated laser source is broader (due to chirp) than in the external modulation case and after postdetection filtering

the interferometric crosstalk is strongly filtered out [7]. We can also observe that the measurements and theory are in relatively good agreement; within a margin of 0.5 dB discrepancy for power penalties less than 2.5 dB. This discrepancy is attributed to measurement error and eventually additionally power penalties due to postdetection electrical signal processing.

Figure 5 presents a comparison of power penalties between the preamplified system and the case without preamplification. As we can observe in Fig. 5 the case with preamplification results in larger power penalties than the system without preamplification, for both types of light source modulation. This is attributed to additional penalties due to crosstalk-ASE beat noise contributions as already pointed out in [12]. The same tendency can also be seen from theoretical results for the crosstalk levels used in the experiment. From our theoretical and experimental study we have observed that optical preamplification does not enhance the system tolerance toward inband crosstalk.

5. Conclusions

We have reported a theoretical and experimental study of the performance of optically preamplified receivers subject to interferometric crosstalk. Systems using directly and externally modulated light source has been used in the experiment. We found that optical preamplification, apart from improving the receiver's sensitivity, does not enhance the systems tolerance toward interferometric crosstalk. Moreover, additional power penalties are observed due to crosstalk-ASE beat noise

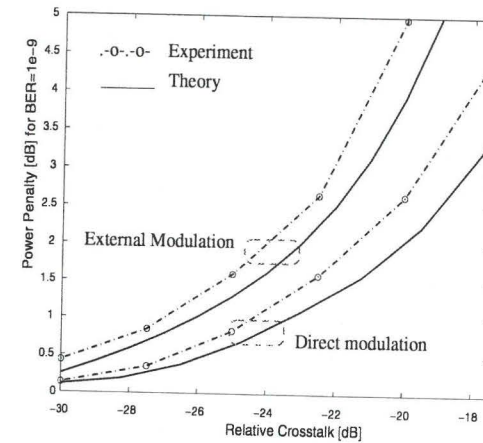


Fig. 4. Crosstalk power penalties for optical preamplified systems with directly and externally modulated laser sources. The solid lines represent the theory while the dash-dotted lines are the measurements.

contributions. The theoretical model yields results in good agreement with experiment.

Appendix A: Moments of γ

This appendix is intended to present a recursive expression for the moments of filtered interferometric crosstalk.

The moment of order k of the variable γ can be found by the following relation [13]

$$\mu_k = E\{\gamma^k\} = \frac{k!}{2^{k-1}T^k} \sum_{\forall a} I_a^{(k)}|_{t=T}, \quad (1)$$

in which

$$I_a^{(n)} = \int_0^t e^{\beta b_n t_n} I_a^{(n-1)} dt_n, \quad (2)$$

with the initial condition $I_a^{(0)} = e^{c\beta\tau_d}$. The parameters b_n , and c are given by (3) and (4), respectively.

$$b_n = \begin{cases} -1 + \sum_{l=1}^n a_l - \sum_{l=n+1}^k a_l & 1 \leq n \leq k-1 \\ -1 + a_k \sum_{l=1}^k a_l & n = k \end{cases} \quad (3)$$

and the term c is given by

$$c = \frac{k}{2} - \sum_{n=1}^k a_n \sum_{l=1}^n a_l. \quad (4)$$

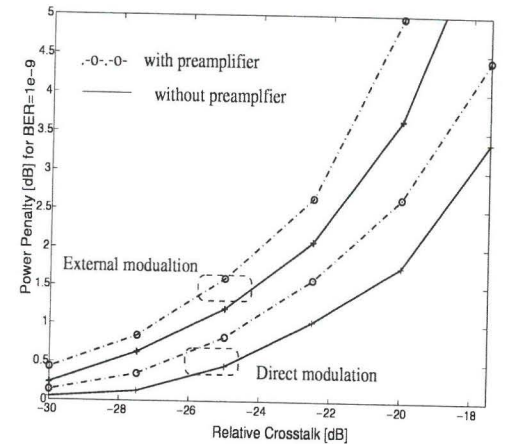


Fig. 5. Measured crosstalk power penalties of systems with and without preamplification using directly and externally modulated light sources.

In (1) by a is denoted a set (a_1, a_2, \dots, a_k) of signs $+1$ or -1 ; see for details [7, 13].

Appendix B: Error probabilities

This Appendix presents the procedure to compute the error probability for the ASK/DD system under investigation. The error probability, given that a binary "one" is transmitted is

$$q_-(\alpha) = P_{r1}(Z < \alpha),$$

where α denotes the decision threshold. Similarly, the error probability, given a binary "zero" is transmitted is

$$q_+(\alpha) = P_{r0}(Z > \alpha).$$

Assuming that the symbols are *a priori* equally probable, the average error probability is

$$P_e = \frac{1}{2}[q_-(\alpha) + q_+(\alpha)]. \quad (1)$$

Analysis by Saddlepoint Approximation

The saddlepoint approximation (SPA) has been proposed by Helstrom [14], as an efficient and numerically simple tool for analyzing communication systems. The SPA has shown a reasonably high degree

of accuracy in the analysis of optical communication systems, e.g., [6].

As shown in [14] the tail probability $q_+(\alpha)$, and $q_-(\alpha)$, are approximately equal to

$$q_+(\alpha) \approx \frac{\exp[\Phi(s_0)]}{\sqrt{2\pi\Phi''(s_0)}}, \text{ and } q_-(\alpha) \approx \frac{\exp[\Phi(s_1)]}{\sqrt{2\pi\Phi''(s_1)}}, \quad (2)$$

respectively, the so-called *saddlepoint approximation*. The function $\Phi(s)$ is related to the MGF for Z , $M_Z(s)$ by

$$\Phi(s) = \ln[M_Z(s)] - s\alpha - \ln|s|. \quad (3)$$

The parameters s_0 , and s_1 are the positive and negative root, respectively, of the equation

$$\Phi'(s) = 0 \quad (4)$$

and $\Phi''(s_{0,1})$ stands for the second derivative of (3) at $s = s_{0,1}$. See [14] or [9] for further details. The error probability is minimized by adjusting the detection threshold α . The optimum value of α and the parameters s_0 , s_1 may be found numerically by solving an appropriate set of equations [9].

References

- Goldstein, E. L., and Eskildsen, L. Scaling limitations in transparent optical networks due to low-level crosstalk. *IEEE Photonics Techn. Lett.*, Vol. 7, No. 1 (Jan. 95), pp. 93–94.
- Goldstein, E. L., Eskildsen, L., and Elrefaie, A. F. Performance implications of component crosstalk in transparent lightwave networks. *IEEE Photonics Techn. Lett.*, Vol. 6, No. 5 (May 1994), pp. 657–700.
- Legg, P. T., Tur, M., and Andonovic, I. Solution paths to limit interferometric noise induced performance degradation in ask/direct detection lightwave networks. *J. Lightwave Technol.*, Vol. 14, No. 9 (Sept. 1996), pp. 1943–1953.
- Tafur Monroy, I., and Tangdiongga, E. Performance evaluation of optical cross-connects by saddlepoint approximation. *J. Lightwave Technol.*, Vol. 16, No. 3 (March 1998), pp. 317–323.
- Herben, C. G. P. et al. Compact integrated polarisation independent optical crossconnect. In *European Conference on Optical Communications*, (Madrid, Spain, September 1998), Vol. 1, pp. 257–258.
- Helstrom, C. Performance analysis of optical receivers by saddlepoint approximation. *IEEE Trans. Commun.*, Vol. 27 (Jan 1979), pp. 186–190.
- Tafur Monroy, I., Tangdiongga, E., and de Waardt, H. On the distribution and performance implications of interferometric crosstalk in WDM networks. *J. Lightwave Technol.*, Vol. 17, No. 6 (June 1999), pp. 989–997.
- Papoulis, A. *Probability, Random Variables, and Stochastic Processes*, second ed. McGraw-Hill Int. Editions, 1991.
- Einarsson, G. *Principles of Lightwave Communications*. John & Wiley, Chichester, 1996.
- Marcuse, D. Calculation of bit-error probability for a lightwave system with optical amplifiers and post-detection gaussian noise. *J. Lightwave Technol.*, No. 4 (April 1990), pp. 505–513.
- Personick, S. D. Applications for quantum amplifiers in simple digital optical communication systems. *Bell Systems Tech. Journal*, Vol. 52, No. 1 (Jan. 1973), pp. 117–133.
- Eskildsen, L., and Hansen, P. B. Interferometric noise in lightwave systems with optical preamplifiers. *IEEE Photon. Technol. Lett.*, No. 11 (Nov. 1997), pp. 1538–1540.
- Roudas, I. *Conception optimale d'un système optique cohérent CPFSK avec récepteur différentiel*. PhD thesis, Ecole Nationale Supérieure des Télécommunications, Paris, France, January 1995.
- Helstrom, C. Approximate evaluation of detection probabilities in radar and optical communications. *IEEE Trans. Aerosp. Electron. Syst.*, Vol. 17 (July 1978), pp. 630–640.

Paper K

Interferometric Crosstalk Reduction in Optical WDM Networks by Phase Scrambling

Idelfonso Tafur Monroy, E. Tangdiongga, and H. de Waardt

© 1999 IEEE. Reprinted, with permission, from *IEEE/OSA J. Lightwave Technol.*, Submitted for publication.

Interferometric Crosstalk Reduction in Optical WDM Networks by Phase Scrambling

Idelfonso Tafur Monroy, Eduward Tangdionga, René Jonker, and Huig de Waardt

Abstract—Interferometric crosstalk, arising from the detection of undesired signals at the same nominal wavelength, may introduce large power penalties and bit-error rate floor significantly restricting the scalability of optical networks. In this paper, interferometric crosstalk reduction in optical WDM networks by phase scrambling is theoretically and experimentally investigated. Enhancement of 7-dB and 5-dB tolerance toward crosstalk is measured in a 2.5 Gbit/s transmission link of 100 km and 200 km of SSMF, respectively. This result proves the feasibility of optical networking in the LAN/MAN domain while tolerating the relatively high crosstalk levels of present integrated optical switching and cross-connect technology. Experiment is in good agreement with theory. Recommendations on the use of phase scrambling to reduce crosstalk in WDM systems are given.

Keywords—Interferometric noise, optical crosstalk, phase scrambling, optical communication, wavelength division multiplexing networks, error analysis.

I. INTRODUCTION

Performance imperfections of optical components (e.g., optical switches, (de)multiplexer and routers) are sources of interferometric crosstalk which constitutes a major limiting factor for the scalability of optical networks, e.g., [1–4]. WDM systems impose strict requirements on the optical crosstalk isolation within the comprising elements. For instance, crosstalk isolation levels better than 35 dB should be used to have power penalties smaller than 1 dB when even a moderated small number of crosstalk interferers are present [2]. This is still a high requirement for the performance of integrated optical switches and cross-connects at the current state-of-the-art [5]. Although improvements in device performance are foreseen, a substantial relaxation of the crosstalk requirements from individual components in optical networks can be achieved by using phase scrambling. In this way, the gap between the stringent crosstalk isolation requirements and the current, still unsatisfactory, achievable values is closed. In this paper we report that power penalties smaller than 1 dB for crosstalk values up to -18 dB are measured in a 2.5 Gbit/s link of 100 km of standard single mode fiber (SSMF). Power penalties smaller than 2 dB for crosstalk values up to -15 dB and -16 dB are measured after transmission over 100 km and 200 km of SSM fiber. This corresponds to an enhancement of the system tolerance to crosstalk of 7 dB and 5.3 dB, respectively. This result demonstrates the feasibility of optical networking in a LAN/MAN domain with the current state-of-the-art in integrated optical technology.

The main contribution of this paper is a complete assessment, experimentally and theoretically, of interferometric crosstalk reduction by phase scrambling in WDM networks. This paper is organized as follows. The phase scrambling principle is described in section II. Implications for transmission over dispersive fibers are studied at Sect. III. Section IV covers the perfor-

mance analysis. The experimental details are given in section V. Experimental and theoretical results are presented and discussed in Sect. VI. Finally, summarizing conclusions and recommendations are outlined in section VII.

II. PHASE SCRAMBLING PRINCIPLE

This section presents the theoretical framework of phase scrambling. Firstly, the receiver model under consideration is introduced. Secondly, the model for interferometric crosstalk is explained. The influence of filtered interferometric crosstalk is quantified by its variance which is mainly determined by the relation between the spectrum of the interferometric crosstalk noise and the post-detection filter bandwidth. Thirdly, the phase scrambling technique to reduce the influence of filtered interferometric crosstalk is introduced.

A. Receiver Model

Lets consider the case of an optical signal disturbed by a number N of interferers operating at the same nominal wavelength. The optical field of the information signal $\vec{E}_s(t)$ and the interferers $\vec{E}_x(t)$ are given by their complex amplitude vectors

$$\vec{E}_s(t) = \sqrt{b_k^s P_0 g_s(t)} \vec{r}_s e^{j\phi_s(t)} \quad (1)$$

$$\vec{E}_x(t) = \sum_{n=1}^N \sqrt{\epsilon_n b_k^{x,n} P_0 g_{x,n}(t)} \vec{r}_{x,n} e^{j\phi_{x,n}(t)} \quad (2)$$

where ϵ is the crosstalk parameter: the ratio of leakage crosstalk to signal power. The indicator b_k is introduced to represent the binary symbols: $b_k \in \{0, 1\}$ ($0 \leq \rho < 1$) at time slot k . For the case of perfect extinction the ratio $\rho = 0$. $\phi_{s,x}$ is the phase of the signal and interferer, respectively. \vec{r}_s and \vec{r}_x are unit vectors representing the signal and interferer polarization state, respectively. The optical peak power is denoted by P_0 and $g(t)$ is the pulse shape.

We consider an ASK direct detection system whose schematic diagram is given in Fig. 1. The photocurrent at the output of the photodetector, $I_{sh}(t)$, is a shot noise process which can be written as

$$I_{sh}(t) = \mathcal{R} |\vec{E}_s(t) + \vec{E}_x(t)|^2, \quad (3)$$

where \mathcal{R} is the detector responsivity.

The receiver thermal noise, denoted by $I_{th}(t)$, is modeled as an additive, zero mean, white Gaussian stochastic process. It is assumed that the optical pulses are of identical shape and confined in the time interval $[0, T]$, i.e. no intersymbol interference (ISI). The signal and the interferers are assumed to exhibit matched polarizations (worst case), and perfect bit alignment.

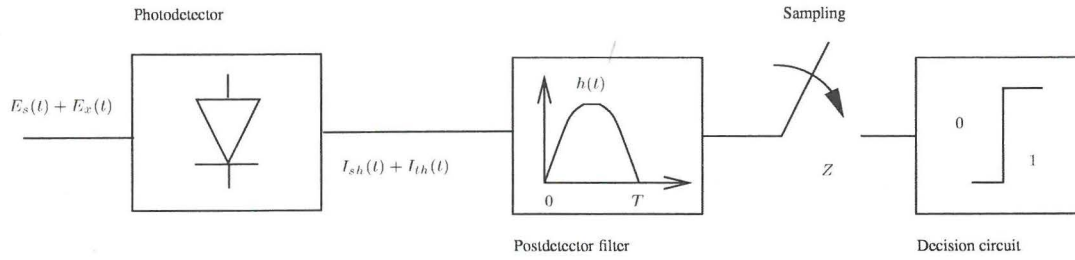


Fig. 1. Schematic diagram of an ASK/DD receiver. At the receiver input $E_s(t)$ represents the optical signal while interferometric crosstalk is denoted by $E_x(t)$.

With the above mentioned assumptions the photocurrent can be written as

$$I_{sh}(t) = P_0 g(t) b_0^s + 2P_0 g(t) \sum_{n=1}^N \sqrt{b_0^s b_0^s} \epsilon_n \cos[\phi_s(t) - \phi_{x,n}(t - \tau_{d,n})] + 2P_0 g(t) \sum_{n=1}^N \sum_{l=1}^{N-1} \sqrt{b_0^{x,n} b_0^{x,l}} \epsilon_n \epsilon_l \times \cos[\phi_{x,n}(t - \tau_{d,n}) - \phi_{x,l}(t - \tau_{d,l})] + P_0 g(t) \sum_{n=1}^N b_0^{x,n} \epsilon_n, \quad (4)$$

where τ_d is the interferometric delay time. The first term is the signal, the second the signal-crosstalk beating, the third the secondary crosstalk-crosstalk beating and the last term is the crosstalk beating with itself.

The photocurrent and thermal noise pass the postdetection filter $h(t)$ whose output is sampled to form the decision variable Z . By comparing the sample value with a preselected threshold α_{tr} , the decision circuit provides an estimate of a transmitted bit in a particular bit interval.

B. Interferometric Crosstalk

The interferometric crosstalk contributions to the photocurrent are of the type

$$\xi(t) = \cos[\phi_s(t) - \phi_x(t - \tau_d)]. \quad (5)$$

The laser phase (variables $\phi_x(t)$, $\phi_s(t)$ in (1)), is modeled as a Wiener process [6]. Then the phase difference

$$\Delta\phi(t) = \phi_s(t) - \phi_x(t - \tau_d) \quad (6)$$

is also a Wiener process, Gaussian distributed with zero mean and variance given by

$$\sigma_{\Delta\phi}^2 = 2\pi\Delta\nu\tau_d = B_L\tau_d, \quad (7)$$

where $\Delta\nu$ equals the 3-dB bandwidth of the Lorentzian shaped laser power spectrum [6].

The autocorrelation function of the process $\xi(t)$ is related to the autocorrelation function of the process $\Delta\phi(t)$ in the following way ([7], Sect. 8.3.2)

$$R_\xi(\tau) = \frac{1}{2} \exp(-[R_{\Delta\phi}(0) + R_{\Delta\phi}(\tau)]) + \frac{1}{2} \exp(-[R_{\Delta\phi}(0) - R_{\Delta\phi}(\tau)]) \quad (8)$$

where $R_{\Delta\phi}(\tau)$ is found to be

$$R_{\Delta\phi}(\tau) = \begin{cases} 2\pi\Delta\nu(\tau_d - |\tau|) & |\tau| \leq \tau_d \\ 0 & |\tau| > \tau_d \end{cases} \quad (9)$$

Substitution of (9) in (8) yields

$$R_\xi(\tau) = \begin{cases} \frac{1}{2} e^{-B_L|\tau|} [1 + e^{-2B_L(\tau_d - |\tau|)}] & |\tau| \leq \tau_d \\ e^{-B_L|\tau|} & |\tau| > \tau_d \end{cases} \quad (10)$$

Incoherent interferometric noise

In most of the application of interest the delay time is of a larger magnitude than the laser coherence time ($B_L\tau_d \gg 1$). This situation is called the incoherent interferometric noise regime. In integrated optical cross-connects the circuit configuration can be chosen such that the amount of crosstalk is minimized and that the dominant crosstalk contributions are in the incoherent regime [5]. For this case the autocorrelation is given by

$$R_\xi(\tau) = \begin{cases} \frac{1}{2} e^{-B_L|\tau|} & |\tau| \leq \tau_d \\ 0 & |\tau| > \tau_d \end{cases} \quad (11)$$

Filtered interferometric crosstalk

At the output of the postdetection filter, $h(t)$, the filtered interferometric noise is denoted by

$$\gamma(t) = \xi(t) * h(t), \quad (12)$$

where $*$ represents the convolution operation.

If we consider an integrate-and-dump postdetection filter, then the variance for filtered crosstalk is given by [8]

$$\sigma_\gamma^2 = \frac{e^{-B_L T} + B_L T - 1}{(B_L T)^2}. \quad (13)$$

In the incoherent regime the mean of filtered interferometric crosstalk approaches the value zero. We may also consider a wider class of postdetection filters. In that case the variance for filtered interferometric crosstalk can be found by using the following relation

$$\sigma_\gamma^2 = 2 \int_0^\infty S_\xi(f) |H(f)|^2 df, \quad (14)$$

where $H(f)$ is the transfer function of the postdetection filter and $S_\xi(f)$ is the interferometric crosstalk power spectrum obtained by Fourier transforming (11).

For comparison reasons we introduce an effective electrical filter bandwidth $B_F = 1/T$. In Fig. 2 is shown the variance of filtered interferometric crosstalk using two different filters: an integrate-and-dump, and a full raised cosine filter. We observe that by increasing the value of B_L/B_F a significant reduction of the noise variance is achieved. This is an important characteristic of filtered interferometric crosstalk. It indicates that we can reduce interferometric crosstalk by strong filtering or by dithering the phase of the light source. As the postdetection filter bandwidth is governed by the operating data rate, we propose to exploit the second fact to reduce the effect of interferometric crosstalk in WDM networks. Namely, we will, intentionally, perform phase modulation of the signals with noise: phase scrambling.

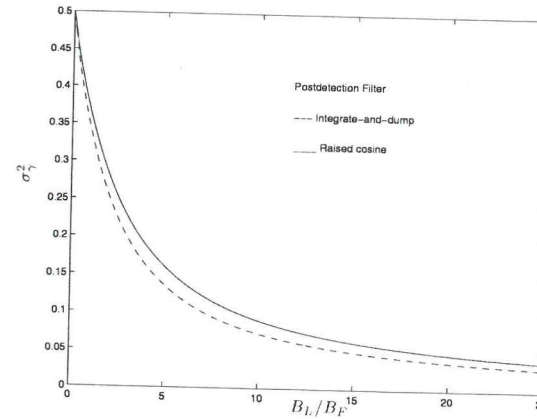


Fig. 2. Variance of filtered interferometric crosstalk as a function of B_L/B_F .

C. Phase scrambling

Interferometric noise reduction by broadening the spectrum (by e.g. phase dithering or phase noise modulation) has already been proposed [9–11]. However, as to our knowledge, a complete assessment of crosstalk reduction by phase scrambling, including transmission, in WDM networks has not been reported yet. This section introduces the theoretical framework of interferometric crosstalk reduction by phase scrambling. The schematic diagram of phase scrambling is presented in Fig. 3. Consider that the optical signals are phase modulated with noise $\psi(t)$. The optical field can be, generally, written as

$$\vec{E}(t) = \sqrt{b_k P_0(t) g(t)} \vec{r} e^{j[\phi(t) + \psi(t)]}, \quad (15)$$

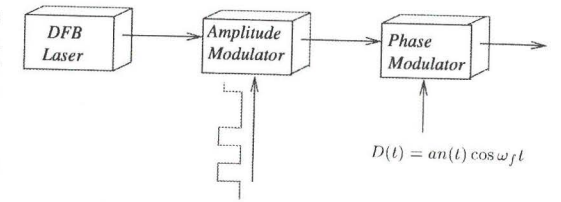


Fig. 3. The signal is phase modulated with noise $D(t)$, centered at an arbitrary frequency ω_f .

and the interferometric crosstalk contributions to the photocurrent are then of the type

$$\xi(t) = \cos[\Delta\phi(t) - \Delta\psi(t)], \quad (16)$$

in which $\Delta\phi(t)$ and $\Delta\psi(t)$ are the phase difference (cf. (6)) of the laser phase and the imposed phase modulation, respectively. By considering $\Delta\phi(t)$ and $\Delta\psi(t)$ to be independent stochastic processes, it can be shown that the autocorrelation function of $\xi(t)$ is given by

$$R_\xi(\tau) = \frac{1}{2} \exp(-[R_M(0) + R_M(\tau)]) + \frac{1}{2} \exp(-[R_M(0) - R_M(\tau)]), \quad (17)$$

in which $R_M(0) = R_{\Delta\phi}(0) + R_{\Delta\psi}(0)$ and $R_M(\tau) = R_{\Delta\phi}(\tau) + R_{\Delta\psi}(\tau)$. We proceed, similarly as in [9], by assuming that $\psi(t)$ is of the form

$$\psi(t) = an(t) \cos \omega_f t, \quad (18)$$

where a is the modulation index and $n(t)$ is a bandpass Gaussian noise centered at a frequency ω_f . The autocorrelation function for $\Delta\psi(t)$ is given by

$$R_{\Delta\psi}(\tau) = \frac{a^2}{2} R_n(\tau) \cos \omega_f \tau + \frac{a^2}{2} R_n(\tau_d) \cos \omega_f \tau_d - \frac{a^2}{2} R_n(\tau - \tau_d) \cos \omega_f (\tau - \tau_d) - \frac{a^2}{2} R_n(\tau + \tau_d) \cos \omega_f (\tau + \tau_d), \quad (19)$$

where $R_n(t)$ is the autocorrelation function of the Gaussian noise $n(t)$. We also define by τ_n the autocorrelation time of the noise $n(t)$. Further, we assume that the time delay exceeds the noise correlation time: $\tau_d \gg \tau_n$. This incoherent regime, as already mentioned above, is applicable in WDM networking. In this case, the calculations for $R_{\Delta\psi}(\tau)$ are simplified. The terms in (19) involving τ_d can be neglected and we get

$$R_{\Delta\psi}(\tau) = \frac{a^2}{2} R_n(\tau) \cos \omega_f \tau. \quad (20)$$

Subsequently, we arrive at

$$R_\xi(\tau) = \frac{1}{2} e^{-B_L|\tau|} e^{-\frac{a^2}{2} [R_n(0) - R_n(\tau) \cos \omega_f \tau]}. \quad (21)$$

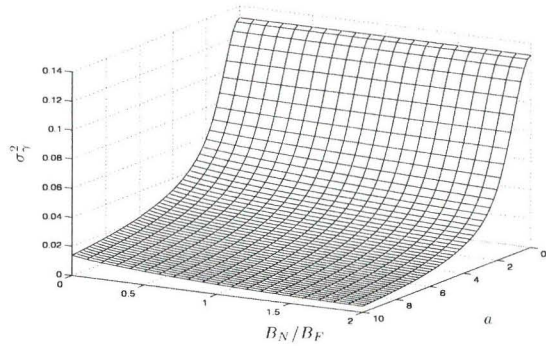


Fig. 4. Variance of filtered interferometric crosstalk as function of the parameters B_N and a for a fixed value of $\omega_f/B_F = 2$.

Let us analyze the dependence of the variance of crosstalk on the parameters of the phase scrambling signal such as the central frequency ω_f , modulation index a and the equivalent noise bandwidth B_N of the modulating noise. The spectral shape of $n(t)$ is taken to be of a Lorentzian shape. It has been shown that the shape of the power spectral density of the modulating noise $n(t)$ is irrelevant for the crosstalk noise reduction [9]. A plot of the variance, given a value for ω_f , as a function of a and B_N is presented in Fig. 4. We observe that the variance decreases substantially as the modulation index increases. The same tendency is observed for the other studied values of ω_f . We also performed similar computations as in Fig. 4 for other combinations of parameters. From our study, we observe that the parameter of major influence is the modulation index a . Moreover, we also observe that for relative large values of B_N/B_F the value of the central frequency has little or insignificant influence on the crosstalk reduction. However, the central frequency should amount some hundreds of MHz to enhance the crosstalk reduction when fiber dispersion restricts the use of a wide bandwidth modulating noise.

In general, we can conclude that phase scrambling with a Gaussian noise source reduces effectively the variance of interferometric crosstalk. The parameter of major influence on the reduction of crosstalk is the modulation index a . The modulating noise source can be centered at an arbitrary frequency ω_f and its equivalent noise bandwidth can be smaller than the bit rate (see Fig. 4). This agrees well with previous results [9] and it is confirmed in our experimental setup.

III. TRANSMISSION OVER DISPERSIVE FIBERS

In this section, the spectral broadening caused by the imposed phase modulation is determined. Subsequently, a model for the relative noise due to phase-to-intensity noise conversion caused by chromatic dispersion is presented.

A. Spectrum of phase modulated signal with Gaussian noise

Determining the spectrum of a phase modulated signal with a Gaussian noise is a topic widely studied in references like e.g. [12, 13]. It is of common practice to specialize the

analysis to certain cases. For instance, to the case of large or small modulation index. As we already observed in the previous section we are interested in a phase modulation with a large modulation index to effectively reduce interferometric crosstalk. Therefore we will consider a large index phase modulation with a Gaussian noise. The spectrum shape of the modulating noise is assumed to be a Lorentzian function. This type of noise may be obtained by low bandpass filtering a white Gaussian noise; say by an RC-circuit.

From (15) we have that the phase modulating signal is given by

$$E_{\phi M}(t) = e^{j\phi(t)} \times e^{j\psi(t)} = E_{\phi}(t) \times E_{\psi}(t). \quad (22)$$

The autocorrelation function of the phase modulated signal $E_{\psi}(t)$ is given by [13]

$$R_{E_{\psi}}(t) = e^{-k(\tau)}, \quad (23)$$

where

$$k(\tau) = R_{\psi}(0) - R_{\psi}(\tau),$$

with $R_{\psi}(\tau)$ the autocorrelation function of the modulating Gaussian noise.

The spectral density $S_{E_{\psi}}(f)$ of $E_{\psi}(t)$ is given by the Fourier transform of (23). For the case of large modulation index this spectral density can be approximated by a Lorentzian spectrum with a 3-dB bandwidth $\Delta\nu_{\psi} = B_N a^2$ [13]. The spectrum of the phase scrambled signal is given by the convolution of the spectrum due to the laser phase noise and the imposed phase modulation:

$$S_{\phi M}(f) = S_{\phi}(f) * S_{\psi}(f). \quad (24)$$

The spectrum due to the phase noise is known to be given by the Lorentzian shape with a 3-dB bandwidth $\Delta\nu$ [6]. The convolution of two Lorentzian shaped spectra is again a Lorentzian spectrum with a 3-dB bandwidth given by the sum of their 3-dB bandwidth. So, we have that the (normalized) spectrum of the phase modulated signal is given by

$$S_{\phi M}(f) = \frac{1}{1 + \left(\frac{f}{\Delta\nu + \Delta\nu_{\psi}}\right)^2}. \quad (25)$$

From this result we may conclude that the effect of phase scrambling on the signal spectrum is to cause spectral broadening yielding a resultant 3-dB bandwidth

$$\Delta\nu_{\phi M} = \Delta\nu + \Delta\nu_{\psi} = \Delta\nu + B_N a^2. \quad (26)$$

B. Propagation in dispersive fibers

Phase scrambling, as shown in the preceding section, reduces interferometric crosstalk, but at the same time the broadening of the laser spectrum may have detrimental effects on the system performance. Namely, laser phase-to-intensity noise conversion by chromatic dispersion may lead to power penalties in optical fiber transmission systems, e.g., [14, 15]. This section presents the analysis of phase-to-intensity noise conversion during

transmission by determining the relative intensity noise (RIN) at the fiber output.

Propagation in a fiber of length L is described by the propagation term $e^{-j\beta L}$ where the phase function β can be expanded in a Taylor series and keeping only the first terms

$$\beta(\omega) = \beta_0 + \beta_1(\omega - \omega_0) + \frac{1}{2}\beta_2(\omega - \omega_0)^2, \quad (27)$$

with the group delay per unit length β_1 and the group velocity dispersion

$$\beta_2 = \frac{-D\lambda^2}{2\pi c}, \quad (28)$$

in which λ is the wavelength and c the velocity of light, and D the common dispersion parameter.

We aim to determine the variance due to RIN. The variance of the RIN contribution to the photocurrent, after postdetection filtering, can be found by

$$\sigma_{\text{RIN}}^2 = \int_0^{\infty} \text{RIN}(f) |H(f)|^2 df, \quad (29)$$

where $\text{RIN}(f)$ is the normalized RIN power spectral density at the dispersive fiber output. The transfer function the postdetection filter is denoted by $H(f)$.

C. RIN Model

This section presents the model of the RIN for a systems using externally modulated light sources. This type of light source exhibits a low magnitude of chirp (spectral broadening) which means that insignificant crosstalk noise filtering will take place at the receiver end. In this case phase scrambling will assure the needed spectral broadening for substantial crosstalk filtering by the electrical postdetection filter. However, spectral broadening may introduce penalties due to dispersion. Yamamoto et al. [15] have studied the effect of phase-to-intensity noise conversion by chromatic dispersion in intensity modulated and direct detected systems. The normalized RIN power spectral density at the dispersive fiber output is related to the laser phase noise and fiber dispersion as follows: [15]

$$\text{RIN}(f) = 8 \left[\sum_{n=0}^{\infty} J_n(\alpha_0) J_{n+1}(\alpha_0) \sin \left\{ \frac{1}{2}(2n+1)\alpha_1 \right\} \right]^2, \quad (30)$$

where $J_n(\cdot)$ is the Bessel function of the first kind, and

$$\alpha_0 = \frac{1}{f} \sqrt{\frac{2\Delta\nu}{\pi}}, \quad (31)$$

$$\alpha_1 = (2\pi f)^2 \beta_2 L. \quad (32)$$

When phase scrambling is employed we proceed by assuming that the effect is equivalent to a laser source with a broader linewidth, namely the resultant 3-dB bandwidth $\Delta\nu_{\phi M}$. This can be deduced from the analysis in Sec. III-A. This fact has also been pointed out in [16].

Systems using directly modulated lasers experience substantial spectral broadening due to chirp which is intrinsic to this type of modulation. Although this spectral broadening results in crosstalk noise filtering at the receiver end, this filtering is not assured for all detection situations because of the bit pattern dependence of chirp. In these systems phase scrambling will also result in crosstalk mitigation. However, the enhancement of the tolerance to crosstalk is expected to be smaller than in the case of systems using externally modulated lasers, for the reason of the already present spectral broadening in directly modulated lasers.

IV. PERFORMANCE ANALYSIS

This section presents the performance evaluation for ASK/DD receivers using phase scrambling to reduce interferometric crosstalk. The question is to evaluate the average error rate P_e of the system under discussion (see Fig. 1). To account for all possible combination of beat terms between the signal and crosstalk we proceed by assuming that μ sources are simultaneously a binary symbol "one", thus $N - \mu$ sources are "zero". The error probability analysis is then conducted by a weighted statistical average of the error probability for each value μ . This probability is given by the binomial distribution function. Hence, the average error probability P_e or bit-error rate (BER), for a given threshold α_{tr} , using the Gaussian approximation and assuming that the symbols are *a priori* equally probably $P_e(\mu)$ can be written as

$$P_e = \frac{1}{2^N} \sum_{\mu=0}^N \binom{N}{\mu} \left\{ \frac{1}{2} Q \left(\frac{E_1(\mu) - \alpha_{tr}}{\sigma_1(\mu)} \right) + \frac{1}{2} Q \left(\frac{\alpha_{tr} - E_0(\mu)}{\sigma_0(\mu)} \right) \right\}, \quad (33)$$

where $E_{1,0}$ is the mean value of the receiver decision variable when a "one", and a "zero" is transmitted, respectively. The variance is denoted by $\sigma_{1,0}^2$. The function $Q(\cdot)$ is the standard Gaussian probability tail function. In the presence of interferometric crosstalk and RIN due to chromatic dispersion after propagation, the variance of the receiver decision variable is approximately given by

$$\begin{aligned} \sigma_{0,1}^2 = & \underbrace{2q\mathcal{R}P_0b_0^2B_FI_2}_{\text{signal shot noise}} + \underbrace{2q\mathcal{R}P_0 \sum_{n=1}^N b_0^{x,n} \epsilon_n B_F I_2}_{\text{xtalk shot noise}} + \\ & \underbrace{(q\mathcal{R}2P_0)^2 \sum_{n=1}^N b_0^{x,n} \epsilon_n \sigma_{\gamma,n}^2}_{\text{signal - xtalk beat}} + \underbrace{\sigma_{th}^2}_{\text{therm. noise}} + \\ & \underbrace{(q\mathcal{R}2P_0)^2 \sum_{n=l+1}^N \sum_{l=1}^{N-1} b_0^{x,n} b_0^{x,l} \epsilon_n \epsilon_l \sigma_{\gamma,n}^2}_{\text{xtalk - xtalk beat}} + \\ & \underbrace{(q\mathcal{R}2P_0)^2 b_0^2 \sigma_{\text{RIN}}^2}_{\text{signal RIN}} + \underbrace{(q\mathcal{R}2P_0)^2 \sum_{n=1}^N b_0^{x,n} \epsilon_n \sigma_{\text{RIN},n}^2}_{\text{xtalk RIN}}, \end{aligned} \quad (34)$$

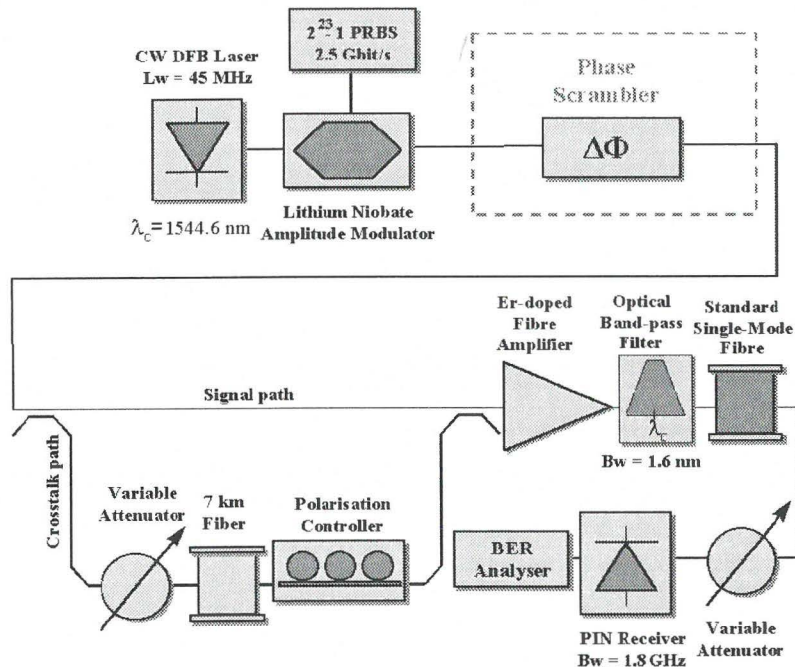


Fig. 5. Experiment setup for the investigation of interferometric noise reduction by phase scrambling.

where q is the electron charge, and I_2 is the Personick parameter [17]. Given a number N of crosstalk sources, the error probability is expeditiously evaluated by (33) accounting for data statistics, and non-perfect extinction ratio. The analysis, however, assumes that RIN contributions due to the beating terms of signal and crosstalk are neglected.

Some words on the use of the Gaussian approximation. As the signal is phase modulation with a Gaussian noise process the RIN due to phase to intensity noise conversion after propagation can also be considered to have a Gaussian distribution. The distribution of filtered interferometric crosstalk may differ from Gaussian statistics, e.g., [8, 18]. However, a Gaussian approximation (using the effective variance given by (14)) works well for crosstalk values resulting in relatively small power penalties. Moreover, the statistics of filtered interferometric noise tends to a Gaussian shape if the signal bandwidth exceeds the electrical filter bandwidth (as in the case of phase scrambling) [8]. We have adopted the Gaussian approximation for assessing the system performance considering the above mentioned features and also on view of its numerical simplicity.

V. EXPERIMENTAL SETUP

The experiment setup for measuring the interferometric crosstalk reduction by using phase scrambling is shown in Fig. 5. The setup works as follows. A commercial available

DFB laser with a measured linewidth of 45 MHz operating at a wavelength 1544.5 nm is the CW source for the system. The CW lightwave is injected to a LiNbO₃ external modulator which is driven by a pseudo-random binary signal generator (PRBS) producing an encoded repetitive sequence of non-return-to-zero (NRZ) pulses. The sequence length is $2^{23} - 1$ and the bit-rate is 2.5 Gbit/s. In this experiment, we have intentionally used an external modulator because of its low-chirp characteristic. In this way, the spectral broadening is determined mainly by the driving current of the phase scrambler. The generated PRBS NRZ format has a measurable 20 dB extinction ratio and the receiver sensitivity has been measured to lie around -27 dBm.

The phase scrambler consists of a commercially available phase modulator, which is driven electrically by a high frequency modulated noise source. In Fig. 6 is shown the spectrum of the phase modulator driving signal with a modulation index equal to π and with a bandpass filtered noise source centered at a frequency of 2.5 GHz. On the spectrum, the high frequency sinewave signal is clearly observed as a sharp peak surrounded by the bandpass filtered noise. The modulating noise bandwidth is measured to be around 200 MHz and the ratio between peak power of the sinewave and the noise amounts approximately 35 dB. The spectrum of the resulting phase scrambled (using a driving signal whose spectrum is shown in Fig. 6) optical signal is given in Fig. 7. In comparison with the original

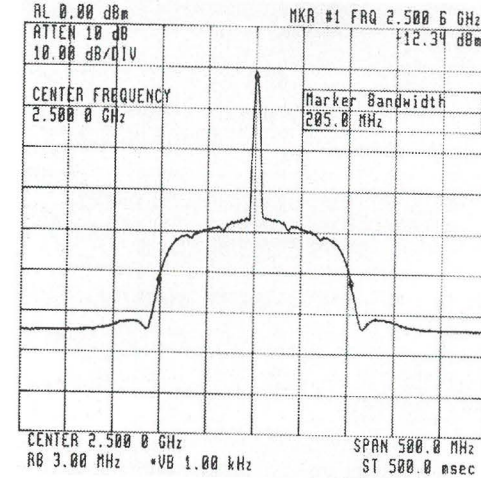


Fig. 6. Spectrum of the phase scrambling driving signal. The driving signal consists of a sinewave centered at 2.5 GHz and a filtered noise source with a bandwidth of 200-MHz.

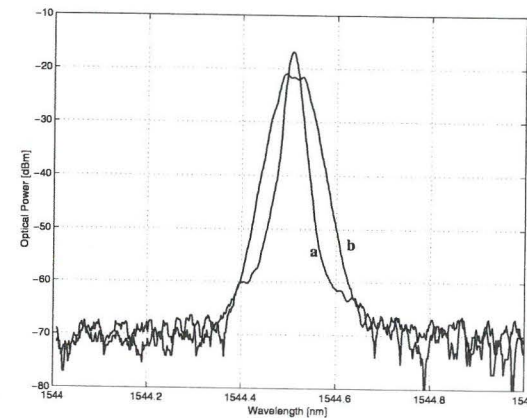


Fig. 7. Spectrum of the 2.5-Gbit/s optical signal: (a) without, (b) with the phase scrambling.

spectrum (curve a in Fig. 7), we measured an increase in spectral bandwidth after phase scrambling of approximately 74 picometers (curve b in Fig. 7). Moreover, the top is flattened by the phase scrambling. We observed also that this flattening is largely affected by the noise source parameter than by the sinewave. Furthermore, increasing the noise level does not show any significant change of the spectrum shape. The signal bandwidth varies significantly if the modulation index is varied to values up to approximately 2. This phenomenon has also been observed early in the theory section. After the phase scrambler, the 2.5-Gbit/s modulated signal is coupled into an unbalanced Mach-Zehnder structure in which the signal is split into two paths. One path is 7 km longer than the other. This length difference largely surpass the coherence length of a

45-MHz linewidth laser. Then, the two signals are mixed to produce interferometric beating noise at the incoherent regime. Polarization alignment between the signal and interferer, to create a worst-case condition, is done by adjusting the polarization controller. Two optical variable attenuators are used. One attenuator adjusts the level of the interferometric crosstalk and the other varies the level of received signal power.

The receiver section consists of an InGaAs PIN photodiode module followed by a variable gain GaAs electrical amplifier to boost received photocurrent. The electrical bandwidth of the receiver circuit is approximately 1.85 GHz, which is suitable to detect signals at a bit-rate of 2.5 Gbit/s without any distortion. The system performance is evaluated by using a BER analyzer. During the BER measurements the decision threshold is automatically optimized, taking a value somewhere between the level for the received binary "one" and "zero", to result in the lowest error probability.

The performance assessment of the system using phase scrambling is summarized in the power penalty curves shown in Fig. 9. The power penalties are related to a BER level of 10^{-9} . As reference we use a back-to-back measurement (no fiber transmission between the MZ and receiver section). In the back-to-back situation (curve a in Fig. 9), crosstalk levels less than -23 dB result in a penalty less than 1 dB. Using the phase scrambling technique, the crosstalk level causing the same penalty can be lowered to around -16 dB. With a transmission span of 100 km SSMF and using an optical amplifier to compensate for the fiber-induced loss, we still obtained a good performance even for crosstalk levels up to -18 dB. This means a crosstalk relaxation of 5 dB. Increasing the transmission span to 200 km and using a second amplifier, resulted in a tolerable crosstalk level of -21 dB. However, even for small values of the crosstalk the power penalty is relatively high, approximately 0.7 dB. This is due to the dispersion as a consequence of the spectrum broadening. We also observe that if we relate to a power penalty level of 2 dB, crosstalk values up to -15 dB and -16 dB are tolerable after transmission over 100 km and 200 km of SSM fiber. This corresponds to an enhancement of the system tolerance to crosstalk of 7 dB and 5.3 dB, respectively. In conclusion, we have demonstrated in a simple experimental setup that significant mitigation of interferometric crosstalk can be achieved using a phase scrambling technique, even for high levels of crosstalk. Transmission with satisfactory BER performance in a link of 100 km and 200 km of SSM fiber has been demonstrated. These transmission spans represent the situation in a LAN/MAN network. The power penalty due to dispersion was measured to be 0.4 dB and 0.7 dB for 100 km and 200 km transmission, respectively.

VI. RESULTS AND DISCUSSIONS

Phase scrambling - no transmission

In Fig. 8 is displayed how power penalties due to interferometric crosstalk are reduced by using phase scrambling. These theoretically obtained curves for a fixed value of $B_N T$ and $\omega_f T$ assume no transmission over dispersive fibers. The dotted line

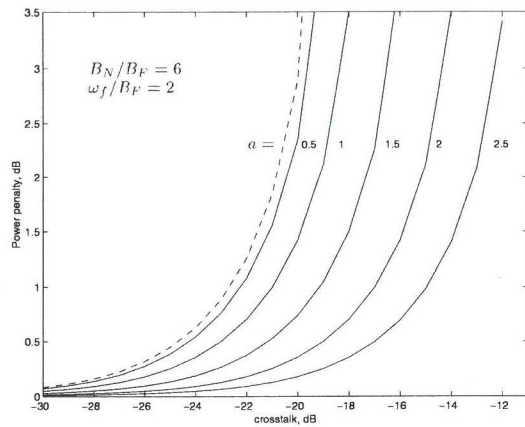


Fig. 8. Reduction of power penalty by phase scrambling as a function of the modulation index a . Theoretical results. The dotted line is the case of no phase scrambling. A fixed value for $B_N/B_F = 6$ and $\omega_f/B_F = 2$ is used. No transmission case.

represents the power penalties without phase scrambling. As the modulation index increases we can observe that system tolerance towards interferometric crosstalk is substantially enhanced.

Phase scrambling and transmission

We examine power penalties after 100 km and 200 km transmission over SSM fiber with $D = 17 \text{ ps/nm km}$. Phase scrambling is applied with a modulation index $a = \pi$. In Fig. 10 are presented the power penalties as function of the crosstalk parameter ϵ . The modulating noise bandwidth is $B_N = 200 \text{ MHz}$. The parameters used in the theoretical computations are in correspondence with the experimental set-up to simulate the measurements. We observe in Fig. 10

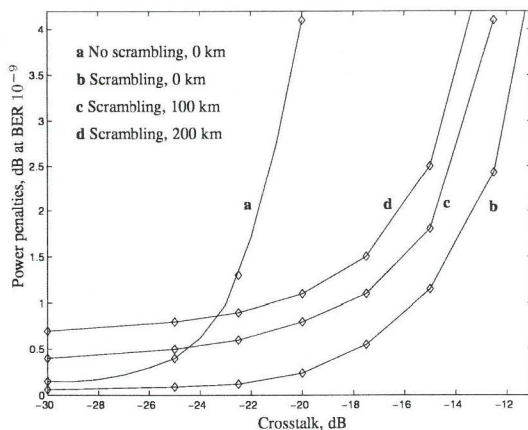


Fig. 9. Measured power penalties. (a) Back-to-back situation, and with phase scrambling (b). Results with phase scrambling and transmission over (c) 100 km, and (d) 200 km of SSMF.

that phase scrambling effectively enhance the tolerance towards crosstalk. However, additional power penalties associated with RIN due to dispersion are incurred. We can conclude that phase scrambling mitigates crosstalk penalties at expenses of network reach. We may compare the theoretical results shown in Fig. 10 with the measurements presented in Fig. 9. We observe good agreement between theory and experiment. The theoretical model predicts well the performance tendency of the system and can therefore be used to determine the proper parameters for phase scrambling in WDM networks.

The scalability of optical networks using phase scrambling is strongly governed by the limitations imposed by fiber dispersion. However, selecting appropriate parameters for the phase scrambling dispersion penalties can be kept small while crosstalk is still significantly filtered out at the receiver end. Limitations caused by the spectral broadening are further reduced in optical networks using dispersion compensating strategies. From our study, significant enhancement of the tolerance to crosstalk and transmission over 200 km SSMF are proven feasible for a system operating at 2.5 Gbit/s.

Besides phase scrambling other methods of crosstalk suppression have been proposed [3, 19]. These include bit pattern misalignment, error correcting codes, among others; see Table III in [3]. Among these methods phase scrambling is a proven crosstalk mitigating technique, but at expenses of network reach due to dispersion penalties.

VII. CONCLUSIONS AND RECOMMENDATIONS

A complete assessment, theoretical and experimental, of crosstalk reduction by phase scrambling in WDM systems is presented. It is experimentally demonstrated that phase scrambling substantially reduces interferometric crosstalk, enhancing the system tolerance to crosstalk. For instance, crosstalk values of -16 dB results in power penalty less than 2

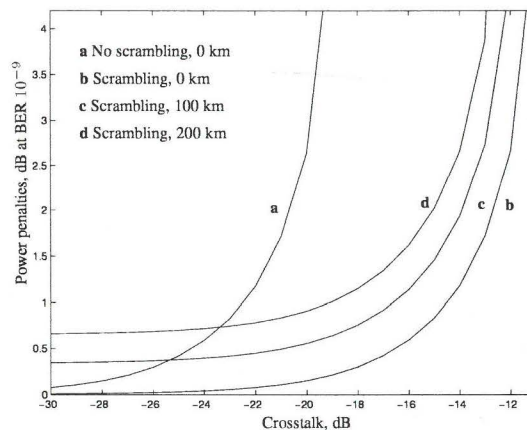


Fig. 10. Theoretical results for power penalties. (a) Back-to-back situation, (b) phase scrambling and no transmission. Results with phase scrambling and transmission over: (c) 100 km and (d) 200 km of SSM fiber.

dB after transmission over 200 km SSM fiber. Such crosstalk values when no phase scrambling is applied would make impossible any transmission of information. Hence, phase scrambling has been proven to effectively mitigate crosstalk extending the scalability properties of WDM optical networks. It is also shown that by properly choosing the noise source for the phase scrambling power penalties due to phase to intensity noise conversion can be kept small. For instance, transmission over 200 km of SSM fiber is successfully demonstrated. This results indicates that phase scrambling make feasible WDM networking in a LAN/MAN environment while making use of the current integrated switching and cross-connect technology.

Phase scrambling mitigates the limitations imposed by interferometric crosstalk at expenses of network reach. Care should be taken to assure that small power penalties due to dispersion are incurred. The presented theoretical model can be used to compute the optimal parameters for phase scrambling. The modulation index a is the parameter of major influence on the crosstalk mitigation. A fast crosstalk reduction is observed for values of a up to π . Larger values of a show a slow rate of reduction of crosstalk variance (see Fig. 4). The modulating noise source can be centered at an arbitrary frequency ω_f and its equivalent noise bandwidth can amount some hundreds of MHz.

Acknowledgment

This work was supported in part by the European Commission ACTS project AC332 APEX.

REFERENCES

- [1] E. L. Goldstein, L. Eskildsen, and A. F. Elrefaie, "Performance implications of component crosstalk in transparent lightwave networks," *IEEE Photonics Techn. Lett.*, vol. 6, pp. 657-700, May 1994.
- [2] E. L. Goldstein and L. Eskildsen, "Scaling limitations in transparent optical networks due to low-level crosstalk," *IEEE Photonics Techn. Lett.*, vol. 7, pp. 93-94, Jan. 95.
- [3] P. T. Legg, M. Tur, and I. Andonovic, "Solution paths to limit interferometric noise induced performance degradation in ASK/direct detection lightwave networks," *IEEE/OSA J. Lightwave Technol.*, vol. 14, pp. 1943-1953, Sept. 1996.
- [4] I. Tafur Monroy and E. Tangdiongga, "Performance evaluation of optical cross-connects by saddlepoint approximation," *IEEE/OSA J. Lightwave Technol.*, vol. 16, pp. 317-323, March 1998.
- [5] C. G. P. Herben *et al.*, "Compact integrated polarisation independent optical crossconnect," in *European Conference on Optical Communications*, vol. 1, (Madrid, Spain), pp. 257-258, September 20-24 1998.
- [6] A. Mooradian, "Laser linewidth," *Phys. Today*, vol. 38, pp. 43-48, May 1985.
- [7] G. Einarsson, *Principles of Lightwave Communications*. Chichester: John & Wiley, 1996.
- [8] I. Tafur Monroy, E. Tangdiongga, and H. de Waardt, "On the distribution and performance implications of interferometric crosstalk in wdm networks," *IEEE/OSA J. Lightwave Technol.*, June 1999. Accepted for publication.
- [9] P. K. Pepeljugoski and K. Y. Lau, "Interferometric noise reduction in fiber-optic links by superposition of high frequency modulation," *IEEE/OSA J. Lightwave Technol.*, vol. 10, pp. 957-963, July 1992.
- [10] A. Yariv, H. Blauvelt, and S. Wu, "A reduction of interferometric phase-to-intensity conversion noise in fiber links by large index phase modulation of the optical beam," *IEEE/OSA J. Lightwave Technol.*, vol. 10, pp. 978-981, July 1992.
- [11] F. W. Willems and W. Muys, "Suppression of interferometric noise in externally modulated lightwave AM-CATV systems by phase modulation," *Elect. Letters*, vol. 29, pp. 2062-2063, Nov. 1993.
- [12] D. Middleton, *An Introduction to Statistical Communication Theory*. McGraw-Hill Book Company, Inc., 1960.
- [13] H. E. Rowe, *Signals and Noise in Communications Systems*. The Bell Telephone laboratories series, D. van Nostrand Company, Inc., 1965.
- [14] A. R. Chraplyvy *et al.*, "Phase modulation to amplitude modulation conversion of cw laser light in optical fibres," *Elec. Lett.*, vol. 22, pp. 409-500, April 1986.
- [15] S. Yamamoto and *et al.*, "Analysis of laser phase noise to intensity noise conversion by chromatic dispersion in intensity modulation and direct detection optical fiber transmission," *IEEE/OSA J. Lightwave Technol.*, vol. 8, pp. 1716-1722, Nov. 1990.
- [16] A. Yariv *et al.*, "An experimental and theoretical study of the suppression of interferometric noise and distortion in am optical links by phase dither," *IEEE/OSA J. Lightwave Technol.*, vol. 15, pp. 437-443, March 1997.
- [17] R. G. Smith and S. D. Personick, *Semiconductor Device for Optical Communication*, ch. Receiver Design for Optical Communication Systems, pp. 89-160. Springer-Verlag, 1987.
- [18] M. Tur and E. L. Goldstein, "Probability distribution of phase-induced intensity noise generated by distributed feed-back lasers," *Optics Letters*, vol. 15, pp. 1-3, January 1990.
- [19] R. Khosravani *et al.*, "Reduction of coherent crosstalk in WDM add/drop multiplexing nodes by bit pattern misalignment," *IEEE Photon. Technol. Lett.*, vol. 11, pp. 134-135, January 1999.

Paper L

Scalability of All-Optical Networks: Study of Topology and Crosstalk Dependence

Idelfonso Tafur Monroy, J. Siffels, H. de Waardt and H. J. S. Dorren
Syben'98. Zurich, Switzerland, May 18-22, 1998, pp 201-207.

Scalability of all-optical networks: study of topology and crosstalk dependence

I. Tafur Monroy, J. Siffels, H. de Waardt and H.J.S. Dorren

Eindhoven University of Technology, Telecommunication Technology and Electromagnetics.

P. O. Box 513, 5600 MB Eindhoven, The Netherlands

ABSTRACT

The influence of in-band crosstalk on the error performance of all optical networks with different topologies is studied. A statistical crosstalk model is used for evaluating the bit-error rate. The model accounts for optical preamplification. We present a network topology having the best performance while using the largest transmission path.

1. INTRODUCTION

All-optical networks offering a large transport capacity, are regarded as a promising solution to the increasing demand of bandwidth in future telecommunication systems. In these networks routing, switching and amplification is performed in the optical domain. In Fig.1, a schematic representation of an optical multi-wavelength cross-connect is presented.

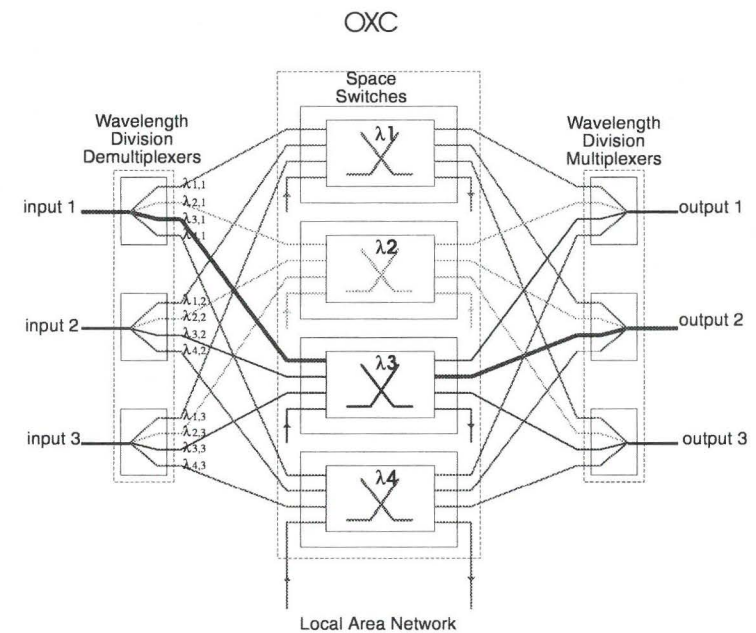


Figure 1. Optical Cross Connect

Suppose we consider a signal at wavelength λ_3 which is switched from input 1 to output 2. It is well-known that due to an imperfect switching array, the output signal is corrupted with contamination of other input signals. This phenomena is called crosstalk. Transparent optical networks impose strict requirements on the crosstalk performance

of the network elements involved.¹ We restrict ourselves to considering the situation that the contamination has the same wavelength as the signal (in-band crosstalk). This type of crosstalk can not be removed by using optical filters and it is therefore necessary to design optical networks with an optimum crosstalk performance. In this paper we focus on crosstalk accumulation which takes place when a signal passes through different nodes in a network. An example is given in Fig. 2. Suppose we have a fixed distribution of nodes which are connected to each other by four different configurations. It is clear that the crosstalk performance is related to the topology involved. We aim to investigate which of the topologies has the best performance with respect to crosstalk accumulation. We approach the problem by using numerical simulation techniques. The model accounts for data-statistics, linear random polarization and a non-perfect extinction ratio. The receiver model also counts for optical preamplification by an erbium-doped fibre amplifier (EDFA). The main result of the paper is that we show that introducing additional links in a network leads to a decreased crosstalk performance. We will consider two situations. In the first case we consider ideal networks, while in the second case we assume that link failures take place.

This paper is structured as follows: Sect. 2 introduces four different network topologies. Section 3 describes the receiver model and explains how the performance analysis is conducted. The mathematical model which is used to compute the crosstalk is explained in Sect. 4. The simulation results are presented in Sect. 5. The paper is concluded with a short discussion.

2. ANALYSIS

The considered networks consist of a core-network which is connected to a number of sub-networks (Fig. 2). We assume that every node in a sub-network is connected to an access network. We search for the largest transmission path in these networks. With this we mean that we compute the set of shortest paths between all possible pairs of nodes in the network. From this set of shortest paths we select the path with the maximum length. From a physical point of view this means that we have selected the largest possible connection between two nodes in the network.

The next step is to calculate the total number of crosstalk sources. We will use this number as a measure for comparing the four studied topologies. The number of crosstalk sources is determined by counting the number of interfering channels. In the following we assume that this number equals the number of fibers connected to the node minus one (which represents the incoming signal).

The first network of Fig. 2 we discuss in detail is *Topology 1* which represents five interconnected ring networks. This implies that every node has a connection to its left-hand-side neighbour and to the right-hand-side neighbour. Rings are commonly used because of the possible alternative routing (self-healing) when a failure occurs. The number of needed connections (fibres) is equal to the number of nodes. Each sub-network has only one connection to the core-network. This can be an unwanted situation because of the absence of a backup route. From this topology, it follows that the nodes in the core-network have two sources of crosstalk. Since it is assumed that the sub-networks are connected to access networks, it follows that every node in the sub-network has two possible sources of crosstalk, except the node with the connection to the core-network. The latter has three sources of crosstalk.

Topology 2 is similar to *Topology 1*, but in the core-network two extra links are introduced (Fig. 2b). With these extra links the core-network is fully connected. With this we mean that every node in the core-network is interconnected to every other node. This implies that by passing the core-network only two nodes have to be visited. On the other hand the number of crosstalk sources in each node of the core-network is increased from two to three.

We proceed by considering *Topology 3*. In this topology the sub-networks are interconnected to each other. This implies that only *Topology 3* has an alternative for re-routing between two sub-networks. The largest path consists of six nodes. However there are two possible routes, one using the core-network and one using the outer-ring. The difference between these two routes is that the route through the core has fourteen crosstalk sources, while the route using the outer ring has nineteen sources of crosstalk.

The last network of Fig. 2 we consider is *Topology 4*. This network consists of a fully connected core-network and fully connected sub-networks. The largest route in this network consists of six nodes, but the number of crosstalk sources has increased to twenty.

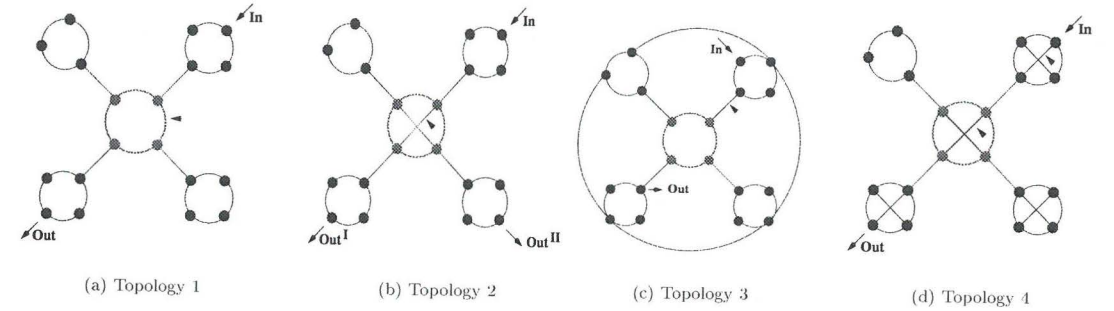


Figure 2. The topologies studied in this paper

3. RECEIVER MODEL

We consider an ASK/DD (direct detection), optically preamplified receiver whose schematic diagram is depicted in Fig. 3. The incoming optical signal $Y(t)$ (informative signal and crosstalk), after traversing one or several optical cross-connections, is amplified and subsequently filtered in order to reduce the effect of the amplified spontaneous emission (ASE) noise $X(t)$. The photodetector output is passed through an integrate-and-dump filter and sampled to form the decision variable Z . The decision device derives an estimate of a transmitted binary symbol by comparing the value of the decision variable with a preselected detection threshold α .

We are interested in evaluating the error performance of the system. To accomplish this goal we use an statistical

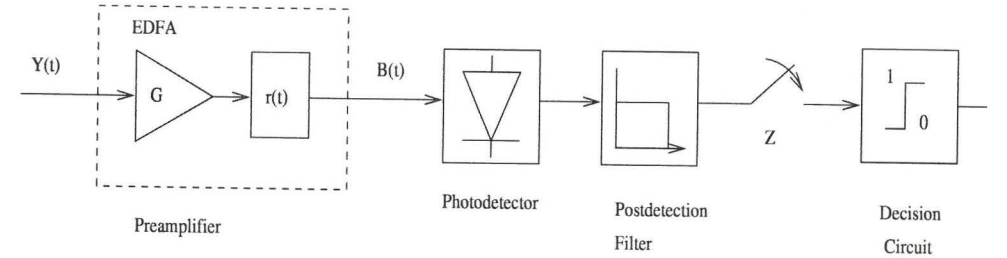


Figure 3. Optical preamplified ASK/DD receiver

method for evaluating the error-probabilities: the so called saddlepoint approximation which makes use of the moment generating function (mgf) for the receiver decision variable. We present here only some key results on the performance analysis for ASK/DD systems subject to crosstalk. For a detailed presentation we refer to.² The mgf of the decision variable Z is given by

$$M_Z(s) = M_{sh}(s)M_{th}(s), \quad (1)$$

where M_{th} is the mgf for a zero mean Gaussian variable with variance σ_{th}^2 : $M_{th}(s) = \exp(s\sigma_{th}^2/2)$. $M_{sh}(s)$ is the mgf of the filtered shot noise (photocurrent) contribution to the decision variable Z . The shot noise is well modeled as a doubly stochastic Poisson process with intensity $\lambda(t)$. Hence, for the case of an integrator postdetection filter, M_{sh} is given by³

$$M_{sh}(s) = M_{\Lambda}(e^s - 1), \quad (2)$$

where $\Lambda = \int_0^T \lambda(t)dt$ is the *Poisson parameter*. The photoelectron intensity $\lambda(t)$, in a normalized way is given by³:

$$\lambda(t) = \frac{1}{2}|B(t)|^2, \quad (3)$$

in which $B(t)$ represents the optical field, equivalent baseband form, falling upon the photodetector. In Sect. 4 we present an explicit expression for the mgf $M_\Lambda(s)$.

3.1. Optical preamplification

Consider an optical signal $Y(t)$ at the input of the EDFA preamplifier which is modeled as an optical field amplifier with power gain G , an additive noise source $X(t)$, representing the spontaneous emission and an optical filter with complex equivalent baseband impulse response $r(t)$. The optical field at the output of the amplifier is

$$B(t) = \sqrt{G}Y(t) + X(t), \quad (4)$$

where $X(t)$ is a white Gaussian stochastic process representing the spontaneous emission noise. The density of $X(t)$ expressed in photons per second is given by⁴:

$$N_0 = n_{sp}(G - 1),$$

in which n_{sp} represents the spontaneous emission parameter. For the further analysis, following Ref. 4, we assume that $Y(t)$ is confined in the bit interval and that the impulse response $r(t)$ is limited to the same time interval. We can therefore expand $B(t)$ in a Fourier series. Subsequently, the optical field $B(t)$ can be written as:

$$B(t) = \sum_{k=-L}^{k=L} (Y_k + X_k) e^{j\pi kt/T}, \quad (5)$$

where $\beta = 2L + 1$ (the number of temporal modes) equals the ratio of the bandwidth B_0 of the optical filter and the data rate $B = 1/T$:

$$\beta = B_0/B.$$

The real and imaginary part of $X_k = X_{ck} + jX_{sk}$ are Gaussian independent variables with equal variances for all $-L \leq k \leq L$: $\text{Var}\{X_{ck}\} = \text{Var}\{X_{sk}\} = N_0 B$.

We can now express Λ as:

$$\Lambda = \frac{T}{2} \left(\sum_{k=-L}^{k=L} [Y_k \sqrt{G} + X_{ck}]^2 + X_{sk}^2 \right). \quad (6)$$

We focus now on the derivation of the mgf for Z , accounting for crosstalk and optical preamplification. Our first step towards the derivation of this mgf is to condition on the value of Y_k and observe that Λ is the sum of 2β independent Gaussian variables with variance equal to $N_0/2$ of which β have mean $Y_k \sqrt{G}$. From the orthogonality of the base functions $e^{j\pi kt/T}$ we have that

$$\int_0^T |Y(t)|^2 dt = T \sum_{k=-L}^{k=L} |Y_k|^2. \quad (7)$$

The conditional (on Y_k) mgf for Z is given by a noncentral chi-square distribution function⁵:

$$M_{\Lambda|Y}(s) = \frac{1}{(1 - N_0 s)^\beta} \exp \left(\frac{\frac{1}{2} s T \sum_{k=-L}^{k=L} |Y_k \sqrt{G}|^2}{1 - N_0 s} \right). \quad (8)$$

The second step is to average over all possible values of Y_k from which we obtain:

$$M_\Lambda(s) = \frac{1}{(1 - N_0 s)^\beta} M_{\Lambda_0} \left(\frac{s}{1 - N_0 s} \right), \quad (9)$$

where Λ_0 is given by

$$\Lambda_0 = \frac{1}{2} \int_0^T |\sqrt{G}Y(t)|^2 dt. \quad (10)$$

Expression (10) is (except for the amplification factor G) the Poisson parameter for a receiver without optical amplification (see Eq. 2). The mgf in Eq. 9 is the principal result of this section. As we can see from Eq. 9 it is easy to obtain the mgf of the decision variable for a preamplified receiver once we know the respective mgf for a receiver without any amplification; see Eq. 13. Subsequently, based on the knowledge of the mgf, the performance analysis is carried out with the help of the saddlepoint approximation.

4. CROSSTALK MODEL

We assume that N sources of crosstalk are present and that $p(\mu)$ is the probability of μ crosstalk sources being simultaneously a “digital one”. Furthermore, the average error probability P_e , bit-error rate (BER), given a detection threshold α , is given by a weighted statistical average of the error probability $P_r(\alpha, \mu)$ for each value μ :

$$P_e = \sum_{\mu=0}^N p(\mu) P_r(\alpha, \mu). \quad (11)$$

In Eq.(11) we assume that $p(\mu)$ is a binomial distribution

$$p(\mu) = \frac{N!}{(N - \mu)! \mu! 2^N}. \quad (12)$$

We proceed by making the following assumptions:

- Perfect signal and crosstalk bit-alignment.
- It is assumed that m photons per bit are received for a transmitted logical “one” while ρm photons are transmitted for a logical “zero”.
- The ratio of leakage crosstalk to signal power is denoted by ϵ .
- We assume that each interferer has the same relative crosstalk power ϵ .
- The crosstalk statistics is assumed to be of the arc-sine type.⁶
- The signal and crosstalk polarisation are linearly random with independent, uniformly distributed, orientation angles.
- The post-detection filter is of the “integrate-and-dump type”.
- The detection threshold is optimized to yield the lowest error-probability.
- The receiver thermal-noise is considered to be Gaussian distributed, zero-mean and with variance σ_{th}^2 .

We proceed by following Ref. 2. In this reference we have that the mgf for Λ (c.f. Eq. 2), given a value μ , for a transmitted logical “one” is given by

$$M_\Lambda(s) = \frac{1}{(1 - N_0 s)^\beta} e^{sm[1 + \epsilon(\mu + (N - \mu)\rho)]} I_0^2 \left(sm\sqrt{\epsilon}\mu \right) I_0^2 \left(sm\sqrt{\epsilon}\rho(N - \mu) \right) \times I_0^2 \left(sm\sqrt{\rho\epsilon}\mu(N - \mu) \right) I_0^2 \left(sm\epsilon\rho(N - \mu)(N - \mu - 1)/2 \right) I_0^2 \left(sm\epsilon\mu(\mu - 1)/2 \right), \quad (13)$$

where $I_0(x)$ is the modified Bessel's function of zero order. Similar expression for the case of transmitted “zero” is also easily obtained. The evaluation of bit-error probabilities P_e is further performed according to the method explained in Ref. 2.

In Fig.4 the bit-error rate as a function of the number of crosstalk sources for different values of ϵ is presented. The extinction ratio is $\rho = 8$ dB while $m = 325$ photons/s. This corresponds to a signal power of -39.82 dBm for a receiver with responsivity equal to 1 A/W, operating at a wavelength of 1.55 μm , and at a bit-rate of 2.5 Gb/s. The amplifier Gain is 20 dB and the spontaneous noise parameter n_{sp} and β are set to unity. The receiver resistance load is equal to 50 Ω .

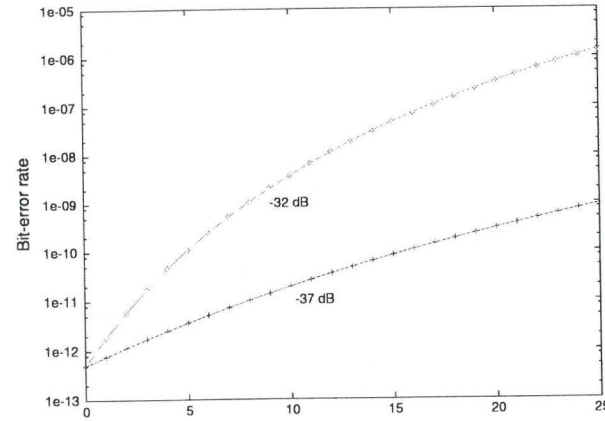


Figure 4. BER dependence on the number of crosstalk sources for values $\epsilon = -32$ dB (dotted line) and $\epsilon = -37$ dB (solid line). The extinction ratio $\rho = 8$ dB, $G = 20$ dB, $n_{sp} = 1$, and $M = 1$.

5. RESULTS

As mentioned in Sect. 1, we consider two situations. In the first situation the case without link failures is considered. In the second case we assume that link failures in the network are present. The place of the link failures are indicated by the \blacktriangle in Fig. 2. We firstly discuss the case without link failures.

5.1. Without link failures

Table 1 presents the performance results for network operating without link failures. The first column in Table 1 represents the topology as indicated in Fig.2. As discussed in Sect. 2, *Topology 3* has two alternative routes, indicated by the upper-index I and II. Column 2 gives the number of nodes in the largest route, while in column 3 the number of crosstalk sources are presented. Finally in column 4 the corresponding BER is given for a crosstalk value $\epsilon = -32$ dB.

topology	nodes	sources	BER
1	9	20	$3.1 \cdot 10^{-7}$
2	8	20	$3.1 \cdot 10^{-7}$
3 ^I	6	14	$3.0 \cdot 10^{-8}$
3 ^{II}	6	19	$2.2 \cdot 10^{-7}$
4	6	20	$3.1 \cdot 10^{-7}$

Table 1. Characteristics of the largest routes. ^I route using the core-network. ^{II} route using the new links.

It can be concluded from Table 1 that *Topology 3^I* has the best error performance. This is related to the fact that this topology has the lowest number of interfering crosstalk sources.

topology	nodes	sources	BER
1 ^I	9	19	$2.2 \cdot 10^{-7}$
1 ^{II}	10	20	$3.1 \cdot 10^{-7}$
2	9	21	$4.3 \cdot 10^{-7}$
3	6	19	$2.2 \cdot 10^{-7}$
4 ^{III}	7	21	$4.3 \cdot 10^{-7}$
4 ^{IV}	7	22	$5.9 \cdot 10^{-7}$

Table 2. Characteristics of the largest routes. ^I using the same route. ^{II} using a new longest route. ^{III} removed link in the core-network. ^{IV} removed link in a sub-net.

5.2. With link failure

In the second case we consider the situation that link failures take place. As reflected in Table 2, link failures will affect the largest route. Similarly as in Table 1, the first column in Table 2 describes the topology discussed.

In *Topology 1* the link failure will not introduce an extra node in the route, but one source of crosstalk is removed. This situation is indicated in Table 2 by the upper-index I. Additionally, another route has become the largest path. This "new largest path" starts in the node marked as "in" and ends in the node marked as "out II". This situation is indicated in Table 2 by the upper-index II. It follows from Table 2 that this route has one additional node. The BER-performance of both cases are presented in Table 2.

In *Topology 4* there are two places where a link failure can occur without blocking the route. The situation marked with upper-index III indicates a link failure in the core-network, while in situation IV the failure occurs in a sub-network. The BER-performance of both situations are given in Table 2.

The second column of Table 2 contains the number of nodes in the largest routes. If we compare this result to the result presented in Table 1, we can conclude that "in average" the number of nodes has increased. As a result of this the number of crosstalk sources has also increased. This results is presented in the third column of Table 2. Finally, in column 4 the resulting BER is given.

6. CONCLUSIONS

We can conclude that inserting just a few, wisely placed, extra connections in the ring-only network (*Topology 3*) improves the operation reliability with respect to crosstalk. Introducing more links will make the route even shorter, but more sources of crosstalk can contaminate the signal.

In general these results indicate that a balance between the number of links and the error-performance with respect to crosstalk exists. It should be noted that it is crucial in the design of future all-optical networks to find an optimum topology with respect to in-band crosstalk.

ACKNOWLEDGEMENT

H.J.S. Dorren is with the KPN-TUE partnership.

REFERENCES

1. E. L. Goldstein and L. Eskildsen, "Scaling limitations in transparent optical networks due to low-level crosstalk," *IEEE Photonics Techn. Lett.* **7**, pp. 93-94, Jan. 95.
2. I. T. Monroy, "Statistical analysis of interferometric noise in optical ASK/direct detection system," To be published in *Syben'98. Broadband European Networks*, EUROPTO Series, EOS/SPIE, (Zürich, Switzerland), May 1998.
3. L. Snyder, *Random Point Processes*, Wiley-Interscience Publ., 1975.
4. G. Einarsson, *Principles of Lightwave Communications*, John & Wiley, 1996.
5. A. Papoulis, *Probability, Random Variables, and Stochastic Processes*, McGraw-Hill Int. Editions, second ed., 1991.
6. M. Tur and E. L. Goldstein, "Probability distribution of phase-induced intensity noise generated by distributed feed-back lasers," *Optics Letters* **15**, pp. 1-3, January 1990.

Paper M

How Does Crosstalk Accumulate in WDM Networks?

H. J. S. Dorren, H. de Waardt, and Idelfonso Tafur Monroy

© 1999 IEEE. Reprinted, with permission, from *IEEE/OSA J. Lightwave Technol.*, Submitted for publication.

How does cross-talk accumulate in WDM-networks?

H.J.S. Dorren, H. de Waardt and I. Tafur Monroy

Abstract— Accumulation of inband crosstalk in all-optical networks is studied. By applying statistical methods, we have investigated how inband crosstalk accumulation influences the performance of optical networks of different configurations. Our study shows that there exists a delicate dependence between network topology and robustness with respect to accumulation of inband cross-talk. A method is proposed to design optical networks with optical paths satisfying a certain level of inband crosstalk performance.

I. INTRODUCTION

Optical WDM-networks offer a large transport capacity and are regarded as a promising solution to the increasing demand of bandwidth in future telecommunication systems. In all optical WDM-networks, routing, switching and amplification is performed in the optical domain. An important component in the WDM-network is the multi-wavelength optical cross-connect which is schematically presented in Figure 1. Suppose we consider a signal at wavelength λ_3 which propagates from input 1 to output 2. It is well-known that due to an imperfect switching array, the output signal is corrupted with leakage of other input signals. This phenomena is called cross-talk. If the contamination has the same nominal wavelength as the signal, we speak about in-band cross-talk. This type of cross-talk can not be removed by optical filters and it is therefore necessary to design optical networks with an optimum cross-talk performance. Transparent optical networks impose strict requirements on the cross-talk performance of the network elements involved [1, 2].

Up until now considerable effort is invested in developing an adequate understanding of cross-talk in optical switches (See ref. [2] and the references therein) as well as improving the cross-talk performance of optical switches. Nevertheless, the applicability of cross-connects in optical networks depends on the cross-talk properties of the device. Modern integrated optical switches introduce cross-talk which is in the order of -35 dB. A signal propagating through an optical network in general passes through more than one switch. As a result of this the overall cross-talk on the signal is larger than -35 dB. It is therefore important to design the optical network in such a way that the effects of cross-talk are minimized. In this paper we deal with the question whether we can reduce the cross-talk accumulation by using a good network design. This will be done by selecting four network designs and investigate, by using statistical methods, what effects are important on the cross-talk accumulation. The results are derived tak-

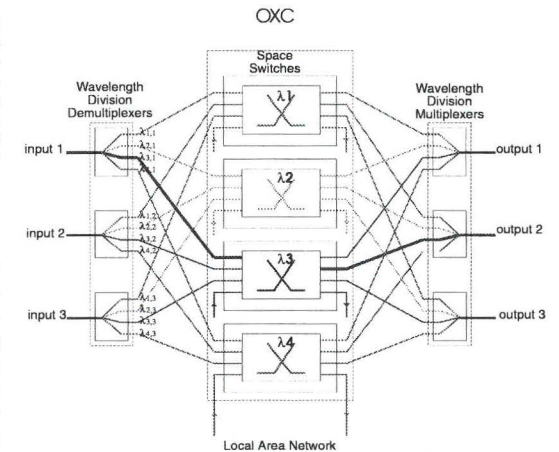


Figure 1. Schematic example of an optical cross-connect.

ing into account that realistic networks are always subject to upgrades. With this we mean that we have assumed that during the course of time more nodes are added in the network. We ask ourselves the question whether particular network designs have a better cross-talk performance with respect to upgrades, and which parameters play an important role in this.

We investigate the problem presented above by using statistical methods. This will be done on two levels. Firstly, we describe the cross-talk in every node by a statistical model in which is accounted for the data-statistics, linear random polarization and a non-perfect extinction ratio. On the other hand we also introduce statistics to cover the properties of the complete network lay-out. The latter has been done to make the results obtained in this paper as independent as possible for a particular network design. We aim to formulate general criteria that cover large generic classes of optical networks. We will show that there is a delicate relationship between the number of optical links in a network and the signal quality with respect to cross-talk. Introducing more links leads to a shorter connection, but on the other hand the number of cross-talk sources increases leading to a worse cross-talk performance.

This paper is structured as follows: In Sec. 2 the investigated networks are discussed as well as the numerical scheme to obtain a Probability Density Function (PDF) which represents the cross-talk performance of the network design. In Sec.3 we discuss how the cross-talk accumulates

through optical networks, and what parameters are governing this process. The paper is concluded with a discussion. Technical matters with respect to the cross-talk model are added as a comprehensive appendix.

II. CONCEPTS

Since realistic optical networks are continuously subject to upgrades, it is inadequate to investigate cross-talk accumulation in one particular network and extrapolate the results to arbitrary networks. We apply statistical techniques to obtain generic results about large classes of networks. To do this we investigate four different network designs which are presented in Figure 2. We do not have the intention to present an optimum network design. The networks which are presented in the following have to be regarded as examples to illustrate and understand the effects which play a role in the cross-talk performance of optical networks. The particular networks have been chosen as presented below, because in agreement with realistic networks, they include examples with rings, grids, and combinations of both. The first network design (Network 1) is presented in Figure

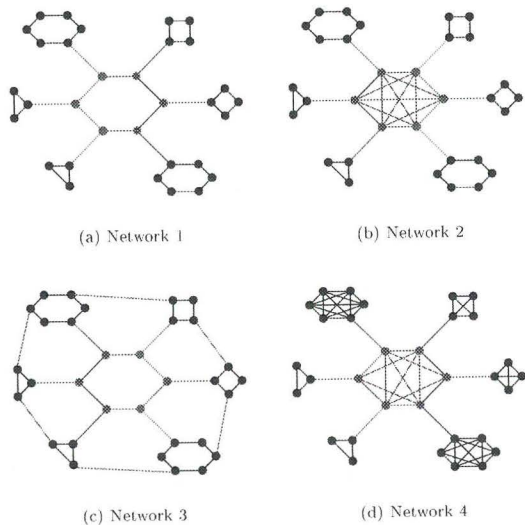


Figure 2. The network configurations as investigated in this paper: a): Network 1, consisting of an inner core which is connected with subnetworks on every node of the core. b): Network 2, similar as Network 1, except the nodes in the core are interconnected. c): Network 3, similar as Network 1, except an outer ring on the sub-networks is implemented d): Network 4, similar as Network 1, with all nodes inter-connected.

2a. The network consists of interconnected ring networks. The nodes in Figure 2 represent cross-connects of the type as presented in Figure 1. Network 1 represents a central core network which is connected to several regional ring-networks. The second network design (Network 2) which is investigated in this paper is presented in Figure 2b. Network 2 only differs from Network 1 by the fact that all

the nodes in the central core-network are interconnected. In the third network (Network 3), which is presented in Figure 2c, a large outer-ring is implemented to interconnect the sub-networks of Network 1. Finally, in the last network design (Network 4), which is presented in Figure 2d, all the nodes in the core-network and sub-networks are interconnected.

If we compare for instance Network 1 and Network 3, we can conclude that the distance between two nodes in adjacent subnetworks is shorter in Network 3. Throughout this paper, we define the “distance” as the number of nodes which are passed by an optical signal. The path-length than equals the number of nodes crossed by an optical signal while traveling through the network. In Network 3, the signal can use the outer-ring, while in Network 1, the signal has to take a path which includes more nodes through the inner core. As a result of this one can expect that the signal in Network 1 is subject to much more cross-talk contamination than a signal in Network 3. Making the path-length between two nodes shorter requires that the remaining optical cross-connects can handle more connections which also introduces new sources of cross-talk. This makes clear that there is a delicate balance between the path-length and the number of interfering cross-talk sources. Before we proceed describing the method which is used to compute cross-talk accumulation in these networks, we want to remark that in Figure 2 only the layout of the network-design is presented. For investigating the cross-talk performance, we have developed a recipe consisting of four steps which are described below.

Step 1: We generate for each of the network design presented in Figure 2, 25 different samples with a size of the inner-core between 5 and 30 nodes. Every node is connected to a ring-shaped sub-network. The number of nodes in the subnetwork is chosen randomly with a uniform distribution, but it has a minimum of three nodes and the maximum number of nodes equals half the number of nodes in the core. Network 2, can be constructed from Network 1, by connecting all the nodes in the core. For Network 3, the nodes which determine the outer ring are also chosen randomly. These networks can be formulated as a directed graph which is represented as a matrix. Network 4, follows from network 2, by simply connecting all the nodes in the sub-networks to each other.

Step 2: As a first step Floyd’s path-search algorithm is used to compute the shortest paths between two nodes in the network [3]. With the shortest path we mean the shortest connection (measured in nodes) between two points in the network. If the optical network is presented as a graph, Floyd’s algorithm provides an efficient tool to compute these paths. When the shortest paths are identified, we can also compute the number of cross-talk interferers. It follows from Figure 2 that the number of cross-talk sources in every node equals the number of neighbors of every node; i.e.: it is assumed that the signal is contaminated in every node with corruption from only the neighboring nodes. Because of reasons of limited computation time, higher order cross-talk accumulation is not taken into account. We

compute the number of cross-talk sources for all shortest connections between all pairs of nodes in the graph.

Step 3: The procedure described in *Step 1* and *Step 2* is repeated 80 times and an ensemble average is taken. An example is given in Figure 3, where the normalized ensemble averages for the number of cross-talk interferers is plotted for all the network designs at a core-size of 30 nodes. Similar histograms are generated for every core-size between 5 and 30 nodes. The normalized histogram has the interpretation of a Probability Density Function (PDF) for the number of cross-talk interferers of a particular network design. Taking ensemble averages is important to make the results independent for particular network configurations, and to obtain generic results.

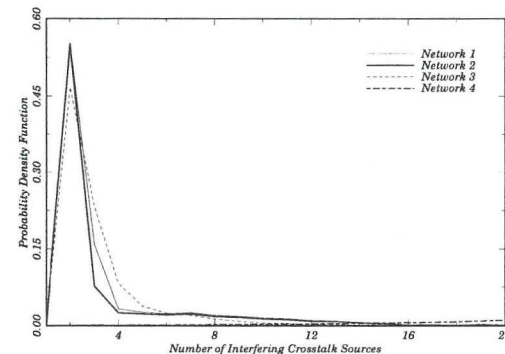


Figure 3. Example of a PDF for the interfering cross-talk sources at a core-size of 30 nodes. It can be shown that all the networks have a characteristic behavior.

Step 4: By using the mathematical model presented in Appendix A, we relate the number of interferers to the Bit-Error-Rate (BER). The method is described in more detail in the next section, but the results are already presented in Figure 4. This also implies that we can compute the PDF for the BER for a certain network design. An example is shown in Figure 4 for a core-size of 30 nodes.

The recipe described above helps us to compute generic results. The fact that we take averages over large ensembles of networks guarantees that the results are independent for specific realizations. Once we have determined the PDFs for the BER, we can formulate a criterion on what conditions a particular ensemble of networks can guarantee a satisfactory QoS (Quality of Service). A criterion could be for instance that the BER should be below a 10^{-9} level. By repeating this procedure for an increasing number of nodes in the core, one can compute how sensitive a particular network design is for cross-talk accumulation after upgrades. In the next section, it will be shown that the network designs which are presented in Figure 2, all have characteristic properties with respect to cross-talk accumulation, and an optimum design can be chosen.

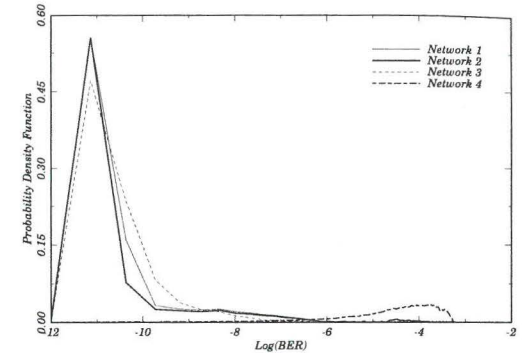


Figure 4. Example of a PDF for the BER at a core-size of 30 nodes. It can be shown that all the networks have a characteristic behavior.

III. RESULTS

In this section, we present the results with respect to cross-talk accumulation in the network designs as presented in Figure 2, following the recipe described in the previous section. In Figure 5, the BER is plotted as a function of the number of interfering cross-talk sources for -33 dB, -37 dB, -50 dB and -80 dB of cross-talk isolation. The BER is computed by using Eq.(A-6). We have chosen the parameters so that if no cross-talk is present a BER of 10^{-12} is obtained. It is witnessed from Figure 5 that in the case of -80 dB cross-talk isolation, nearly no degradation for the BER takes place. However, in the case of -33 dB cross-talk isolation (this corresponds to presently available optical switches) less than 10 interfering cross-talk sources can be handled. This result implies that the cross-talk per optical switch has to be improved to -50 dB or preferable -80 dB, before this kind of switches can be used in realistic optically transparent networks.

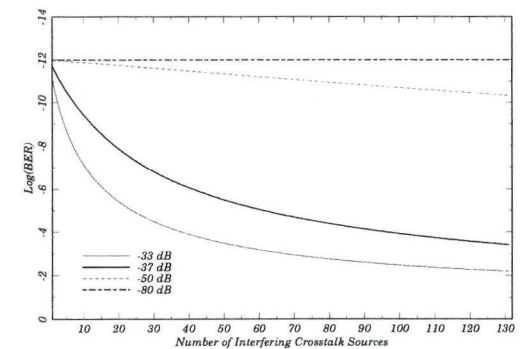


Figure 5. The BER as a function of the number of interfering cross-talk sources computed according Eq.(A-6) for -33dB, -37dB, -50dB and -80dB cross-talk respectively.

In Figure 3, as an example, the PDF of the four network designs is computed for a core-size of 30 nodes. The results are obtained after an ensemble averaging of 80 realizations, following the recipe as presented in the previous section. A similar behavior also takes place for different number of nodes in the core. It can be concluded that Network 3 has the best cross-talk performance since the probability to find paths having more than 12 cross-talk sources is negligible. Network 4 has the poorest cross-talk performance since it has a large number of paths with more than 40 cross-talk sources (this result is not visible in Figure 3, but is follows from the raw data and manifests itself as a large BER in Figure 4). The performance with respect to the number of cross-talk sources of Network 1 and Network 2 is slightly worse than the performance of Network 3. One may conclude from the results presented in Figure 3 that by counting the number of interfering cross-talk sources (*i.e.* the number of neighboring nodes) insight can be obtained about the relationship between the network lay-out and the cross-talk performance. It is clearly visible in Figure 3 that the network designs of Figure 2 have a characteristic cross-talk performance.

By using the results presented in Figure 5, we can also compute the performance with respect to the BER. In Figure 4 the probability of the BER is presented for the same network as presented in Figure 3. We have assumed that the cross-talk is -37 dB. Due to the nonlinear relation between the number of interferers and the BER, our conclusions derived from Figure 3 have to be changed. If we relate the cross-talk performance to the decay of the BER-tail in Figure 4, we would draw a similar conclusions as drawn in the previous paragraph. On the other hand if we implement a criterion that only paths with a BER performance below 10^{-9} are satisfactory, it appears that Network 1 has the best performance. To distinguish this, we have computed the surface underneath the curves:

$$S_i = \int_{x_{min}}^{x_{max}} f_i(x) dx \quad (1)$$

where S_i determines the surface underneath the PDF $f_i(x)$ for network-design i between the under-limit x_{min} and the outer-limit x_{max} . We can conclude that in order to estimate the cross-talk performance of a network, it is not sufficient to count the number of cross-talk interferers because the latter represents a property which is not linearly related to the BER.

If we plot the surface S_i for variable number of nodes in the core, we obtain Figure 6. It follows clearly from Figure 6 that every network design has its characteristic properties with respect to an increasing number of nodes. Clearly Network 1 has the best properties. This is related to the fact that the number of interfering cross-talk sources is low as well as the number of paths which crosses a large number of nodes. The other extreme is network 4 in which all the rings are completely connected. As a result of this in every node a large amount of cross-talk contamination takes place. It is also interesting to remark that up to 15 nodes, Network 2 and Network 3 have a comparable cross-

talk performance.

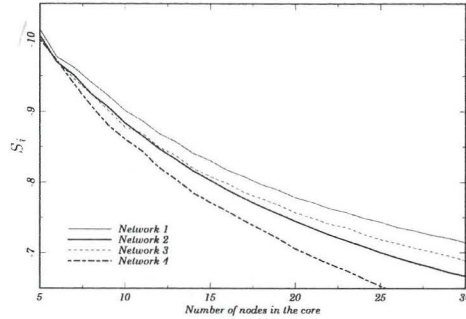


Figure 6. The averaged BER as a function of the core-size.

IV. CONCLUSIONS

We have introduced a method to determine the robustness of optical networks with respect to cross-talk accumulation. An underlying consideration for the work conducted in this paper is that integrated optical switches always introduce a certain level of cross-talk. It is therefore necessary to identify network configurations which minimize cross-talk accumulation. We have approached the problem sketched above by implementing statistical methods. By taking averages over large ensembles of networks with a similar topology, we obtain results which are generic and representative for large classes of networks.

We can conclude that for cross-talk accumulation in optical networks two "parameters" are important. The first parameter is the number of nodes in a network. This can be understood easily since more nodes means more sources of cross-talk. One wants to design a network that minimizes the number of nodes to be crossed from an arbitrary signal traveling through the network. Minimizing the number of nodes can be done by introducing more connections. The second parameter is the number of cross-talk interferers per connection. This implies that after enlarging the network the number of cross-talk interferers increases, and hence a poorer cross-talk performance takes place. It is therefore crucial to find the optimum number of connections per node.

The work conducted is far from complete and the network topologies only form an illustration for the effect we describe. An important issue which is not considered in this paper, is the impact of fiber-cuts. As broken fiber implies that the traffic has to be re-routed, in general more nodes have to be crossed. In Ref. [4], it is shown that the impact of broken fibers does not affect the results drawn in this paper.

Acknowledgments

We thank J. Siffels for making figures available. The critical comments by Prof. Khoe were greatly appreciated

APPENDIX A

Cross-talk model

This Appendix presents the cross-talk model used in the performance analysis. The receiver considered is an ASK/DD receiver whose schematic diagram is presented in Figure 7.

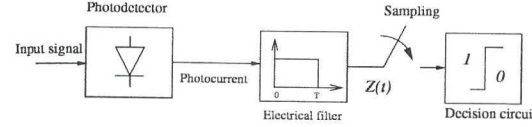


Figure 7. Schematic diagram of an ASK/DD receiver.

The proposed cross-talk model is a balance between accuracy and complexity. We want the model to be as accurate as possible, but it must be not prohibitive in terms of computing time needed to run the simulation for the set of networks under investigation. We choose the commonly used Gaussian approximation for the bit-error probability evaluation. Although cross-talk has been shown to exhibit non-Gaussian statistics, *i.e.* [5], the Gaussian approximation, which is numerically simple, gives us in particular a good indication of how cross-talk affects the system performance if the number of cross-talk sources is large [1]. We proceed by making the following assumptions and definitions:

- Perfect signal and cross-talk bit-alignment (worst case scenario).
 - Extinction ratio is denoted by φ .
 - It is assumed that m photons per bit are received for a transmitted "one" while φm are for a transmitted "zero".
 - The ratio of leakage cross-talk to signal power is denoted by ϵ .
 - There are N cross-talk sources operating at the same nominal wavelength as the informative signal.
 - We assume that each interferer has the same relative cross-talk power ϵ (worst case scenario).
 - The cross-talk statistics is assumed to be Gaussian having zero-mean with a normalized variance which is equal to 1/2.
 - The signal and cross-talk polarization are linearly random and its induced intensity noise is assumed to be Gaussian with zero-mean and with a normalized variance which is equal to 1/2.
 - A post-detection filter which is of the "integrate-and-dump" type.
 - The detection threshold is fixed to be a midway point between the signal level for a transmitted "zero" and "one".
 - The receiver thermal-noise is assumed to be Gaussian distributed, zero-mean and with variance σ_{th}^2 .
- The photo-current at the output of the photo-detector, shot noise, and the thermal noise current pass the electrical post-detector filter. The filtered signal $Z(t)$ is further sampled at $t = t_0 + kT$ time instants to form the decision variable. The post-detector filter is assumed to be an integrator over the time interval $[0, T]$. With no loss of

generality we consider the time interval $[0, T]$ ($k = 0$) and denote the decision variable by $Z = Z(t = T)$. By comparing the sample value with a preselected threshold, the decision circuit derives an estimate of a transmitted bit in a particular bit interval.

The expression for the decision variable takes the following form [6]:

$$\begin{aligned} Z = & mb_0^s + 2\sqrt{\epsilon m} \sum_{n=1}^N \sqrt{b_0^s b_0^{x,n}} \vec{r}_s \cdot \vec{r}_{x,n} \times \cos(\phi_s - \phi_{x,n}) \\ & + 2\epsilon m \sum_{j=n+1}^N \sum_{n=1}^{N-1} \sqrt{b_0^{x,n} b_0^{x,j}} \cos(\phi_{x,n} - \phi_{x,j}) \\ & + \epsilon m \sum_{n=1}^N b_0^{s,n} + X_{th} \end{aligned} \quad (A-1)$$

where b_k represents the binary symbols. The variables ϕ_s and ϕ_x are the phase of the signal and cross-talk respectively. The unit vectors \vec{r}_s and \vec{r}_x represent the signal and the cross-talk state of polarization. The thermal noise contribution, X_{th} , is a zero mean, Gaussian distributed variable with variance σ_{th}^2 given by

$$\sigma_{th}^2 = \frac{2K_B T_k T}{q^2 R} \quad (A-2)$$

K_B being the Boltzmann's constant, T_k the temperature in Kelvin, q the electron charge, and R is the receiver resistance load.

A. Performance analysis

The question is to evaluate the average error rate P_e of the system under discussion. We are going to treat the case of amplitude shift keying (ASK) modulation format. To account for all possible combinations of signal and cross-talk interfering bits we proceed by assuming that μ interferers are simultaneously a logical "one", thus $N - \mu$ interferers are "zero". The error probability analysis is conducted by a weighted statistical average of the error probability for each value μ . This probability is given by the binomial distribution:

$$P(\mu) = \frac{N!}{(N - \mu)! \mu! 2^N} \quad (A-3)$$

Hence, the average error probability P_e , for a given threshold α , is given by

$$P_e = \langle P_e | \mu \rangle_{P(\mu)} \quad (A-4)$$

Using the Gaussian approximation $P_e | \mu$ can be written as

$$P_e | \mu = \frac{1}{2} Q\left(\frac{E_1 - \alpha}{\sigma_1}\right) + \frac{1}{2} Q\left(\frac{\alpha - E_0}{\sigma_0}\right), \quad (A-5)$$

where $E_{0,1}$ is the mean of the received signal when a "single zero", and a "single one" is sent, respectively. The variance is denoted by $\sigma_{0,1}^2$, and the decision threshold by

α . The function $Q(\cdot)$ is the standard Gaussian probability tail function.

With (A-3), and assuming that the symbols are *a priori* equally probable, the average BER (A-4) can be written as

$$P_e = \frac{1}{2^N} \sum_{\mu=0}^N \binom{N}{\mu} \left\{ \frac{1}{2} Q\left(\frac{E_1(\mu) - \alpha}{\sigma_1(\mu)}\right) + \frac{1}{2} Q\left(\frac{\alpha - E_0(\mu)}{\sigma_0(\mu)}\right) \right\} \quad (\text{A-6})$$

If we consider the case for a transmitted symbol "one" ($b_0^s = 1$), then the mean (E_1) and variance (σ_1^2) for the decision variable Z are presented in (A-7) and (A-8).

$$E_1 = m + \epsilon m (\mu + (N - \mu)\varphi) \quad (\text{A-7})$$

$$\begin{aligned} \sigma_1^2 = & \mu (2m\sqrt{\epsilon})^2 \frac{1}{4} + (N - \mu) (2m\sqrt{\varphi\epsilon})^2 \frac{1}{4} \\ & + (2m\epsilon)^2 \frac{1}{4} \frac{\mu(\mu-1)}{2} + (2m\sqrt{\varphi\epsilon})^2 \frac{1}{4} \mu(N - \mu) \\ & + (2m\epsilon\varphi)^2 \frac{1}{4} \frac{(N - \mu)(N - \mu - 1)}{2} + E_1 + \sigma_{th}^2 \end{aligned} \quad (\text{A-8})$$

where the first term in (A-8) represents the beat terms between the signal and the μ cross-talk sources which are "one". The factors $\frac{1}{4}$ arise from the variance of the polarization, and cross-talk, respectively. The second term accounts for the beating terms which are "zero". The next three terms represent the cross-talk-cross-talk beating terms. Firstly, the $\frac{\mu(\mu-1)}{2}$ possible combinations of "one-one" beating terms are considered. Secondly, there are $\frac{(N-\mu)(N-\mu-1)}{2}$ combinations of "zero-zero" beating terms. Lastly, beating terms for "one" and "zero" are accounted for in the fourth term. This implies that all possible cross-talk-cross-talk combination are covered in this simple formula. The variance of the shot-noise is according to the Poisson statistics for photo-detection equal to the mean of the photo-current. In a similar manner one could derive that under the assumption that the signal contains a "zero" ($b_0^s = 0$), the mean (E_0) and variance (σ_0^2) are:

$$E_0 = m\varphi + \epsilon m (\mu + (N - \mu)\varphi) \quad (\text{A-9})$$

$$\begin{aligned} \sigma_0^2 = & \mu (2m\sqrt{\epsilon\varphi})^2 \frac{1}{4} + (N - \mu) (2m\sqrt{\varphi\epsilon})^2 \frac{1}{4} \\ & + (2m\epsilon)^2 \frac{1}{4} \frac{\mu(\mu-1)}{2} + (2m\epsilon)^2 \frac{1}{4} \frac{\mu(\mu-1)}{2} \\ & + (2m\sqrt{\varphi\epsilon})^2 \frac{1}{4} \mu(N - \mu) \\ & + (2m\epsilon\varphi)^2 \frac{1}{4} \frac{(N - \mu)(N - \mu - 1)}{2} + E_0 + \sigma_{th}^2 \end{aligned} \quad (\text{A-10})$$

Given a number N of cross-talk sources, the error probability is expeditiously evaluated by (A-6). In the computations used in this paper we used an extinction ratio of $\varphi = 8$ dB while m is $1.3 \cdot 10^4$ photons/s for a BER of 10^{-12} . This corresponds to a signal power of -24 dBm for a receiver with responsivity equal to 1 A/W, operating at a wavelength of $1.55\mu\text{m}$. The receiver resistance load is equal to 50Ω .

REFERENCES

- [1] E. Goldstein and L. Eskildsen, *Scaling limitations in transparent optical networks due to low level cross-talk*, IEEE Photon. Technol. Lett., **1**, 93-95, 1995.
- [2] E. Goldstein, L. Eskildsen, and A. F. Elrefaie *Performance implications of component cross-talk in transparent lightwave networks*, IEEE Photon. Technol. Lett., **6**, 657-660, 1994.
- [3] R. Gould, *Graph Theory*, Benjamin/Cummings, Amsterdam, 1988.
- [4] J. Siffels, I. Tafur Monroy, H. de Waardt and H.J.S. Dorren, *How does optical cross-talk depend on the network topology?*, In Proceedings of the IEEE/LEOS symposium, Benelux Chapter, 1997.
- [5] A. Arie, M. Tur, and E. L. Goldstein, *Probability-density function of noise at the output of a two-beam interferometer*, J. Opt. Soc. Am. A., vol. 8, pp. 1936-1942, Dec. 1991.
- [6] I. Tafur Monroy and E. Tangdiongga, *Performance evaluations of optical cross-connects by saddle-point approximation*, J. Lightwave. Technol., **16**, pp. 317-323, 1998.

Paper N

Scalability of Optical Networks: Crosstalk Limitations

Idelfonso Tafur Monroy

Photonic Network Communications, Submitted for publication.

Scalability of Optical Networks: Crosstalk Limitations

Idelfonso Tafur Monroy

Abstract— Optical networks represents a promising solution for the future high capacity and flexible transport network. This paper presents a model for the performance evaluation of optical networks with respect to linear crosstalk and accumulated spontaneous emission noise.

Keywords— Communication networks, interferometric noise, optical crosstalk, optical communication, wavelength division multiplexing networks, error analysis.

I. INTRODUCTION

All-optical networks are regarded as a promising solution for the high speed and flexible transport network of future broad-band telecommunications services. These networks are composed of optical nodes, mainly optical cross-connects (OXC), in which the routing, switching and add/drop of channels take place. At present, major efforts are directed toward the development of devices and concepts for implementing such optical cross-connects [1, 2]. At the main time, performance limitations due to optical crosstalk have being identified. Crosstalk or power leakage from undesired channels, arises from performance imperfections of devices like optical switches and (de)multiplexers. Crosstalk has been reported to degrade the performance, introducing large power penalties and bit-error rate floors, of a variety of optical networks, e.g., all-optical trunk networks and WDM system, e.g., [3–6]. Hence, it is of relevance to assess the impact of crosstalk on the scalability of all-optical networks.

This paper presents a simple model for the performance analysis of optical networks with regard to linear optical crosstalk and accumulated spontaneous emission noise. The proposed model is useful for evaluating the crosstalk requirements on the devices needed to support an optical network with a certain numbers of nodes and with a given level of error probability. The rest of the paper is structured as follows. In Sec. II the optical cross-connect architecture is described. The crosstalk mechanism is explained. A signal path thru the optical network is described in detail. Scalability calculations and discussion are presented in Sec. III. Conclusions are drawn in Sec. IV. Finally, crosstalk modeling, EDFA gain model, and details of the performance analysis computations are given in the Appendix.

II. SYSTEM MODEL

A. Cross-connect architecture

Let consider a network of interconnected optical cross-connects (see Fig. 1(a)). The functionality of the optical

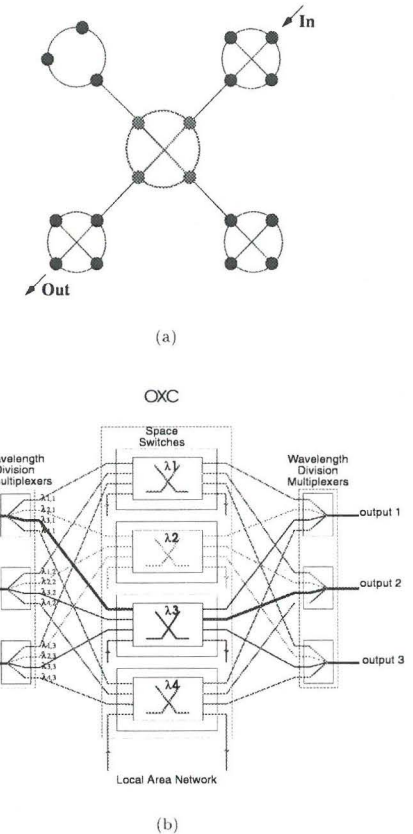


Fig. 1. a) Example of optical network. b) Schematic diagram of an optical cross-connect (OXC).

cross-connect is to switch, route and add/drop channels; see Fig. 1(b). The number of input fibers to a node is denoted by N_f . Each fiber supports a number N_λ of wavelengths. Moreover, it is assumed that each node has a fiber connection intended to add/drop channels. An example of such a node with $N_f = 3$ and $N_\lambda = 4$ is shown in Fig. 1(b). We assume also that at the input of a node an optical amplifier compensates for the power loss, and at the output of the node another optical amplifier boosts the signal to the next node; see Fig. 2. In the OXC nodes under consideration the optical switches are optimized for a given

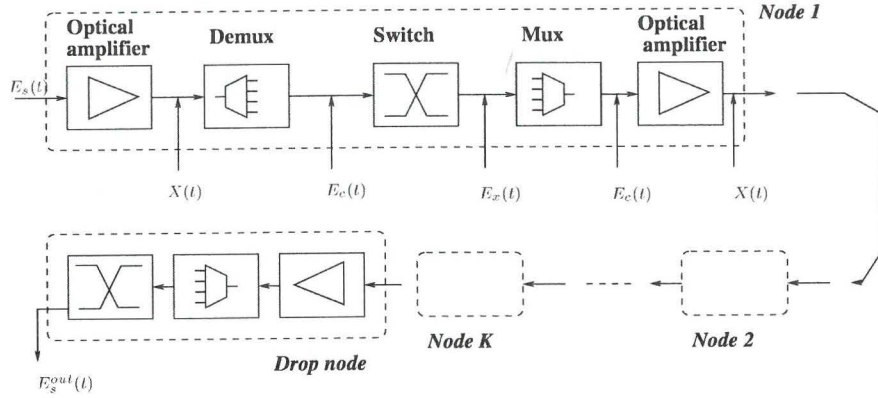


Fig. 2. Model of the optical path in a cross-connected network

wavelength. The channel (de)multiplexing (DE)MUX is assumed to be performed by phase arrays (PHASAR). Due to performance imperfections of (DE)MUX and optical switches an optical signal propagating thru the network will experience accumulation of undesired power leakage from other channels, i.e. *crosstalk*. Moreover, amplified spontaneous emission (ASE) noise from optical amplifiers will also be added to the signal. In a complex optical network other effects may take place (e.g. dispersion loss, wavelength instability), but in this work we will restrict ourselves to the case of linear optical crosstalk and an ASE accumulation.

B. Crosstalk mechanism

In an optical cross-connect we distinguish two types of linear crosstalk: inband crosstalk and interband crosstalk, according to whether it has the same nominal wavelength as the desired signal or not. The effect of interband crosstalk can be reduced by concatenating narrow-bandwidth optical filters. Inband crosstalk, however, cannot be removed as the signal and the crosstalk operates at the same wavelength. The detrimental effect of inband crosstalk is further intensified in cascaded optical nodes due to its accumulative behavior.

Inband crosstalk

Lets us consider the case of an optical informative signal disturbed by a number N of interferers operating at the same nominal wavelength (inband crosstalk). The optical field of the information signal $\vec{E}_s(t)$ and the interferers $\vec{E}_x(t)$ is given by their complex amplitude vectors

$$\vec{E}_s(t) = \sqrt{b_k^s P_0 g_s(t)} \vec{r}_s e^{j\phi_{s,t}(t)} \quad (1)$$

$$\vec{E}_x(t) = \sum_{n=1}^N \sqrt{\epsilon_n b_k^{x,n} P_0 g_{x,n}(t)} \vec{r}_{x,n} e^{j\phi_{x,n,t}(t)} \quad (2)$$

where ϵ is the crosstalk parameter: the ratio of leakage crosstalk to signal power. The indicator b_k is introduced to represent the binary symbols: $b_k \in \{0, 1\}$ ($0 \leq \epsilon < 1$).

For the case of perfect extinction the ratio $\rho = 0$. $\phi_{s,x}$ is the phase of the signal and interferer, respectively. \vec{r}_s and \vec{r}_x are unit vectors representing the signal and interferer polarization state, respectively. The optical peak power is denoted by P_0 and $g(t)$ is the pulse shape.

Interband crosstalk

The optical field from interfering channels at other wavelength (interband crosstalk) is given by

$$\vec{E}_c(t) = \sum_{l=1}^M \sqrt{\gamma_l b_k^{c,l} P_0 g_{c,l}(t)} \vec{r}_{c,l} e^{j\phi_{c,l,t}(t)} \quad (3)$$

where γ_l is the interchannel crosstalk power. The magnitude of γ_l is a function of the channel spacing, (DE)MUX characteristics and the signal spectrum shape. In the Appendix we present a simple model for the interchannel crosstalk in optical nodes using PHASARs as (DE)MUXs.

C. Spontaneous emission noise

Optical amplifiers are going to be used in order to compensate for the power loss (cross-connect and fiber) and to enhance the receiver sensitivity. In optical amplifiers the ASE noise is dependent on the optical frequency, and the incoming signal power, among other factors. We will however assume that the amplifiers have a flat gain and operate in the linear region. In a system where ASE noise accumulates from node to node, as in our case, the total accumulated ASE noise power may be sufficiently large to saturate the amplifiers. In our study, we will require that the accumulated ASE noise power should be less than saturation output power of the current amplifier. This condition will restrict the maximum signal power and represents a scalability limitation of optical systems incorporating optical amplifiers [7]. The model for the EDFA gain is presented in the Appendix. For accumulated ASE noise we use the simple lumped amplifier model of [8].

D. The optical path

For illustrative reasons we give an example of the optical path of a signal crossing K nodes. Keeping in mind the node architecture already described, the optical path is illustrated in Fig. 2. At the input of every node the signal, $E_s(t)$, is amplified and consequently ASE noise $X(t)$ is added. Further, the signal is demultiplexed and interchannel crosstalk $E_c(t)$ is added. The optical switch performs the routing of the signal. Due to imperfections of the optical switch inband crosstalk $E_x(t)$ is introduced. The optical switch is characterized by the crosstalk relative power ϵ . Further, the multiplexer may introduce interchannel crosstalk $E_c(t)$ and secondary inband crosstalk. At the output of the node an optical amplifier is placed to compensate for the fiber power losses during transmission to the next optical node. The above described optical path for a single node is repeated in every node until the signal reaches the destination node. At the end node the signal is routed to the drop output after being demultiplexed. The output optical signal $E_s^{out}(t)$ will then be a superposition of the input signal field, $E_s(t)$, and the various optical fields from crosstalk and ASE noise contributions. We have developed a statistical model to evaluate the bit-error rate (BER) for a signal traversing K nodes in an optical network as described in this section. The details of the model and BER evaluations are presented in the Appendix.

III. CALCULATIONS AND DISCUSSION

A. Reference node: $N_\lambda = 4$, $N_f = 3$

Consider an optical network composed of K nodes; each node with a number of input fibers $N_f = 3$ and a number of channels per fiber $N_\lambda = 4$. The EDFA at the input of the OXC compensates totally for the node power loss L_{node} . The fiber loss L_f is compensated by the EDFA booster at the output of the OXC ($GL_{node} = 1$, $GL_f = 1$). We assume that the EDFAs have the following parameters. Gain $G = 22.5$ dBm, noise figure $N_F = 4.8$ dB and input saturation power of $P_{in}^{sat} = -11$ dBm. A list of parameters of the system considered in the computations is given in Table I.

Description	Value
Bit rate	2.5 Gb/s
Laser Linewidth	45 GHz
Extinction ratio	13 dB
Receiver load	50 Ohm
Phasar 3-dB λ_P	46 GHz
Inband Crosstalk	variable
Interband Crosstalk	-32 dB
EDFA gain	22.5 dB
EDFA noise figure	4.48 dB
P_{in}^{sat}	-11 dBm

TABLE I
SYSTEM SPECIFICATIONS

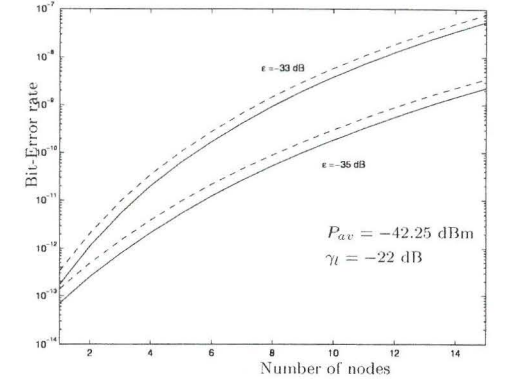


Fig. 3. Bit-error rate as a function of the number of nodes for crosstalk values $\epsilon = -33, -35$ dB, $\gamma_l = -22$ dB. Without ASE accumulation. The solid lines are the result when only inband crosstalk is present. The dotted lines are the result when both inband and interband crosstalk are taken into account.

Crosstalk only

As starting point, we consider the performance analysis of the network with respect to solely inband and interband crosstalk (without EDFAs). We assume that interband crosstalk take place only at the last optical node and that it is due only to the two nearest channels. This assumption is based on the fact that this crosstalk contribution is dominant compared to crosstalk from far separated or strong filtered channels. In Fig. 3 is shown the BER for different nodes as a function of inband and interband crosstalk. We can see that the optical switch crosstalk isolation should be better than 35 dB if ten nodes are to be traversed with a BER lower than 10^{-9} .

Accumulated ASE

When EDFA are used, ASE noise and crosstalk accumulates as signals propagate along the optical network. Hence the input power to the EDFA may reach the saturation power level. We imposed the condition that the input power to EDFA is less than the P_{in}^{sat} . We compute the P_{in} under the following assumptions:

- all channels on the fiber has traversed K nodes in the network.
- the OXCs are full loaded. This means that each channel has accumulated the maximum number of crosstalk sources and ASE noise.
- EDFA saturates at average input power levels.

This calculation gives us an indication of how many OXCs can be reached without saturating the EDFAs.

In Fig. 4 is displayed the P_{in} as function of the number of concatenated OXC for a given value of the interband crosstalk and inband crosstalk. Two different values of the 3-dB bandwidth $\Delta\lambda_P$ of the optical (DE)MUX are considered. We can see that narrow optical filters reduce the effect of accumulated ASE. However, in practical systems the bandwidth can not be chosen arbitrarily narrow as ISI

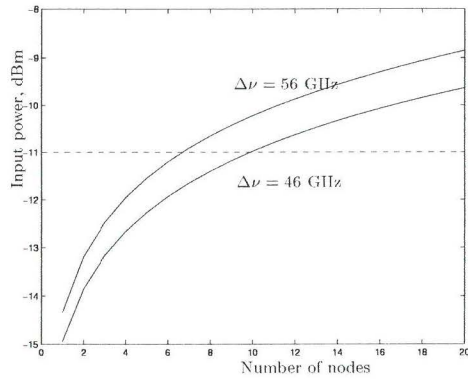


Fig. 4. Input power to the EDFA at different optical nodes for two different values of the 3-dB bandwidth $\Delta\lambda_P$ of the (DE)MUX

can be incurred or high requirement on wavelength stability are then imposed. From Fig. 4 we can see that ten nodes can be passed before the EDFA is saturated, given that (DE)MUXs of a 3-dB bandwidth $\Delta\lambda_P = 46$ GHz are used. In optical networks it is expected that optical gain management is going to be used. For example, in every node a gain equalization block may be used.

Node scalability

In Fig. 5 is shown the BER as a function of the number of traversed nodes when EDFAs are used. A fixed value of crosstalk power and signal power is used in the computations. We can see that taking into account accumulation of ASE noise the BER degrades more rapidly than without ASE accumulation. This indicates that more signal power is required to maintain a signal-to-noise ratio of enough value to assure a certain level of bit-error rate. This topic is further investigated in Fig. 6 in which it is displayed the required received signal power to assure a BER of 10^{-9} as a function of the numbers of nodes. Two values of the crosstalk parameter ϵ are considered (-33, -37 dB). We can also see that with ASE accumulation the requirements on the optical switch crosstalk isolation become more stringent. However, we see that ten nodes can be traversed with a BER of 10^{-9} when $\epsilon = -37$ dB. We note also that saturation of the EDFA is not reached according to our gain model; see Fig. 4.

B. Scalability with respect to N_λ and N_f

Until now we conducted scalability calculations for the reference node ($N_\lambda = 4, N_f = 3$). We analyze now the situation when N_λ or/and N_f is increased. Let consider a situation with $N_\lambda = 4$ and different number of input fibers N_f . This means that more sources of inband crosstalk are present at each node. In Fig. 7 is shown the required received power for a BER of 10^{-9} as a function of the number of nodes for two values of inband crosstalk ($\epsilon = -33, -37$ dB). We can observe that as the number of input fibers increases the required power also increases. At some value

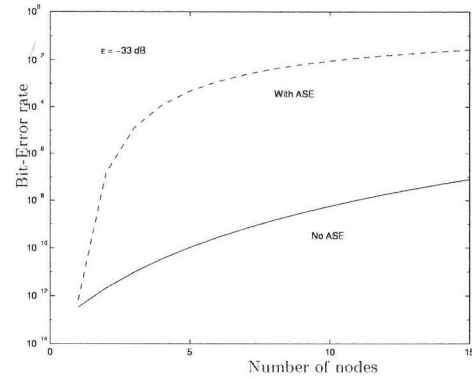


Fig. 5. Bit-error rate as function of the number of optical nodes. The solid line is the result without ASE accumulation while the dotted line is the result when EDFAs are used.

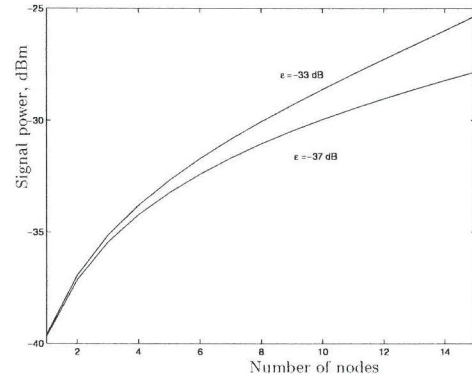
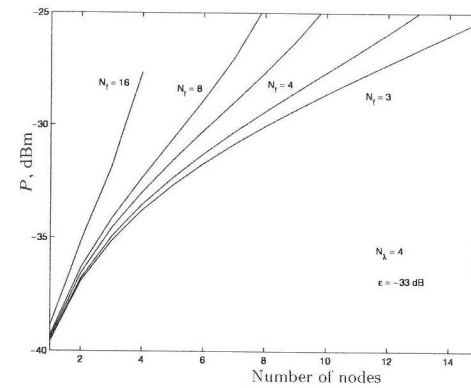
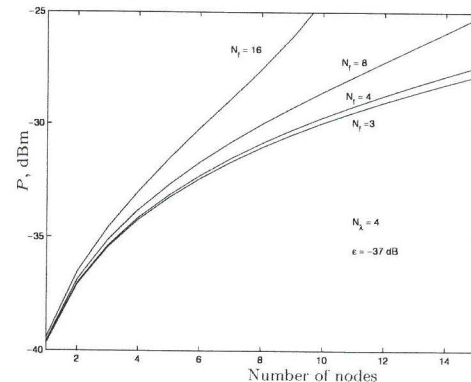


Fig. 6. Required signal power to assure a BER of 10^{-9} as a function of the number of traversed optical nodes.

of inband crosstalk and after traversing a certain number of nodes a BER floor will finally take place. In Fig. 7(a) we may observe that a BER floor is reached after four nodes for inband crosstalk $\epsilon = -33$ dB and $N_f = 16$. If inband crosstalk is reduced to -37 dB, then nine nodes can be traversed before a BER floor is reached. If we consider scalability with respect to the number of channels per fiber, then the first limitation encountered is the increase of accumulated ASE and input power than may saturates the EDFAs. If we restrict ourselves to an operating situation of unsaturated EDFAs, scalability with respect to N_λ is quite limited. In Fig. 8 is displayed the amount of P_{in} as a function of the number of nodes with N_λ as parameter. Considering our example ($P_{in}^{sat} = -11$ dBm) we have that four nodes can be traversed when $N_\lambda = 6$ while only two nodes can be reached for the case of $N_\lambda = 8$. Unsaturated operation of EDFAs is a very strict condition. Optical amplifiers can operate with certain degree of saturation and still yield a satisfactory signal-to-noise ratio [8]. To conduct more accurate scalability analysis of optical nodes with EDFA the



(a) $\epsilon = -33$ dB



(b) $\epsilon = -37$ dB

Fig. 7. Scalability with respect to N_f . a): $\epsilon = -33$ dB. b): $\epsilon = -37$ dB.

gain model should account for gain saturation. However, the present model clearly indicates the scalability limitations imposed by crosstalk and accumulated ASE noise.

IV. CONCLUSIONS

As optical cross-connects are cascaded the requirements on optical switch crosstalk isolation become more stringent. For the reference node is found that inband crosstalk should be lower than -37 dB in order to reach ten nodes. If more input fibers are added to the optical node less optical nodes can be reached unless the crosstalk parameter is improved. For instance, keeping $N_\lambda = 4$ and $N_f = 16$, the number of nodes that can be cascaded before a BER floor at 10^{-9} takes place is four for $\epsilon = -33$. This number can be increased to ten if the crosstalk value is improved to $\epsilon = -37$ dB (see Fig. 7). We also have found that the use

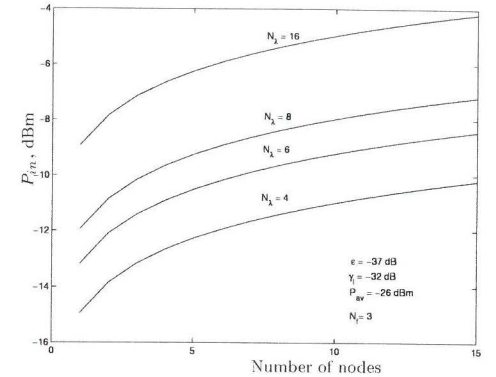


Fig. 8. Input power P_{in} to the EDFA as function of the number of nodes with N_λ as a parameter.

of EDFAs made the requirements on the crosstalk isolation even more stringent. Moreover, more power per channel is required to maintain a satisfactory signal-to-noise ratio. This is a consequence of the accumulation of ASE noise in a cascade of optical amplifiers. If we consider unsaturated EDFA operation, then a small number of nodes can be cascaded. Saturation of EDFAs will also limit the scalability of optical nodes. After traversing a certain number optical nodes the required signal power per channel may exceed the available transmitter power.

We can conclude that with crosstalk levels lower than -37 dB a cascade of ten reference nodes ($N_\lambda = 4, N_f = 3$) operating at a BER better than 10^{-9} is feasible. This also will apply for a network with a shortest largest optical path of ten (reference) nodes [9]. We also see that scalability with respect to the number of channels per fiber (N_λ) is strongly limited by the increase of accumulated ASE noise and saturation gain characteristics of the optical amplifiers.

This paper has studied the scalability of optical networks with respect to crosstalk. A statistical model, which includes optical crosstalk, ASE noise and data statistics, has been presented for the performance analysis of ASK systems. Although accumulation of ASE noise is taken into account, we consider only unsaturated EDFA operation. This condition is rather restrictive as EDFAs can operate under certain gain saturation and still provide a satisfactory signal-to-noise ratio. A more accurate scalability analysis should include a EDFA gain saturation model. However, the present analysis gives correct indications on the scalability of optical networks with respect to linear optical crosstalk. The present model can be used to evaluate the crosstalk requirements on the optical devices so that a given level of bit-error rate is assured in an all-optical network.

APPENDIX

This appendix is intended to present the model for inband and interband crosstalk. The EDFA gain model and

the model for the performance evaluation are also given.

A. Interband Crosstalk

We present a model for determining the amount of interchannel crosstalk power. Consider a channel at a wavelength λ_l . We follow [10] and considered a neighbor channel k at a wavelength $\lambda + \Delta\lambda$, where $\Delta\lambda$ is the channel spacing. We denote by P_l the optical power falling upon a photodetector due to channel l , and by P_k the power from the neighbor interfering channel. These magnitudes are given by

$$P_l = \int_{-\infty}^{\infty} S_l(\lambda) D_l(\lambda) d\lambda \quad (4)$$

$$P_k = \int_{-\infty}^{\infty} S_k(\lambda) D_l(\lambda) d\lambda \quad (5)$$

where $S_{k,l}(\lambda)$ is the power spectral density of the signal in channel l and k , respectively. The function $D(\lambda)$ represents the demultiplexer power transfer function. The relative interband crosstalk power is then given by

$$\gamma_l = 10 \log \frac{P_k}{P_l}. \quad (6)$$

In order to compute γ_l we have to specify the of spectrum shape of the light source, and the spectral transfer function $D(\lambda)$, and $M(\lambda)$ for the (DE)MUXs. We assume that the (DE)MUX are implemented by PHASARs. For a PHASAR designed to pass a channel at wavelength λ_l , and with a 3-dB spectral bandwidth λ_P , the power transfer function can be approximated by [11]

$$T(\lambda) = \exp[-(\lambda - \lambda_l)^2 / a^2], \quad (7)$$

where $a = 0.6\lambda_P$.

For a CW operating laser its spectrum is found to have a Lorentzian shape type with a 3-dB bandwidth $\Delta\nu_0$. For a digital modulated signal the spectrum is given by a convolution of the original CW spectrum with the spectral characteristic of the pulse shape and the data statistics. Roughly approximated, the bandwidth of the modulated laser is at least $\Delta\nu = \Delta\nu_0 + B$, with the data rate denoted by B . In this work we don't carry out detailed computations for the spectrum of the modulated laser but consider two situations: a) a Lorentzian and b) a Gaussian shaped spectrum with a 3-dB bandwidth $\Delta\nu$. We are interested in computing the amount of interchannel crosstalk in an optical node as described in Sec. II. The expression for the interband crosstalk is given by

$$\gamma_l = 10 \log \frac{\int_{-\infty}^{\infty} S_k(\lambda) M_k(\lambda) D_l(\lambda) d\lambda}{\int_{-\infty}^{\infty} S_k(\lambda) M_l(\lambda) D_l(\lambda) d\lambda}. \quad (8)$$

For a Gaussian shaped spectrum a closed form expression for γ_l is easily found:

$$\gamma_l = -12.06 \frac{(1 + \rho^2)}{1 + 2\rho^2} \Delta\lambda^2, \quad (9)$$

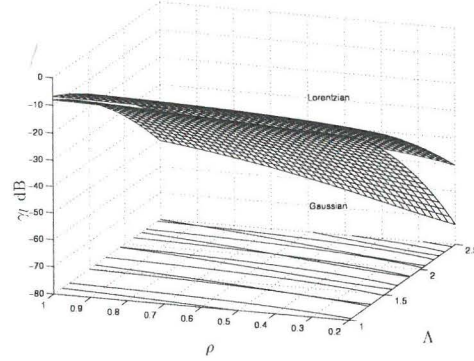


Fig. 9. Interchannel crosstalk as a function of the normalized channel spacing $\Delta\lambda$ and the parameter ρ

where $\Delta\lambda = \Delta\lambda / \lambda_P$ is the normalized channel separation and $\rho = \Delta\nu / \lambda_P$ [10]. Assuming a Lorentzian spectrum,

$$S(\lambda) = \frac{1}{1 + (\frac{\lambda - \lambda_l}{\Delta\nu})^2}, \quad (10)$$

the interband crosstalk is the given by

$$\gamma_l = 10 \log \frac{r e^{-\Delta\lambda^2 / 0.36} \int_{-\infty}^{\infty} \frac{\exp(-x^2 + \sqrt{2} \Delta\lambda x / 0.6)}{r^2 + x^2} dx}{\pi \operatorname{erfc}(r) e^{r^2}}, \quad (11)$$

where $r = \sqrt{2}\rho / 0.6$.

The relations (9) and (11) give us the amount of interband crosstalk from a next neighbor channel as a function of the normalized channel separation $\Delta\lambda$ and the ratio between channel bandwidth and (DE)MUX 3-dB bandwidth ρ . Expression (11) is easily evaluated by numerical methods like Gaussian quadrature rule integration.

In Fig. 9 is shown the relative interband crosstalk as a function of $\Delta\lambda$ and ρ for a Lorentzian and a Gaussian spectrum. We can consider (9) and (11) as a lower and upper bound on the value of interchannel crosstalk, respectively. The Lorentzian spectrum has a slowly decreasing tail and it is expected to give an overestimate result for interchannel crosstalk. The Gaussian spectrum is the resultant spectrum if the optical pulse has a Gaussian shape and the laser source exhibits no phase noise or chirp. In practical systems other effects like wavelength stability may influence the amount of interband crosstalk. Ultimately, measurements can be conducted to establish more accurate values for γ_l in a given system. In Table II are presented the computed values of γ_l for some parameters $\Delta\lambda$ and λ_P assuming a system operating at 2.5 Gbits/s.

If a number n of (DE)MUXs (PHASARs) are concatenated, then the resultant power spectral transfer function has also a Gaussian shape with a narrower 3-dB bandwidth given by $\lambda_P^n = \lambda_P / \sqrt{n}$. In this way we can also use expressions (9) and (11) in the case of cascaded optical nodes. In the analysis presented here we assume that interchannel crosstalk take place in latest optical node. This is due to

$\Delta\lambda$, GHz	λ_P	$\Delta\nu$	γ_l , dB (1)	γ_l (2)
100	56	2.54	-33.94	-38.38
100	46	2.54	-45.68	-56.82
75	56	2.54	-20.63	-21.59
75	46	2.54	-28.35	-31.97

TABLE II

INTERCHANNEL CROSSTALK γ_l . 1) LORENTZIAN SIGNAL SPECTRUM. 2) GAUSSIAN SIGNAL SPECTRUM.

the fact that this contribution appears to be the dominant one.

B. Inband crosstalk

The inband crosstalk contributions to the filtered photocurrent are of the type [12]

$$\xi_{s,x} = \frac{1}{T} \int_0^T \cos[\phi_s(t) - \phi_x(t - \tau_d)] dt, \quad (12)$$

given an integrate-and-dump postdetection filter. The bit duration time is denoted by T and τ_d is the interferometric delay time. The laser phase is modeled as Wiener process (variables $\phi_x(t)$, $\phi_s(t)$ in (1), and (2)) [13]. In most of the application of interest the delay time is of a larger magnitude than the coherence time ($B_L \tau_d \gg 1$). This situation is called the incoherent interferometric noise regime. In integrated optical cross-connects the circuit configuration can be chosen such that the amount of crosstalk is minimized and that the dominant crosstalk contributions are in the incoherent regime [2]. In the incoherent regime the mean of filtered inband crosstalk approaches the value zero and the variance is given by [12]

$$\sigma_{\xi}^2 = \frac{e^{-B_L T} + B_L T - 1}{(B_L T)^2}, \quad (13)$$

in which $B_L = 2\pi\Delta\nu_0$, where $\Delta\nu_0$ is the 3-dB bandwidth of the Lorentzian shaped laser power spectrum.

C. EDFA gain model

In an optical network a signal traverses more than one (DE)MUX which represent filtering for the ASE noise. We denote by $H_{\text{path}}(f)$ the equivalent transmission function for the optical path. This transmission curve is determined by the transmission function of the (DE)MUX of the number of traversed optical nodes. ASE noise is modeled as a Gaussian stochastic variable with a spectral noise power density given by

$$N_{\text{ASE}}^{\text{out}}(f) = N_{\text{ASE}}(f) |H_{\text{path}}(f)|^2 df \quad (14)$$

where $N_{\text{ASE}}(f)$ is the ASE noise power spectral density at the output of the optical amplifier, which is given by

$$N_{\text{ASE}}(f) = n_{\text{sp}}(G - 1) h f, \quad (15)$$

in which h is the Planck's constant, n_{sp} is the spontaneous emission coefficient, and G the amplifier gain. We assume that the amplifier gain is constant for input power values below the saturation level $P_{\text{sat}}^{\text{sat}}$.

D. Receiver model

We consider an ASK (NRZ) direct detection system whose schematic diagram is given in Fig. 10. The photocurrent at the output of the photodetector, $I_{sh}(t)$, is a shot noise process which can be written as

$$I_{sh}(t) = P_0 g(t) b_0^s + 2P_0 g(t) \sum_{n=1}^N \sqrt{b_0^s b_0^x} \epsilon_n \cos[\phi_s(t) - \phi_{x,n}(t - \tau_{d,n})] + 2P_0 g(t) \sum_{n=l+1}^N \sum_{l=1}^{N-1} \sqrt{b_0^x b_0^x} \epsilon_n \epsilon_l \times \cos[\phi_{x,n}(t - \tau_{d,n}) - \phi_{x,l}(t - \tau_{d,l})] + P_0 g(t) \sum_{n=1}^N b_0^{x,n} \epsilon_n + P_0 g(t) \sum_{l=1}^M b_0^{c,l} \gamma_l + I_{\text{ASE} \times s} + I_{\text{ASE} \times x} + I_{\text{ASE} \times c} + I_{\text{ASE} \times \text{ASE}}. \quad (16)$$

The first term is the signal, the second the signal-crosstalk beating, the third the secondary crosstalk-crosstalk beating, is the inband crosstalk, the fifth term is the interband crosstalk, and the last terms are the contribution from the ASE fields.

The derivation of (16) includes the following assumptions:

- the optical pulses are of identical shape and confined in the time interval $[0, T]$, i.e. no intersymbol interference (ISI) is assumed.
- The signal and the interferer are assumed to exhibit matched polarizations (worst case), and perfect bit alignment.

The photocurrent and thermal noise pass the postdetection filter $h(t)$ and further the filtered signal is sampled to form the decision variable. By comparing the sample value with a preselected threshold α_{tr} , the decision circuit provides an estimate of a transmitted bit in a particular bit interval.

E. Performance analysis

The question is to evaluate the average error rate P_e of the system under discussion (see Fig. 10). To account for all possible combination of beat terms between the informative signal and crosstalk we proceed by assuming that μ sources are simultaneously a binary symbol "one", thus $N - \mu$ sources are "zero". Similarly, all possible outcomes of the interchannel crosstalk l are considered. The error probability analysis is then conducted by a weighted statistical average of the error probability for each value μ and l . This probability is given by the binomial distribution function.

Hence, the average error probability P_e , for a given threshold α_{tr} , using the Gaussian approximation and assuming that the symbols are *a priori* equally probably $P_e(\mu)$ can be written as

$$P_e = \frac{1}{2^N} \frac{1}{2^M} \sum_{\mu=0}^N \binom{N}{\mu} \sum_{l=0}^M \binom{M}{l} \left\{ \frac{1}{2} Q \left(\frac{E_1(\mu, l) - \alpha_{tr}}{\sigma_1(\mu, l)} \right) + \frac{1}{2} Q \left(\frac{\alpha_{tr} - E_0(\mu, l)}{\sigma_0(\mu, l)} \right) \right\} \quad (17)$$

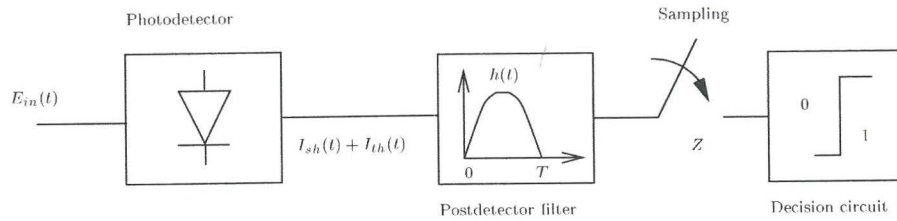


Fig. 10. Schematic diagram of an ASK/DD receiver. At the receiver input $E_{in}(t)$ represents the received optical signal.

where $E_{1,0}$ is the mean value of the receiver decision variable when a "one", and a "zero" is transmitted, respectively. The variance is denoted by $\sigma_{1,0}^2$. The function $Q(\cdot)$ is the standard Gaussian probability tail function. The variance of the receiver decision variable is approximately given by

$$\sigma_{0,1}^2 = \underbrace{2qRP_0b_0^2BF I_2}_{\text{signal shot noise}} + \underbrace{2qRP_0 \sum_{n=1}^N b_0^{x,n} \epsilon_n BF I_2}_{\text{inb. xtalk shot noise}} + \underbrace{(qR2P_0)^2 \sum_{n=1}^N b_0^{s,1} b_0^{x,n} \epsilon_n \sigma_{\xi,s,n}^2}_{\text{signal - inb. xtalk beat}} + \underbrace{\sigma_{th}^2}_{\text{therm. noise}} + \underbrace{(qR2P_0)^2 \sum_{n=l+1}^N \sum_{l=1}^{N-1} b_0^{x,n} b_0^{x,l} \epsilon_n \epsilon_l \sigma_{\xi,x,l}^2}_{\text{inb. xtalk - inb. xtalk beat}} + \underbrace{2qRP_0 \sum_{l=1}^M b_0^l \gamma_l^2 + \sigma_{ASE}^2}_{\text{interb. xtalk}} \quad (18)$$

where q is the electron charge, and I_2 is the Personick parameter [14]. The magnitude σ_{ASE}^2 accounts for the variances due to all ASE, signal and crosstalk beat contributions. The expressions for σ_{ASE}^2 are taken from [7]. Given a number N of inband and M interband crosstalk sources, the error probability is expeditiously evaluated by (17) accounting for data statistics, and non-perfect extinction ratio. Some words on the use of the Gaussian approximation. The distribution of filtered interferometric crosstalk may differ from Gaussian statistics, e.g., [12, 15]. However, a Gaussian approximation (using the effective variance; see (13)) works well for crosstalk values resulting in relatively low power penalties. We have adopted the Gaussian approximation for assessing the system performance considering the above mentioned features and also on view of its numerical simplicity.

REFERENCES

- [1] C. G. P. Herben *et al.*, "A compact integrated inp-based single-phasar optical crossconnect," *IEEE Photon. Technol. Lett.*, vol. 10, pp. 678-680, May 1998.
- [2] C. G. P. Herben *et al.*, "Compact integrated polarisation independent optical crossconnect," in *European Conference on Optical Communications*, vol. 1, (Madrid, Spain), pp. 257-258, September 20-24 1998.
- [3] E. L. Goldstein, L. Eskildsen, and A. F. Elrefaie, "Performance implications of component crosstalk in transparent lightwave networks," *IEEE Photonics Techn. Lett.*, vol. 6, pp. 657-700, May 1994.
- [4] E. L. Goldstein and L. Eskildsen, "Scaling limitations in transparent optical networks due to low-level crosstalk," *IEEE Photonics Techn. Lett.*, vol. 7, pp. 93-94, Jan. 95.
- [5] P. T. Legg, M. Tur, and I. Andonovic, "Solution paths to limit interferometric noise induced performance degradation in ask/direct detection lightwave networks," *J. Lightwave Technol.*, vol. 14, pp. 1943-1953, Sept. 1996.
- [6] I. Tafur Monroy and E. Tangdiongga, "Performance evaluation of optical cross-connects by saddlepoint approximation," *J. Lightwave Technol.*, vol. 16, pp. 317-323, March 1998.
- [7] N. A. Olsson, "Lightwave systems with optical amplifiers," *J. Lightwave Technol.*, vol. 7, pp. 1071-1082, July 1989.
- [8] C. R. Giles and E. Desurvire, "Propagation of signal and noise in concatenated erbium-doped fiber optical amplifiers," *J. Lightwave Technol.*, vol. 9, pp. 147-154, Feb. 1991.
- [9] I. Tafur Monroy, J. Siffels, H. de Waardt, and H. J. S. Doreen, "Scalability of all-optical networks: study of topology and crosstalk dependence," in *Broadband European Networks and Multimedia Services*, vol. 3408 of *EUROPTO Series*, (Zürich, Switzerland), EOS/SPIE, 18-20 May 1998.
- [10] G. Murtaza and J. M. Senior, "Wdm crosstalk analysis for systems employing spectrally-sliced led sources," *IEEE Photon. Technol. Lett.*, 1996.
- [11] H. Takahashi *et al.*, "Transmission characteristics of arrayed waveguide $n \times n$ wavelength multiplexer," *J. Lightwave Technol.*, vol. 13, pp. 447-455, March 1995.
- [12] I. Tafur Monroy, E. Tangdiongga, and H. de Waardt, "On the distribution and performance implications of interferometric crosstalk in wdm networks," *J. Lightwave Technol.*, June 1999. Accepted for publication.
- [13] A. Mooradian, "Laser linewidth," *Phys. Today*, vol. 38, pp. 43-48, May 1985.
- [14] R. G. Smith and S. D. Personick, *Semiconductor Device for Optical Communication*, ch. Receiver Design for Optical Communication Systems, pp. 89-160. Springer-Verlag, 1987.
- [15] M. Tur and E. L. Goldstein, "Probability distribution of phase-induced intensity noise generated by distributed feed-back lasers," *Optics Letters*, vol. 15, pp. 1-3, January 1990.

Chapter 7

Conclusion, Recommendations, and Further Work

7.1 Conclusions

Chapter 4: Phase noise analysis

Phase noise from signal oscillators impair the performance of a wide class of communications system. Optical communication systems where signals are derived from a laser light source are no exception. Chapter 4 presented a study of phase noise in optical systems. Firstly, we presented a direct analysis of phase noise in heterodyne optical systems (see paper A). Secondly, a recursive formula for the moments of filtered phase noise was derived (see paper B).

Chapter 5: Optical preamplified receivers

The analysis of optically preamplified receivers with Fabry-Perot optical filters was presented in detail. A closed form expression for the MGF of the receiver decision variable, implicitly incorporating a Fabry-Perot filter, was derived (see paper C).

A modified integrating postdetection filter and equalization was found to improve the performance and allow the use of narrower optical filters. This is of relevance in dense wavelength division multiplexing (DWDM) systems with closely spaced channels. A simple and accurate analytical approach to the analysis of optically preamplified receivers was introduced. It allows us to determined the optimum 3-dB bandwidth for arbitrary optical filters and arbitrary postdetection filters resulting in the best balance between ASE noise rejection and ISI (see paper D).

Several preamplified On-Off keying (OOK) receiver configurations, including different types of optical filters, were also studied. This problem constitutes the classic communication situation of determining the statistics for the filtered output of squared envelope detectors with colored Gaussian noise input. Closed form expressions for the MGF of the receiver decision variable were derived. These expressions are believed to be new. The derived MGFs were then applied to the problem of finding the quantum limit for OOK, optically preamplified receivers (see paper E). We also discussed the question of what the

ultimate quantum limit is for OOK, when using optically preamplified receivers. A receiver configuration resulting in a very low quantum limit was presented (see paper **F** and comments in Sec. 5.3).

In conclusion, the analysis of optically preamplified receivers is a complex task. This is due to the nonlinear character of photodetection. An important parameter for the design of an optically preamplified receiver is an optimum 3-dB bandwidth of the optical filter resulting in the best balance between ASE noise rejection and ISI. A simple analytical approach was presented for the analysis of preamplified receivers incorporating an arbitrary optical filter and an arbitrary electrical postdetection filtering.

Chapter 6: Crosstalk in optical networks

Interferometric crosstalk is a serious limiting factor for the scalability of all-optical networks. Interferometric crosstalk translates into intensity noise at the receiver end. For a proper performance analysis of a communication system an accurate description of noise is required. A detailed statistical description of filtered crosstalk was presented in paper **I**. An important contribution is the implicit incorporation in the statistics of the relation between the 3-dB bandwidth of the optical signal and the 3-dB bandwidth of the postdetection filter. This finding allowed us to explain, from the statistical analysis point of view, the experimental observation that systems using directly modulated lasers are less vulnerable to crosstalk than those using externally modulated light sources. The reason is the inherent spectral broadening in directly modulated laser diodes due to chirp. Experiments and computer simulations demonstrated the validity of the theory.

In the computational aspect of the performance analysis, an accurate and numerically simple method was introduced by making use of the saddlepoint approximation. The saddlepoint approximation is based on the moment generating function (MGF) for the receiver decision variable. The advantage of this method becomes more noticeable in the presence of multiple sources of crosstalk. The complexity of the method does not depend on the number of crosstalk interferers compared to other methods where this is the case; e.g. numerical convolutions of probability density functions (see papers **G** and **H**).

Scalability of optical networks with respect to crosstalk and its dependence on the network topology were studied. The result is that there is a delicate relationship between the crosstalk performance of an optical network and its topology. This means that during upgrades or (re)designs of an optical network special attention should be paid to this relationship (see papers **L** and **M**).

If optical amplifiers are used in the network for optical loss compensation, the requirements on crosstalk isolation become more severe. Moreover, a strategy of gain management should be employed to avoid detrimental effects from gain saturation and unequal amplification of channels (see papers **J** and **N**).

Phase scrambling as a technique to reduce crosstalk in WDM optical networks was theoretically investigated and experimentally assessed. The trial systems operated at 2.5 Gbit/s.

It was demonstrated that significant crosstalk reduction can be achieved. Enhancement of approximately 8 dB tolerance towards crosstalk was observed. Phase scrambling results in spectral broadening of the optical signal. As a consequence, power penalties are incurred due to dispersion during transmission over SSMF. However, by properly selecting the parameters for phase scrambling, transmission length of 100-200 km are viable. This indicates that phase scrambling permits WDM optical networking in a LAN/MAN environment while making use of the current integrated WDM technology. Phase scrambling substantially relaxes the crosstalk requirement for optical components (see paper **K**).

In conclusion, if the comprising components in an optical network suffer from crosstalk leakage, serious performance degradation will arise due to interferometric crosstalk. Accumulation of crosstalk in optical networks is strongly related to the network topology and number of fiber connections per optical node. Interferometric crosstalk can be electrically filtered if the laser bandwidth exceeds the receiver electrical postdetection filter bandwidth. Based on this fact, an efficient technique for crosstalk reduction is phase modulation of optical signals with noise: phase scrambling. A series of recommendations on the use of this technique are given in the following section.

7.2 Recommendations

This section gives a series of recommendation concerning the operating regime of the following optical communication systems: (a) Systems disturbed by inband crosstalk and (b) systems using phase scrambling to reduce the effect of inband crosstalk. (c) Optically preamplified receivers. The most relevant aspects are highlighted below.

Inband crosstalk

- Optimization of the receiver detection threshold results in an improved performance of systems disturbed by inband crosstalk (Appendix A).
- Power penalties due to inband crosstalk are less pronounced if the system has a laser with a large extinction ratio (Appendix A).
- Systems using directly modulated (semiconductor) light sources result in smaller power penalties than those using externally modulated sources. The reason is that in directly modulated diode sources the inherent amount of chirp broadens the spectrum, allowing filtering of crosstalk noise power at the receiver end. However, chirp in DFB lasers is deterministic and bit-sequence dependent so that no crosstalk reduction will take place in this particular case. When using externally modulated light sources no crosstalk filtering will arise (paper **I**), as crosstalk noise will fall within the receiver bandwidth.
- Optical preamplification in the presence of interferometric crosstalk does not enhance the receiver tolerance toward power penalties. Moreover, additional power penalties (added to the ones due to crosstalk) arise from beat term between ASE and crosstalk (see paper **J**).

Scalability

- In the presence of one crosstalk source, a crosstalk level better than -24 dB (-20 dB) results in power penalties smaller than 1 dB. This concerns a system operating at 2.5 Gbit/s, and using a directly (externally) modulated light source. As the number of crosstalk sources increases, the requirement on crosstalk source isolation becomes more stringent. So, for three interferers the crosstalk level should be less than -30 dB to yield power penalties smaller than 1 dB (see papers G, H, and I).
- In the presence of ASE noise and inband crosstalk, additional power penalties due ASE-crosstalk beats are incurred. The penalty level depends on the ASE noise level from the amplifier, laser extinction ratio, and crosstalk level. For example, in a system operating a 2.5 Gbit/s (using both directly and externally modulated light sources) it is found that at a level of 1 dB inband crosstalk penalty the additional penalty is about 0.5 dB. However, if we would like to perform below the 1 dB power penalty, the crosstalk isolation should be improved by ≈ 1.5 dB and ≈ 1 dB for a system with a directly modulated light source and a for system using an external modulator, respectively (see paper J). These conclusions are drawn for the case of one crosstalk source being present. As the number of interferers increases, the requirement on crosstalk isolation becomes more severe (see paper N).
- Accumulation of inband crosstalk is closely related to the network topology. Therefore, while upgrading or designing optical networks special attention should be paid to the relationship between network topology, connectivity (number of nodes and connections), and crosstalk accumulation (see papers L and M).

Phase scrambling (paper K)

- Phase scrambling significantly reduces crosstalk power penalties due to inband crosstalk. It was found, theoretically and experimentally, that at a level of 1 dB power penalty, an increase in tolerance toward crosstalk of around 6 dB can be achieved. This conclusion is applicable for a single crosstalk source case and no fiber transmission.
- The main parameter for phase scrambling is the modulation index of the modulating noise. Higher values of the modulation index assure better reduction of inband crosstalk. The correlation characteristics of the modulating noise are irrelevant for the crosstalk reduction effectiveness. In the case of a system operating at 2.5 Gbit/s, the 3-dB bandwidth of the noise can be of a moderate magnitude at the range of hundreds of MHz, and the center frequency can be arbitrarily chosen to have a value of some hundreds of MHz.
- Proper selection of the phase scrambling parameters can allow transmission over some 100-150 Km of SSMF at a bitrate of 2.5 Gbit/s. Crosstalk reduction still is effective (some 8 dB of tolerance enhancement) and the penalties due to dispersion can be kept low. The reach of a network using phase scrambling is limited by dispersion due to the intentionally introduced spectral broadening.

Optically preamplified direct detection receivers

- For a receiver using a Fabry-Perot optical filter and a postdetection filter of the integrate-and-dump type, the optimum optical filter 3-dB bandwidth B and bit-time T product is found to be $BT = 7.5$ (see papers C and D).
- A modified postdetection integration time $[\epsilon T, T]$ yields a better performance. A suitable value for ϵ is found to be $\epsilon = 0.4/BT$, which should be used with an optical filter with a 3-dB bandwidth so that $BT = 3.7$. This combination results in an improved receiver performance (see paper E).
- Further performance improvement can be achieved by using postdetection equalization (see paper E).

7.3 Further work

In this section the author would like to identify some areas for further work. Naturally, the success of all-optical networking depends on the availability, high performance, reliability, and low cost of the constituent optical components. This is an area full of challenges for further research.

With regard to the scalability of optical networks, further research should be directed towards the interplay between network topology, access/multiplexing methods, connectivity, and crosstalk performance. It is also of importance to expand the theoretical models used in this thesis to cover more aspects of optical signal transmission and networking. These include nonlinear transmission, optical amplifier gain management, wavelength conversion, and other issues. In this way, the performance limitations, scalability and benefits of optical networks can be more accurately assessed and understood. It is expected that optical networks will support higher and higher transmission capacities, and that more complex optical elements (cross-connects, receivers, transmitters, etc.) are going to be used. A large amount of traffic is going to be transported, which will mean significant costs for the operators. In view of this, network optimization, monitoring, restoration, and network management is expected to be an area for intensive further research.

Ongoing attempts are being made to exploit the bandwidth of the optical fiber as an information transmission medium in a more effective way. As a consequence, channel spacing in WDM is reduced, optical filters, and wavelength selective elements are introduced, etc., in order to get more use out of the fiber bandwidth. Efficient strategies to reach this goal may be found by conducting research in the area of optical communication theory. This includes the study of novel modulation schemes (power efficient schemes), pulse shapes, and codes, among other aspects, that may improve the quality of information transmission over the optical fiber while making efficient use of its bandwidth. Topics covering optical filtering (dispersion effects, phase distortion, and intersymbol interference) are also of relevance. Effective and simple techniques for clock-recovery are also of crucial importance for the implementation of all-optical networks.

Appendix A

Characteristics of Interferometric Crosstalk

Parameters like polarization statistics, laser extinction ratio, and receiver detection threshold are determining factors regarding how the performance of a system is influenced by interferometric crosstalk. This Appendix shows how the performance of an ASK/DD receiver, disturbed by interferometric crosstalk, is affected by the abovementioned parameters. The analysis presented here concerns a single crosstalk interferer.

A.1 Polarization statistics

It is common practice to consider a so-called worst-case detection situation for the performance analysis of a communication system. This gives insights into how a system should be design to fulfill a particular performance requirement even in the worst-case scenario. In our situation, the worst-case means that the signal and the crosstalk interferer exhibit matched state of polarization. However, it is important to obtain a more detailed description of how the performance is affected by a polarization misalignment that is different from the worst-case. To study this issue a special case is going to be considered: the signal and crosstalk are assumed to exhibit a linear polarization with random, independent orientation angles θ_s and θ_x , respectively. Consequently, the parameter $\vec{r}_s \vec{r}_x$ in expression 6.1 takes the form $\zeta(\theta_s, \theta_x) = |\cos(\theta_s - \theta_x)|$ where $\theta_s - \theta_x$ is assumed to be a random variable, uniformly distributed in $[0, 2\pi]$. The probability density function of ζ is given by the doubled, nonnegative part of an arcsine distribution [86].

$$f(\zeta) = \begin{cases} \frac{2}{\pi\sqrt{1-\zeta^2}} & 0 < \zeta < 1 \\ 0 & \text{elsewhere} \end{cases} \quad (\text{A.1})$$

A mathematical model was developed to compute the error probabilities for systems disturbed by interferometric crosstalk. Here we present the results yielded by the model while the details can be found in the papers **G** and **H**. The power penalties, with respect to a bit-error rate level of 10^{-9} , for different values of the crosstalk parameter ϵ (relative crosstalk to signal power) are shown in Fig. A.1. We observe in Fig. A.1 that there is no substantial difference in performance between the worst-case and the linear polarization situation.

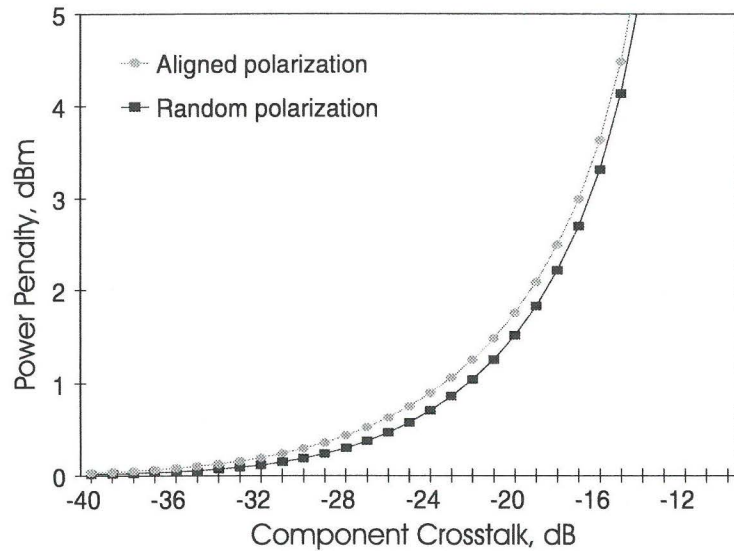


Figure A.1: Power penalties due to crosstalk. A comparison between the worst-case and a random linear polarization alignment of the signal and crosstalk.

This applies for any arbitrary value of the crosstalk parameter. This result indicates that optical networks should be designed taking into account a worst-case polarization alignment between the signal and crosstalk.

A.2 Detection threshold

The setting of the receiver detection threshold influences the system performance. It is common practice to use a detection threshold set to be a midway point between the “zero” and “one” received level. This is not an optimum detection threshold, in the sense of yielding the lowest bit-error probability. The optimum detection threshold can be found numerically by applying a minimization procedure on the bit-error rate (see papers **G** and **H**). Figure A.2 shows that at the level of 1 dB power penalty there is a difference in performance between the optimum and fixed midway detection threshold setting of 4 dB. In conclusion, an optimized detection threshold is desirable in systems disturbed by interferometric crosstalk. An optimized detection threshold provides an enhancement of more than 4 dB tolerance to crosstalk.

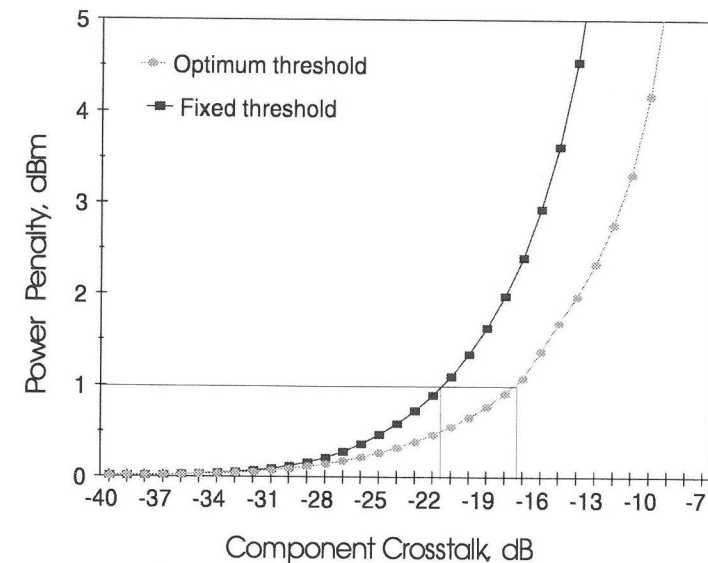


Figure A.2: Power penalties due to crosstalk. This figure shows the effect of an optimized detection threshold on the receiver performance. The power penalties are related to a bit-error rate level of 10^{-9} .

A.3 Non-perfect extinction ratio

By laser extinction ratio (ER) is meant the relation $\rho = \frac{P_0}{P_1}$ between the light source power level P_0 when a “zero” is transmitted and the level P_1 for a transmitted “one”. When the laser extinction ratio is perfect ($\rho = 0$), only the binary symbols “one” contribute to the signal-crosstalk beat term of the receiver photocurrent. In the case of non-perfect extinction ratio, both the binary “one” and “zero” transmitted symbols contribute to crosstalk interference. Thus, we have four possible beat terms $\{b^s b^x\}$ for a signal binary symbol b^s and a crosstalk interferer symbol b^x .

The power penalties shown in Fig. A.3 are calculated for the perfect and non-perfect ($\rho = 0, 0.17$) extinction ratio. We observe that the difference in performance is insignificant for small values of the component crosstalk parameter ϵ , while for high crosstalk values there is a relevant difference in the incurred power penalties.

An optimized detection threshold results in a better performance. For example, there is a difference in tolerance to crosstalk of 4.5 dB between the perfect extinction ratio $\rho = 0$ and the case of $\rho = 0.17$ (7.7 dB). This observation concerns a midway detection threshold setting. For the case of an optimized detection threshold the difference in power penalties is 1.2 dB. We can conclude that the better the extinction ratio the larger the tolerance for

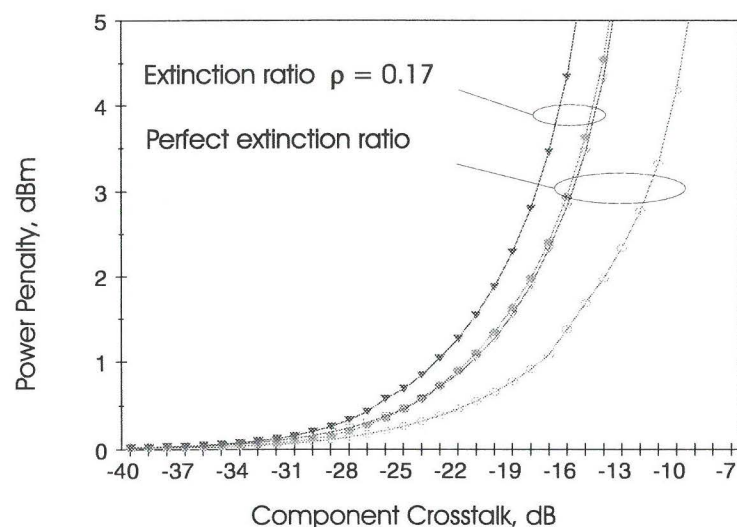


Figure A.3: This figure shows the effect of non-perfect extinction ratio on the power penalties due to crosstalk. Perfect extinction ratio $\rho = 0$: marker \circ ; extinction ratio $\rho = 0.17$: marker ∇ . The open and filled markers represent optimum and fixed threshold detection, respectively.

crosstalk. We can also conclude that detection threshold optimization is important to incur smaller power penalties due to crosstalk. The analysis presented here concerns the case of a single crosstalk interferer. How to conduct the analysis for the case of multiple crosstalk interferers is explained in papers G and H.

Bibliography

- [1] K. C. Kao and H. G. A., "Dielectric-fiber surface waveguides for optical frequencies," *IEEE Proceedings*, vol. 133, pp. 191–198, June 1986. Pt. J.
- [2] A. Werts, "Propagation de la lumière cohérent dans les fibre optiques," *L'Onde Electrique*, vol. 46, pp. 967–980, September 1966.
- [3] R. J. Mears, L. Reekie, I. M. Jauncey, and D. N. Payne, "Low-noise erbium-doped fibre amplifier operating at $1.54\mu\text{m}$," *Elec. Lett.*, vol. 23, pp. 1026–1028, September 1987.
- [4] L. F. Mollenauer and P. V. Mamyshev, "Massive wavelength-division multiplexing with solitons," *IEEE J. Quantum Electronics*, vol. 34, pp. 2089–2101, November 1998.
- [5] T. R. I. COBRA, "Photonics in communication technologies." Research proposal, Eindhoven University of Technology, The Netherlands, July 1998.
- [6] E. Mos and H. de Waardt, "Laser neural network demonstrates data switching functions," in *ICANN'98, Proceedings of the 8th international conference on artificial neural networks*, vol. 2, pp. 1165–1170, Springer, 1998.
- [7] H. Kobrinski, "Cross-connection of wavelength division multiplexed high speed channels," *Elec. Lett.*, vol. 23, pp. 974–975, 1987.
- [8] G. R. Hill, "A wavelength routing approach to optical communications networks," *Br. Telecom Techn. J.*, pp. 24–31, July 1988.
- [9] H. J. Westlake *et al.*, "Reconfigurable wavelength routed optical networks: a field demonstration," in *Proc. ECOC*, 1991.
- [10] G. Hill *et al.*, "A transport networks layer based on optical networks elements," *IEEE/OSA J. Lightwave Technol.*, vol. 11, pp. 667–679, May/June 1993.
- [11] G. D. Khoe, H. v.d. Boom, and E. v.d. Put, "LAN interconnection based on a cross-connected multi-wavelength layer," in *LEOS 1994, Summer topical meetings digest*, pp. 40–41, July 8–8 1994.
- [12] *IEEE/OSA J. Lightwave Technol.*, vol. 14 (Special Issue on Multiwavelength Optical Technology and Networks), June 1996.

- [13] P. E. Green, "Optical networking update," *IEEE J. Selected Areas in Communications*, vol. 14, pp. 764–779, June 1996.
- [14] G. Prati, ed., *Photonic Networks*. London: Springer, 1997.
- [15] C. G. P. Herben *et al.*, "A compact integrated InP-based single-phaser optical cross-connect," *IEEE Photon. Technol. Lett.*, vol. 10, pp. 678–680, May 1998.
- [16] J. S. Wellen, *Modelling, design and fabrication of a GaAs-based integrated photoreceiver for short distance optical communication*. PhD thesis, Eindhoven University of Technology, April 1997.
- [17] K. Steenbergen, *High Capacity Integrated Optical Receivers*. PhD thesis, Delft University of Technology, June 1997.
- [18] ACTS programme 3002, "Advanced photonic experimental x-connect, technical annex," 1998.
- [19] O. M. van Deventer *et al.*, "Node functionalities and architectures for the optical network layer, results from eurescom p615," in *NOC'97, European Conference on Networks and Optical Communications*, (Antwerpen, Belgium), June 1997.
- [20] K. Mueller *et al.*, "Application of amplitude histograms for quality of service measurements of optical channels and fault identification," in *European Conference on Optical Communications*, vol. 1, (Madrid, Spain), pp. 707–708, September 20–24 1998.
- [21] L. E. Nelson, S. T. Cundiff, and C. R. Giles, "Optical monitoring using data correlation for WDM systems," *IEEE Photon. Technol. Lett.*, vol. 10, pp. 1030–1032, July 1998.
- [22] K. J. Park, S. K. Shin, and Y. C. Chung, "A simple monitoring technique for WDM networks," in *Optical Fiber Communication Conference*, pp. 152–154, OSA, technical digest, February 1999.
- [23] E. Radius *et al.*, "The BOLERO project at KPN Research," in *1998 IEEE/LEOS Symposium*, (Gent, Belgium), pp. 17–20, November 1998.
- [24] "Optical internetworking forum (OIF)," URL: <http://www.oiforum.com>.
- [25] I. Shake *et al.*, "Monitoring of optical signal quality using sum-frequency-generation optical sampling," in *Symposium on Optical Fiber measurements*, NIST 930, pp. 87–90, National Institute of Standards and Technology, 1998.
- [26] M. Renaud, "Components for advanced WDM networks," in *European Conference on Optical Communications*, vol. 3, (Madrid, Spain), pp. 33–37, September 20–24 1998.
- [27] M. S. Borella *et al.*, "Optical components for WDM lightwave networks," *Proc. IEEE*, vol. 85, no. 5, pp. 1274–1307, 1997.
- [28] J. Buus, "Tunable laser diodes," in *Photonic Networks* (G. Prati, ed.), pp. 91–102, London, UK: Springer, 1997.

- [29] M. Zirngibl, "Multifrequency lasers and applications in WDM networks," *IEEE Comm. Magazine*, pp. 39–41, December 1998.
- [30] E. R. M. Taylor *et al.*, "A 1300nm Nd³⁺-doped glass amplifier," in *European Conference on Optical Communications*, vol. 1, (Madrid, Spain), pp. 45–46, September 20–24 1998.
- [31] J. G. L. Jennen *et al.*, "4x10 Gbit/s NRZ transmission in the 1310nm window over 80km of standard single mode fiber using semiconductor optical amplifiers," in *European Conference on Optical Communications*, vol. 1, (Madrid, Spain), pp. 235–236, September 20–24 1998.
- [32] M. K. Smit and C. Van Dam, "Phaser-based WDM-devices: principles, design and applications," *IEEE J. of Selected Topics in Quantum Electronics*, vol. 2, pp. 237–250, June 1996.
- [33] S. Turley, "Technology choices abound for the optical network," *Lightwave*, pp. 51–60, February 1998.
- [34] E. Ollier and P. Mottier, "Low voltage wavelength and polarization independent micro-opto-mechanical switch integrated on silicon," in *Photonics in Switching*, vol. 10 of *Technical Digest Series*, (Stockholm, Sweden), OSA, April 2–4 1997.
- [35] R. Dangel and W. Lukosz, "Electro-nanomechanically activated integrated-optical interferometric switches," in *Photonics in Switching*, vol. 10 of *Technical Digest Series*, (Stockholm, Sweden), OSA, April 2–4 1997.
- [36] M. Gustavsson, "Technologies and applications for space-switching in multi-wavelength networks," in *Photonic Networks* (G. Prati, ed.), pp. 157–171, London, UK: Springer, 1997.
- [37] K. E. Stubkjaer *et al.*, "Wavelength conversion technology," in *Photonic Networks* (G. Prati, ed.), pp. 103–117, London, UK: Springer, 1997.
- [38] H. Yoshimura, K. Sato, and N. Takachio, "Future photonic transport networks based on WDM technologies," *IEEE Comm. Magazine*, pp. 74–81, February 1999.
- [39] E. Iannone, F. Matera, M. A., and M. Settembre, *Nonlinear Optical Communication Networks*. Microwave and optical engineering, John Wiley & Sons, Inc., 1998.
- [40] D. M. Spirit and M. J. O'Mahony, eds., *High Capacity Optical Transmission Explained*. John Wiley & Sons, 1995.
- [41] F. Heismann, "Polarization mode dispersion: fundamental aspects and impact on optical communication systems," in *European Conference on Optical Communications*, vol. 2, (Madrid, Spain), pp. 51–79, September 20–24 1998.
- [42] Y. Fukada, T. Imai, and A. Mamoru, "BER fluctuation suppression in optical inline amplifier systems using polarisation scrambling technique," *Elec. Lett.*, vol. 30, pp. 432–433, 1994.

- [43] D. R. Lutz, "A passive depolariser," *IEEE Photon. Technol. Lett.*, vol. 4, pp. 463–465, 1993.
- [44] E. A. Golovchenko, V. J. Mazurczyk, and S. M. Abbot, "Implementing optical noise loading to estimate margin in WDM systems," in *Optical Fiber Communication Conference*, pp. 335–337, OSA, Technical digest, February 1999.
- [45] G. Einarsson, *Principles of Lightwave Communications*. Chichester: John & Wiley, 1996.
- [46] G. P. Agrawal, *Fiber-optic communication systems*. Wiley-Interscience, 1997.
- [47] P. E. Green, *Fiber Optic Networks*. Prentice Hall, 1993.
- [48] *IEEE J. Quantum Electronics*, vol. 34 (Feature Issue on Fundamental Challenges in Ultrahigh-Capacity Optical Fiber Communication Systems and Networks), November 1998.
- [49] *IEEE Communications Magazine*. No. 2 (Optical Networks: Communications Systems, and Devices), February 1999.
- [50] G. Foschini and G. Vannucci, "Characterizing filtered light waves corrupted by phase noise," *IEEE Trans. Inform. Theory*, vol. 34, pp. 1437–1448, Nov 1988.
- [51] I. Garret and G. Jacobsen, "Phase noise in weakly coherent systems," *IEE Proceedings*, vol. 136, pp. 159–165, June 1989.
- [52] R. Taylor, V. Poor, and S. Forrest, "Phase noise in coherent analog AM-WIRNA optical links," *IEEE/OSA J. Lightwave Technol.*, vol. 15, no. 4, pp. 565–575, 1997.
- [53] T. Pollet, M. van Bladel, and M. Moeneclaey, "BER sensitivity of OFDM systems to carrier frequency offset and Wiener phase noise," *IEEE Trans. Commun.*, vol. 43, pp. 191–193, Feb./March/April 1995.
- [54] L. Tomba, "On the effect of wiener phase noise in OFDM systems," *IEEE Trans. Commun.*, vol. 46, no. 5, pp. 580–583, 1998.
- [55] W. P. Robins, *Phase noise in signal sources*, vol. 9 of *IEE Telecommunications series*. London, UK: Peter peregrinus, 1984.
- [56] Z. Xiaopin, "Analytically solving the Fokker-Planck equation for the statistical characterization of the phase noise envelope detection," *IEEE/OSA J. Lightwave Technol.*, vol. 13, p. 1787, August 1995.
- [57] D. J. Bond, "The statistical properties of phase noise," *Br. Telecom Technol. J.*, vol. 7, pp. 12–17, Oct. 1989.
- [58] G. L. Pierobon and L. Tomba, "Moment characterization of phase noise in coherent optical systems," *IEEE/OSA J. Lightwave Technol.*, vol. 9, pp. 996–1005, Aug. 1991.

- [59] J. B. Waite and D. S. L. Lettis, "Calculation of the properties of phase noise in coherent optical receivers," *Br. Telecom Technol. J.*, vol. 7, pp. 18–26, Oct. 1989.
- [60] A. Mooradian, "Laser linewidth," *Phys. Today*, vol. 38, pp. 43–48, May 1985.
- [61] G. H. Golub and J. H. Welsh, "Calculation of Gaussian quadrature rules," *Math. Comput.*, vol. 23, pp. 221–230, April 1969.
- [62] E. Snitzer, "Optical maser action of Nd^{+3} in a barium glass," *Physical review Letters*, vol. 7, pp. 444–446, December 1961.
- [63] C. J. Koester and E. Snitzer, "Amplification in a fiber laser," *Applied Optics*, vol. 3, pp. 1182–1186, October 1964.
- [64] V. S. Letokhov and B. D. Pavlik, "Nonlinear amplification of optical surface waves in active optical waveguide," *Soviet Physics- Technical Physics*, vol. 11, pp. 1628–1632, June 1967.
- [65] R. J. Mears, L. Reekie, s. B. Poole, and D. N. Payne, "Low-threshold tunable CW and Q-switched fibre laser operating at $1.55\mu\text{m}$," *Elec. Lett.*, vol. 22, pp. 159–160, January 1986.
- [66] P. S. Henry, "Error-rate performance of optical amplifiers," in *Proceedings, OFC*, 1989.
- [67] M. Kac and A. J. F. Siegert, "On the theory of noise in radio receivers with square law detectors," *J. of Applied Physics*, vol. 18, pp. 383–397, April 1947.
- [68] S. O. Rice, "Mathematical analysis of random noise," *Bell Sys. Tech. J.*, vol. 23 and 24, pp. 282–332 and 46–156, 1954.
- [69] A. J. F. Siegert, "A systematic approach to a class of problems in the theory of noise and others random phenomena -part II, examples," *IRE Trans. Information Theory*, pp. 38–43, March 1957.
- [70] D. Slepian, "Fluctuations of random noise power," *Bell Sys. Tech. J.*, pp. 163–184, Jan. 1958.
- [71] M. I. Schwartz, "Distribution of the time-average power of a Gaussian process," *IEEE Trans. Inform. Theory*, vol. 16, pp. 17–26, Jan. 1970.
- [72] C. W. Helstrom, "Distribution of the filtered output of a quadratic rectifier computed by numerical contour integration," *IEEE Trans. Inform. Theory*, vol. 32, pp. 450–463, July 1986.
- [73] C. W. Helstrom, *Elements of Signal Detection and Estimation*. ISBN 0-13-808940-x, Englewood Cliffs, NJ.: Prentice Hall, 1995.

- [74] O. Lindunger and E. Almström, "Time dependence of interferometric crosstalk in all-optical networks," in *Photonics in Switching*, vol. 10 of *Technical Digest Series*, (Stockholm, Sweden), OSA, April 2-4 1997.
- [75] R. Khosravani *et al.*, "Reduction of coherent crosstalk in WDM add/drop multiplexing nodes by bit pattern misalignment," *IEEE Photon. Technol. Lett.*, vol. 11, pp. 134-135, January 1999.
- [76] E. Goldstein *et al.*, "Polarization statistics of crosstalk-induced noise in transparent lightwave networks," *IEEE Photon. Technol. Lett.*, vol. 7, pp. 1345-1347, November 1995.
- [77] P. T. Legg, M. Tur, and I. Andonovic, "Solution paths to limit interferometric noise induced performance degradation in ASK/direct detection lightwave networks," *IEEE/OSA J. Lightwave Technol.*, vol. 14, pp. 1943-1953, Sept. 1996.
- [78] S. L. Danielsen *et al.*, "Analysis of interferometric crosstalk in optical switch blocks using moment generating functions," *IEEE Photon. Technol. Lett.*, vol. 10, pp. 1635-1637, Nov. 1998.
- [79] Y. Yamada *et al.*, "Tolerance for optical coherent crosstalk of a novel manchester-code receiver," in *European Conference on Optical Communications*, vol. 1, (Madrid, Spain), pp. 61-62, September 20-24 1998.
- [80] P. K. Pepeljugoski and K. Y. Lau, "Interferometric noise reduction in fiber-optic links by superposition of high frequency modulation," *IEEE/OSA J. Lightwave Technol.*, vol. 10, pp. 957-963, July 1992.
- [81] A. Yariv, H. Blauvelt, and S. Wu, "A reduction of interferometric phase-to-intensity conversion noise in fiber links by large index phase modulation of the optical beam," *IEEE/OSA J. Lightwave Technol.*, vol. 10, pp. 978-981, July 1992.
- [82] F. W. Willems and W. Muys, "Suppression of interferometric noise in externally modulated lightwave AM-CATV systems by phase modulation," *Elect. Letters*, vol. 29, pp. 2062-2063, Nov. 1993.
- [83] Y. Pan, C. Qiao, and Y. Yang, "Optical multistage interconnection network: new challenges and approaches," *IEEE Comm. Magazine*, pp. 50-56, February 1999.
- [84] E. L. Goldstein and L. Eskildsen, "Scaling limitations in transparent optical networks due to low-level crosstalk," *IEEE Photonics Techn. Lett.*, vol. 7, pp. 93-94, Jan. 95.
- [85] C. G. P. Herben *et al.*, "Compact integrated polarisation independent optical crossconnect," in *European Conference on Optical Communications*, vol. 1, (Madrid, Spain), pp. 257-258, September 20-24 1998.
- [86] A. Papoulis, *Probability, Random Variables, and Stochastic Processes*. McGraw-Hill Int. Editions, second ed., 1991.

Curriculum Vitae

Idelfonso Tafur Monroy was born in El Castillo (Meta), Colombia, in 1968. In November 1985 he completed and approved the 11th grade of Colombian High School ('Bachiller') at the Departamental Integrado School Fontibon, Bogotá, D. C. In the period between September 1986-July 1987 he studied Russian language and approved the University Preparatory course at the Kharkov Polytechnic Institute, Kharkov, Ukraine. In September 1987 he joined the Bonch-Bruевич Institute of Communications, St. Petersburg, Russia, where he received in 1992 the M.Sc. degree in Multichannel Telecommunications. In 1993 he enrolled as a graduate student in the Department of Signals, Sensors and Systems at the Royal Institute of Technology, Stockholm, Sweden, where he received in 1996 the Technology Licenciata degree in Telecommunication Theory. The same year he started pursuing the PhD degree in the Department of Electrical Engineering at the Eindhoven University of Technology, The Netherlands. His research interests are in the area of optical communication networks, communication theory, stochastic processes, and applied probability theory.

Stellingen behorende bij het proefschrift

**Performance Evaluation of Optical
Communication Networks**

door Idelfonso Tafur Monroy
9 september 1999

1. The beliefs that shape our historical foresight represent ... our *Erwartungshorizonten*, or “horizons of expectation”.
(Stephen Toulmin, *Cosmopolis: the hidden agenda of modernity*, The University of Chicago Press, 1990)
2. Assessment of optical crosstalk in optical systems is most accurately achieved by analyzing the resulting filtered photocurrent at the receiver end.
(This thesis, paper **I**)
3. Although optical preamplification enhances the receiver sensitivity, it does not mitigate crosstalk and moreover it introduces additional power penalties due to the occurrence of beats between crosstalk and spontaneous emission noise.
(This thesis, paper **J**)
4. The performance of optical networks with respect to crosstalk is topology dependent.
(This thesis, paper **M**)
5. Phase scrambling mitigates interferometric crosstalk at the expense of network reach.
(This thesis, paper **K**)
6. Det tunga i livet:
 vilja men inte kunna.
 Det onda i livet:
 kunna men inte vilja.
(Gunnel Vallquist, *Steg på vägen*, Libris, Örebro, 1995)
7. Using maximum entropy in crosstalk analysis has been a rather distracting task. It is supposed that the more the crosstalk the higher the entropy, but the whole point here was to eliminate crosstalk!
8. The performance of optical receivers can still be improved by using electrical postdetection signal processing.
(This thesis, paper **D**)
9. It should be possible to achieve more power and/or bandwidth efficient transmission over the optical channel by using novel modulation techniques.
10. Writing these “stellingen” I discovered that my thesis was mostly about combining the best of my Latin culture with the Dutch culture: *crosstalk* and *performance*.
11. !Viva la paz, pero con los ojos abiertos!
(Gabriel García Márquez)

